Improving the quality of future protein: an exploration of amino acid profile malleability in *Fusarium venenatum*

Kamil J. Szepe MSc.

Thesis submitted to the University of Nottingham for the degree of Doctor of Philosophy.

December 2024

Acknowledgements

Firstly, I'd like to thank Professor Simon Avery for all the guidance and help with navigating this project. I'd also like to thank Professor Paul Dyer as well as my industrial supervisors Professor Rob Johnsons and Dr Ivey Geoghegan for valuable inputs throughout the project. Thank you to Marlow Foods and Future Food Beacon Nottingham for providing the funding for the project. I'd like to also thank Matthew Kokolski and the rest of technical team over at The School of Life Sciences, and Dr Dongfang Li for the assistance with LCMSMS analysis. Thank you, to all the friends and colleagues in B44 and B85, that passed through the labs over the years (including the Transformation King – Xu Mingzhi). I'd also like to thank Professor Tom Reader for all the help with the statistical analysis.

Chciałbym pozdrowić całą swoją rodzinę. Kochani rodzice, mimo to, że nie mieliście bezpośrednio wpływu na pisanie tej pracy, to chciałem podziękować Wam, za wychowanie i wsparcie, bez którego wiem, że nie mógłbym być tu gdzie jestem teraz. Mam nadzieję, że jesteście i będziecie ze mnie dumni. Chciałem także podziękować mojej babci za ciągłe bezwarunkowe wsparcie i zawsze bycie gotową do wysłuchania i porozmawiania.

Okres po ukończeniu tego doktoratu okazał się jak do tej pory, najważniejszym w moim życiu, i przyniósł ze sobą wiele przemyśleń i objawień. Zdałem sobie sprawę, że owszem, wszystkie interakcje, nawet najmniejsze mają wpływ na charakter człowieka, ale nie filtrując tychże interakcji, bardzo łatwo jest się zgubić. Dopiero niedawno, dzięki rozmowom z miłością mojego życia, zdałem sobie sprawę jak ważne jest ciągła pielęgnacja swojego charakteru, i jak łatwo można z tej drogi zboczyć. Niczym krople drążące skałę, te wspomniane kontakty tępiły ostre krawędzie pozostawiając coraz to nudniejszy, i pospolity krajobraz. Szczęśliwie, było mi dane zdać sobie sprawę z kierunku w jakim zmierzałem. Teraz jestem w stanie odżywić części siebie które były przez lata uśpione i z nowym, lepszym punktem widzenia pokierować swoim życiem tak jak zawsze chciałem. Najbardziej chcę podziękować sobie za to, że udało mi się dopiąć to do końca, mimo wszystkich przeszkód które stanęły na mojej drodze. Chcę podziękować Y.K., najważniejszej osobie w moim życiu, mimo, że pojawiła się w nim tak późno, jestem pewny, że bez niej ciągle błądziłbym bez celu, znudzony, nie potrafiąc doceniać piękna i najważniejszych aspektów tego życia.

Covid Impact statement

As everyone is acutely aware in the beginning of 2020 the global pandemic of Covid-19 has been declared with governments across the world taking action to deal with the spread of the virus, limit casualties and buy time for development of a vaccine. My PhD project was affected to a major extent by the combination of UK government policies, policies of the University of Nottingham and of the pandemic impact on my personal well-being which I will try to discuss in this statement.

The most visible impact of the Covid lockdown was the time lost which I feel was specifically significant for my project. The project relied on access to LCMSMS facilities that were to become available within 2 months of the project starting date in July 2019. Due to issues with construction this deadline was pushed early 2020, which then was halted again due to Covid-19 lockdown. Consequently, I was only able to start conducting the AA analysis experiments (key component of the project) in early 2021 – almost 2 years into the project. This turn of events led to the need to remove some planned parts of the project from the plan (like in-vivo digestion assays and sensory testing of generated products) and for a time changed the feel of the project from exploring the scientific process to racing against time to get enough results for a PhD thesis before the end of project deadline.

The closing of school of Life Sciences lasted specifically from March 2020 until late August 2020, upon which a week in/week out working system was in place for a couple of months making catching up with lost time difficult. Not long after full time return to the lab was permitted (although Covid-19 restrictions regarding e.g., number of people allowed per room were still in place slowing down work), the UK left the EU in January 2021 causing delays of key consumables to the lab slowing down/completely stopping some types of experiments once again for a couple of months (e.g., 2-month delay of 96-well plate shipment). Due to ongoing restrictions and self-isolation regimes due to Covid less staff were available to carry out repairs to any crucial equipment needing servicing was delayed (e.g., biosafety cabinet).

Of course, steps were taken to mitigate the impact of the lockdown but that also fell victim to unfortunate timing. The lockdown started not long after I've submitted my 1st year review meaning that unlike colleagues whose reviews were scheduled for June (or more senior colleagues who could work on their theses) I did not have a major piece of work to focus on. Initially (when lockdown was supposed to last a couple of weeks) the plan was to plan future experiments which quickly became very abstract as it became clear that the return to labwork was not in sight. Next my focus went into writing a review article that ended up being published – a valuable experience that broadened my knowledge and improved my writing skills, but due to the topic of the review had little impact on the development of my actual PhD project. I also took part in a few online conferences to broaden my knowledge. I also attended a Nutrition Society 2020 online conference to broaden my knowledge. Lastly, we tried to organise work placement at labs of our industrial partners at, but initially that was not possible due to company Covid policy, and later due to lack of open accommodation/restaurants in the area (due to UK Government Covid restrictions).

Finally, I only received 8 weeks of funding extension to my project (where 6 months of unfunded extension to the thesis submission were, because of circumstances outlined above I did need every day of that time to finish my research and thesis on time. However receiving only 8 weeks of funded extension meant that after August 2023 I had to take part time jobs to in addition to my lab work/thesis writing to financially survive in the UK among the growing

cost of living. Towards the end of November my supervisor find a way to secure some funding form me which was extremely helpful and removed a great deal of stress, but the time that could have been spent on additional experiments that would benefit this thesis was inadvertently lost.

The aspects above are of course do not include the psychological pressure that that was added by all these circumstances during a PhD project which in normal times can be quite an isolating experience.

ABSTRACT

Meeting the food demand of a growing population whilst dealing the with effects of climate change is one of the biggest challenges facing humanity this century. The current food system is considered unsustainable, and alternatives are required to face the challenges. Some microorganisms can provide an alternative, sustainable and high quality source of dietary protein which, due to the organisms' short generation times and general amenability to laboratory studies, also offers unique opportunities for improvement including by non-GM methods. The mycoprotein product from the fungus *Fusarium venenatum* has a high quality amino (AA) profile which, as shown here, is stable in different growth conditions. There was no significant difference in AA composition of *F. venenatum* cultured at industry or laboratory scale, supporting the extrapolation of laboratory-based experimental results to industrial production. The growth medium (RHM) used for industrial scale production of *F. venenatum* is not a prerequisite for the mycoprotein AA profile as culture of the fungus in different growth media did not change the AA profile and neither did substituting glucose with sucrose, an alternative carbon source. Supplementing cultures with agents that stimulate AA mis-incorporation (mistranslation) during protein synthesis by cells did not induce a detectable change to the AA profile of the fungus. High branch chained AA selection medium caused an enrichment in the AAs in the *F. venenatum* hydrolysate, but subsequent adaptive evolution experiments did not enhance the effect as intended. Furthermore AA (leucine) over-producing isolates of *F. venenatum*, selected via culture on the leucine derivative 5'5'5-tri-fluoro-leucine, showed no change in protein-AA profile despite up to a ~10 fold increase in free leucine. The stability of the *F. venenatum* AA profile supports the possibility of using alternative fermenter conditions and growth substrates (e.g. waste streams as components of the growth medium).

Table of contents

1 Chapter 1 – General Introduction 10

1.1 Challenges facing the food system 10
1.1.1 Global food production and food security 10
1.1.2 Importance of protein quality in human nutrition. 10
1.1.3 Climate and sustainability 12

1.2 Alternative proteins 13
1.2.1 Types of alternative proteins 14
1.2.2 Single cell proteins – the past 15
1.2.3 Microbial renaissance 16
1.2.4 Opportunities and challenges of single cell proteins 17

1.3 Quorn Mycoprotein 19
1.3.1 History of Quorn mycoprotein 20
1.3.2 Genus *Fusarium* 21
1.3.3 *F. venenatum* A3/5 as Quorn mycoprotein producer 24
1.3.4 Industrial scale production of *F. venenatum* mycoprotein 25
1.3.5 Mycoprotein and nutrition 27

1.4 Thesis aims 28

2 Chapter 2 Investigation of properties of *F. venenatum* AA profile and its response to different growth conditions 29

2.1 Introduction 29

2.2 Chapter aims 30

2.3 Materials and Methods 30
2.3.1 Chemicals 30
2.3.2 Fungal strains and growth conditions 30
2.3.3 Growth media and culture in shake flasks 30
2.3.4 Microplate reader culture conditions 31
2.3.5 Calculating the doubling times 31
2.3.6 Media 31
2.3.7 Biomass measurements and preparation. 31
2.3.8 Protein hydrolysis and sample preparation for LCMSMS analysis. 32
2.3.9 Preparation of LCMSMS standards and sample dilution 32
2.3.10 UHPLC-MS/MS Instrumentation 33
2.3.11 LCMSMS chromatograph analysis. 34
2.3.12 HPLC conditions 34
2.3.13 Free amino acid extraction for HPLC analysis 35
2.3.14 Protein extraction and Bradford assay analysis. 35
2.3.15 Statistical analysis 35

2.4 Results 38
2.4.1 Growth of *F. venenatum* in microplate cultures 38
2.4.2 Growth in baffled flask cultures 39

2.4.3 Validation of total protein content measurements with Bradford assay. 39
2.4.4 The relationship between growth stage and protein content 40
2.4.5 Comparison of AA profiles of *F. venenatum* in flask culture and airlift fermenter cultures 43
2.4.6 Comparison of the relative and absolute AA profiles of flask grown *F. venenatum* cultures at 30 h and 36 h 46
2.4.7 Comparison of free AA profiles 47
2.4.8 Comparison of AA profiles and growth in other fungal media 50
2.4.9 Effect of carbon source substitution on the AA profile of *F. venenatum* 55

2.5 Discussion 59
2.5.1 Use of flask cultures for testing effects of growth medium 59
2.5.2 Robustness of the AA profile of *F. venenatum* 59
2.5.3 Limitations and future work 60

3 Chapter 3 - Investigation of the AA composition of *F. venenatum* c-variant mutants 61

3.1 Introduction 61

3.2 Chapter Aims 62

3.3 Methods 63
3.3.1 Procurement and maintenance of *F. venenatum* C-variant strains 63
3.3.2 Culture growth 63
3.3.3 Sample preparation 63
3.3.4 Analysis of free AA by LCMSMS 63

3.4 Results 66
3.4.1 Acquisition and selection of mutants 66
3.4.2 Growth of C variant mutants in flask cultures 68
3.4.3 The AA profile of C-variant mutants C4 and C5 70
3.4.4 Changes to free AA profile in the C5 isolate. 73

3.5 Discussion 75
3.5.1 General conclusions 75
3.5.2 Presence of taurine in *F. venenatum* 76

4 Chapter 4 – Targeting translation as means of amino acid profile manipulation 78

4.1 Introduction 78

4.2 Chapter Aims 81

4.3 Materials and Methods 81
4.3.1 Media preparation 81
4.3.2 Chemicals 81
4.3.3 Tube race setup and protocol 81

4.4 Results 84
4.4.1 Identification of subinhibitory concentration of paromomycin for *F. venenatum* in plate reader cultures 84

4.4.2 Identification of subinhibitory concentration of paromomycin with *F. venenatum* in flask cultures 85
4.4.3 Measurements of effect of paromomycin treatment on the AA profile of *F. venenatum* 85
4.4.4 Identification of subinhibitory H_2O_2 concentrations against *F. venenatum* growth in microplate cultures 91
4.4.5 Growth curve with H_2O_2 in in flasks 92
4.4.6 Effects of H_2O_2 on AA profile 92
4.4.7 Adaptive mistranslation setup rationale 95
4.4.8 Growth with low nitrogen (N) 95
4.4.9 Effect of high BCAAs medium on biomass 96
4.4.10 Effect of high BCAA medium on AA profile 97
4.4.11 The effect of removal of valine from the BCAA mix in selection medium. 100
4.4.12 The effect of tube race selection in liquid medium on the AA hydrolysate composition of *F. venenatum* 104
4.4.13 The effect of tube race selection in agar medium on the AA hydrolysate composition of *F. venenatum* 109

4.5 Discussion 116
4.5.1 Chemically induced mistranslation 116
4.5.2 Effects of BCAA selection media on *F. venenatum* hydrolysate AA profile 117
4.5.3 The effect of tube race selection 118

5 Chapter 5 Targeting leucine biosynthesis as a means of altering the amino acid profile of *F. venenatum*..... 119

5.1 Introduction 119

5.2 Chapter Aims 122

5.3 Materials and Methods 122
5.3.1 Chemicals 122
5.3.2 Buffers 122
5.3.3 Culture media 123
5.3.4 Culture conditions 123
5.3.5 Molecular cloning 123
5.3.6 Pre-germination of *F. venenatum* spores 128
5.3.7 UV mutagenesis conditions 128
5.3.8 Mycotoxin assay 129

5.4 Results 129
5.4.1 Prediction of a potential gene target enabling selection for increased leucine synthesis in *F. venenatum* 129
5.4.2 The effect of TFL on growth of *F. venenatum* 129
5.4.3 Pre-germinated *F. venenatum* spores can be fully inhibited by TFL. 130
5.4.4 Determining the appropriate UV irradiation time of pre-germinated *F. venenatum* spores 131
5.4.5 TFL selection screen and validation of gain of TFL resistance 132
5.4.6 Free-AA analysis of the TFL screen isolates 133
5.4.7 Comparison of AA profile of Iso2 and WT hydrolysates 139
5.4.8 Amplification and sequencing of IPMS from TFL isolates 142
5.4.9 Bioassay for mycotoxin production by the high free-leucine Iso 2 isolate 145
5.4.10 The extent of loss of free leucine (and other AAs) during the RNA lowering step of mycoprotein production 146

5.5 Discussion 147

5.5.1 The resistance to TFL in *F. venenatum* spores. 148
5.5.2 Changes to IPMS in Iso2 148
5.5.3 The utility of Iso2 and other potential isolates 149

6 General discussion 150

6.1 The stability of *F. venenatum* amino acid profile **150**

6.2 The translation focused amino acid profile manipulation approach **151**

6.3 Concluding remarks **152**

7 Appendix 153

8 References 185

1 Chapter 1 – General Introduction

1.1 Challenges facing the food system

The growing worldwide population and climate change are among the most important issues that humanity will have to deal with within this half of the century. The current food system is already strained, and it is unlikely that in its current form it can be expanded to accommodate for the growing population. Additionally, the farming practices and effects of climate change contribute to decrease in current food yields due to factors like animal and crop disease, floods, or draughts. To address these challenges, it is necessary to understand the problems with the current way food is produced to avoid similar pitfalls in the future. At the same time a plethora of solutions are being proposed to both find novel ways of producing food as well as making the current food production process less environmentally damaging and more efficient. The first half of this chapter will attempt to briefly summarise the current dynamic between agriculture and environment as well as give an overview of some of the proposed solutions.

1.1.1 Global food production and food security

The global human population is projected to reach 10 bn by 2050 (UN, 2017). However by some estimates the population is supposed to peak in 2064 and decline afterwards (Vollset et al., 2020), others think that growth will continue but likely at lower rate (UN, 2022). In any case past 2050 the growth in global population is projected to slow down significantly, stop, or even reverse. A significant part of the increase in the population is a result of increasing life expectancy, this is likely to add pressure to the food system, as an increasing amount of studies show the importance of enhanced nutrition in the elderly to delay onset of age related diseases (expanded in **1.1.2**) (Lonnie et al., 2018). High levels of meat consumption in western countries are associated with wealth and as a consequence many countries with developing middle classes are projected to increase their meat consumption, e.g. India is projected to shift to levels of meat consumption typical of western diets (Alexandratos and Bruinsma, 2012). To meet this demand the global food production should be 60% higher in 2050 than it was in 2005/2007 (FAO, 2009). This may be challenging because the water and land resources are already stretched and overall crop yields have decreased -a trend that is feared to possibly be irreversible. In general the sustainability of the current food system is fairly questionable (expanded in **1.1.3)(FAO, 2021)**.

In summary, the increasing demand for food production due to a growing population will likely not continue indefinitely and start plateauing after 2050. That said, trying to achieve levels of food production needed by simply expanding current operations is unlikely to be feasible. The decisions of how to meet the demand of this final biggest increase in human population is likely one of the key contemporary issues.

1.1.2 Importance of protein quality in human nutrition.

The estimated required energy intake - kcal/per person/per day (k/p/d) is 2500 kcal for men (2000 kcal for women). As of 2005/2007 28% of the population consumes on average over 3000 kcal (overconsumption) and 35 % of the world population consumes under 2500 kcal (malnutrition) (FAO, 2013). The amount of kcal per day is not the only factor required for good nutrition, enough micro and macronutrients, dietary fibre etc. are also required. In the diet, energy itself can be produced from carbohydrates, fats or proteins, but essential AAs can

only be obtained from dietary protein (or as free AAs). In humans, there are nine essential amino acids (EAAs) (histidine, isoleucine, leucine, lysine, methionine, phenylalanine, threonine, tryptophan and valine) meaning they cannot be synthesised at all, or in sufficient amounts so need to be provided through diet (FAO, 2013).

Protein intake mirrors the global caloric intake to an extent. In developed countries, many individuals consume considerably more protein (and calories) than required to maintain health and some evidence suggests this could contribute to high incidence of obesity, diabetes and related conditions putting a strain on healthcare systems, quality of life and ability to work (Drummen et al., 2018; Neff et al., 2018). Additionally, because excess protein is not stored in the human body, it is secreted out as ammonia – making overconsumption not only wasteful but also contributing to environmental pollution. In other parts of the world, populations may suffer from insufficient protein/AA intake. As mentioned earlier, EAAs must be provided through diet in sufficient amounts for development/maintaining health. High quality protein is characterised by an appropriate balance of EAAs, good digestibility and absence of anti-nutritional factors (e.g. trypsin inhibitors in unprocessed legumes or uricogenic nucleobases in certain microorganisms) (Gilani et al., 2012; Gorissen et al., 2018). An ideal protein source meets EAA requirements without further supplementation (**Figure 1.1**). According to the FAO-preferred method of AA profile evaluation (DIAAS; Digestible indispensable amino acid score, used to replace PDCAAs (Protein digestibility corrected amino acid score) in 2013) protein sources scoring close to ideal include eggs and milk (WHO, 2007; FAO, 2013).
These factors highlight that for sufficient nutrition not only is the quantity of the protein important but also quality. In parts of the world where dietary protein relies on poor variety of crops, some EAAs might not be taken in sufficient amounts from the diet (**Figure 1.1),** resulting in developmental issues in children e.g. due to insufficient dietary lysine in Nigerian children (de Vries-Ten Have et al., 2020). Protein is also an important modulator of satiety, so its lack in the diet can lead to abnormalities regarding appetite (Lonnie et al., 2018).
In situations where high quality protein is not available, but other sources of food are, this protein starvation may paradoxically lead to obesity, as individuals are likely to keep experiencing the feeling of hunger if the diet consists only of, e.g. carbohydrates (Siddiqui et al., 2020).

The daily recommended intake of high-quality protein for young adults is 0.8 g/kg/day, however, this should be seen as a bare minimum to prevent net protein loss. In adults over 40 years, there is a progressive loss of muscle mass at a rate of around 8 % per decade from 40-70 years of age and 15 % per decade afterwards known as sarcopenia (Larsson et al., 1979). As increasing life expectancy is one of the main drivers of population growth, for elderly adults, whose numbers are increasing in many developed countries, 1.2–2 g/kg/day is recommended to help prevent sarcopenia (Baum et al., 2016; Lonnie et al., 2018). Despite these elevated protein intake requirements, many older adults are not consuming enough dietary protein. Reportedly, in North America ~ 40 % of older adults consume less protein than recommended (Houston et al., 2008). Data from the UK suggests that the protein intake decreases with increasing age, e.g., protein intake in adults over 75 years was 11-19 % lower than in adults aged 64 and below (Public Health England, 2020). Despite this many elderly people feel like they consume appropriate amounts of protein and are sceptical about increasing the intake (Banovic et al., 2018). This is problematic as elderly adults with poor protein knowledge are more likely to suffer from sarcopenia related symptoms (Visser et al., 2021)

In summary, in addition to providing quality nutrition to the existing populations, the growing and ageing population will require additional sources of high-quality protein to allow for high quality life and to decrease the burden on healthcare systems, so the future challenges lay not only in producing more food but also increasing its quality and availability worldwide.

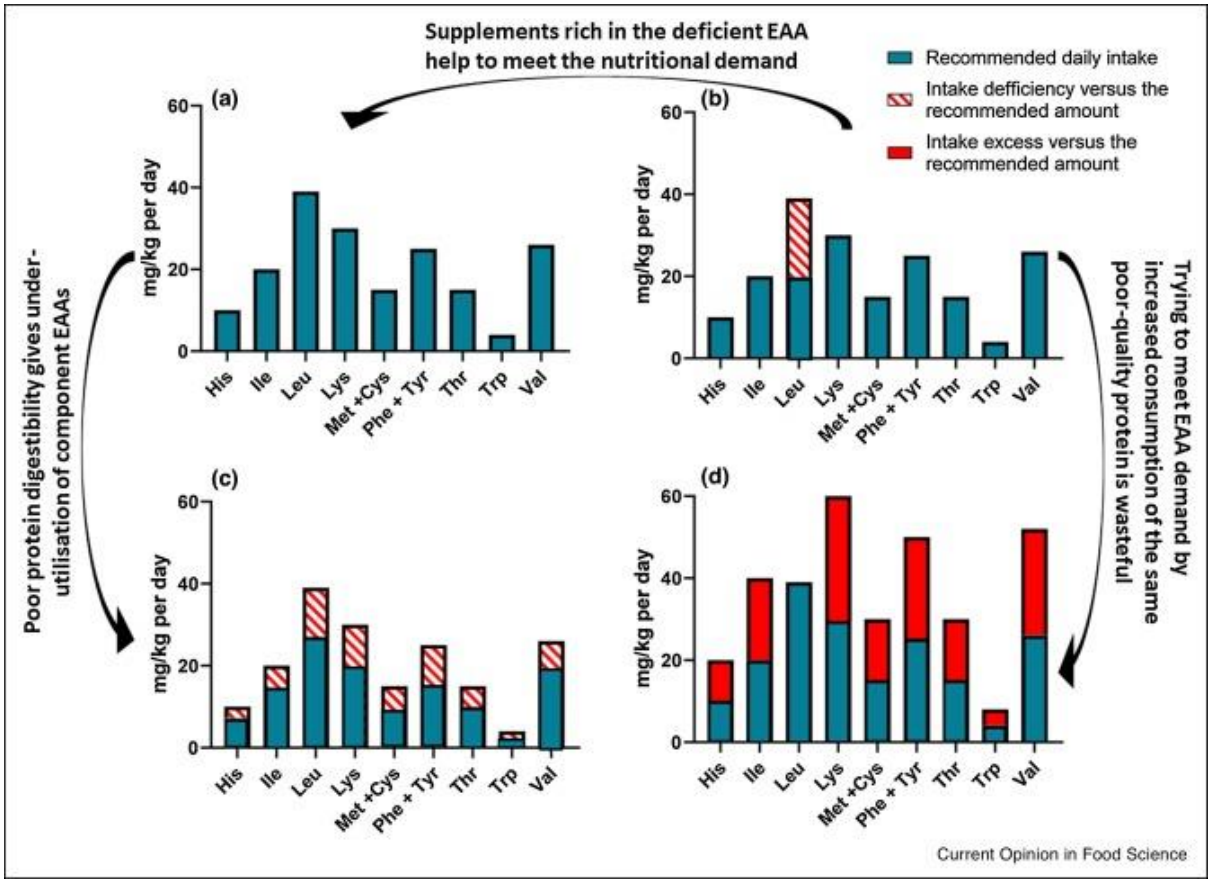

Figure 1.1 Potential protein-quality scenarios and effects on dietary essential amino acid (EAA) supply. (a) EAA profile (x axis) of 60 g of a protein source of an ideal quality (based on (WHO, 2007). **(b)** EAA profile of a near ideal protein source deficient in Leu. **(c)** Poorly digestible protein or protein containing antinutritional compounds may not be completely utilised despite having a good EAA profile **(d)** Consuming more poor-quality protein to compensate for particular deficiencies (b) leads to excess consumption of EAAs that are already available in sufficient amounts (Figure taken from (Szepe et al., 2021) .

1.1.3 Climate and sustainability

As mentioned above (**1.1.1**), maintaining the current trajectory of the food system is likely to accelerate climate change, but also is likely to be further affected by changing temperatures. Increases in beef production – as a result of the overall trend of increased meat demand is a significant factor driving deforestation in the Amazon. Building transport infrastructure and pastures for cattle to meet the growing predicted trend of increased global demand for meat is likely to exacerbate this deforestation trend (Recanati et al., 2015). This pasture expansion is linked to 80% of all of Amazon deforestation in the last 30 years, and despite policies and public pressure to stop this precedent, it continues to this day (Skidmore et al., 2021). Deforestation also leads to depletion of animal habitats, decreases biodiversity and increases the chances of pathogen jumping from wild animals to livestock and humans (Esposito et al.,

2023). In general, high intensity farming of animals produces prime conditions for the development of zoonosis, e.g., the 2013 outbreak of H7N9 avian influenza infections in Shanghai in 2013 (Li et al., 2016). In general, attempts to scale up meat production by expansion of land on which to rear livestock or increasing the intensity of farming are likely to lead to increased emergence of novel zoonotic pathogens that risk more pandemics (Hayek, 2022). Livestock production also contributes significantly to emissions of greenhouse gasses in form of methane (produced via fermentation of plant material in the guts of ruminants) and nitrous oxide emitted from manure, which have 28 and 265 times higher global warming potential respectively compared to CO_2 (Grossi et al., 2018). For some time, aquaculture was seen as an alternative because it can produce large amounts of protein efficiently, but this becomes increasingly unsustainable. Mangrove forests are removed to construct new aquafarms and the system is reliant on fishmeal (often produced from caught wild fish) increasing demand which contributes to overfishing (Macusi et al., 2023; Martinez-Porchas and Martinez-Cordova, 2012).

The global temperatures are rising at unprecedented rates because of increasing CO_2 and other greenhouse gas emissions. This phenomenon is at the centre of the issues, yet the precise consequences are only beginning to be understood. For example, increasing CO_2 emissions to process and designate more land as arable can be counterproductive as increased CO_2 levels have already been shown to lower yields of crops like soybean and maize (Jägermeyr et al., 2021). Our monoculture based agricultural system as well as increasing temperatures contribute to accelerating spread of crop pathogens which is likely to further limit the efficiency of the food production (Singh et al., 2023a). In similar vein increasing crop and animal production requires additional water which is already becoming more scarce due to climate change that causes increasing amounts of draughts every year (UN, 2023).

In summary, the food system in the current state can be considered both a driver of climate change as well as being negatively affected by the consequences of climate change risking falling into a vicious cycle.

1.2 Alternative proteins

The current way agriculture is run is very resource heavy and reliant on monocultures. 75 % of global food (and consequently energy and proteins) comes from just 12 crops (rice, wheat, sugarcane, corn, soy, potatoes, palm oil, cassava, sorghum, millet, groundnuts and sweet potatoes) and 5 animals (cattle, chicken, buffalo, pig and goat) (FAO, 2000). Grains are the largest contributors to proteins sources with the exception of a few countries where meat and dairy are the biggest contributors. 94% of all non-human mammalian biomass comes from livestock, with livestock birds making up 71 % of total bird biomass (Bar-On et al., 2018). 70 % of global fresh water supplies are used for agriculture and 78 % of all global water body pollution is related to agriculture (Poore and Nemecek, 2018; FAO, 2021). Food production also accounts for an estimated 26 % of global greenhouse gas emissions (FAO, 2021). This state of things is generally unsustainable as explained in the preceding sections. Simultaneously, the lack of variety in diet, due to hegemony of only a few food sources can lead to less diverse diets and a lack of necessary nutrients in parts of the population. Alternative protein is a term that can be used to collectively describe sources of protein that do not belong to the 17 mainstream food sources, this can include sources of protein that have been used for centuries like underutilised crops or insects, or more recent inventions like single cell proteins or lab grown meat.

1.2.1 Types of alternative proteins

A lot of commercially used crops are nutrient poor and show low resilience to the less stable climate (IPCC, 2019). However, there are a multitude of other crops that were not commercialised on mass scale but have been known to local populations historically, these come under a collective term of underutilised crops. Legumes are a group of underutilised crops that show nutritional variability as well as adaptability to European agricultural system. Species like *Vicia faba* or *Pisum sativum* were shown to contain high quality protein and good digestibility making them good candidates for diversification of crop production in Europe (Mecha et al., 2023). Another example of an underutilised legume that gained interest in recent years is the winged bean (*Psophocarpus tetragonolobus)*. Winged bean grows in hot, humid, equatorial countries of Southern Asia, Melanesia and the Pacific area (Tanzi et al., 2019). It is a good candidate for a crop in subtropical and tropical area, and its high efficiency in nitrogen fixing and storage make it a perfect candidate for use as a rotational crop. What is more, all parts of the winged bean are edible and contain a similar nutrient and AA profile to that of soybean, with similar digestibility after processing, making it a good alternative to reduce the reliance on soybean (Mohanty et al., 2020). Another example of an underutilised crop of high interest is Quinoa (*Chenopodium quinoa Willd*.) also known as the "Golden Grain" which is native to the Andean region of South America. The latter name of the crop comes from its resilience to cold, draught, and high salinity, as well as its unique highly nutritional value (Angeli et al., 2020). Due to its environmental resilience Quinoa can be farmed on marginal soils. Additionally, Quinoa contains a higher amount (11 – 19 %) of protein than other cereals (like wheat and barley) or soybean, whilst simultaneously being a good source of vitamins like riboflavin and thiamine and micronutrients (calcium, magnesium, iron, copper and zinc). Unlike many other cereals, Quinoa also does not contain gluten to which may be considered as many conditions such as celiac disease, irritable bowel syndrome, and Crohn's disease that are or can be triggered by consumption of gluten (Roszkowska et al., 2019; Azizi et al., 2020).

Using insects as animal feed or directly for human consumption is another possible alternative. Insects were historically, and are to this day, consumed in many cultures around the world but due to hegemony of western culture which did not typically contain insects, over time insects became seen as a less desirable (van Huis, 2013). However, insects constitute a good source of protein and rearing is estimated to be more efficient and environmentally sustainable compared to traditional livestock. Like traditional livestock, insects produce CO_2 and ammonia, however current knowledge suggests that these levels are lower compared to livestock emissions (van Huis and Oonincx, 2017; Alexander et al., 2017). The land and water use are also lower with added potential for rearing insects using industry side streams. Among other benefits are, better feed to biomass conversion ratio and lower risk of zoonotic disease due to a more distant evolutionary relationship with humans (van Huis, 2013).A digestibility study showcased that insect protein can be a viable protein source for humans (Hermans et al., 2021). However, chitin from the insect exoskeleton might be a potential drawback as it can trigger allergic reactions in people with shellfish allergy, which is one of the leading causes of allergy globally (Tham and Leung, 2018; De Marchi et al., 2021). As mentioned earlier, the acceptance of insects as food source in western culture can be low due to negative associations, but insects can also be used in other ways, e.g. by replacing fish meal as feed for fish in aquaculture, or used as an ingredient (e.g. insect flour) to increase the protein content of food products (Hartmann et al., 2015). Other cultures see insects as a source of food with more acceptance so studies aimed at identifying the causes of

the approach can be useful to designing strategies to promote insect proteins in the western culture.

Lab grown meat is a more recent way of producing meat and other animal products in a more sustainable way. The idea is to use animal cell lines to cultivate animal muscle tissues or fats and use them to produce meat products that do not rely on rearing the actual animal (Ching et al., 2022). Even though this may never turn out to be cheaper than animal derived meat it would diversify the food market, increasing its resilience and providing consumers with "ethical" ways of getting high quality protein (Stephens et al., 2018). Examples of other alternative proteins include treatment of keratin (protein found in e.g., sheep wool, an abundant waste product of sheep rearing) to break down the sulphate bonds of the protein and allow digestibility (Dias et al., 2022). This protein was shown to be comparable to casein in a rat model, providing an alternative source of protein free from fats or carbohydrates (Dias et al., 2022).

Highlighted here is only a brief overview of various alternative proteins, all of which have their own advantages and disadvantages but are not the focus of this thesis. A large area of alternative protein also lies in using microbial organisms to either produce animal/plant derived molecules or to use microbial organisms such as bacteria, fungi and microalgae as a direct source of food for animals or humans. This latter is referred to as single cell proteins (SCP)

1.2.2 Single cell proteins – the past

Single cell proteins are referred to as proteins derived from microbial organisms that are used as a food source. The term was coined in the 1960s but the idea was described and implemented half a century earlier. Use of excess yeast from the beer brewing process as a source of food for people and livestock, due to their high nutritional value, was first highlighted by Max Delbrück and colleagues in Germany (Völtz, 1916) (Delbruck, 1910). During WW1, Germany compensated for the loss of imports by incorporating this yeast into diets, and even starting operations dedicated to directly producing yeast biomass as a food source. After the war improvements to the method were made and batch-fed fermentation as a method was first developed. This allowed a higher final biomass yield to be achieved from fermentation or to trigger desired metabolic pathways (Ugalde and Castrillo, 2002).

The use of yeast as a food continued in Germany and during WW2 the interest in microbe derived protein spread across the world, spawning projects such as use of *Candida utilis* in USA to produce biomass from waste sulphate liquor from wood production (Harris, 1949). In the 1960s, the UN published a report that predicted a global protein crisis by the year 2000, when the population was projected to grow from 2.5 bn to 5 bn people, based on available crop yields and prices of the time (Ugalde and Castrillo, 2002). This report spawned an increasing interest in alternative protein sources including SCP. During that time, even more developed nations started their own SCP projects, such as Finnish SCP using fungus *Paecilomyces varioti* in a Pekilo process to produce animal feed (Koivurinta et al., 1979). Similarly in Britain, bacterial SCP that used *Methylophilus methylotrophus* to ferment methanol and produce pig feed trademarked as Pruteen was developed (Marstrand, 1981). Another British company, Quorn developed an SCP product using fungus *Fusarium venenatum* intended for direct human consumption (Whittaker et al., 2020). In the USSR, large scale operations intended to produce SCP from yeast using hydrocarbons were also in place (CIA, 1977).

In the 1980s, the improvement in plant breeding and geopolitical changes increased the agricultural output and decreased the cost below what was previously thought possible. The green revolution combined with local developments such as agricultural reforms in China contributed to significant increases in global crop production (FAO, 2000). Additionally, the prospects of the end of the Cold War brought hopes for liberalisation of the global food markets which culminated in signing of the General Agreement on Trades and Tariffs in 1994 in Marrakesh that was signed by 118 countries and introduced new rules for a global open free market (WTO, 1994; Ugalde and Castrillo, 2002). These factors combined drastically increased the availability and reduced the cost of staple crops worldwide rendering many SCP operations not commercially viable, which resulted in discontinuations, rendering almost the whole sector effectively dormant until more recently. For more detail about the historical perspective of the SCP the reader is encouraged to read the review written by Ugalde and Castrillo (2002).

1.2.3 Microbial renaissance

Since its temporary dormancy the SCP sector seems to be entering a global reawakening with microbial protein gaining a lot of publicity and investment in the last couple of years (Ritala et al., 2017; Graham and Ledesma-Amaro, 2023). In the first seven months of 2020, 435 million USD were invested in fermentation globally, the highest investment levels recorded to that point (GFI, 2020). The EU, which is already the largest market for alternative proteins sales, continues to provide further funding for innovation, research and legislation for the development and upscaling of alternative proteins including a lot of SCP projects (GFI, 2023). The new SCP projects come in many shapes, from reviving previously discontinued ventures like the Pekilo project, now in the phase of upscaling under the Finnish company EniferBio (https://enifer.com/), building on existing solutions like production of vegan meat substitutes done by Swedish Mycorena (https://mycorena.com/), or to novel ventures such as the use of Knallgas bacteria to produce biomass using CO_2 as carbon source in fermentation developed by Solar Foods (https://www.solein.com/) which recently was approved for the first time for human consumption in Singapore (Solar Foods, 2023).

The growing interest and investments in recent years has produced and rejuvenated a lot of ideas in terms of methods of cultivation and organisms used in the area of SCP. A common disadvantage of SCP is that they generally contain relatively high levels of nucleic acids (a necessary prerequisite for their fast growth) which need to be lowered to safe levels if the product is intended for human consumption. Broadly, SCPs can be divided into three groups, being derived from bacteria, microalgae or fungi, with each group possessing unique features (Ritala et al., 2017). Typical bacterial candidates for SCP contain 50 – 80 % protein by dry weight and tend to be rich in methionine content (up to 3%) as well as containing a variety of micronutrients, vitamins and phospholipids (Ritala et al., 2017). An added benefit is that production of bacteria is relatively easy as they can often grow on very simple minimal media e.g. utilising methane or CO_2 as a source of carbon with some hydrogen fixing bacteria like *Nocardioides nitrophenolicus* being cultivated using gas fermentation (Ritala et al., 2017) (Nyyssölä et al., 2021). Microalgae can grow using photosynthesis meaning the minimal requirement is sunlight and CO_2. Species like *Chlorella vulgaris* and *Dunaliella salina* contain 50-80 % protein by dry weight and are a good source of A, B, C, E vitamins, chlorophyll and omega fatty acids (Janssen et al., 2022). To date however, microalgae derived products are mostly used as supplements in other products rather than a whole source

of protein (Ritala et al., 2017). The last general group of SCP candidates are fungi which for SCP purpose will typically contain between 30 – 50 % of protein by dry weight with protein usually high in lysine and threonine but with low methionine content when compared to meat. Additionally, fungi contain a lot of B-complex group vitamins and good fibre content, the in vivo dietary impact of fungal SCP is probably best described among all sources of SCP (expanded on in **1.3.5**) Filamentous fungi can form more diverse morphologies providing additional benefits for texturing (that have been first capitalised by Marlow Foods Quorn Mycoprotein) or even creating "whole cut" fungal meat substitutes like products being developed by Adamo Foods (https://www.adamofoods.com/).

Another application of microbes in alternative protein production is precision fermentation where microbial organisms genetically modified to express molecules derived from animals are used to produce an animal derived product without the use of an animal, e.g. producing cow's milk by expressing proteins from cow in yeast cells (Nyyssölä et al., 2022). Use of these methods of protein cultivation though are reliant on shifts from public perception and legislation perspective towards the use of genetic modification in food (expanded in **1.2.4**).

1.2.4 Opportunities and challenges of single cell proteins

Use of microbes to produce protein either as SCP or in precision fermentation brings a lot of exciting ideas and opportunities to not only find more sustainable ways of producing food, to also upcycle a lot of materials, which currently are simply waste or even contribute to pollution. Some microbial protein sources are less resource intensive than production of animal meat e.g., replacing beef protein with fungal derived mycoprotein is estimated to not only have lower emissions but also able to reach price parity with beef in terms of g per g of high-quality protein (Humpenöder et al., 2022). The versatility of microbes and the variety of sources these can be grown on open a lot of possibilities for integration into a circular economy. The goal of a circular economy is an increase in sustainability by focusing on returning product components and materials back into the production cycle so that they can be used multiple times, with the overarching goal of reducing as much as reasonably possible the use of non-renewable natural resources (Klenk et al., 2020). A simple example of such reduction in wastage is the use of waste from processing date fruits which was shown to be useful as a medium component to culture SCP producing filamentous fungus *Fusarium venenatum* (Hashempour-Baltork et al., 2020). Elsewhere it was demonstrated that municipal wastewater has the potential to be converted biomass by fermentation with a mixed culture of methanotrophic bacteria composed in large of *Methylomonas* and *Methylophilus* species (Zha et al., 2021). More intricate ideas for applying a circular economy approach to SCP production also exist. *Cupriavidus nectator* is a bacterium able to produce polyhydroxyalkanoates (PHA) an alternative to synthetically produced plastics, however separating the bioplastic from surrounding protein rich biomass can be costly (de Mello et al., 2023; Chee et al., 2019). To purify the plastic and utilise the surrounding protein it was proposed that the *C. nectator* biomass can be fed to larvae of mealworm beetle (*Tenebrio molitor)* which are able to digest the protein and pass on the plastic effectively purifying it to be ready for downstream uses, the insects themselves then can then be used as source of food for humans or as feed for livestock (Chee et al., 2019). Another idea is the use of industrial residues to produce biomass for aquaculture feed, this has a double benefit of reducing reliance on fishmeal but also prevents discharges of these residues into water bodies and reduces overall levels of contamination (Pereira et al., 2022; Jones et al., 2020). Important factors to consider in such ideas however are the costs and energy required to run such operation. Depending on the type of waste it might need to be treated to be usable by

microbes, e.g., by liquification. Presence of toxins like heavy metals in the waste substrate can also lead to accumulation of toxins in the resulting biomass (Hashempour-Baltork et al., 2020). Another aspect is logistics of operations – will an enterprise be able to maintain a steady stream of waste of sufficient quality to maintain uninterrupted production whilst balancing the cost of transport of said waste to the production facilities.

Another idea feeding into circular economy and sustainability aspect of SCPs is using mostly renewable sources of energy for production of biomass. An example of this is the use photovoltaics to run electrolysis to produce hydrogen, methanol or formate to be used as electron donors and simultaneously using solar energy to run direct carbon capture (DAC) to provide CO_2 as a carbon source for the fermentation process (Leger et al., 2021). This solution was estimated to give more efficient biomass production per land area vs traditional crops. However, the question here is whether such an enterprise on industrial scale is, at this point in time, actually more sustainable. DAC systems use high amounts of energy to capture relatively small amounts of CO_2 with many critics saying that use of renewable sources of energy to use DAC system would actually harm attempts to reduce CO_2 emissions as the renewable energy sources would be more effectively used to displace the use of fossil fuels directly (Realmonte et al., 2019; Collins, 2021). Overall development of circular economy frameworks is in itself novel with many challenges and pitfalls (Klenk et al., 2020).

Most if not all SCP projects are carried out in closed sterile systems. This makes the emergence of pests that could impair production unlikely compared to industrial crop and animal production. Similarly due to the nature of production in a closed system as well as a large evolutionary distance from humans, emergence of pathogens able to infect humans from SPC production is virtually impossible. However, it is worth noting that depending on the organism various levels of sterility of equipment and media will be required, which is associated with additional costs. Production of SCPs is more conservative in terms of water and land usage compared to traditional livestock, e.g., producing 1 kg of *F. venenatum* mycoprotein (which has a comparable nutritional quality to animal meat) requires 10 times less water and land compared to 1 kg of beef or 3 times less land and 2 times less water compared to producing 1 kg of poultry meat (Finnigan et al., 2017a). Another benefit of working within a closed system is that fermentation is not affected by external factors like unpredictable weather – an increasingly common phenomenon related to climate change (Gornall et al., 2010; Ebi et al., 2021). Working within a closed system also brings opportunities for better waste management and water recycling. Of course, these closed systems do not exist in a vacuum and factors like transportation of components to the production site and costs related to production of growth media e.g. plant derived sugar or CO_2 obtained from direct air capture have to be taken into consideration to properly assess the sustainability aspect (Voutilainen et al., 2021). Additionally, some SCPs like mycoproteins can constitute an overall beneficial addition to human nutrition (expanded in **1.3.5**).

Another aspect adding to the versatility of microbes as food source is that their biology does not pose many ethical issues like wellbeing in case of animals, and that their quick generation times and rapid adaptability can be exploited for attaining specific parameters for the biomass. Because of their fast cell-doubling times, fungi or bacteria can be selected over hundreds or thousands of generations in weeks or months, in marked contrast to most animals and plants. Thus, adaptive evolution is often used for strain improvement, and this avoids use of genetic engineering and its attendant restrictions for food purposes. Knowledge of metabolite biosynthesis pathways in fungi and bacteria provides additional opportunities for

targeted manipulation of AA profiles (Szepe et al., 2021). For example, culturing yeast with 5,5,5-trifluoro-DL-leucine (TFL) — a non-metabolised leucine analogue — can select cells that overproduce leucine due to loss of feedback inhibition of leucine production (focused on in Chapter **5**) (Oba et al., 2006). Other approaches may not require targeted manipulation of specific biosynthesis pathways. Simple changes in sugar source can alter the AA content of *Fusarium* species (Anderson and Solomons, 1984). Continuous adaptive selection was used to find mutants of the bacterium *Corynebacterium glutamicum* (which is used for industrial AA production) that could grow rapidly without the need for addition of expensive growth-boosting additives (Graf et al., 2019). A potential method for manipulation of the AA composition of the microbial biomass may lay in targeting the translation mechanism of the cells Chapter 4 (**4.1**) (Szepe et al., 2021).

Use of genetic modification (GM) is also a natural fit for work with microbes due to their relatively simple genomes and extensive use as model organisms in some species. However, the use of GM in food remains a topic that is not widely accepted by the wider population and regulations hamper application and innovation in the area (Halford, 2019). Lastly customer acceptance of novel foods including SCPs cannot be neglected and appropriate communication of research on safety and promotion of novel foods will be required for mass adoption needed to drive further development (Siddiqui et al., 2022).

Overall SCP and precision fermentation represent very young fields relative to traditional agriculture i.e., livestock and crops, so groundbreaking discoveries might still be on their way and equally some of the currently proposed solutions may show to be unviable as our knowledge and expertise increases.

1.3 Quorn Mycoprotein

Quorn mycoprotein is a food product made from mycelium of the filamentous fungus *Fusarium venenatum* sold by Marlow Foods Ltd. The first product was introduced on the shop shelves in the UK in 1985 but the inception of the company predates this event by over 2 decades (Whittaker et al., 2020). Marlow Foods Ltd. currently sell their products in 20 different countries. In the UK, Quorn mycoprotein was also used to introduce vegan products into ranges of prominent fast food companies in the UK e.g. vegan sausage roll (and vegan bake) at Greggs or vegan chicken at KFC (KFC, 2019; Quorn, 2020). The company has seen strong growth in the past with a recent slowdown due to partial collapse of the plant based protein market (Devlin, 2023). In spite of that, it persists with innovation and exploring new ways of popularising mycoprotein by establishing a sister company Marlow Ingredients that aims at providing raw ingredients and solutions for companies that plan to use mycoprotein in their own products (Marlow Ingredients, 2023). One of the selling points of mycoprotein is its higher sustainability compared to meat. Production of mycoprotein uses less land and water per 1 kg of protein compared to beef and can be considered resulting in net gain to protein production as the carbohydrate fraction of crops is used as the glucose source for growing the fungus. In addition, a recent analysis indicates that mass production of mycoprotein can compete with global beef production in terms of cost, making a good candidate for replacing/limiting expansion of beef production (Risner et al., 2023).

1.3.1 History of Quorn mycoprotein

As stated above, Quorn branded mycoprotein was commercialised sold in 1985 and until recently it was the only SCP product on the market intended for direct human consumption. The concept however, began much earlier, in fact prompted by the previously mentioned (in **1.2.2**) 1960's UN report predicting a global protein shortage. The initial idea came from Lord Rank [of Rank Hovis McDougal (RHM)] who wanted to create an alternative protein source that would be suitable for direct human consumption. RHM was a major producer of cereals so the original idea intended to use starch from the production process as a carbon feedstock for the candidate organism (Whittaker et al., 2020). The type of organisms chosen as candidates were filamentous fungi, due to the ease with which filaments can be extracted from liquid culture and the potential for the mycelial strands to create a better texture which would be more appealing to consumers by mimicking the texture of meat. The search began by spraying starch on a field in hopes of isolating candidate organisms by selecting for effective growth on starch (Angold et al., 1989). The first candidate obtained by this method was *Penicillium notatum* which reportedly had an AA profile that resembled that of casein. After 3 years of trials, the organism unfortunately needed to be abandoned because it was unsuitable to grow in continuous culture as it was rapidly colonising internal structures of the fermenter (Finnigan, 2012). Later, the search for a new candidate was broadened worldwide. Between 1967 and 1972, 3000 isolates were harvested, catalogued and screened for parameters like mycotoxin production, pigmentation, pathogenicity and growth in continuous culture (Whittaker et al., 2020; Moore et al., 2011). Ultimately, *Fusarium graminearum* A3/5 (later reclassified as *F. venenatum* A3/5*)* was selected on the basis of suitability for fermentor growth, low odour and favourable protein production (O'Donnell et al., 1998; Anderson and Solomons, 1984). Ironically, despite sampling from all over the world, the final candidate was found in a heap of compost in Marlow Bottom, 4 miles away from Lord Rank Research Centre in Marlow Buckinghamshire (Whittaker et al., 2020).

Following the isolation of the strain, 10 years were spent on safety testing between 1970-80. Potential for mycotoxin presence was a major food safety concern as *Fusarium* species, in particular *F. graminearum* (which the strain was then classified as) are prolific producers of mycotoxins (expanded on in **1.3.2**)(Ji et al., 2019; Nelson et al., 1993). Feed trails on 11 animals species, including larger mammals such as pigs or cows were performed to assess the safety of *F. venenatum* biomass. The results indicated no negative effects of *F. venenatum* diet (Whittaker et al., 2020). Later the new food named "mycoprotein" was approved by UK Food Standards Agency, because the product contains significant amounts of protein derived from fungi. This was followed by a human trial with 2500 volunteers that identified no immunological reactions or other symptoms related to consumption of mycoprotein. In 1985 the product was approved for sale in UK and given name Quorn™ which originates from a name of a village in Leicestershire. In 1994 further toxicology test were performed and submitted to United States Federal Food and Drug Administration (FDA) (Miller and Dwyer, 2001).

A more detailed history of Quorn mycoprotein, the search and ultimate discovery of the *F. venenatum* A3/5 as a mycoprotein producing organism was researched and compiled by Jack Whittaker (Whittaker et al., 2020; Whittaker, 2022).

1.3.2 Genus *Fusarium*

The genus *Fusarium* is a ubiquitous filamentous fungus taxon, demonstrating worldwide distribution with greater than 300 distinct species discovered to-date, comprising 20 species complexes (**Figure 1.2)** (Summerell, 2019). The members of the *Fusarium* genus were first catalogued based on the shape of their characteristic banana shaped conidia in 1809 with the name "*Fusarium*" being sanctioned in 1821 with new species being discovered and added since then. The taxonomy of these fungi has had a confusing history with many species being erroneously classified as *Fusarium* but with the advancement of molecular techniques e.g. classification by comparing the sequence of RNA polymerase 1 and 2, many organisms within the family group were reclassified with higher confidence (Summerell, 2019). At the same time, novel species are still being discovered e.g. recently 6 new fungi classified as *Fusarium* were found in Australia (Laurence et al., 2016).

Fusarium spp. are an important food crop pathogen e.g. head blight of wheat is currently the most economically important disease of wheat worldwide caused principally by *F. graminearum*. However, recent analysis indicates that other *Fusarium* species may also have a significant contribution to the wheat disease (Alisaac and Mahlein, 2023). Another major pathogen from the *Fusarium* genus is *F. oxysporum* affecting a variety of crops. Perhaps most famously, *F. oxysporum* was responsible for the outbreak of, "*Fusarium* wilt" also known as Panama Disease that completely wiped out Gros Michel banana industry in globally in the mid of the 20th century (Dita et al., 2018). Worryingly new strains of *F. oxysporum* were confirmed to cause outbreaks in the currently used Cavendish banana variety going as far back as 2015 (Pegg et al., 2019). Members of *Fusarium* genus are not exclusively plant pathogens, *F. oxysporum* and *F. solani* in particular can be found as opportunistic pathogens in humans and animals and due to their relative abundance can often be found as opportunistic pathogens in immunocompromised patients with mortality rates reaching nearly 100 % (Nucci and Anaissie, 2007; Batista et al., 2020). The cases of infections in humans and animals have been on the rise in recent years possibly due to the widespread use of antifungals in agriculture (Sáenz et al., 2020). Despite some members of the genus being prolific pathogens, not all *Fusarium* are pathogenic e.g. many non-pathogenic *Fusarium* species were found to be co-occurring alongside pathogenic *Fusarium* species in infections of cacao plant (*Theobroma cacao L.*) (del Castillo et al., 2016). Interestingly, non-pathogenic strains of *F. oxysporum* are known to protect plants from infection from virulent strains and ideas exist to use them as biocontrol agents against the pathogenic *F. oxysporum* and *Pythium aphanidermatum* infections of crops (Sajeena et al., 2020).

Outside of killing crops, *Fusarium* pathogens present other threats, namely they are prolific producers of many types of mycotoxins – a group of secondary metabolites produced by fungi. These metabolites can contaminate crops and cause poisoning in humans and animals when the mycotoxins make their way into the food, this is a major problem as recently it was estimated that up to 25 % of global food production ends up contaminated with mycotoxins (Eskola et al., 2020). For this reason Initial hypothesis for the reason of mycotoxin synthesis postulated that it helps compete with other organisms for nutrient sources like seeds or fruits (Janzen, 1977). To date however, many other functions of mycotoxins were revealed including acting as chemical signals, virulence factors or as a defence mechanism against insect predation (Reverberi et al., 2010). There are three prominent classes of mycotoxins produced by *Fusarium spp*.: trichothecenes, zearalenone (ZEN), and fumonisins (FBs). Among these trichothecenes are the most important class of mycotoxins in *Fusarium*. The compounds in this group can range in size from 200 to 500 Da with over 200 toxins known

(Ji et al., 2019). Trichothecenes have been divided into four subgroups (A-D) that are characterised by the substitutions mode of the core structure of 12,13-epoxytrichothec-9-ene (ETP) (McCormick et al., 2011). Of these toxins, type A and B are most common as food contaminants due to their higher toxicity compared to types C and D.

Figure 1.2 Combined RNA polymerase 1 and 2 (RPB1/2) data set indicating the phylogenetic relationship between the major species complexes in the Fusarium genus based on the phylogeny published in (Laurence et al., 2016). Abbreviations: CI, confidence interval; PIC, preinitiation complex; RI, repeat interval. Figure taken from (Summerell, 2019)

1.3.3 *F. venenatum* A3/5 as Quorn mycoprotein producer

As mentioned above **(1.3.1**) *F. venenatum* A3/5 was accidentally discovered on the heap of compost and initially classified as *Fusarium graminearum.* In 1998, the strain was reidentified as *F. venenatum* based on morphological, molecular and mycotoxin analysis (O'Donnell et al., 1998). This finding was later corroborated in another independent study (Yoder and Christianson, 1998). This finding was a promising development for Marlow Foods due to the lower potential for virulence compared in *F. venenatum* compared to *F. graminearum*. Indeed, in 2018, genome analysis of *F. venenatum* identified that although some genes encoding production of mycotoxins are present in the genome, the potential for pathogenicity and mycotoxin production is overall significantly lower compared to *F. graminearum* (King et al., 2018). Additionally, experiments assessing the extent of *F. venenatum* virulence have shown that the fungus was not capable of infecting wheat and caused only a mild infection on a tomato plant after long period of incubation (King et al., 2018).

However, *F. venenatum* is still capable of producing mycotoxins which was demonstrated under laboratory conditions (Laraba et al., 2021) . Factors like nitrogen starvation, deregulation of carbohydrate metabolism or growth in presence of sucrose all were identified as triggers of mycotoxin production in *F. venenatum A3/5* (Altomare et al., 1995; O'Donnell et al., 1998; Whittaker, 2022; Miller and MacKenzie, 2000). When *F. venenatum* is cultured in appropriate conditions (expanded in **1.3.4**) mycotoxin production is not triggered (Miller and Dwyer, 2001). During mycoprotein production routine checks for presence of mycotoxins are in place, and to date mycotoxin presence has never been detected (Whittaker et al., 2020).

As mentioned earlier, most microbes contain relatively high levels of nucleic acids that can cause disease in humans if consumed in excess (**1.2.4**). In *F. venenatum* fermentation, the nucleic acid levels are between 8-9 % of the biomass. Consequently, during production, the nucleic acid levels need to be lowered to ~1 % (expanded in **1.3.4** so that consumption of higher amounts of mycoprotein does not exceed 2 g of nucleic acid intake per day). The benefits of *F. venenatum* mycoprotein include relatively high protein content and quality compared to some meats and overall good nutritional profile (discussed more in depth in **1.3.5**).

F. venenatum A3/5 strain used in mycoprotein production is haploid and to date is only known to reproduce asexually. However, there is an interest in finding a sexual cycle as this would allow for selective breeding regimes to e.g., improve the growth rate in different media compositions or slow down the emergence of undesirable morphological variants (discussed in **Chapter 3**). Sexual breeding of fungal strains can be an efficient method of selection of desirable traits without the need for genetic engineering – which is currently advantageous in production of food (Ashton and Dyer, 2016).This approach has been successfully implemented in *Penicillium roquerforti* where discovery of a sexual cycle allowed for selection of a variety of cheese producing strains with custom attributes such as flavour or colour (Dyer and Kück, 2017). The reasoning for the existence of a sexual cycle in *F. venenatum* is that closely related species like *F. graminearum* and *F. sambucinum* have identified sexual cycles (Trail, 2009; Crous et al., 2021). Additionally mating type genes that are a necessary pre-requisite for sexual reproduction in fungi have been recently discovered in *F. venenatum* (Dyer et al., 2016; Whittaker et al., 2020). The efforts to identify a sexual

cycle in *F. venenatum* are currently ongoing in other *F. venenatum* related projects (Dyer, P., Pate, A., pers. comms.).

1.3.4 Industrial scale production of *F. venenatum* mycoprotein

After *F. venenatum* was selected as the source of the eventual food product the suitable method of production needed to be selected. Batch, fed-batch and continuous fermentation processes were tested for production of mycoprotein selecting continuous fermentation as most suitable. This was because a continuous fermentation method allowed to run the fermentation for longer periods of time whilst continuously extracting biomass as well as allowed for better control of the filamentous fungi culture compared to batch techniques (Whittaker et al., 2020).

The fermentors used by Quorn Foods utilise airlift technology as opposed to more common stirred reactors. This is beneficial for growth of mycelial cultures as the airlift design prevents hyphae from shearing, allowing for longer strands to develop – a desirable trait for generating intended meat like texture of the products. The added benefit is lower energy consumption compared to stirred reactors which adds to sustainability of Quorn. The oxygen saturation and mixing in airlift fermenters is achieved via influx of sterile air into the culture medium which then mixes the culture. This contrasts with mechanical impellers used in stirred fermenters. The oxygen transfer occurs primarily at the base of the riser where the air is pumped into the vessel taking advantage of high hydrostatic pressure (**Figure 1.3)**. The turbulence generated via the pumped air, together with the hydrostatic pressure result in good transfer of oxygen from gaseous to aqueous phase. As a result, the riser is filled with a mix of air and mycelial culture in which air bubbles make up to 50 % of the volume. Past the riser the air levels decrease to about 10 % of the volume present near the riser, the drop in pressure results in nitrogen, leftover oxygen, and CO_2 to be released from the culture via the gas disengager. Then the culture enters the downcomer depleted of oxygen, there fresh oxygen is being pumped in to prevent cell death. Once the culture passes the downcomer it is directed back to the riser where it is aerated again closing the cycle. During the fermentation cycle the culture is kept at 30 ^{o}C and the pH is kept at 6.0 via addition of ammonia (that also constitutes nitrogen source for the culture). The culture is operated as a glucostat – a condition where glucose is always in excess allowing the fungus to constantly maintain growth speed close to its maximum specific growth speed (Anderson et al., 1975). This maximum specific growth rate is usually achieved 4 days after inoculation at which point biomass can start to be continuously removed from the fermenter and being replaced with fresh growth medium allowing for continuous biomass production.

After extraction from the main loop of the fermenter, the mycelium is heated at 68 ^{o}C (**Figure 1.3**) to decrease the levels of nucleic acids to a level that is safe for human consumption, as discussed earlier in this chapter (**1.2.4**). The minimal length of the extracted hyphae must be between 400-700 µm otherwise the final product would exhibit a crumbly texture (Finnigan et al., 2017b; Finnigan, 2011). Egg albumin or other non-animal binding agents like agar or locust bean gum (*Ceratonia siliqua*) are used to a mimic a cross linking structure prominent in muscle fibres but absent in fungal hyphae. The final texture is produced by freeze texturization of the fibre-gel complex, where the controlled growth of ice crystals pushes the fungal mycelium together resulting in a fibrous bundle that resembles the texture of muscle fibres. This process is described in more depth in (Finnigan et al., 2017b).

Quorn currently operates three fermentors which are the biggest units of this type worldwide. A single 155 m^3 fermentor is capable of producing 6500 tonnes of mycoprotein per annum. Once the extraction of biomass starts ~4 day post inoculation, the production has a theoretical potential to go on indefinitely as long as fresh media are being provided (Moore et al., 2011). Unfortunately, in reality, the fermentation is stopped around every 1000 h upon which the fermenter needs to be emptied, cleaned and sterilised causing drop in productivity. This is because growth in a glucostat results in selection of undesirable morphological variants, in the case of *F. venenatum* biomass production in airlift fermenters over time increasing the presence of highly branched, short hyphae C-variant (covered more in depth in **Chapter 3** of this thesis) that affect the texture of the final product by increasing crumbliness (Finnigan, 2011; Wiebe et al., 1994a).

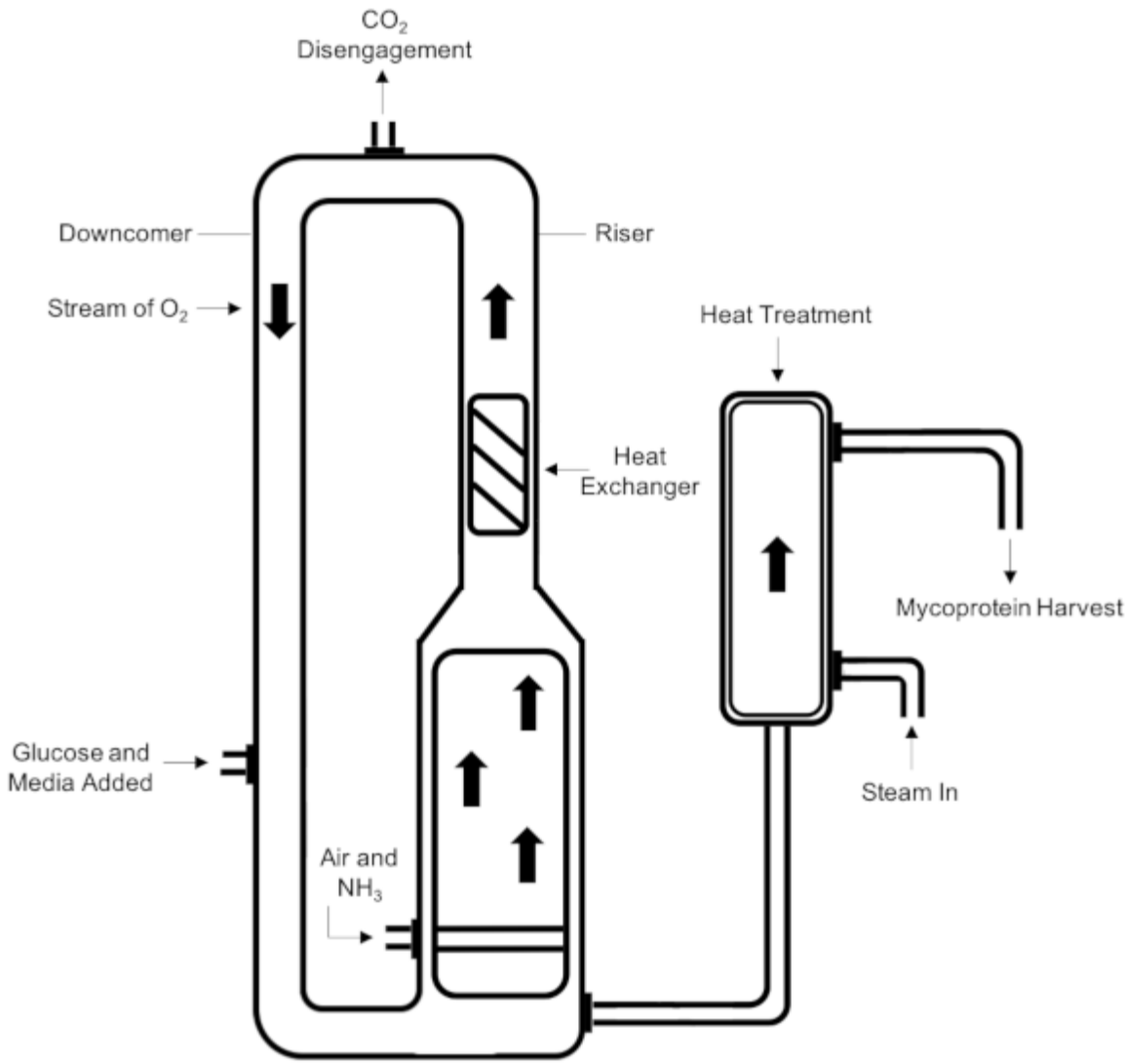

Figure 1.3 Schematic of the airlift fermenter used by Quorn Foods. Taken from (Whittaker, 2022)

1.3.5 Mycoprotein and nutrition

From the moment of its inception, the selling point of mycoprotein was intended to be its "nutritional competitiveness" with meat. When the protein quality was assessed, mycoprotein has gained a near perfect PDCAAS (covered in **1.1.2**) score of 0.99 (out of maximum 1) making mycoprotein a better source of protein than some types of meat e.g., beef scores 0.92 (Cummings and Edwards, 2010). The mycoprotein also contains a good variety of nutrients. Per 100 g of dry weight, it was shown to contain 45 g protein, 25 g fibre, 13 g fat, 10 g of carbohydrate, and a range of micronutrients and vitamins (Finnigan et al., 2017b). Allergic reactions to mycoprotein are known but these are estimated to have lower incidence in population than allergies to soy or eggs (Hunter, 2014).

More importantly the effects of mycoprotein on the human body were and continue to be extensively researched in humans *in vivo*. Previously, mycoprotein consumption was correlated with lowering the blood levels of cholesterol (Finnigan et al., 2017b; Turnbull et al., 1992).This was confirmed with more recent studies and additionally it has been have shown that replacing red meat and processed meat with mycoprotein can improve cardiovascular disease risk markers (Farsi et al., 2023a; Coelho et al., 2021). This, in addition to the sustainability argument gives consumers another strong incentive to replace some or all of their beef/processed meat intake with mycoprotein. Another important aspect of mycoprotein vs meat is its ability to facilitate muscle synthesis. A randomised control trail in older adults showed that a vegan mycoprotein based high protein diet stimulated muscle synthesis in the participants to the same extent as equivalent omnivorous diet (Monteyne et al., 2021). Similarly, another trial revealed that a mycoprotein diet stimulated muscle synthesis in young exercising men to the same extent as a high meat diet (West et al., 2023). Despite this, meat remains a much more protein dense food: 100 g of wet weight mycoprotein i.e. how it is found in food products, contains only 11.5 g of protein vs 30.2, for roasted chicken breast (Finnigan et al., 2017b; Marangoni et al., 2015). The upside of this is that it can prevent overeating whilst giving a feeling of satiety to the consumer (Burley et al., 1993). The downside is that it may hamper potential use as a high protein source for e.g., elderly who typically have reduced appetite and may struggle to reach their recommended daily protein intake even with more protein dense food sources like meat (Banovic et al., 2018). One way to address this problem could be to mix smaller amounts of mycoprotein with a dose of branch chained AAs (BCAAs), AAs known to be involved in muscle synthesis. High intake mycoprotein was shown to increase the muscle synthesis to a higher degree compared to a lower dose supplemented with a mix of BCAAs (Monteyne et al., 2020). This indicates that supplementing mycoprotein with BCAAs as is, is unlikely to give better results in stimulating muscle synthesis in elderly compared to meat. The comparison of mycoprotein with meat diet also was shown to decrease the genotoxicity of faecal and amount of excreted nitroso compounds (that are carcinogens) compared to red meat diet showing potential for decreasing the risk of colorectal cancer (Farsi et al., 2023b). Additionally, the mycoprotein was also shown to increase the amounts of beneficial microbes (*Lactobacillus, Roseburia* and *Akkermansia*) in the microbiome compared to meat diet.

Overall, in the last 30 years a lot of research on the effects of mycoprotein has been done not only proving it a valuable nutrient but also potentially cementing it as a future benchmark for comparison for new alternative proteins entering the market.

1.4 Thesis aims

The need for alternative protein and increase in investment in SCP sector means a lot of work is required for the sector to "catch up" with the traditional livestock and plant agriculture sector. In this thesis, this is attempted by exploring the possibility of amino acid (AA) profile manipulation in *F. venenatum* A3/5, a well-established producer of mycoprotein sold as Quorn. The far reaching goal of this is to inform of possible ways of tailoring the AA profile. To achieve this the following goals were set out:

1.To set up a laboratory method for the analysis of the AA profile of *F. venenatum* that is representative of *F. venenatum* from continuous fermentation in airlift fermenters by comparison of the AA profiles of from the industrial process with samples produced on bench scale.

2. To assess the extent to which the AA profile of *F. venenatum* is reliant on the specific medium used during the current industrial process by monitoring changes in the AA profile in response to changes in the culture medium.

3. To explore the possibilities for altering the AA profile by targeting protein translation via chemical treatment with substances known to increase the translational error rate, adaptive evolution regimes promoting incorporation of branch chained AAs into the AA profile, and selection of *F. venenatum* isolates with deregulated leucine synthesis.

4. To test any promising isolates to assess factors relevant to potential use in large scale fermentation such as growth rate or changes to mycotoxin production.

2 Chapter 2 Investigation of properties of *F. venenatum* AA profile and its response to different growth conditions

2.1 Introduction

The amino acid (AA) profile of organisms can be, to a varying extent, influenced by environmental conditions and genetics (Szepe et al., 2021). In livestock animals this variability in the protein content can be seen in different sexes or breeds of an animal (Hollo et al., 2001), diet and habitat (Mohanty et al., 2014), or parts of the animal carcass (Hamm, 1981). Diet can also have a modest effect on other animal products, e.g., the AA profile of milk from dairy cows can change in different dietary regimes (Jenkins and McGuire, 2006) but other research suggests that these regimes only have a limited effect on the expression levels of different milk proteins and consequently the overall potential to change the AA profile (Haug et al., 2007). Pathological conditions such as wooden breast myopathy affecting industrial poultry was shown to result in a decrease in the levels of specific AAs resulting in a negative change to the AA profile (Zotte et al., 2020). Overall, besides the effects of disease, protein quality in each type of animal is not largely sensitive to changes in growth environment and so can provide reliable protein quality in diverse conditions.

The plant AA profile on the other hand is more malleable both to targeted manipulation as well as general growth conditions. Factors like quality of the soil, type of fertiliser, elevated levels of CO_2 or presence of tropospheric ozone can change the amounts of AAs in plants. The elevated levels of CO_2 and presence of the ground level ozone both decrease the amount of AAs in the crops and therefore decrease their nutritional value (Taub et al., 2008; Broberg et al., 2017). Different fertilisers can also result in plants with varying levels of AAs depending on the rate at which the nitrogen from the fertiliser is released throughout the plants development (Carillo et al., 2012; Armesto et al., 2020). Historically, humans have capitalised on the malleability of the plant proteome through advances in selective breeding techniques, e.g., by producing “quality protein maize” (Prasanna et al., 2001). Adoption of genetic engineering methods allowing for expression of specific proteins can affect the overall AA profile of plants without detrimental effects on growth. For example, high lysine maize (LY038) has reported increases in both protein- and free-lysine from 2.55 and 0.09 mg/g to 3.70 and 0.96 mg/g respectively (Lucas et al., 2007). This was achieved by embryo-specific expression of feedback-insensitive dihydrodipicolinate synthase from bacteria – the native enzyme in plants is sensitive to inhibition by pathway end-product valine, but its bacterial counterpart is less sensitive to inhibition by valine resulting in overall higher levels of valine production (Dizigan et al., 2007; Lucas et al., 2007; Grant Pearce et al., 2017). In conclusion plant AA profiles are much more tolerant of changes than those of animals (Galili and Amir, 2013; Szepe et al., 2021) which bring an opportunity for improvement of protein quality, but it also means that certain external conditions, such as increased CO_2 levels, can lead to lowering of agricultural protein output (Jayawardena et al., 2021).
Because many microorganisms, including fungi, possess a good ability to adapt to varied conditions, e.g., by modifying their protein expression according to environmental demands, their proteomes can be reasonably plastic. A further advantage of microbial protein as a food source is the fact that industrial waste/side streams can be used as potential sources of growth medium (Spalvins et al., 2018). *Fusarium venenatum*, the filamentous fungus used for mycoprotein fermentation at Quorn Foods, is grown in airlift fermenters in continuous culture where glucose levels are kept constant and the organism grows at constant maximum specific growth rate (Simpson et al., 1998). Since its original use for this purpose, the industrial

growth regime of *F. venenatum* (strain A3/5) has barely changed. Therefore, not much is known about the influence that changing the composition of the medium might have on, for example, protein quality. *F. venenatum* A3/5 has the capacity to produce mycotoxin. However, mycotoxin was never detected throughout production history in the industrial setting (R Johnson, pers. comm.), giving a disincentive to try changing the growth method. In an experimental setting, changing the carbon source from glucose to ribose in batch cultures was shown to reduce the total AA content of *F. venenatum* (494 mg/g vs 394 mg/g respectively) (Anderson and Solomons, 1984). Another study aiming to identify cheaper alternatives to glucose found that *F. venenatum* growth speed and biomass accumulation in sucrose was comparable to that of glucose up to the 10 l fermenter scale (Whittaker, 2022). However, because the structure of fructose – a subunit of sucrose - is similar to that of ribose, there is a risk of an undesirable change to the AA profile of *F. venenatum* cultivated with sucrose. One of the benefits and selling points of Quorn mycoprotein as a meat substitute is its protein quality, mycoprotein has a protein digestibility corrected amino acid score (PDCAAS) of 0.99, which is nutritionally comparable to chicken meat and more nutritious in terms of AA content than that of beef (Finnigan et al., 2019). Therefore, any consideration of change to the mycoprotein production process, like switching of carbon source or using an industrial waste stream as medium, requires that the nutritional quality of the mycoprotein is not negatively affected.

2.2 Chapter aims

As mentioned above, the industrial growth regime for *F. venenatum* mycoprotein has barely changed since the 1960s. This chapter focuses on:

a) Establishing a laboratory method for cultivation of *F. venenatum* biomass that gives a total-protein and AA profile representative of the fungus in the industrial growth regime.
b) Investigating the extent to which altered growth conditions alter the AA profile of *F. venenatum*.

2.3 Materials and Methods

2.3.1 Chemicals

All chemicals used in this project were obtained from Sigma, UK unless stated otherwise.

2.3.2 Fungal strains and growth conditions

The filamentous fungus *F. venenatum* A3/5 was provided by Marlow Foods Ltd. *F. venenatum* was maintained and grown on potato dextrose agar (PDA) (Oxoid, UK) at room temperature (21°C). Conidia (asexual spores) were harvested in 0.1% [v/v] Tween 80 after 5-10 days on PDA plates and filtered through miracloth. Spore concentrations were determined by hemocytometry.

2.3.3 Growth media and culture in shake flasks

Cultures were grown in 250 ml or 500 ml Kimble^{TM} baffled flasks (Dixon, Kent, UK) at 28 ^{o}C with shaking at 150 rev/min. The starting spore concentration used was 10,000 spores/ml.

Starter cultures were grown for 24 h after which 1% v/v of starter culture was used to inoculate experimental flasks.

2.3.4 Microplate reader culture conditions

In 96 a well microplate (Greiner Bio-One, UK) 300 µl of medium containing 10 000 spores/ml were aliquoted in each well. The plate was taped with masking tape over the edges to minimise evaporation. The microplates were statically incubated in EPOCH 2 plate reader (Agilent, USA) at 28 ^{o}C with readings taken every 1 h. The software used was Gen5 v3.08. Exported data was analysed using Microsoft Excel, background absorbance was corrected for by subtracting the OD values of wells containing uninoculated medium.

2.3.5 Calculating the doubling times

Doubling times of the culture were determined for each growth curve by selecting two time points on the exponential phase of growth on the growth curve and calculated using **Equation 2.1** (Vidal et al., 2006), where "Duration" is the amount of time between the two selected points, final cell concentration and initial cell concentrations are the OD values of the later and earlier selected timepoints respectively.

Equation 2.1 Equation used to calculate doubling time of a cell culture.

$$Doubling\ time = \frac{Duration\ \times \ln(2)}{\ln\left(\frac{Final\ cell\ concentration}{Initial\ cell\ concentraion}\right)}$$

2.3.6 Media

Cultures were grown in 250 ml or 500 ml Kimble^{TM} baffled flasks (Dixon, Kent, UK) at 28°C with shaking at 150 rev/min. The starting spore concentration used was 10,000 spores/ml. Starter cultures were grown for 24 h after which 1% v/v of starter culture was used to inoculate experimental flasks. The broth media used for shake flask culture were: RHM (KH_2PO_4 20 g, NH_4Cl 4.4 g, K_2SO_4 0.3 g, $MgSO_4 \cdot 7H_2O$ 0.25 g, biotin 0.03 µg, 5 ml of RHM trace element solution [$FeSO_4 \cdot 7H_2O$ 2.8 g, $ZnCl_2$ 1 g, $MnCl_2 \cdot 7H_2O$ 1 g, $CuCl_2$ 0.2 g, $CoCl_2 \cdot 6H_2O$ 0.37 g, Na_2MoO_4 0.2 g, $CaCl_2 \cdot 2H_2O$, citric acid 1.5 g per 1L] per 1L; *Aspergillus complete medium* (ACM) (10 g glucose, 1 g yeast extract, 2 g bacteriological peptone, 1 g casamino acids, 0.075 g adenine, 10 ml *Aspergillus* vitamin solution per 1L), vitamin solution was prepared as described in Paoletti et al. (2005) , *Aspergillus* minimal medium (AMM) (20 g glucose, $ZnSO_4 \cdot 7\ H_2O$ 1 crystal, $FeSO_4 \cdot 7H_2O$ 1 crystal, bacteriological peptone 2 g, KH_2PO_4 1.52 g, $MgSO_4 \cdot 7\ H_2O$ 0.52 g, KCl 0.52 g, $NaNO_3$ 6 g per 1L)

2.3.7 Biomass measurements and preparation.

Flask contents were vacuum filtered through pre-weighed Whatman qualitative 110 mm filter papers (No .1001-110) (Merck, Darmstadt, Germany). The flasks were rinsed with sterile deionised water (SDW) until all visible biomass was washed out. The biomass was then rinsed with SDW to remove traces of growth medium. The paper filter with biomass was placed in a falcon tube at – 80°C and freeze dried using Thermo Savant Modulyod benchtop freeze dryer (Thermo Fisher, UK) with a RV8 vacuum pump (Fisher Scientific, UK). The final mass of the sample was measured by subtracting the original weight of the paper from

the total and correcting for the loss of mass produced by drying a clean paper (with no biomass). Dried biomass was then separated from the filter paper and ground in liquid nitrogen using a mortar and pestle.

2.3.8 Protein hydrolysis and sample preparation for LCMSMS analysis.

Freeze dried and powdered biomass samples containing ~5 mg nitrogen were suspended in 2.5 ml oxidation solution (1 part 30% hydrogen peroxide, 9 parts formic acid/phenol solution v/v); the formic acid/phenol solution was prepared by mixing 735 ml 98-100% LCMSMS-grade formic acid, 111 ml dH_2O, 4.73 g phenol. Samples were left in the fridge for 16-18 hours after which the oxidation reagent was neutralised by adding 0.42 g of sodium metabisulphite. Then 2.5 ml of 12M HCl and 0.5 ml of hydrolysis reagent (49.2 ml 12 M HCL, 1 g phenol, made up to 100 ml with dH_2O) were added. Tubes were sealed and placed in a 110°C pre-heated oven (GP/20/SS/F/250/DIG; LABQUIP LTD, UK) for 24 h. After hydrolysis the pH of the samples was adjusted to 2.8 pH with 4 M ammonium formate solution (252.4 g ammonium formate dissolved to 1 l volume with dH_2O) and made up to 50 ml with 20 mM ammonium formate buffer pH 2.8. The samples were centrifuged for 10 min at 1509x g. The supernatant was passed through a 22 µm microfilter (Sartorius, Goettingen, Germany) and diluted as described in section **2.3.9**.

2.3.9 Preparation of LCMSMS standards and sample dilution

Amino acid LCMSMS standard and internal standard were prepared by using a combination of a pre-made AA LCMSMS grade standard mix and stocks of individual AAs, the chemicals used in preparation of the standards were: amino acid standard, 2.5 µmol/ml (Cat. No. AA-S-18) (containing 2.5 µmol/ml of L-alanine; ammonium chloride; L-arginine; L-aspartic acid; L-glutamic acid; glycine; L-histidine; L-isoleucine; L-leucine; L-lysine, L-methionine; L-phenylalanine; L-proline; L-serine; L-threonine; L-tyrosine; L-valine, and 1.25 µmol/ml cystine), cysteic acid (Cat. No. C7630), methionine sulfone (Cat. No. M0751), Cell free amino acid mixture (CFSIL) – 13C,15N (Cat No. 767964).

Concentrated standard solution of cysteic acid and methionine sulfone (1.25 µmol/ml) was prepared by dissolving 0.234 g of cysteic acid and 0.2265 g of methionine sulfone in 200 ml pH 2.75 20 mM ammonium formate buffer and made up to 1 l with pH 2.75 20 mM ammonium formate buffer.

Internal standard (ISTD) preparation

CFSIL 1/2000 dilution was prepared by diluting 0.5 ml of CFSIL in 20mM ammonium formate pH 2.75 buffer to 1 l volume in volumetric flask.

LCMSMS Standard preparation

AA standard stock was prepared by mixing previously prepared solutions as outlined in **Table 2.1.** The concentrations of standards used for LCMSMS calibration are as listed in **Table 2.2.** Preparation of internal standards is described in above**.**

Table 2.1 Preparation of standard stock

	Stock concentration (mM)	Volume	Concentration (µM)		Final concentration
AA standard mix (18 AAs)	2.5 mM (except cystine - 1.25 mM)	64 µl	400 µM (except cystine - 200 µM)	200 µl of stock is then mixed with 200 µl of ISTD (1/2000 CFSIL dilution)	200/100 µM
Cysteic acid + Methionine Sulfone	1.25 mM	64 µl	200 µM		100 µM
Tryptophan	10 mM	16 µl	400 µM		200 µM
Ammonium formate 20 mM pH 2.75		272 µl			CFSIL dilution 1/4000

Table 2.2 Concentrations of AA standards used for calibration of LCMSMS for quantification of AAs in samples.

Standard number	Concentration (µM)
AA14	200/100
AA13	100
AA12	50
AA11	25
AA10	12.5
AA9	6.25
AA8	3.125
AA7	1.563
AA6	0.781
AA5	0.391
AA4	0.195
AA3	0.098
AA2	0.049
AA1	0.024
AA0	0

2.3.10UHPLC-MS/MS Instrumentation

UHPLC

All calibration standards and hydrolysed samples prepared as described above (**2.3.8**, **2.3.9**) were separated and analysed using a Thermo-Fisher Vanquish (uHPLC) and Altis Triple Quadrupole Mass spectrometer (MS/MS) with heated electrospray ionization (H-ESI) probe. Positive ion mode was used for all amino acids. A 1 µl aliquot was injected on a Thermo Scientific™ Acclaim™ Trinity P1 mixed mode column (150 mm x2.1 mm, 3 µM) at 30 °C. Mobile phases consisted of ammonium formate in water at pH 2.75 for phase A and a mixture of ammonium formate in water and acetonitrile (80/20 v/v) for phase B. Chromatographic separation was achieved by gradient elution under the conditions described in **Table 2.3**

Table 2.3 UHPLC gradient used in this work.

Time (min)	Flow Rate (ml/min)	%A	%B
0	0.3	100	0
5	0.3	100	0
7	0.3	0	100
14	0.3	0	100
14.5	0.35	100	0
16.5	0.35	100	0
17	0.3	100	0
18	0.3	100	0

Mass Spectrometry

A Thermo Scientific™ TSQ Altis™ triple quadrupole mass spectrometer equipped with a Thermo Scientific™ Opta-Max NG ion source with a heated electrospray ionization probe has caused. Sheath gas was set at 45 arbitrary units, auxiliary gas at 15 arbitrary units, and spray voltage at 3500 V for positive ionization and at 2700 V for negative ionization. The vaporizer temperature was set to 370 °C and transfer tube temperature to 270 °C, while source fragmentation was applied at 15 V. Data was acquired in Selected Reaction Monitoring (SRM) mode using a resolution of 0.7 full width at half maximum (FWHM) for both quadrupoles. All compounds were detected at positive mode.

2.3.11 LCMSMS chromatograph analysis.

Trace Finder 4.1 software was used to quantify the detected amounts of AAs. Peaks were individually inspected and manually curated where automatic detection failed.

2.3.12 HPLC conditions

Preparation of reagents

HPLC grade water was produced with a Purelab Flex (ELGA, High Wycombe, UK) water purifier. O-phthalaldehyde (OPA) reagent was prepared fresh each time by mixing under nitrogen 20 mg phthaldialdehyde (Alfa Aesar, Heysham, UK) and 20 mg of 3–mercaptoprionic acid (Alfa Aesar) made up to 1 ml with 0.4 M boric acid (Sigma, UK) and adjusted to pH 10.2 with NaOH, then passed through a 22 µm filter into an HPLC vial. Borate buffer was prepared by adjusting 0.4 M boric acid to pH 10.2 with NaOH. For phase A, 20 mM phosphate buffer was prepared by dissolving 2.76 g $NaH_2PO_4 \cdot H_2O$ (Sigma, UK) in 800 ml dH_2O, adjusting to pH 7.80 with NaOH and making up to 1000 ml with dH_2O. The solution was then passed through a 22 µm filter. Mobile phase B comprised acetonitrile, methanol, water at ratios of 45/45/10 (v/v/v). Amino acid standards were prepared by using equal molar amounts of 18 analytical grade AAs (L-Asp, L-Glu, L-Asn, L-Ser, L-Gln, L-His, Gly, L-Thr, L-Arg, L-Ala, L-Tyr, L-Val, L-Met, L-Trp, L-Phe, L-Ile, L-Leu, L-Lys) and dissolving them in 0.1M HCl. The solution was passed through 22 µm microfilter and was diluted with 0.1M HCl to 1000, 600, 400, 100, 10 µM per amino acid.

HPLC analysis

Analysis was performed using a Dionex Ultimate 3000 HPLC (Thermo Scientific, UK) equipped with a solvent rack with degasser (SRD-3400), pump (HPG-3200 SD), autosampler (WPS-3000TSL), column compartment (TCC-3000) and diode array detector (DAD-3000). The OPA method used was as described by Agilent and validated by Bartolomeo and Maisano (2006). Briefly, borate buffer, dH_2O vial without cap for washing the needle, OPA reagent, water vials were in positions A1-A4 on the sample rack respectively. The autosampler was programmed as described by Bartolomeo and Maisano (2006).
The column used was a Zorbax Eclipse AAA 4.6 x 150 mm, 5µm (Agilent, Santa Clara, USA). The analysis was performed at 40ºC with detection at 338 nm. The separation was obtained at a flow rate of 2 ml min^{-1} with gradient programme. The % of liquid phase A or B being pushed through the system were: 1.9 min at 0% B, then a 16.3min step that gradually raised phase B to 53%. Then washing at 100% B and equilibration at 0% B was performed in a total analysis time of 26 min. Peaks were analysed using Chromeleon 7.2 SR4 software and amino acid amounts quantified using the calibration function built into the software, by comparison with peaks for the amino acid standards.

2.3.13 Free amino acid extraction for HPLC analysis

Freeze dried powdered samples were resuspended in 1ml of 0.1M HCl and boiled at 100ºC for 15 min. Afterwards, samples were centrifuged for 30min at 21130x g. The supernatant was passed through a 22 µm filter into a HPLC vial (Thermo Scientific, UK). Samples were stored frozen at -20ºC until analysis.

2.3.14 Protein extraction and Bradford assay analysis.

Total protein was extracted from freeze-dried powdered mycelium with a modified version of a previous method (Mæhre et al., 2016) . Samples were suspended in 1ml of extraction buffer (0.1M NaOH, 3.5% NaCl dissolved in dH_2O) and vortexed until homogenous. Tubes were incubated in dry heat thermostat (Grant instruments, Shepreth, UK) at 60ºC for 3h. The samples were then centrifuged at 21130x g for 30 min at 4ºC. The supernatant was collected and diluted with dH_2O (usually 1/800). 800 µl of diluted supernatant followed by 200ul of Bradford reagent (Bio-Rad, UK) was pipetted into a 1.5 ml cuvette (Thermo Scientific, Massachusetts, USA) and left to incubate for at least 5 minutes at room temperature. Absorbance was measured by spectrophotometry (DS-11FX+, DeNovix, Wilmington, USA) at 595 nm. A calibration curve for the protein calculation was prepared fresh before each experiment using bovine serum albumin (BSA) (Sigma, UK) as protein standard in concentrations of 1.2, 2.4 ,4.8 and 10 µg/ml of BSA.

2.3.15 Statistical analysis

To compare the absolute and relative AA profiles within each experiment a Principal Components Analysis (PCA) was performed using R studios software on the combined hydrolysate AA dataset. The data were standardised by normalisation, a covariance matrix was produced and examined (**Figure 2.1**, **A**) and PCA was performed on the data. The PCA produced 17 principal components (PCs) the first three of which explained 81.28 % of variability in the dataset (**Figure 2.1**, **B**). Eigen values of the PCs were examined with only PC1-3 having eigenvalues > 1 (9.37, 2.87, 1.51) respectively, confirming that these three PCs should be used for further analysis. The loading factors of the first three PCs (**Table 2.4**)

were examined, and it was determined that PC1 measures the total AA production and indicates changes to the overall AA profile between treatments. PCA2 contrasts Ala, Asp, Gly and Pro with His and Val, with higher values indicative of a treatment that produces a profile enriched in the former group of AAs and lower/negative values for a profile enriched in the latter. PC3 contrasts Cys with Leu, Ile, Gly and Asp with higher values indicating a higher Cys enrichment and lower enrichment in the latter group. For analysis of the individual experiments PC1-3 values were extracted for each treatment group and compared by One-Way ANOVA and post hoc tests (Tukey's multiple comparisons – unless stated otherwise).

For free AA experiments where the total amount of data was lower and number of the variables too high to warrant a PCA, the means of individual AAs were compared between treatments by multiple T-tests/One-Way ANOVAs.

The statistical analysis was conducted using R studio software (version 2024.04.0+735).

Table 2.4 Factor loadings of principle components 1-3.

	PC1	PC2	PC3
Ala	**0.036**	**0.443**	**0.018**
Arg	**0.279**	**-0.086**	**0.127**
Asp	**0.126**	**0.377**	**-0.466**
Cys	**0.025**	**0.183**	**0.651**
Glu	**0.248**	**0.237**	**0.076**
Gly	**0.129**	**0.344**	**-0.437**
His	**0.255**	**-0.305**	**-0.119**
Ile	**0.276**	**-0.181**	**-0.098**
Leu	**0.303**	**0.012**	**-0.091**
Lys	**0.309**	**-0.047**	**-0.017**
Met	**0.257**	**0.145**	**0.208**
Phe	**0.312**	**-0.130**	**0.022**
Pro	**0.234**	**0.307**	**0.211**
Ser	**0.275**	**0.085**	**0.042**
Thr	**0.266**	**0.143**	**0.138**
Tyr	**0.282**	**-0.216**	**-0.063**
Val	**0.231**	**-0.335**	**-0.026**

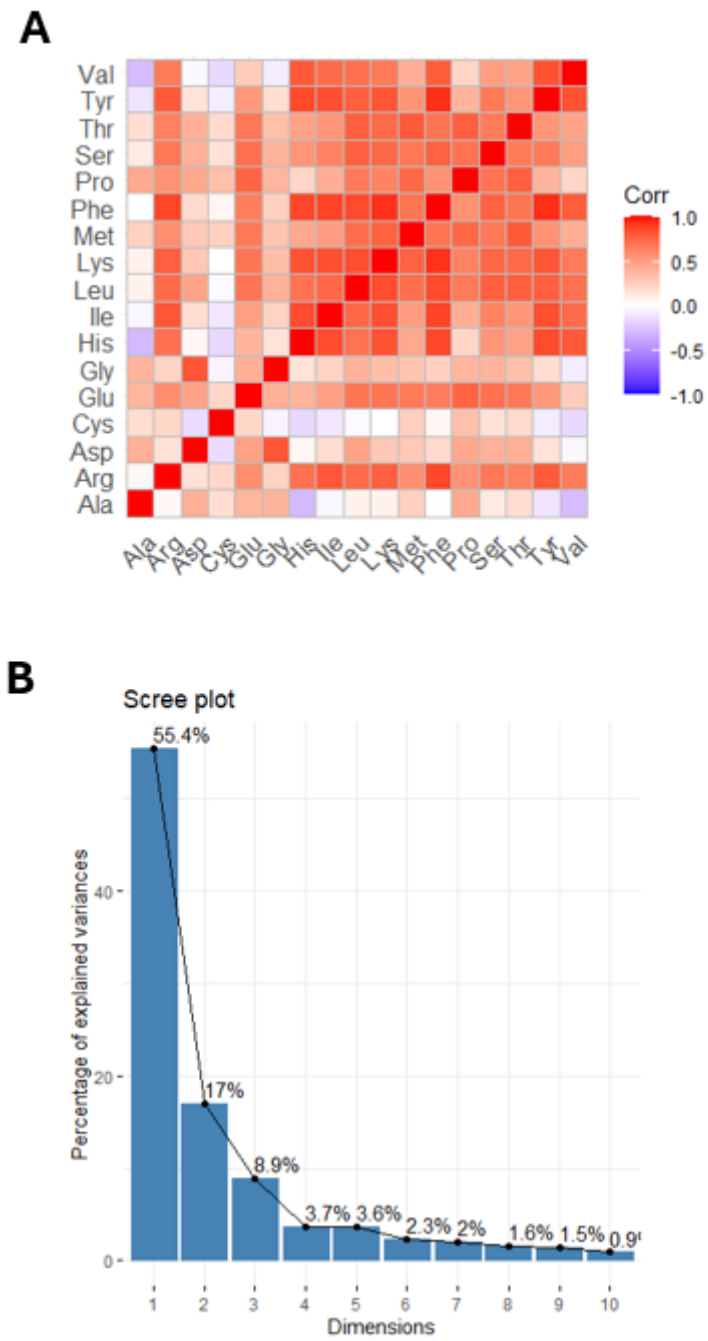

Figure 2.1. Visual representation of relevant Principal Component Analysis data. A) Covariance matrix of the normalised AA dataset, magnitude of the correlation is described in terms of colour type and intensity with more positive correlation in red and negative correlation in blue (right hand Y axis). B) Scree plot representing the variance accounted for by the principal components (PC) of the PCA (PCA 11-17 not included).

2.4 Results

2.4.1 Growth of *F. venenatum* in microplate cultures

Initial experiments to establish the growth pattern of *F. venenatum* under laboratory conditions were conducted in 96 well microplates, using a microplate reader (**Figure 2.2**). The plates were incubated in the microplate reader statically at 28 ^{o}C for 72 h with OD readings at 600nm every 1 h. No shaking was used at any stage of incubation in the microplate readers to prevent formation of undesirable pellets from the mycelium (Whittaker, 2022). This meant that it was likely that in a flask culture with shaking where the aeration and nutrient availability is higher the growth would be quicker, but this experiment provided a timeframe in which *F. venenatum* is likely to grow exponentially. The growth of *F. venenatum* in these conditions appeared to follow two distinct phases of exponential growth: between ~16 and ~28h and between ~40 to ~56 h, with a brief period between these phases during which growth was decelerating. The shortest doubling time occurred between 20-24 h (4.1 h), whereas the second growth phase between 40-56 h had an average doubling time of 9.02 h.

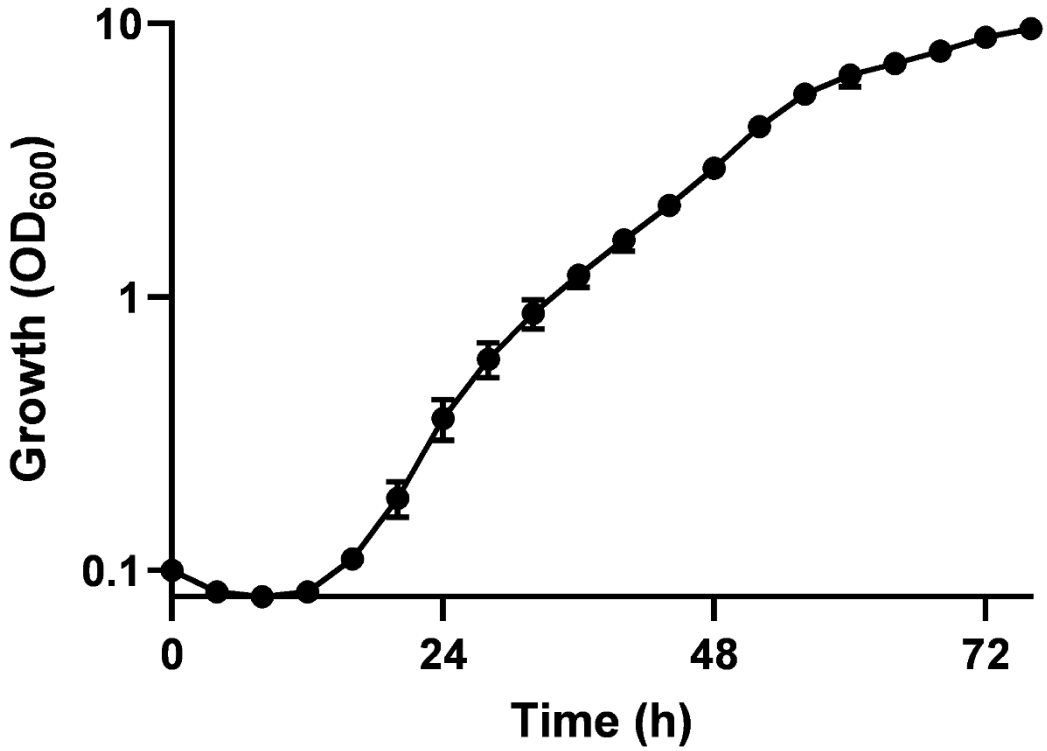

Figure 2.2 Growth curve of *F. venenatum* in microplate culture. RHM medium was inoculated with 10,000/ml of spores and 300 ul of the suspension was deposited into wells and incubated statically at 28° C for 72 hours with OD measurements taken every 1 h for 72 h. Data points indicate mean average, ± SD, n = 3.

2.4.2 Growth in baffled flask cultures

The growth curve of *F venenatum* was examined in RHM medium in 250 ml baffled flasks. Freeze-dried biomass was weighed at intervals (as described in **2.3.2** and **2.3.3**). The biomass increased exponentially between approximately 24 and 36 h (additional time points in this period would delimit exponential-phase growth more accurately) with a calculated mean doubling-time of 3.32 h between 24 – 36 h. Growth subsequently slowed, and no further biomass increase was observed after 41 h indicating that the culture had reached a stationary phase. This entry to stationary phase occurred sooner than in microplate cultures. Visual examination revealed that before 24 h of growth the hyphae are not long enough and therefore not representative of *F. venenatum* biomass extracted from the airlift fermenters at Quorn. Therefore, timepoints between 30 and 41 h were selected as points of extraction for the future experiments.

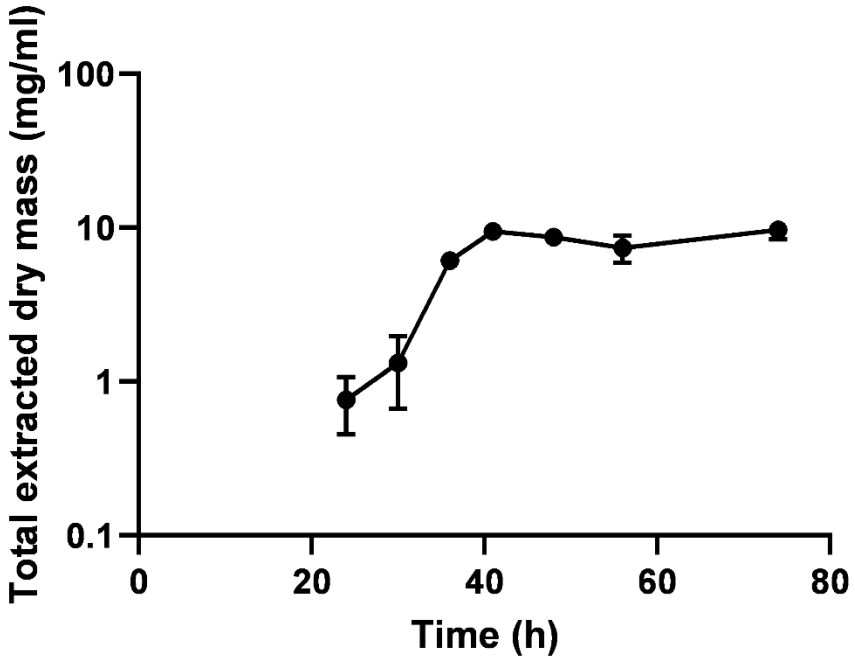

Figure 2.3 Growth curve of *F. venenatum* in flask cultures. RHM medium was inoculated with 10 000/ml of spores and 50 ml of the suspension was deposited into 250 ml baffled flasks and incubated statically at 28° C with shaking (150 rev/min). The biomass was extracted at 24, 30, 36, 41, 48, 56 and 74 h. Data points indicate mean average, ± SD, n = 3.

2.4.3 Validation of total protein content measurements with Bradford assay.

In addition to measuring the biomass (above), for this thesis it was important to consider whether protein content changes during growth in batch culture. The mycoprotein obtained from airlift fermenters exhibits a consistent protein quantity (**Figure 2.4**) throughout extraction. Assessing total protein content of a sample by expressing it as a % of the total AAs detected by LCMSMS analysis vs the dry weight of the sample is considered one gold standard (Mæhre et al., 2016). However, LCMSMS analysis is time consuming, costly and requires ~5 mg of nitrogen per sample which can be problematic for monitoring early growth timepoints where biomass is low. Nitrogen analysis is low cost and requires small amounts of biomass but can be problematic for less commonly tested samples as specific nitrogen to protein conversion factors are not available and for fungal derived samples, presence of chitin

(nitrogen containing polysaccharide) in fungal cell walls can also skew the results (Mæhre et al., 2016). The Bradford protein assay with an appropriate protein extraction method was reported to give comparable values to those derived by LCMSMS analysis. Here, four replicate samples of *F. venenatum* biomass were extracted from flask cultures at 30 h and each was split into two for analysis by either LCMSMS (after biomass hydrolysis – **2.3.8**) or Bradford assay (after protein extraction - **2.3.14**). The derived total protein amounts were comparable between the two assays (p = 0.49), around a value of 40% protein in the dry biomass (**Figure 2.4**).

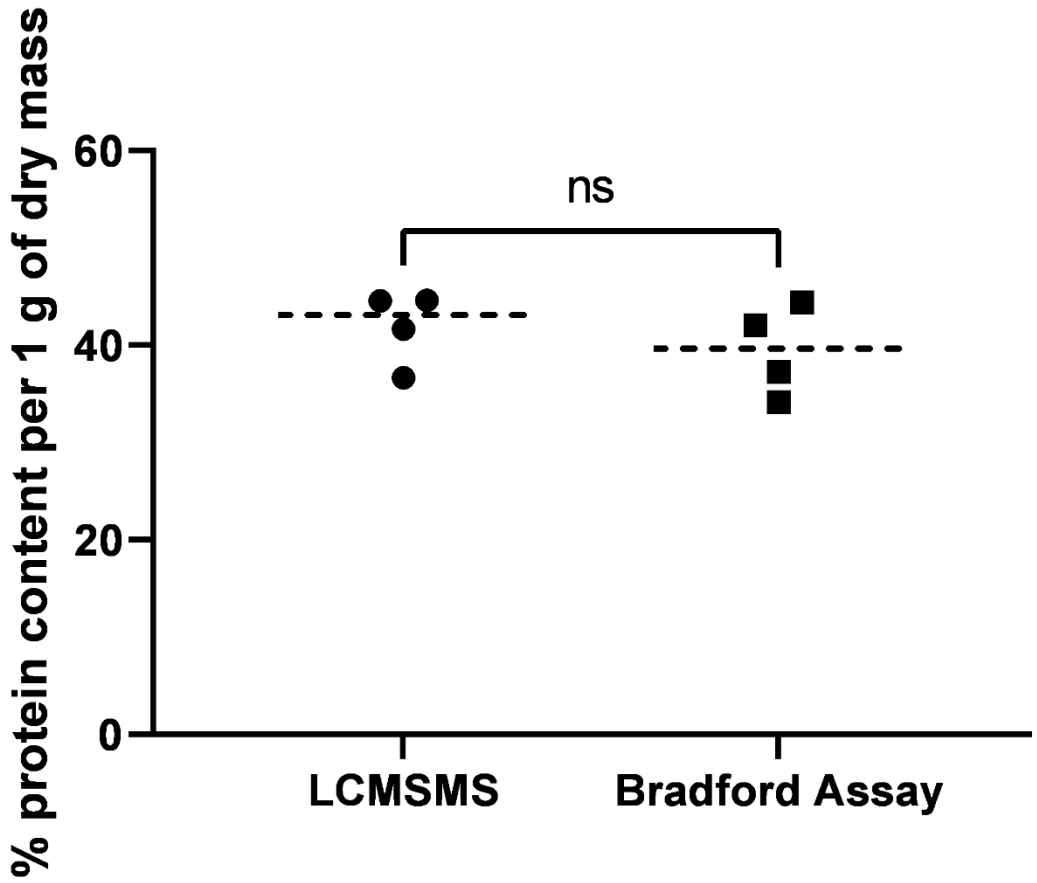

Figure 2.4 Comparison of % protein for the same biomass samples measured by LCMSMS and Bradford assay. Data points indicate individual values for biological replicates from flasks cultures extracted at 30 h after inoculation. The dotted lines indicate mean values. SDs (not shown) were 3.74 and 4.64 for LCMSMS and Bradford assay, respectively. The sets were compared using the Mann-Whitney test: U = 5, Two-tailed p = 0.4857, n = 4.

2.4.4 The relationship between growth stage and protein content

After validating total protein content measurement by Bradford assay (based on comparison with those by the LCMSMS AA analysis), the Bradford assay was used to monitor changes to the total protein content throughout growth in flask cultures. This was not done for microplate cultures because the culture growth conditions were different to those in a continuous fermenter. The cultures were grown in flasks in RHM medium. The samples used for biomass measurement were subsequently used for total protein extraction and the protein

content determined by Bradford assay. As expected, there was a marked increase in protein content from the spore stage used for inoculum and the vegetative state after 20 h growth, the earliest growth timepoint at which sufficient biomass enabled protein determination (**Figure 2.5 A**). After 24 h, there was a downward trend in protein content as growth progressed through exponential phase and slowed towards stationary phase, with biomass having lower protein % per gram of dry mass from 24 to 72 h ($p = 0.021$) (**Figure 2.5 B**). The relationship between dry mass and % protein was considered further (**Appendix Figure 1**). Here, replicate data were plotted separately as it had been noted that replicate cultures for the same treatment were not identical in their protein content. Dry total masses of individual samples inversely correlated with protein content of the sample – samples of lower total culture mass tended to have higher protein content (**Appendix Figure 1**). This relationship between the downward change in protein content as biomass increased during exponential phase may help explain the large variation in protein content across replicates at certain timepoints noted above, i.e., due to potential divergences in growth progress between replicate cultures. It also suggests that experimental conditions which affect growth progress in flask cultures (e.g., use of a different growth medium) might affect the total protein content purely on the basis of growth stage attained by particular timepoints rather than specifically because of the condition (e.g., composition of the tested medium).

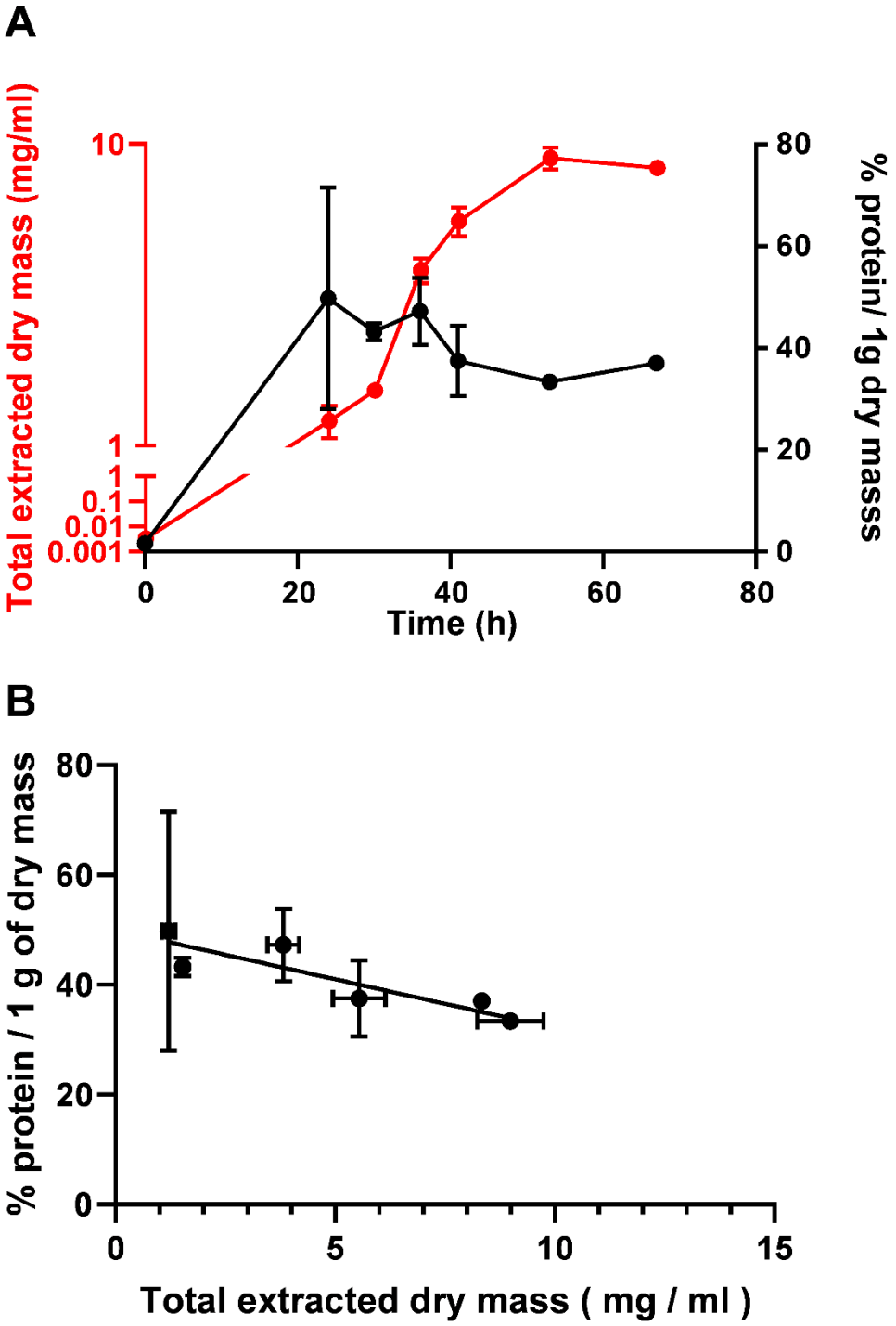

Figure 2.5 Protein content of *F. venenatum* during flask culture in RHM medium. A) Cultures were inoculated with 10 000 spores per ml and grown at 28ºC and 150 rev/min. At indicated timepoints, biomass from a flask was extracted, freeze dried and weighed to give extracted dry mass (± SD). The dry mass was then powdered and analysed via Bradford assay to determine protein % per 1 g of dry mass. The 0 h timepoint was determined in the same way but with ~10 million freeze dried spores. **B)** Pearson correlation: r (22) = – 0.8791, p (two-tailed) = 0.021

2.4.5 Comparison of AA profiles of *F. venenatum* in flask culture and airlift fermenter cultures

As for the case of *F. venenatum* growth in 96 microwell plates versus flask cultures, the conditions will differ between the latter and industrial scale continuous fermentation in airlift fermenters. Therefore, the AA profiles of *F. venenatum* biomass sampled from airlift fermenters at the Quorn production facility were determined. The samples came from two Quorn airlift fermenters (Q3 and Q5) and were sampled 5 times from each fermenter over a 40-hour period during routine fermentation cycles (I. Geoghegan, pers. Comm., Marlow Foods Ltd.). Analysis of protein content via Bradford assay showed that the protein content fluctuated around 40% as a proportion of biomass dry weight. There were no significant differences between the total protein contents of biomass derived from flask cultures and either of the airlift fermenters ($p = 0.8626$) (**Figure 2.6**).

Biomass from the samples was hydrolysed and the AA profile was measured via LCMSMS. The AA composition of samples from flasks and airlift fermenter cultures was comparable: One-Way- ANOVA of the PC1 values from the experiment revealed no statistically significant effect of growth in flask versus fermenter on AA profiles of *F. venenatum* biomass ($p = 0.699$) (**Table 2.5).** There were also no significant differences in PC2 and PC3 ($p = 0.7699$, $p = 0.8601$) indicating no change in levels of individual AAs between the samples. The absolute and relative AA profiles of the samples are shown in (**Table 2.5**, **Figure 2.7**, **Appendix Table *2***). Overall, no significant differences in individual AAs or total AA amounts between flask grown and Quorn fermenter biomass were found suggesting that exponential phase biomass grown in flask cultures can be used as reasonable proxy for determination of potential changes to AA profile of *F. venenatum* under different conditions.

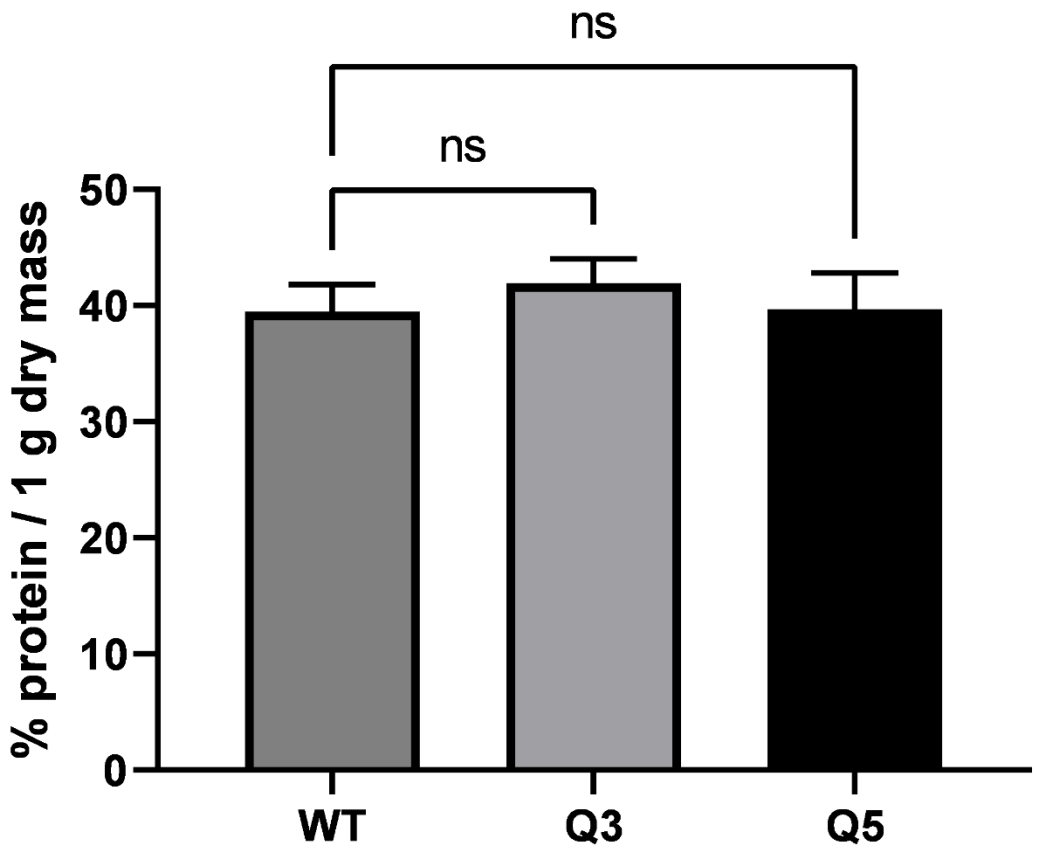

Figure 2.6. Total protein content of *F. venenatum* biomass from flask cultures is comparable to samples from industrial scale continuous fermentation. Here WT indicates samples from flask cultures, Q3 and 5 indicates samples extracted from respective airlift fermentors. 30 h extracted flask culture samples were compared Kruskal-Wallis test with Dunn's multiple comparisons (H = 0.3600, df = 2 p = 0.8626) n = 4 (WT), n = 5 (Q3 and Q5).

Table 2.5. **Comparison of AA profiles of *F. venenatum* biomass hydrolysate extracted from flask cultures at 30 h and airlift fermentors.** Values indicated g/kg of dry mass ± SD. The bottom three rows indicate the principal component values ± SD. The PC1-3 from different treatments were compared by One-Way ANOVA (F = 0.3804, df = 2, p = 0.699; , F = 0.7699, df = 2 p = 0.5039; F = 0.1546, df = 2, p = 0.8601) respectively. n = 3.

AA g/kg	Flask	Airlift Q5	Airlift Q3
Ala	38.5 ± 4.2	40.2 ± 0.4	40.4 ± 6.9
Arg	29.1 ± 2.8	29.6 ± 1.0	31.0 ± 3.1
Asp	34.7 ± 3.9	32.5 ± 2.0	32.9 ± 1.1
Cys	3.0 ± 0.4	2.9 ± 0.3	2.8 ± 0.4
Glu	78.5 ± 16.5	66.3 ± 5.2	61.3 ± 4.5
Gly	18.5 ± 1.8	16.3 ± 0.9	16.3 ± 0.9
His	10.0 ± 1.2	10.3 ± 0.6	9.9 ± 0.3
Ile	20.2 ± 2.4	19.9 ± 2.1	20.7 ± 0.7
Leu	31.2 ± 4.5	29.4 ± 2.2	30.8 ± 1.2
Lys	33.9 ± 3.7	33.6 ± 2.3	32.5 ± 0.9
Met	11.2 ± 2.6	10.2 ± 1.5	9.9 ± 0.1
Phe	18.8 ± 2.2	17.6 ± 1.6	17.6 ± 0.6
Pro	18.0 ± 1.8	18.2 ± 1.4	17.8 ± 0.7
Ser	17.1 ± 2.3	15.4 ± 1.4	15.7 ± 0.9
Thr	21.3 ± 2.9	20.0 ± 1.1	20.0 ± 1.2
Tyr	9.7 ± 1.8	8.5 ± 0.8	8.7 ± 0.3
Val	26.0 ± 4.1	26.4 ± 1.9	25.8 ± 0.8
Total	419.6 ± 37.3	397.3 ± 25.7	393.7 ± 21.8
PC1	0.12 ± 2.0	-0.73 ± 1.3	-0.78 ± 0.6
PC2	0.5 ± 0.8	0.10 ± 0.3	-0.04 ± 0.5
PC3	1.43 ± 0.55	1.47 ± 0.34	1.29 ± 0.32

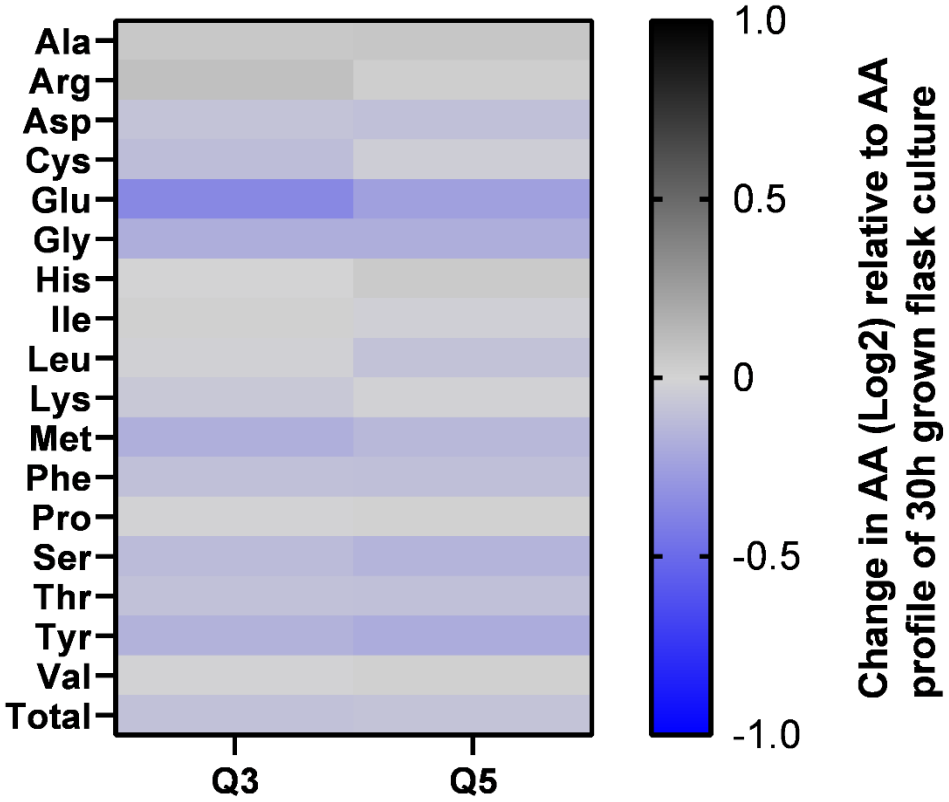

Figure 2.7. **Heat map illustration of individual-AA levels of *F. venenatum* from airlift fermenter samples relative to those for flask cultures.** The values (converted to heat map according to the right-hand scale) are normalised to the flask cultures and expressed as Log2 of the values, n=3.

2.4.6 Comparison of the relative and absolute AA profiles of flask grown *F. venenatum* cultures at 30 h and 36 h

As shown in section (**2.4.4)** the protein content within flask cultures tends to decrease with increasing biomass even through exponential growth phase. To see whether this decrease in protein content over time in flask cultures also affects the relative AA composition – that is the proportion that each AA makes up in the total AA content – relative AA profiles of samples from flask cultures extracted at 30 and 36 h were compared. Between flask samples extracted at 30 and 36 h the absolute levels of individual AAs remained comparable as expected for both replicas as evidenced by no significant differences in when PC1 values were compared by One-Way ANOVA ($p = 0.74$, $p = 0.35$, for replicas 1 and 2 respectively) (**Appendix Table 2**). In replica 1, comparison of PC2 and 3 did not reveal any significant differences to the AA profile ($p = 0.16$, $p = 0.58$, respectively), likewise in PC3 in replica 2 ($p = 0.08$). However PC2 in replica 2 did indicate a significant change in the levels of AAs described by this PC ($p = 0.035$). Lower value of PC2 at 36 compared to 30 h suggested a decreased level of Ala in both absolute (32 vs 49 g per kg) (**Appendix Table 2**) and relative terms (6.55 vs 9.39 %) (**Appendix Table 3**).

Hydrolysate AA profiles at 30 vs 36 h are fairly similar, and it seems like most of the variation in AA profiles of flask cultured *F. venenatum* samples comes from the variation in the levels of Ala.

2.4.7 Comparison of free AA profiles

Although the relative composition AA of the hydrolysates from flasks between 30 and 36 h is comparable (**2.4.6)** AAs like glutamate and alanine tend to fluctuate the most both within the timepoint and between them. Free glutamate is stored in cells to be converted into other AAs and support protein translation and AA signalling (Yoo et al., 2020). In yeast the free AA pool may change in response to shift metabolic shift or change in growth conditions (Martinez-Force and Benitez, 1995) and this change is more rapid than in case of the proteome. This change to the free AA profile was corroborated by additional analysis in the present study comparing the free AA profiles in *F. venenatum* across different growth points. The free AA profile of *F. venenatum* was changing throughout growth, with alanine and glutamine levels generally getting lower at later growth points with levels of some other AAs, especially lysine getting higher (**Appendix Figure 2**).

To determine the extent to which changes to the free AA pool can influence the overall AA profile of *F. venenatum* hydrolysate (AAs in proteins + free AAs), free AAs from *F. venenatum* biomass grown in flasks cultures were extracted at 30 and 36 h and the profiles were measured via LCMSMS. The two free AA profiles were different with biggest absolute change in the amount of glutamate and alanine ($p = 0.005$, $p = 0.0014$, respectively) (**Table 2.6**). At 36 h a change to the AA profile can be seen presumably as an effect of metabolic shift as a result of growth slowdown (**Appendix Table 2**, **Appendix Table 3**, **Figure 2.8**). In some experiments however, free AA profiles of samples extracted at 36 h resembled the profile of 30 h extracted samples, presumably due to slightly slower growth in the flask (data not shown). 30 h was concluded to be more suitable point to look at the free AA profiles because it consistently produced a replicable free AA profile. Comparing the free AA profiles and hydrolysate proteins from the 30 h samples (**Table 2.4 and Table 2.6)** showed that the free AAs make on average 14.8 % of the total cellular AA content (**Table 2.7**). Free alanine and glutamate make up the highest proportion of their respective AA pools 12.91 and 39.9 % these two free AAs also make up 58 % of the whole free AA pool. Other free AAs make up a varying degree of their respective AA pools, e.g., free leucine makes up only 0.7 % of the leucine pool, but free histidine makes up 7 % of the total histidine pool, but with exception of alanine and glutamate the other free AAs individually represent ≥ 0.56% of the total AAs found in the hydrolysate (**Table 2.7**). Changes to the free AA profile could explain the fluctuations in the levels of free glutamate and alanine between different samples pointed out earlier in this chapter, but due to relatively low abundance of other free AAs it is unlikely that fluctuations in their level would noticeably affect the AA profile of the *F. venenatum* hydrolysate.

Table 2.6. Comparison of free AA profiles of *F. venenatum* biomass extracted from flask cultures at 30 h and 36 h. Values of amino acids are expressed as g/kg ± SD. Different letters in superscript between cells in the same row indicate statistically significant difference between values ($p < 0.006$) derived multiple unpaired T-test (df = 4) with false discovery rate at 1 %. Lack of any superscript letters indicates lack of significant difference within a row. N/D - not detected, N/I - not included.

AA g/kg	RHM 30 h (n = 3)	RHM 36 h (n = 3)
Ala	4.97 ± 0.55 ^{A}	8.33 ± 0.50^{B}
Arg	2.35 ± 0.03	1.55 ± 0.38
Asx	0.51 ± 0.01	N/I
Asp	2.28 ± 0.17	2.02 ± 0.78
Cys	0.06 ± 0.01	N/D
Glu	31.34 ± 2.1 ^{A}	17.48 ± 3.87 ^{B}
Glx	0.14 ± 0.03	N/I
Gly	0.82 ± 0.04 ^{A}	0.46 ± 0.03 ^{B}
His	0.7 ± 0.1	0.84 ± 0.14
Ile	0.19 ± 0.02 ^{A}	0.87 ± 0.13 ^{B}
Leu	0.22 ± 0.02 ^{A}	0.60 ± 0.07 ^{B}
Lys	0.69 ± 0.04	1.41 ± 0.47
Met	0.34 ± 0.01 ^{B}	0.06 ± 0.01 ^{B}
Phe	0.32 ± 0.02	0.48 ± 0.06
Pro	0.61 ± 0.02	0.49 ± 0.17
Ser	1.61 ± 0.05	1.22 ± 0.22
Thr	1.97 ± 0.06	1.56 ± 0.21
Trp	0.12 ± 0.01	0.49 ± 0.24
Tyr	0.15 ± 0.01 ^{A}	1.35 ± 0.19 ^{B}
Val	0.9 ± 0.06 ^{A}	0.10 ± 0.03 ^{B}
Total	62.15 ± 2.56 ^{A}	39.30 ± 7.52 ^{B}

Table 2.7. Table outlining the amount of the free AAs found in the hydrolysate. The AA profile is expressed as % abundance of individual free AAs within the free AA pool and within the hydrolysate profile and as % abundance of individual AAs relative to the total amount of AAs in the hydrolysate.

AA g/kg	% of the individual AA	% of total profile
Ala	12.91	1.19
Arg	8.07	0.56
Asp	6.56	0.54
Cys	2.04	0.01
Glu	39.90	7.48
Gly	4.46	0.20
His	7.01	0.17
Ile	0.95	0.05
Leu	0.70	0.05
Lys	2.03	0.16
Met	3.04	0.08
Phe	1.69	0.08
Pro	3.38	0.15
Ser	9.42	0.38
Thr	9.24	0.47
Tyr	1.50	0.03
Val	3.47	0.22
Total	14.84	14.84

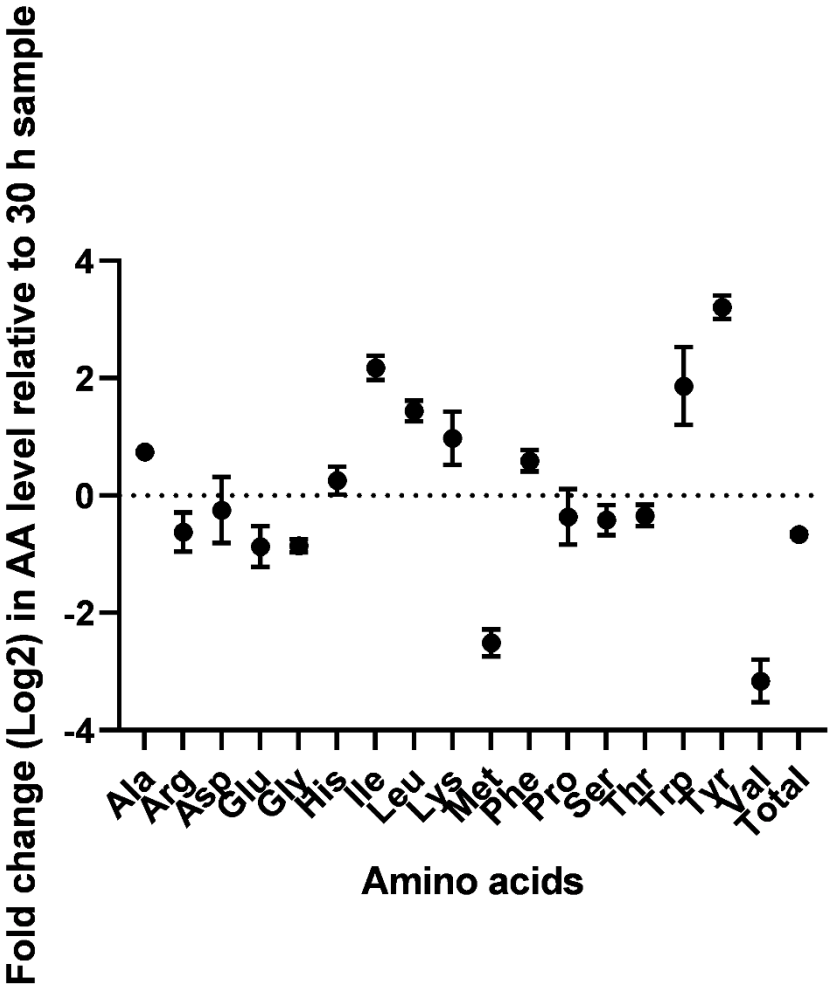

Figure 2.8. Change to free AA profile between 30 and 36 h extracted samples of *F. venenatum* grown in RHM medium. The points on the graphs are the levels of each AA from the 36 h sample normalised against the relevant AA level from the 30 h sample (**Table 2.6**). The values are expressed as $\log_2$ fold-change (n = 6, biological replicates).

2.4.8 Comparison of AA profiles and growth in other fungal media

To test whether the above observations were specific to growth in RHM, the AA profile and protein content were examined in *F. venenatum* cultured in two other commonly used fungal growth media (ACM and AMM).

Exponential-phase *F. venenatum* growth was slightly faster in AMM and ACM media (which contain yeast extract and bacteriological peptone) than in RHM (which does not). Fastest growth was identified between approximately 24 and 36 h with average doubling times of 6 h 21 min, 6 h 51 min, 6 h 21 min in AMM, ACM and RHM media respectively (**Figure 2.9 A, Figure 2.10 A;** RHM shown in **Figure 2.5 A**). There was a significant downward trend in protein content (% protein per gram dry mass) between 24 to 72h (p = 0.0096, 0.0442) for AMM, ACM respectively (**Figure 2.9 B, Figure 2.10 B)**. Biomass grown in ACM, AMM media was collected at 30 and 41 h, hydrolysed and analysed by LCMSMS to compare AA profiles with the profiles of hydrolysate from biomass grown in RHM medium.

At 30 h there was no significant effect of the medium used on the absolute, overall hydrolysate AA profiles of samples grown in the three different media as indicated by analysis of the PC1 ($p = 0.199$) (**Table 2.8**). Comparison of PC2 and 3 revealed no further differences between the treatments ($p = 0.9$, $p = 0.09$) indicating no change in levels of individual AAs between the samples.

At 41 h analysis of the PC1 showed, that there was a significant effect of the medium on the overall abundance of the AAs in the hydrolysate profiles ($p = 0.0018$) (**Table 2.8**). Tukey's multiple comparisons test revealed a significant difference between the RHM and ACM treatment ($p = 0.0017$) and RHM and AMM treatment ($p = 0.013$), in both cases the overall level of AAs is lower than in RHM control. Analysis of PC2 indicated a significant effect of the treatment ($p = 0.0118$), Tukey's multiple comparison test revealed a significant difference between the RHM and ACM treatments ($p = 0.009$). This result indicates a relative increase in Ala, Asp, Gly and Pro relative to His and Val in the ACM treatment (PC2 = 1.52) compared to the RHM treatment (PC2 = -3.98) (**Table 2.8**, **Appendix Table 4**, **Figure 2.11**). Analysis of the PC3 showed no significant difference between the treatments ($p = 0.0941$).

The absolute and relative values for both experiments are presented in (**Table 2.8**, **Appendix Table 4**, **Figure 2.11**)

The results show that the AA profiles of cell hydrolysates from the three media are more similar after 30 h growth than after 41 h growth. One factor that could have influenced this difference is that there were differences in growth rate between media – e.g., *F. venenatum* grown in ACM (**Figure 2.9**) at 41 h had spent longer outside of exponential phase than RHM (**Figure 2.5**) grown fungus.

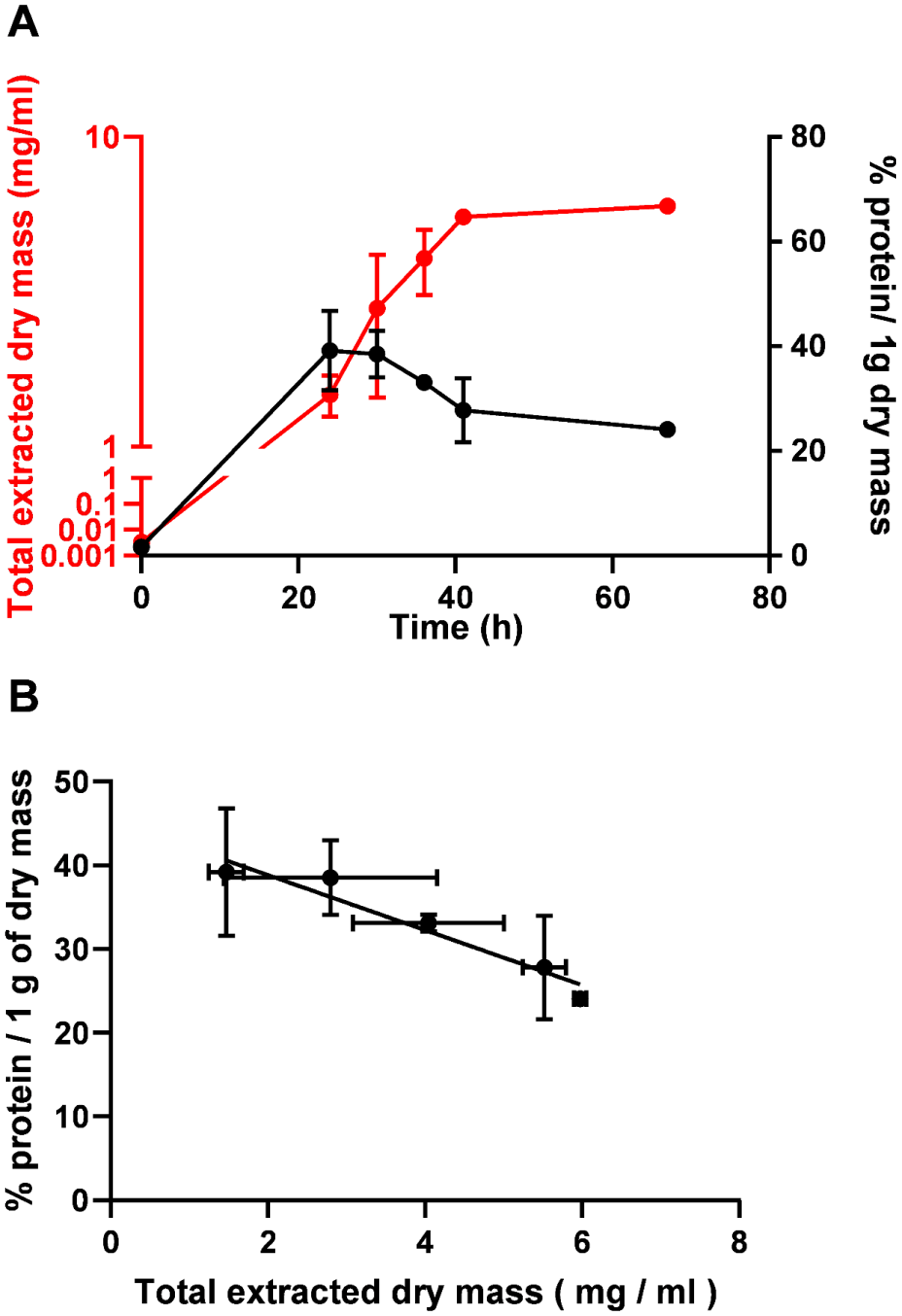

Figure 2.9. The relationship between biomass density during growth and protein content of *F. venenatum* grown in ACM medium. Cultures were inoculated with 10 000 spores per ml and grown at 28ºC at 150 rev/min. At indicated timepoints biomass from whole flask was extracted, freeze dried and weighed to give extracted dry mass (±SD). The dry mass was then powdered and analysed by Bradford assay to determine protein % per 1 g of dry mass. The 0 h timepoint was determined by weighing ~10 million freeze dried spores and calculating the corresponding mass for the inoculum used. The same samples were then analysed with Bradford assay to estimate protein. **A)** Dry weight (red) and protein content (black) of samples plotted for different timepoints, **B)** The relationship between the dry mass of the sample and its protein content. Pearson correlation: r (20) = – 0.-9677, p (two-tailed) = 0.0096.

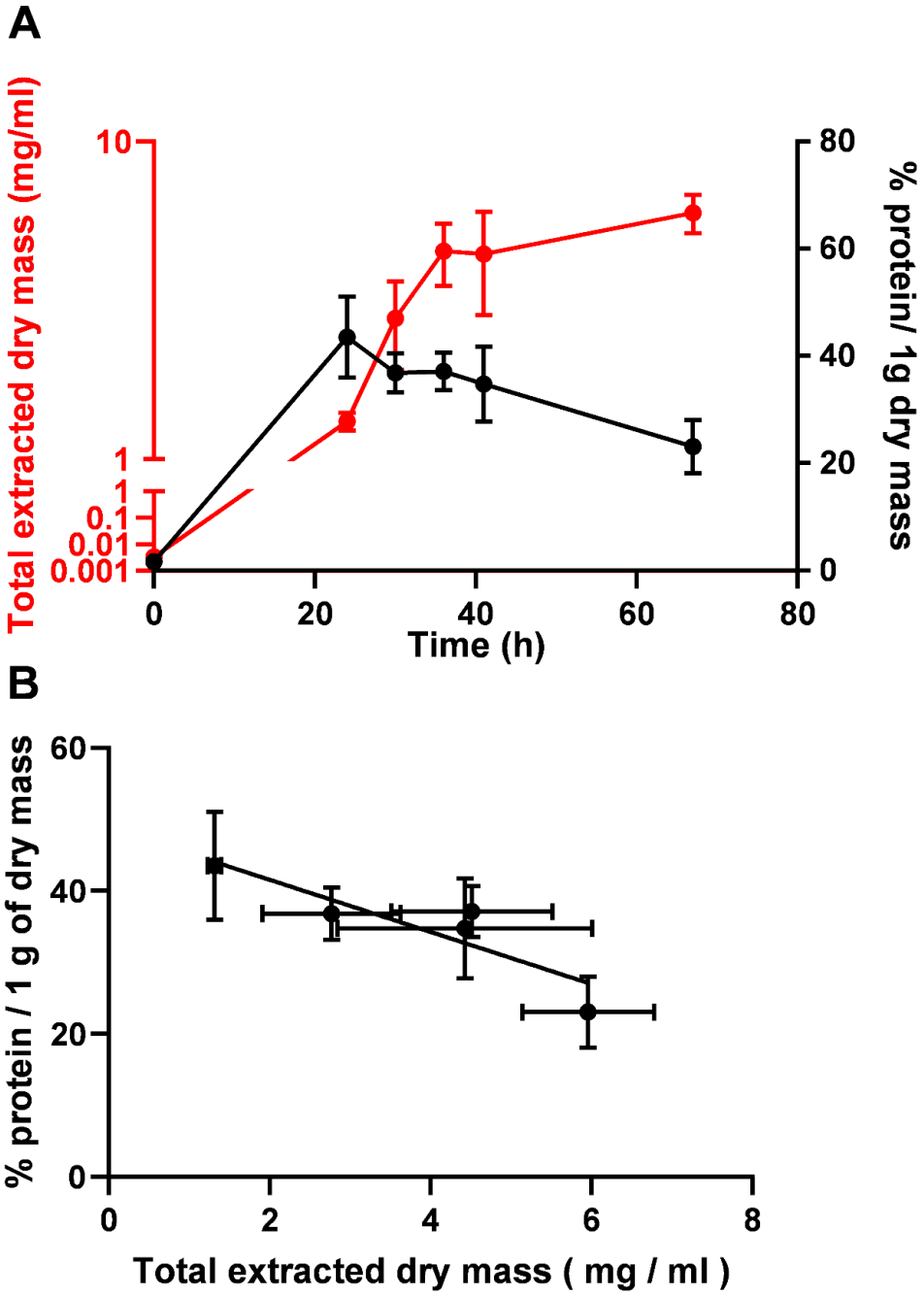

Figure 2.10 The relationship between biomass density during growth and protein content of *F. venenatum* in AMM medium. Cultures were inoculated with 10 000 spores per ml and grown at 28ºC at 150 rev/min. At indicated timepoints biomass from whole flask was extracted, freeze dried and weighed to give extracted dry mass (±SD). The dry mass was then powdered and analysed via Bradford assay to determine protein % per 1 g of dry mass. The 0 h timepoint was determined by weighing ~10 million freeze dried spores and calculating the corresponding mass for the inoculum used. The same samples were then analysed with Bradford assay to estimate protein. **A)** Dry weight (red) and protein content (black) of samples plotted for different timepoints, **B)** The relationship between the dry mass of the sample and its protein content. Pearson correlation: r (20) = – 0.8880, p (two-tailed) = 0.0442

Table 2.8. Absolute amino acid profiles of *F. venenatum* biomass hydrolysate in different media after growth for 30 h and 41 h. Values of amino acids are expressed as g/kg ± of dry mass SD. The bottom three rows indicate the principal component values ± SD. The PC1-3 from different treatments were compared by One-Way ANOVA (F = 1.942, df = 2, p = 0.199; , F = 0.0954, df = 2 p = 0.909; F = 3.1082, df = 2, p = 0.094) respectively for 30 h growth subset and (F = 13.716, df = 2 p = 0.002; F = 7.570, df = 2, p = 0.0118; F = 3.108, df = 2, p = 0.094) respectively for 41 h growth subset. For the PC rows, different letter in superscript indicates a significant difference between the compared PCs, lack of any letters indicates lack of statistically significant difference. n = 4. The corresponding relative % values for AA composition are given in (**Appendix Table 4**) and represented by heat map below (**Figure 2.11**).

AA g/kg dry biomass	30 h growth			41 h growth		
	RHM	AMM	ACM	RHM	AMM	ACM
Ala	36.7 ± 4.9	36.4 ± 2.3	29.6 ± 3.6	31.9 ± 3.9	35.5 ± 8.3	26.0 ± 4.5
Arg	29.1 ± 2.3	23.0 ± 1.7	27.1 ± 4.6	31.58 ± 6.47	33.59 ± 11.39	26.9 ± 3.0
Asp	35.6 ± 3.6	30.6 ± 3.9	36.0 ± 6.1	48.5 ± 4.9	36.7 ± 1.7	33.4 ± 1.3
Cys	3.0 ± 0.3	3.5 ± 1.1	3.6 ± 1.1	5.3 ± 0.9	4.3 ± 0.6	3.8 ± 0.2
Glu	79.9 ± 13.7	63.7 ± 10.9	71.6 ± 16.6	74.5 ± 4.3	66.0 ± 5.9	51.6 ± 12.3
Gly	18.9 ± 1.7	17.0 ± 2.5	19.3 ± 4.0	23.3 ± 2.8	18.4 ± 1.1	17.0 ± 1.3
His	9.9 ± 1.0	8.0 ± 0.3	9.4 ± 1.4	7.1 ± 3.3	5.5 ± 3.4	5.3 ± 3.4
Ile	19.1 ± 2.8	16.6 ± 0.9	17.7 ± 2.2	18.9 ± 0.9	15.0 ± 1.5	14.4 ± 0.7
Leu	31.1 ± 3.7	26.8 ± 3.1	28.5 ± 4.5	30.7 ± 1.7	24.5 ± 2.8	22.9 ± 1.8
Lys	34.3 ± 3.1	28.2 ± 1.9	35.5 ± 5.9	30.6 ± 4.5	22.5 ± 4.0	24.7 ± 7.9
Met	11.4 ± 2.2	9.1 ± 2.3	10.6 ± 3.1	10.2 ± 2.2	8.2 ± 1.7	8.3 ± 2.7
Phe	18.8 ± 1.8	15.1 ± 1.0	17.1 ± 2.9	18.0 ± 0.8	14.4 ± 1.4	13.7 ± 1.2
Pro	18.0 ± 1.5	15.9 ± 1.6	17.7 ± 2.8	20.3 ± 2.4	16.1 ± 0.9	14.4 ± 1.7
Ser	16.8 ± 2.0	14.1 ± 1.9	16.0 ± 2.8	17.9 ± 1.0	14.3 ± 0.7	13.1 ± 1.6
Thr	21.3 ± 2.3	17.3 ± 2.1	19.9 ± 3.6	22.3 ± 1.3	17.3 ± 0.8	15.8 ± 1.6
Tyr	10.0 ± 1.6	8.0 ± 1.3	9.1 ± 2.5	10.6 ± 1.0	8.7 ± 0.9	8.1 ± 0.7
Val	25.3 ± 3.6	21.1 ± 1.1	24.4 ± 3.2	24.9 ± 1.7	20.1 ± 1.6	18.2 ± 1.0
Total	418.8 ± 37.3	354.2 ± 36.7	392.65 ± 68.0	419.7 ± 14.9	357.5 ± 39.4	334.2 ± 26.5
PC1	0.1 ± 1.7	0.56 ± 0.6	1.41 ± 0.4	0.21 ± 0.7 ^{A}	1.76 ± 0.9 ^{B}	2.37 ± 0.5 ^{B}
PC2	- 0.81 ± 2.9	0.38 ± 1.1	1.64 ± 0.9	- 3.98 ± 1.8 ^{A}	- 0.14 ± 0.6 ^{A}	1.52 ± 0.4 ^{B}
PC3	- 2.78 ± 1.5	0.27 ± 1.0	1.51 ± 0.9	- 2.82 ± 0.9	0.76 ± 0.5	1.98 ± 0.5

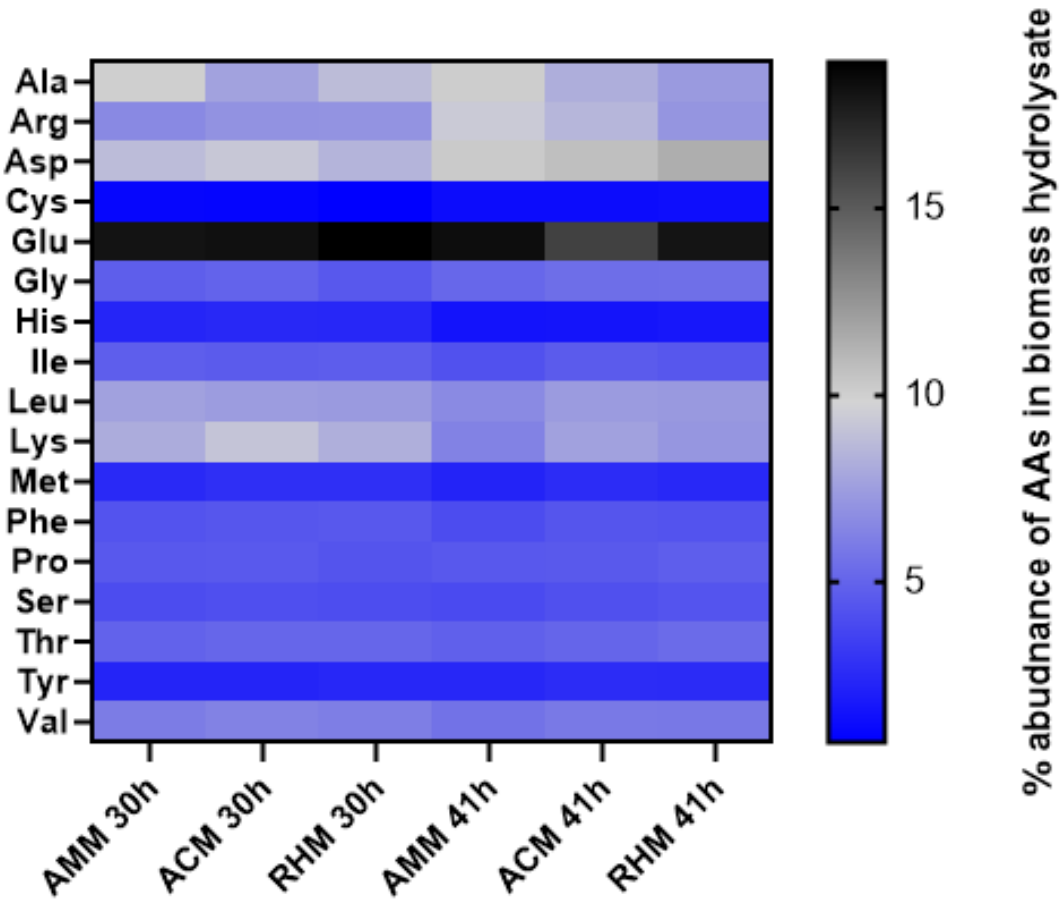

Figure 2.11. Relative AA abundance of *F. venenatum* biomass hydrolysate. Absolute amounts of individual AAs in each condition were expressed as % of total AAs in the condition and plotted on the heat map.

2.4.9 Effect of carbon source substitution on the AA profile of *F. venenatum*

Sucrose has been identified as a potential alternative to glucose as a carbon source for supporting growth of *F. venenatum* (Whittaker, 2022). However, changing the carbon source might affect the organism's AA profile (Anderson and Solomons, 1984). To consider sucrose as an alternative sugar source, it was important to evaluate whether substituting glucose with sucrose changes the AA profile. *F. venenatum* was cultured in flasks for 30 h and 36 h in RHM medium with either 3% glucose, 3% sucrose or a 50/50 glucose/sucrose mix (1.5% each) as a carbon source. It has previously been shown that growth of *F. venenatum* in these alternative sugar sources does not change the growth parameters of the culture compare with standard 3 % glucose (Whittaker, 2022).

Comparisons of the PC1-3 by One-Way ANOVA for the 30 h grown subset of samples revealed no significant differences ($p = 0.4903$, $p = 0.127$, $p = 0.1487$) respectively (**Table 2.9**). Similarly, there were no significant differences between the PC1-3 from the 36 h grown samples subset ($p = 0.7374$, $p = 0.7458$, $p = 0.617$). The absolute and relative values of the AA profiles are presented in (**Table 2.9**, **Appendix Table 6**, **Figure 2.12**) The unusually high total AA level of the hydrolysate of the sucrose grown samples from the comparison made at 30 h (>600 g/kg) might be related to low biomass at the extraction time (**Appendix Table 5**).

Overall, the AA profile of F. venenatum does not seem to change when glucose is substituted for sucrose as a carbon source. This finding is valuable as it means that from protein content and quality perspective sucrose is as good of a sugar source as glucose for production of F. venenatum mycoprotein.

Table 2.9. Absolute AA profiles of *F. venenatum* biomass hydrolysates following growth in RHM with different carbon sources. Values of amino acids are expressed as g/kg ± SD. The bottom three rows indicate the principal component values ± SD. The PC1-3 from different treatments were compared by One-Way ANOVA (F = 0.8248, df = 2, p = 0.4903; , F = 3.2069, df = 2 p = 0.127; F = 2.8576, df = 2, p = 0.1487) respectively for 30 h growth subset and (F = 3.9258, df = 2 p = 0.7374; F = 0.3081, df = 2, p = 0.7458; F = 0.5238, df = 2, p = 0.617) respectively for 36 h growth subset.

	30 h			36 h		
AA g/kg	**Glucose 3% (n=3)**	**Sucrose 3% (n=2)**	**Glucose/Sucrose 1.5/1.5% (n=3)**	**Glucose 3% (n=3)**	**Sucrose 3% (n=3)**	**Glucose/Sucrose 1.5/1.5% (n=3)**
Ala	**56.2 ± 13.3 [A, B]**	**68.1 ± 14.7 [A]**	**47.7 ± 5.5 [B]**	**33.3 ± 8.4**	**39.7 ± 3.4**	**37.9 ± 2.9**
Arg	**30.8 ± 3.0**	**31.7 ± 1.2**	**31.2 ± 4.2**	**21.3 ± 7.3**	**22.9 ± 3.9**	**25.5 ± 6.8**
Asp	**75.5 ± 18.5**	**108.7 ± 21.7**	**71.6 ± 4.8**	**60.4 ± 6.1**	**59.4 ± 1.6**	**59.6 ± 4.4**
Cys	**1.7 ± 0.6**	**1.4 ± 0.2**	**1.8 ± 0.3**	**1.3 ± 0.6**	**1.1 ± 0.4**	**1.4 ± 0.3**
Glu	**89.2 ± 11.7**	**94.5 ± 1.5**	**88.2 ± 10.8**	**55.0 ± 18.5**	**59.2 ± 12.1**	**70.0 ± 16.1**
Gly	**32.7 ± 8.7**	**46.4 ± 9.2**	**31.1 ± 1.2**	**25.9 ± 3.6**	**28.8 ± 6.2**	**25.7 ±1.2**
His	**10.3 ± 1.3**	**10.5 ± 0.4**	**10.3 ± 1.5**	**7.5 ± 2.3**	**8.1 ± 1.5**	**9.2 ± 2.3**
Ile	**22.7 ± 2.6**	**23.3 ± 1.2**	**22.8 ± 2.5**	**17.1 ± 5.5**	**16.3 ± 3.4**	**19.8 ± 5.5**
Leu	**36.0 ± 5.4**	**45.9 ± 8.6**	**35.9 ± 1.6**	**27.4 ± 7.8**	**28.3 ± 5.1**	**31.1 ± 6.2**
Lys	**37.5 ± 4.4**	**39.2 ± 4.3**	**37.4 ± 5.6**	**25.6 ± 8.2**	**27.1 ± 5.1**	**32.2 ± 8.0**
Met	**10.2 ± 1.3**	**10.9 ± 0.4**	**10.5 ± 1.0**	**7.7 ± 2.7**	**8.1 ± 1.8**	**8.9 ± 2.6**
Phe	**19.5 ± 2.0**	**20.5 ± 0.7**	**19.6 ± 2.4**	**14.2 ± 4.7**	**14.7 ± 2.3**	**17.0 ± 4.6**
Pro	**19.3 ± 2.0**	**19.8 ± 1.0**	**19.2 ± 2.5**	**14.0 ± 4.8**	**14.3 ± 2.6**	**16.5 ± 4.4**
Ser	**17.0 ± 2.4**	**19.6 ± 0.6**	**17.7 ± 2.2**	**13.0 ± 4.1**	**13.5 ± 2.8**	**14.7 ± 3.5**
Thr	**22.1 ± 2.8**	**22.1 ± 0.6**	**21.6 ± 2.4**	**16.4 ± 5.4**	**17.4 ±3.6**	**19.5 ± 5.6**
Tyr	**11.3 ± 1.4**	**12.9 ± 1.2**	**11.0 ± 1.2**	**8.7 ± 2.8**	**8.7 ± 1.2**	**9.8 ± 2.6**
Val	**25.8 ± 2.8**	**30.2 ± 4.2**	**25.4 ± 3.00**	**19.4 ± 5.0**	**19.5 ± 2.2**	**20.3 ± 3.7**
Total	**517.7 ± 62.0**	**605.7 ± 70.5**	**454.4 ± 73.4**	**369.3 ± 96.9**	**387.2 ± 47.1**	**419.0 ± 79.4**
PC1	**1.85 ± 2.1**	**3.86 ± 1.6**	**1.79 ± 2.1**	**- 3.20 ± 4.1**	**- 2.68 ± 2.3**	**- 1.01 ± 3.8**
PC2	**3.02 ± 1.4**	**5.17 ± 1.6**	**2.48 ± 0.6**	**0.75 ± 1.1**	**1.22 ± 0.5**	**1.14 ± 0.6**
PC3	**-1.99 ± 1.8**	**- 4.36 ± 1.4**	**- 1.67 ± 0.3**	**- 2.13 ± 0.7**	**-2.29 ± 1.0**	**- 1.61 ± 0.8**

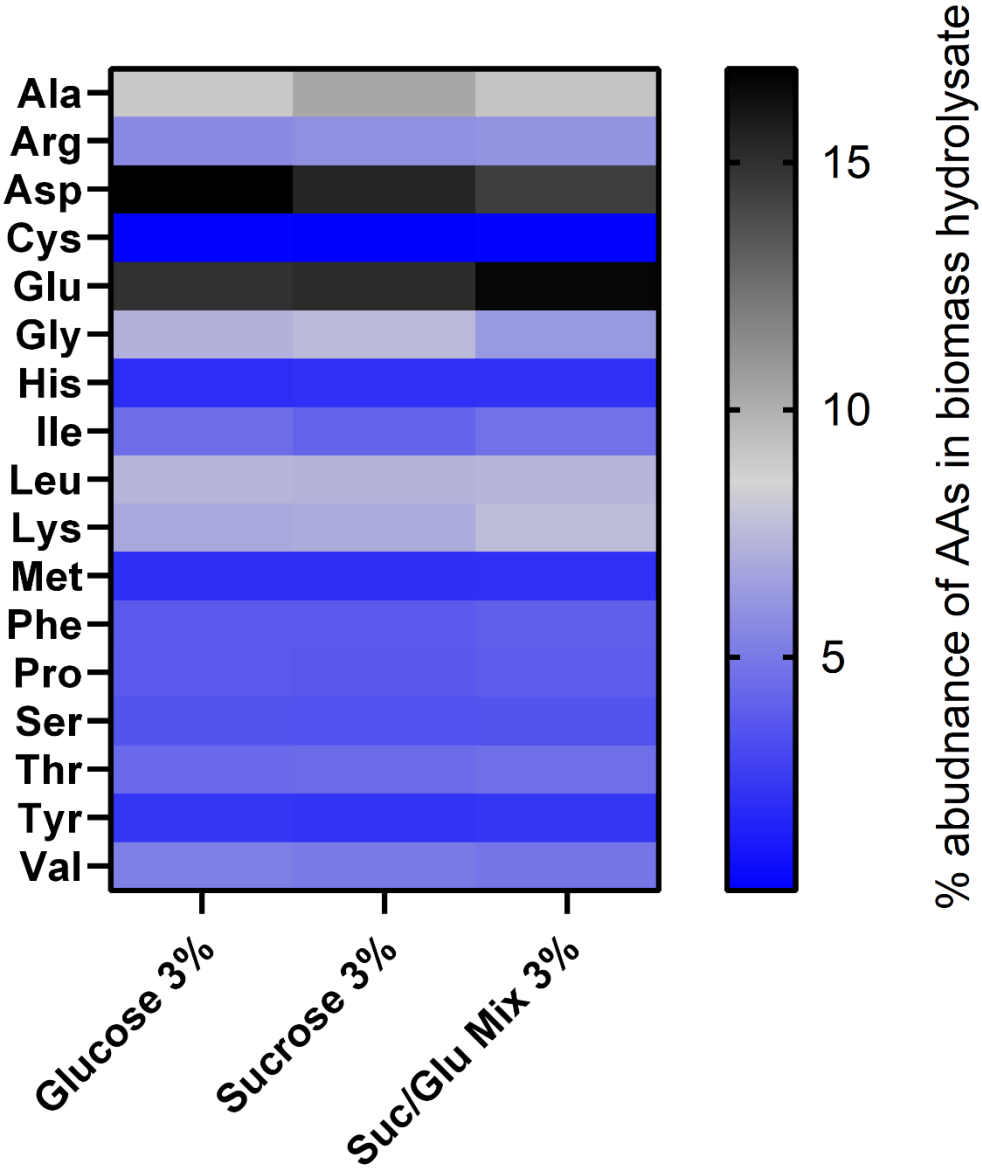

Figure 2.12. Relative AA abundance of *F. venenatum* biomass hydrolysate grown for 36 h. Absolute amounts of individual AAs presented in in each condition were expressed as % of total AAs in the condition (**Appendix Table *6***) and plotted on the heat map. Suc/Glu mix is composed of 1.5% sucrose and 1.5% glucose (totalling 3%).

2.5 Discussion

2.5.1 Use of flask cultures for testing effects of growth medium

The use of baffled flasks cultures for the initial stages of the investigation seemed to be a suitable system for the purpose of assaying for changes to AA profiles, given that there was no significant difference between hydrolysate AA profiles in these compared with those sampled from the industrial fermenters (**2.4.5**). The method does have drawbacks compared to continuous fermentation, e.g., the window of fastest growth during which samples representative of exponential-phase growth were assumed to occur can be reliably extracted lasts only ~6 h for hydrolysates and probably less for free AA profiles (between 30 and 36 hours the free AA profiles can change dramatically (**Figure 2.7**): the AA profile changed after exponential phase and was no longer representative of the profile of mycelium from the continuous culture (**2.4.8**). Moreover, extraction of exponential-phase mycelium at ~30 h can sometimes be problematic due to insufficient biomass from flasks at this stage. This resulted in a lower number of assayable replicates in some treatments (where listed n < 3). This could be mitigated by setting up larger numbers of cultures for each experiment and selecting only those where biomass accumulation was adequate or using larger-volume cultures, but either option would have resource- or space-implications. Additionally, the identified changes in protein content of *F. venenatum* during the assumed exponential phase must be kept in mind, especially when testing media that significantly change the growth rate as profiles for cultures extracted at the same timepoint may be influenced by different biomass densities. Nevertheless, with awareness of these limitations the flask culture setup seems to offer a convenient alternative to growth by airlift fermentation for studying the condition-dependency of AA profiles. The method could be improved by employing real time growth measurements through the shake flask, e.g., by optical backscatter measurements (Riel, 2020). This would allow for precise extraction of replicate samples from flask cultures at the same target culture density rather than fixed timepoints.

2.5.2 Robustness of the AA profile of *F. venenatum*

Overall, the AA profile of *F. venenatum* seems to be stable and not sensitive to general changes to growth conditions, such as change in the growth medium (**2.4.8)** and in carbon source from glucose to sucrose (**2.4.9**). It needs to be acknowledged that the LCMSMS analysis of different biological replicates for samples grown in the same conditions could produce results that differed in the quantified AA values (**Appendix Table 2**). When the same datasets were expressed as relative AA profiles such differences were no longer visible (**Appendix Table 3**). The difference in the absolute AA values between LCMSMS runs could arise from the relationship between hyphal development and protein content – as explained previously lower biomass in an exponentially growing culture appeared to correlate with higher protein content (**2.4.4**). This effect could be enhanced by the fact that between replicas of flask cultures extracted at the same timepoint the total biomass could differ due to higher or, lower growth in particular flask. This could be a result of a quorum sensing mechanism that coordinates germination of spores in individual flask culture (Mehmood et al., 2019). Because throughout this project the LCMSMS AA analysis method was being developed after installation at the University, only data from the same runs were ever compared directly. For other projects using an established framework for LCMSMS analysis, there should be less potential issues with varying AA values between different LCMSMS

runs. This variation can additionally be mitigated by incorporating a standard reference material in each run and correcting the values of quantified AAs accordingly.

Overall, the apparent stability of the AA profile of *F. venenatum* is a promising outcome from the perspective of mycoprotein production as it supports the possibility of alternative growth regimes (at least as regards AA profile), e.g., incorporation of more sustainable components such as waste/side streams into the growth media. It is also promising for the work in the later chapters of this project which looks at deliberate manipulation of the AA profile of the fungus – because the profile is generally stable it should be easier to identify changes specifically induced by experimental treatments. However, it is worth pointing out that in each case where changed growth condition affects or not the AA profile of *F. venenatum*, additional tests in continuous fermentation cultures should be carried out if to extrapolating the results to industrial production, as flask culture versus fermenter may not give the same outcomes in every test scenario.

2.5.3 Limitations and future work

The reproducibility of measurements from the flask cultures method could be optimised by considering OD measurements that directly reflect real-time growth in each flask culture as suggested in **2.5.1.** This would reduce materials usage and workload by removing the need for creating growth curves by extracting total biomass from flask cultures at multiple points. Additionally, ability to select the growth points more precisely could increase sensitivity to pick up any genuine changes to the AA profile.

The total AA content of an organism is the sum of the free AAs and all the AAs contained in all the proteins of the cells. By performing a proteome analysis and identifying proteins that are most abundantly expressed within cells, it is possible to develop a picture of which proteins are mainly responsible for the AA profile of *F. venenatum* (Carberry and Doyle, 2007). This could be used to predict AA changes in different growth conditions according to anticipated changes to regulation of metabolic pathways (Wang et al., 2021) and proteome composition (Kolkman et al., 2006). Work in this chapter focused solely on the AA composition of the *F. venenatum.* However, to obtain the full picture of physiological differences of the organism between flask culture and airlift fermentation other factors of course need to be taken into consideration, including (but not limited to) lipid profiles (Grapes et al., 1989), vitamin and micronutrient content (Md Noh et al., 2020) or hyphal morphology (Riquelme et al., 2018). In addition, the mycoprotein digestibility assays (Bryan et al., 2018**)** need to be in place if bioavailability of nutrients in any modified product is a concern. Overall, setting up a standardised framework for monitoring all the nutritional and sensory aspects not only of *F. venenatum* but also other single cell protein candidate organisms will help to assess the stability of microbial food sources under varying conditions.

3 Chapter 3 - Investigation of the AA composition of *F. venenatum* c-variant mutants

3.1 Introduction

The process of continuous fermentation used for production of *F. venenatum* mycoprotein puts selective pressure on the organism that results in the selection of morphologically distinct variants (Wiebe et al., 1994a; Withers et al., 1994). In *F. venenatum* continuous growth in high glucose conditions, after 500-1000 h results in the reproducible emergence and replacement of the wild type *F. venenatum* with a specific morphological colonial variant (C-variant) (**Figure 3.1**) (Wiebe et al., 1994a; Wiebe et al., 1994b; Trinci, 1992). This phenomenon is not limited to *F. venenatum* as emergence of morphologically distinct variants in continuous cultures has been described in *Aspergillus niger* and *Aspergillus nidulans* (Swift et al., 2000) and *Aspergillus oryzae* (Withers et al., 1994). The emergence of these morphologically distinct variants is the result of selection of mutations that increase maximum specific growth rate in the absence of nutrient limitation and/or decrease the saturation constant (the concentration of nutrient that supports half-maximal rate of growth) of the organism (Trinci, 1992). The short hyphae, a result of the highly branched morphology of these so-called C-variants of *F. venenatum* does not produce the desirable strand like structure of mycoprotein that mimics the texture of meat, although the nutritional quality is reportedly unchanged (**Figure 3.1**). Due to the emergence of the C-variant during mycoprotein production the fermentation process is routinely stopped after around 1000 hours to maximise the mycoprotein yield before the c-variant accumulation affects the sensory properties of mycoprotein, with the process then restarted after cleaning and sterilisation of the fermenter which causes a down-time in production (Whittaker, 2022). Because of this there is an interest in stopping or delaying the emergence of C-variant. In the past, co-culture of different *F. venenatum* strains during the fermentation has been employed as this increased the time before emergence of the C-variant (Wiebe et al., 1994a; Wiebe et al., 1994b). A more recent approach aimed to exploit insights gained by identifying the mutations that accumulate in the *F. venenatum* genome and which give rise to the C-variant phenotype, a task made feasible following the sequencing of the *F. venenatum* genome (King et al., 2018). A previous project (Connel, J., NIAB, unpublished data) identified a group of mutations in 19 C-variant isolates and current efforts aim to understand which genes are important in control of hyphal branching and growth and could offer opportunities for improving the strain robustness (UKRI, 2023). Another idea has been to utilise product arising from the C-variant for the pet food market (R. Johnson, Marlow Foods Ltd. pers.comms.) as reportedly the AA profile of the C-variant is not different to that of the wild type (Trinci, 1994). In use as pet food the heating step designed to lower the amount of RNA in the mycelium could probably be foregone as, unlike apes, the majority of animals possess uricase enzymes that allow for metabolism of higher levels of dietary RNAs (Li et al., 2022).

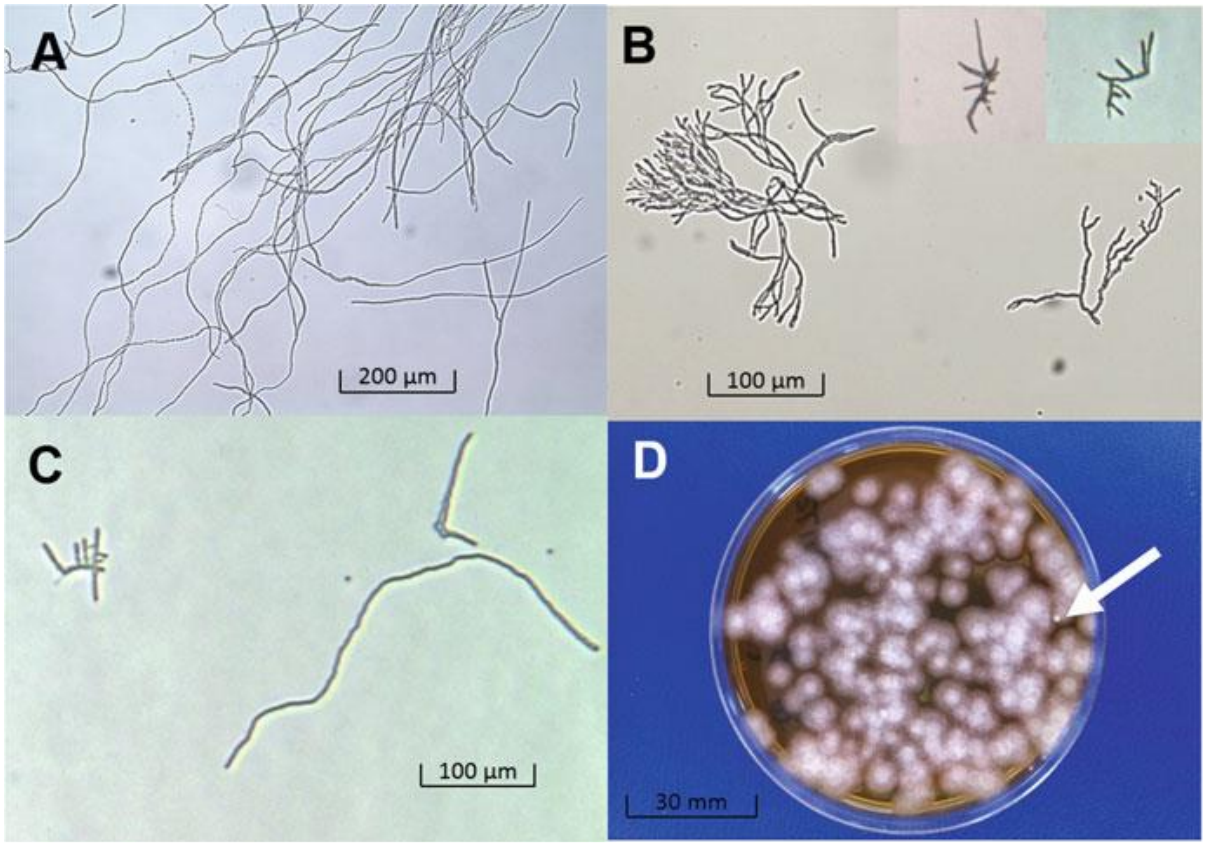

Figure 3.1 Morphology of *Fusarium venenatum* variants visualised under microscope (A-C) or on agar (D). A) Standard morphology of *F. venenatum (*A-variant). B) Morphological mutant (C-variant) with decreased hyphal and internodal length, increased branching frequency. C) direct comparison between C-variant (left) and A-variant (right). D) agar plate (90 mm) after incubation at 25 ºC for 48 hours, showing wild type colonies of *F. venenatum* in addition to the morphological mutant indicated by the white arrow. Figure taken from (Whittaker et al., 2020)

3.2 Chapter Aims

As mentioned in the introduction the emergence of the c-variant negatively affects the texture of mycoprotein and results in loss of productivity. Here using genotyped C-variant isolates from another study the aim is to:

1. Investigate the branch chain amino acid (BCAA) profile in hydrolysates in *F. venenatum* C-variant isolates with known mutations in BCAA catabolism linked genes.
2. To assess the broader AA profiles of *F. venenatum* C-variants, including in hydrolysates and free AAs of the mycelium.

3.3 Methods

3.3.1 Procurement and maintenance of *F. venenatum* C-variant strains

C-variant isolates (C1-19) (**Table 3.2Error! Reference source not found.**) were sent from NIAB (East Malling, UK) on agar plates sealed with parafilm. Agar samples with colonies were cut out with a sterile scalpel and diced into small pieces before using these as inoculum to RHM medium adjusted to 10% of the normal NH_4Cl content. Flasks were sampled between 5-15 days for the presence of macroconidia. Where the presence of macroconidia was confirmed, the culture was filtered through a 40 µm cell strainer and centrifuged at 4000x g. The supernatant was removed, and spores resuspended in 0.1 % Tween 80 with 10 % glycerol, flash frozen in liquid nitrogen and kept at -80 ºC for further use.

3.3.2 Culture growth

Baffled flasks (250 ml) were filled with 50 ml of standard RHM medium containing 3% glucose. The medium was inoculated with 10,000 spores/ml of medium. The cultures were incubated with orbital shaking at 150 rpm at 28 ºC.

3.3.3 Sample preparation

Preparation of samples for hydrolysate LCMSMS analysis was carried out as described in **Chapter 2 (2.3.8).**

3.3.4 Analysis of free AA by LCMSMS

Preparation of reagent stocks: A solution of 20 mM ammonium formate pH 2.75 was prepared as described in **Chapter 2 (2.3.9)**. An internal standard cell-free amino acid mixture (ISTD CFSIL) labelled with stable isotopes: ^{13}C and ^{15}N : 1/4000 dilution was prepared by diluting 0.25 ml of CFSIL (5-100 mM in water, concentrations of individual AAs vary and are as described on Sigma-Aldricht website, product ID: 767964) in 975 ml of 20 mM ammonium formate pH 2.75 buffer in a volumetric flask. A 30 % (w/v) solution of 5-sulphosalicylic acid (SSA) (Merck, UK, Cat No 15640900) was prepared by dissolving 30 g of SSA in 80 ml of 20 mM ammonium formate pH 2.75 then making up to volume in a 100 ml volumetric flask. Stock was stored at 4 ºC.

Amino acid standard solutions:

Physiological amino acids standard containing **acidic** and **neutral** amino acids (**PAN)** for calibrating amino acid analysers (Cat. No. A6407) in 0.1 N HCL contained: 2.5 µmol/ml each of β-alanine; L-Alanine; L-α-aminoadipic acid; L-α-amino-n-butyric acid; D,L-β-aminoisobutyric acid; L-asparginine; L-aspartic acid; citrulline; cystathionine; L-cystine; L-glutamic acid; glycine; hydroxy-L-proline; L-isoleucine; L-leucine; L-methionine; L-phenylalanine; O-phospho-L-serine; O-Phospo-ethanolamine; L-proline; L-sarcosine,; L-serine; taurine; L-threonine, L-tyrosine; L-valine, and 1.25 µmol/ml of L-cystine.

Physiological amino acids standard containing **basic** amino acids (**PB**) for calibrating amino acid analysers (Sigma. Cat. No. A 1585) in 0.1 N HCl contained each: 2.5 µmol/ml of γ-amino-

n-butyric acid, ammonium chloride, L-arginine, L-carnosine, ethanolamine, L-histidine, δ-hydroxylysine, L-lysine, 1-methyl-L-histidine, 3-methyl-L-histidine, L-ornithine and 1.25 µmol/m of L-anserine and L-homocysteine.

A concentrated solution of L-glutamine was prepared by dissolving 0.7305 ± 0.0001 g in 100 ml 20 mM ammonium formate buffer pH 2.75, transferred to a 500 ml volumetric flask and made up to volume with the ammonium formate buffer. A concentrated solution of D-tryptophan was prepared by dissolving 0.1021 ± 0.0001 g transferred to a 500 ml volumetric flask and made up to volume with ammonium formate buffer.

Calibration and internal standard preparation

A standard solution for calibration purposes was prepared by mixing 80 µl each of the PAN and PB standards (above) and 20 µl each of the concentrated solutions of D-tryptophan and L-glutamine, resulting in final concentration of 1000 µM of each amino acids (500 µM each for L-cystine, L-anserine and L-homocysteine). Standards were then diluted with 20 mM ammonium formate buffer pH 2.75 according to **Table 3.1**. Finally, 50 µl of each standard dilution was transferred to HPLC vials and 5 µl of 30% SSA solution and 450 µl of 1/4000 CFSIL were added.

Table 3.1 Concentrations of AA standards used for calibration of LCMSMS for detection. The concentration column describes the µM concentration of each AA in the AA standard mix (L-Alanine; L-α-aminoadipic acid; L-α-amino-n-butyric acid; D,L-β-aminoisobutyric acid; L-asparginine; L-aspartic acid; citrulline; cystathionine; L-cystine; L-glutamic acid; glycine; hydroxy-L-proline; L-isoleucine; L-leucine; L-methionine; L-phenylalanine; O-phospho-L-serine; O-Phospo-ethanolamine; L-proline; L-sarcosine,; L-serine; taurine; L-threonine, L-tyrosine; L-valine, γ-amino-n-butyric acid, ammonium chloride, L-arginine, L-carnosine, ethanolamine, L-histidine, δ-hydroxylysine, L-lysine, 1-methyl-L-histidine, 3-methyl-L-histidine, L-ornithine, L-Glutamine, D-Tryptophan) *with exception of L-cystine, L-anserine and L-homocysteine for which the concentration is always ½ of the value indicated in the table.

Standard number	Concentration of individual AAs*(µM)
1	0
2	40
3	80
4	120
5	160
6	200
7	400
8	600
9	800
10	1000

Sample preparation

The free AAs were extracted as previously described in **Chapter 2 (2.3.13).** The free AA extract samples were cooled to 4 ºC and 10 µl of 30% SSA was added for every 100 µl of free AA extract. The samples were vortexed for 30 s, incubated on ice for 30 min and centrifugated at 21130 g for 5 min. The supernatant was filtered through a 0.2 µm filter and diluted as needed (usually 1:1) with 20 mM ammonium formate pH 2.75. An aliquot (55 µl) of the sample was then transferred to a HPLC vial and 450 µl of CFSIL 1/4000 was added. 1 µl of sample was used for injection in LCMSMS analysis.

LCMSMS conditions

The running conditions and apparatus were the same as described in **Chapter 2 (2.3.10).**

3.4 Results

3.4.1 Acquisition and selection of mutants

In other projects co-sponsored by Marlow Foods, nineteen *F. venenatum* A3/5 c-variant isolates that arose from independent fermentation cycles have been genome sequenced and mutations in 26 different genes were identified across these 19 isolates. Seven of the most prevalent mutations were present in 15 or more out of 19 genotyped strains (**Table 3.2)**. Another two types of mutation were present in 9 and 7 out of all isolates, with remaining mutations appearing in only 1 to 4 out of all genotyped strains. One mutation of interest for this project was a SNP in gene '3588'. This gene is predicted to encode the alpha subunit of 2-oxoisovalerate dehydrogenase, which participates in the degradation of the branch chained amino acids (BCAA) leucine, isoleucine and valine (Ævarsson et al., 1999). Another gene of interest was gene 1654, suspected to encode methylmalonate semialdehyde dehydrogenase (I. Geoghegan, pers. comms.) which is another enzyme involved in BCAA degradation (Sokatch et al., 1968). A SNP in gene 3558 was present in two of the 19 c-variant isolates, while a SNP in gene 1654 occurred in 17 out of the isolates 19 strains. In both cases, mutation to each of these genes was limited to a single, common SNP across the isolates (**Table 3.2**) Three isolates were selected for AA analysis: isolate C4, containing the SNP in gene 3558 but not gene 1654; isolate 11, containing the SNP in 1654 but not 3558; isolate C5 containing both the SNPs in both genes. It should be noted that these three isolates also contained mutations in other genes from **Table 3.2**. The three mutants all contained mutations in genes 1595, 3891, 4254, 9757, 12587, in addition C4 and C5 had mutations in 2745, 3465, C5 and C11 in 1942, and C5 in 9315, 8011, 11498 and C11 in 1483.Because of this any differences between the AA profiles cannot by ascribed to the mutations in genes 3558 and 1654 that informed the choice of isolates.

Table 3.2 Mutations previously identified from genome sequencing of a set of *F. venenatum* c-variants isolated from commercial fermentations. Each of the 19 isolates arose from independent fermentation cycles (unpublished sequencing results kindly provided by John Connell (NIAB) via Ivey Geoghegan (Marlow Foods); gene functions were determined from BLAST searching using AA sequences derived from the *F. venenatum* genome sequencing).

Gene number	Number of different SNPs	Number of isolates with mutation (out of 19)	Predicted protein function (*F. venenatum*)
2745	6	7	Hypothetical protein
2243	5	4	Hypothetical protein
3465	4	4	Rho-type GTPase-activating protein 1 (*F. langsethiae* 98.61%)
4254	4	15	Hypothetical protein
203	3	1	Uncharacterized protein
1942	3	15	Hypothetical protein
7536	3	2	Putative amino acid-n-acetyltransferase (*F. flagelliforme* 97.48%)
9315	3	1	Pectin lyase precursor (*F. oxysporum* 97.33%)
1483	2	9	Hypothetical protein
4774	2	4	Uncharacterised protein
5882	2	2	N amino acid transport system protein (*F. culmorum* 99%)
9657	2	17	Vegetative incompatibility protein HET-E-1
1595	1	19	Small GTPase rab family (*F. sporotrichioides* 99.03%) Hypothetical protein
1654	1	17	Hypothetical protein
2208	1	2	Hypothetical protein
3588	1	2	2 – oxoisovalarate dehydrogenase subunit alpha
3891	1	19	SERAC1 (*F. oxysporum* 83.93%)
4995	1	2	Catalase-peroxidase 2
5018	1	1	Hypothetical protein
5477	1	1	Heterokaryon incompatibility protein-domain-containing protein
5796	1	1	Vitamin H transporter (*F. culmorum* 98.34%)
8011	1	2	S-adenosyl-L-methionine-dependent methyltransferase
10099	1	1	Serine/threonine-protein kinase CLA4
11498	1	1	Fungal-specific transcription factor domain-containing protein
12523	1	1	Hypothetical protein
12587	1	16	Hypothetical protein

3.4.2 Growth of C variant mutants in flask cultures

The growth curve of *F venenatum* mutants C4, C5 and C11 was examined in RHM medium in 250 ml baffled flasks. Biomass was sampled at intervals and weighed after freeze drying (as described in **2.3.2** and **2.3.3**). Baffled flasks were used for growth as it had been found that the C-variants do not grow well in microplate reader conditions (I. Geoghegan, Marlow Foods Ltd., pers. comms.). The glucose content of the RHM medium was increased to 3 % for these experiments (1% is standard) as 3 % glucose was the condition in which these mutants evolved and they grow poorly in RHM medium containing 1 % glucose (**Appendix Figure 3).** In RHM medium with 3 % glucose content the C-variant mutants grew at a rate similar to that of the WT (**Figure 3.2 A)**. The growth in C-variants was slightly faster which is expected from a morphological mutant that outcompetes WT *F. venenatum* in continuous culture by achieving higher growth rate. This is evidenced by on average lower doubling times between 24 and 36 h for mutants C4 and C5 (Kruskall-Wallis test, $p = 0.0108$, no significance from multiple comparisons analysis), as well as higher doubling times between 30 – 36 h of growth (Kruskall-Wallis test: $p = 0.0382$, Dunn's multiple comparisons: WT vs C5, $p = 0.0287$) indicating that C-variant mutants in flask cultures got closer to achieving stationary growth phase at 36 h (**Figure 3.2 B)**. Samples extracted at 36 h were selected for further hydrolysation and AA analysis.

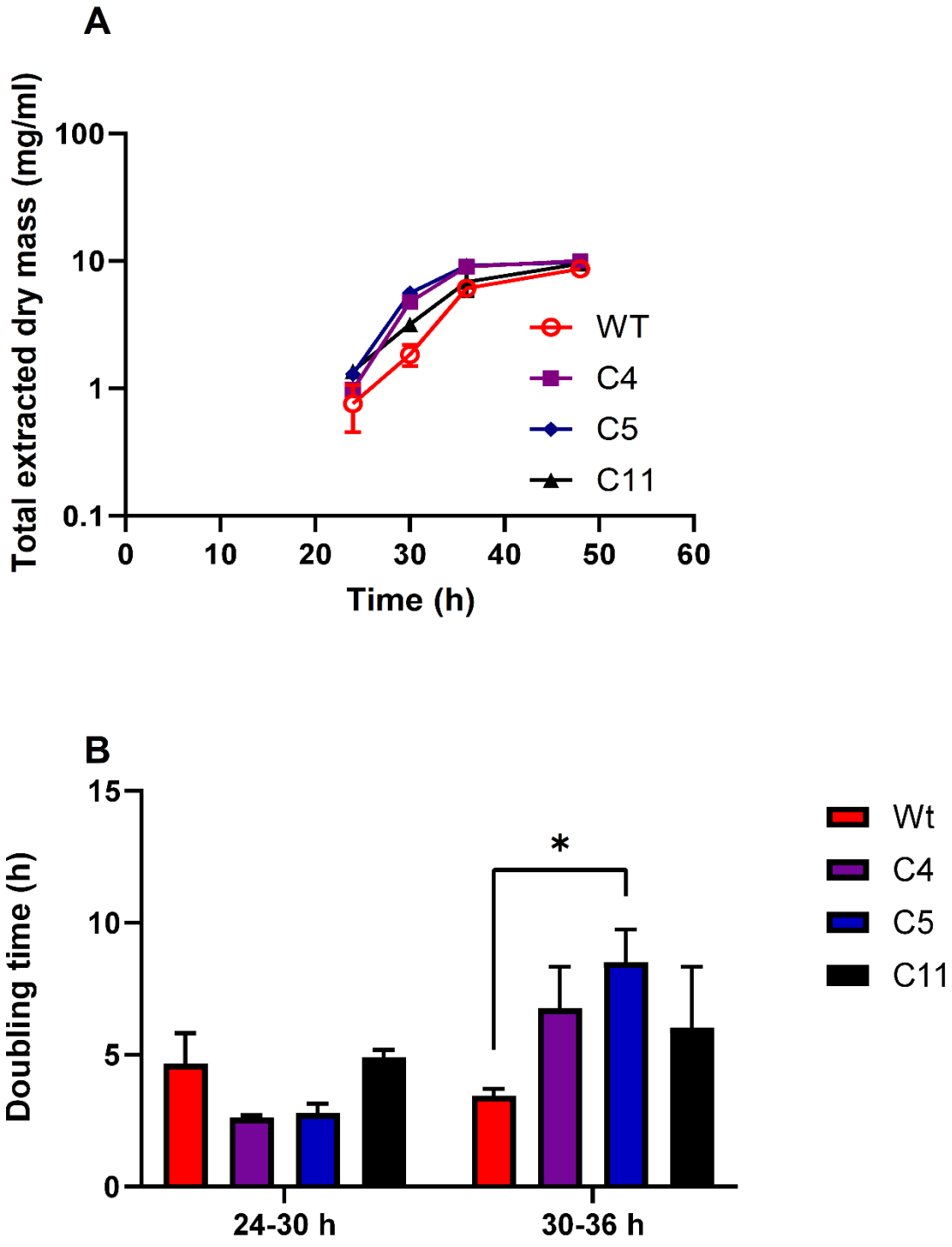

Figure 3.2 Growth curves of *F. venenatum* C variant isolates in flask cultures. A) RHM medium containing 3 % glucose was inoculated with 10,000/ml of spores and 50 ml of the suspension was deposited into 250 ml baffled flasks and incubated at 28° C with shaking (150 rev/min). The biomass was extracted at 24, 30, 36, 48 h. B) Doubling times were compared using Kruskall-Wallis test with Dunn's multiple comparisons for 24-30 h (H = 8.436, df = 3, p = 0.0108) for 30 – 36 h (H = 7.205, df = 3, p = 0.0382, Dunn's multiple comparisons WT vs C5 p = 0.0276) Data points indicate mean average, ± SD, n = 3.

3.4.3 The AA profile of C-variant mutants C4 and C5

The AA profile of hydrolysate from the C variant isolates 4, 5 and 11 was compared to the hydrolysate AA profiles of WT samples. Analysis of the PC1-2 in sets 1 ($p = 0.62$, $p = 0.98$, respectively) and 2 ($p = 0.24$, $p = 0.09$, respectively) showed no significant differences in the overall AA levels between the WT and mutants as well as no difference in the relative abundance of Ala, Asp Gly and Pro vs His and Val (**Table 3.3**). One-Way ANOVA analysis of the PC3 for the set 1 revealed a statistical difference between the datasets ($p = 0.0164$), with Tukey's multiple comparisons revealing a significant difference in PC3 between the WT and C4 mutant ($p = 0.016$) and for set 2 there was a nearly significant difference in the PC3 values of WT and C5 mutant ($p = 0.0526$). In both cases the values of PC for the mutants C4 and C5 were more negative indicating a relative decrease in the Cys to Leu, Gly and Asp. The absolute and relative data of the AA profiles are presented in (**Table 3.3**, **Appendix Table 8**). There was no clear indication of BCAA-specific changes in the mutants versus the wild type. A decrease in cysteine content was common between the three variants, with an average ~40% drop in the cysteine contents (**Figure 3.3**), this was corroborated by the significant difference between the PC3 values from WT and C4 mutant and of potential interest to the industrial collaborators (I. Geoghegan, Marlow Foods Ltd., pers.comms.). In C5 there was also an indication (from the absolute values, albeit not measured by the PCA) of lowered content methionine content and overall drop in levels of all AAs compared to WT (**Table 3.3**, **Figure 3.3**). This again was of interest to industrial partners and led to the mutant C5 begin chosen for further analysis.

Table 3.3 The AA profiles of hydrolysates from C-variant mutants. All the samples were produced by growth in flask cultures in RHM medium with 3 % glucose and extraction 36 h after inoculation. Values of amino acids are expressed as g/kg of dry mass ± SD. The bottom three rows indicate the principal component values ± SD. The PC1-3 from different treatments were compared by One-Way ANOVA (F = 0.5199, df = 2, p = 0.6236; , F = 0.0231, df = 2 p = 0.9773; F = 10.438, df = 2, p = 0.0164) respectively for the set 1 and (F = 1.8887, df = 1 p = 0.2413; F = 5.1246, df = 1, p = 0.0863; F = 7.4407, df = 1, p = 0.0527) respectively for the set 2. Different letters in superscript in the last three rows indicate statistically significant difference between values derived from One-Way-ANOVA with Tukey's multiple comparisons. Lack of any superscript letters indicates lack of significant difference within the relevant part of a row.

	Set 1			Set 2	
	WT (n = 3)	**C4 (n = 3)**	**C11 (n = 2)**	**WT (n = 3)**	**C5 (n = 3)**
Ala	**36.05 ±1.94**	**31.76 ± 3.65**	**35.18 ± 0.17**	**45.73 ± 7.08**	**35.36 ± 4.21**
Arg	**32.42 ± 0.62**	**30.77 ± 4.16**	**33.83 ± 0.04**	**31.21 ± 0.64**	**27.61 ± 3.26**
Asp	**50.11 ± 0.72**	**53.30 ± 13.47**	**53.05 ± 2.99**	**45.41 ± 1.18**	**45.04 ± 3.81**
Cys	**2.88 ± 0.03**	**1.93 ± 0.21**	**2.03 ± 0.11**	**2.20 ± 0.36**	**1.47 ± 0.57**
Glu	**77.26 ± 4.05**	**62.01 ± 5.54**	**78.60 ± 3.75**	**75.54 ± 1.48**	**63.93 ± 7.92**
Gly	**21.29 ± 1.33**	**29.02 ± 10.93**	**27.04 ± 3.29**	**18.78 ± 0.75**	**19.05 ± 3.57**
His	**12.60 ± 0.39**	**11.40 ± 2.26**	**12.03 ± 0.14**	**9.95 ± 0.32**	**8.32 ± 1.66**
Ile	**21.89 ± 0.91**	**19.53 ± 2.90**	**23.94 ± 1.00**	**23.09 ± 0.74**	**20.22 ± 2.77**
Leu	**34.75 ± 0.74**	**34.62 ± 6.81**	**39.72 ± 1.18**	**33.99 ± 0.22**	**30.67 ± 4.08**
Lys	**39.13 ± 1.00**	**36.18 ± 6.04**	**38.18 ± 0.74**	**35.23 ± 0.70**	**32.45 ± 3.27**
Met	**11.36 ± 0.25**	**11.57 ± 2.80**	**11.73 ± 0.04**	**11.29 ± 1.03**	**9.78 ± 1.30**
Phe	**20.08 ± 0.22**	**17.09 ± 2.60**	**19.22 ± 0.02**	**19.10 ± 0.65**	**17.73 ± 1.87**
Pro	**20.05 ± 0.40**	**17.47 ± 1.95**	**20.10 ± 0.54**	**19.04 ± 0.60**	**18.19 ± 1.76**
Ser	**15.94 ± 0.64**	**15.47 ± 3.82**	**16.47 ± 1.07**	**16.30 ± 0.42**	**15.78 ± 2.34**
Thr	**29.30 ± 0.63**	**26.56 ± 6.17**	**26.30 ± 0.54**	**21.01 ± 1.54**	**18.84 ± 1.91**
Tyr	**10.52 ± 0.35**	**9.24 ± 1.58**	**10.80 ± 0.16**	**12.21 ± 0.50**	**11.59 ± 1.52**
Val	**25.59 ± 0.59**	**22.50 ± 3.47**	**26.30 ± 0.39**	**31.46 ± 1.19**	**29.75 ± 4.70**
Total	**461.21 ± 11.89**	**430.39 ± 70.18**	**474.52 ± 3.06**	**451.54 ± 4.43**	**405.75 ± 47.41**
PC1	**1.85 ± 0.38**	**0.52 ± 3.2**	**2.2 ± 0.1**	**1.00 ± 0.3**	**- 0.6 ± 2.0**
PC2	**1.04 ± 0.1**	**1.13 ± 1.1**	**1.17 ± 0.2**	**0.52 ± 0.1**	**- 0.9 ± 0.4**
PC3	**0.91 ± 0.06^{A}**	**- 0.71 ± 0.6^{B}**	**-0.32 ± 0.5**	**0.46 ± 0.4**	**- 0.34 ± 0.31**

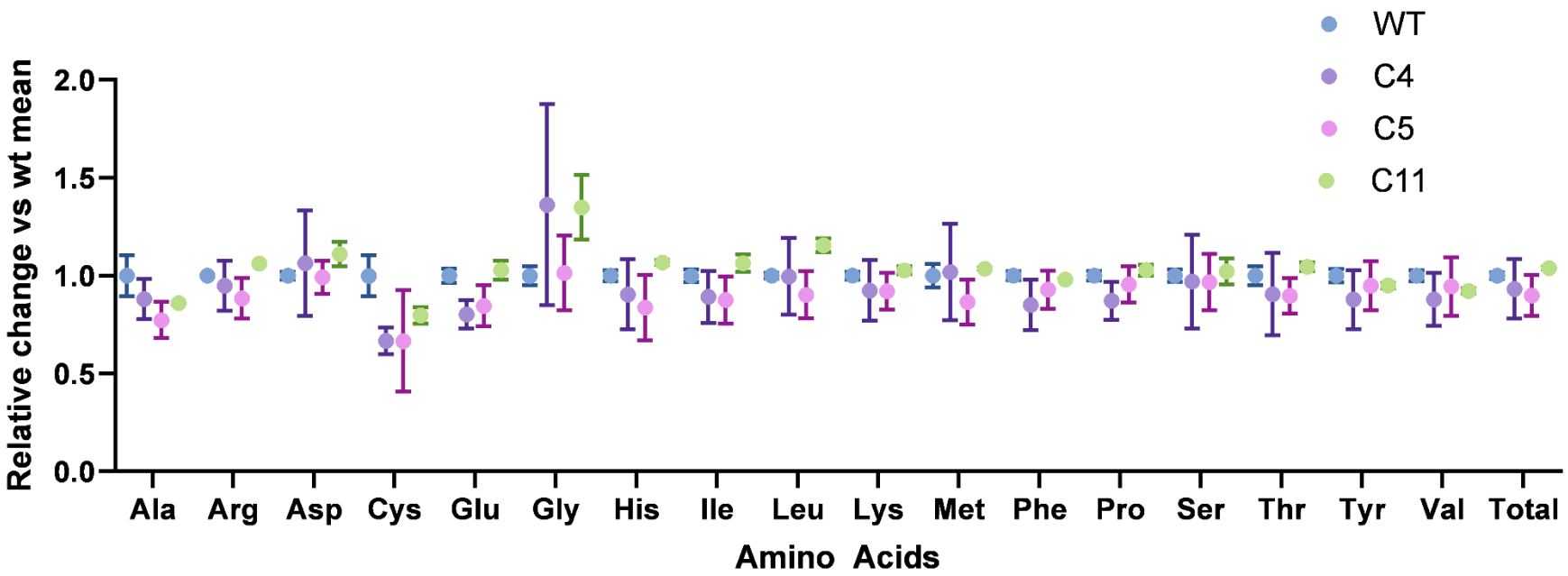

Figure 3.3. Relative differences versus wild type in absolute AA amounts in C-variant mutants C4 and C5. The datapoints are expressed as a fold change relative to the mean of absolute AA values from WT *F. venenatum* biomass hydrolysate extracted from flask cultures at 36 h (**Table 3.3**) WT, n = 6 ; C4 and C5, n = 3; C11, n = 2. Values are derived from the data in Table 3.3.

3.4.4 Changes to free AA profile in the C5 isolate.

To further investigate changes to AA composition in the C-variants, free AA profiles were examined. The C5 variant was selected for this as it had the most significantly altered hydrolysate AA profile. A physiological free-AA standard containing 41 AAs was used for the free AA analysis (18 AAs were used as calibration standard for LCMSMS analysis of hydrolysate). This was in order to be able to assay a wider range of the free AA pools. The absolute free-AA profile of the C5 isolate overall was different to that of the wild type (2-Way ANOVA, $p < 0.0001$). Regarding specific amino acids, the C5 variant had 47 %, 76 % and 92 % lower amounts of methionine, aspartate and taurine, but a >10-fold greater amount of glutamine (multiple t-test, $p < 0.0001$, $p = 0.0001$, $p < 0.0001$ respectively, **Table 3.4**). In addition, similar to the observation made between the hydrolysate AA profiles, the levels of free cysteine were lower in the C5 variant, where they were not measurable. It was noted that AAs which are substrates in the transsulphuration pathway (Ripps and Shen, 2012) (cystine, cystathionine, methionine, taurine, glycine) were all present at a lower abundance in the free form (decreased by 41, 47, 36, 92 % respectively, excluding cystine) in the C5 variant compared to the WT.

Table 3.4. Comparison of the free AA profiles of wild type and C-variant C5 isolate of *F. venenatum*. The values in the table are expressed as g of free AA per kg of dry weight biomass. The data were analysed by multiple unpaired T-test (df = 4) with false discovery rate of 1 % and significance threshold at $p < 0.01$. *Cystine peaks were present on the chromatograph, but the area was too small to quantify reliably being outside of the calibration range. Different letters in superscript between cells in the same row indicate statistically significant difference between values derived the multiple T-test. Lack of any superscript letters indicates lack of significant difference within a row.

	WT 30 h	C5 30 h	Fold Change in abundance relative to WT
α-aminoadipic acid	0.45 ± 0.04	0.51 ± 0.03	1.14
α -aminobutyric acid	0.20 ± 0.00	0.19 ± 0.01	0.93
Alanine	4.97 ± 0.55	4.82 ± 0.41	0.97
Arginine	2.35 ± 0.03	2.64 ± 0.50	1.13
Asparagine	0.51 ± 0.01 [a]	0.27 ± 0.08 [b]	0.54
Aspartate	2.28 ± 0.17 [a]	0.55 ± 0.10 [b]	0.24
β-Alanine	0.04 ± 0.01 [a]	0.02 ± 0.00 [b]	0.51
Citrulline	0.26 ± 0.02	0.37 ± 0.05	1.42
Cystathionine	0.27 ± 0.03 [a]	0.16 ± 0.01 [b]	0.61
Cystine	0.06 ± 0.01	N/D *	N/A
Ethanolamine	0.48 ± 0.02	0.51 ± 0.03	1.05
γ-aminobutyric acid	0.94 ± 0.32	0.13 ± 0.02	0.14
Glutamate	31.34 ± 2.10	30.74 ± 0.73	0.98
Glutamine	0.14 ± 0.03 [a]	1.38 ± 0.25 [b]	9.86
Glycine	0.82 ± 0.04	0.52 ± 0.15	0.64
Histidine	0.70 ± 0.10	0.53 ± 0.06	0.76
Hydroxy-proline	0.06 ± 0.01	N/D	N/A
Isoleucine	0.19 ± 0.02	0.15 ± 0.01	0.76
Leucine	0.22 ± 0.02	0.15 ± 0.03	0.7
Lysine	0.69 ± 0.04	0.58 ± 0.04	0.85
Methionine	0.34 ± 0.01 [a]	0.18 ± 0.01 [b]	0.53
Ornithine	1.83 ± 0.24	1.92 ± 0.32	1.05
Phenylalanine	0.32 ± 0.02 [a]	0.18 ± 0.00 [b]	0.55
Phosphoethanolamine	0.05 ± 0.00	0.06 ± 0.01	1.34
Phosphoserine	0.05 ± 0.00 [a]	0.02 ± 0.00 [b]	0.47
Proline	0.61 ± 0.02	0.79 ± 0.04	1.29
Serine	1.61 ± 0.05 [a]	1.12 ± 0.04 [b]	0.7
Taurine	7.23 ± 0.56 [a]	0.57 ± 0.10 [b]	0.08
Threonine	1.97 ± 0.06	2.03 ± 0.08	1.03
Tryptophan	0.12 ± 0.01 [a]	0.06 ± 0.00 [b]	0.51
Tyrosine	0.15 ± 0.00 [a]	0.08 ± 0.00 [b]	0.57
Valine	0.90 ± 0.06	1.02 ± 0.05	1.13
Total	62.15 ± 2.56	52.30 ± 0.87	0.84

3.5 Discussion

3.5.1 General conclusions

The work in this chapter was carried out at the request of our industrial partners who in one of their other projects identified mutations to genes involved in BCAA metabolism in some of the C-variant mutants that evolved during continuous fermentation process during routine mycoprotein production. The AA analysis did identify some changes between the AA profiles of 3 tested C-variant mutants and the WT but these were not specific to the BCAAs. From the three tested mutants, only C5 had a significantly different absolute AA profile to the WT (**Table 3.2**). However, the other two mutants did exhibit changes in the levels of particular amino acids relative to WT and these were mostly similar between the C4, C5 and C11 mutants, with methionine being exception and lower only in the C5 mutant, this change was not statistically significant but of interest to our industrial partners which prompted further investigation (I. Geoghegan, Marlow Food Ltd., pers. comms.) (**Figure 3.3**).

The comparison of the free AA profiles of the C5 mutant and WT did not exactly reflect the changes observed with the hydrolysate. The levels of free glutamate and alanine were comparable in free AA pools, but lower in the hydrolysate in the case of isolate C5 (**Table 3.3**, **Table 3.4**). The free aspartate was 76 % lower in free AA pools of the C5 isolate versus WT, but the aspartate level was comparable in their hydrolysates. Such discrepancy between the hydrolysate and free aspartate levels could suggest higher incorporation of aspartate into proteins or increased loss from cells in the C5 variant; a proteomic analysis or aspartate-radiotracing assay could help to distinguish such possibilities.
Due to our industrial partner interest further focus was placed on the observed non-significant decrease in cysteine and methionine (substrates of the transsulphuration pathway (Ripps and Shen, 2012)) appeared 43 and 13 % lower in the C5 isolate than WT hydrolysates, while in free AA pools detectable substrates of the transsulphuration pathway were all lowered in the C5 mutant, with a statistically significant 92 % decrease in taurine. Aside from the taurine, there were no significant differences between the levels of other substrates of transsulphuration. Up and downregulation of the transsulphuration pathway in *Aspergillus flavipes* was shown to change fungal morphology and dramatically alter protein expression (El-Sayed et al., 2015). In other examples differences, in methionine biosynthesis may also occur upon morphological transformation of fungal cells e.g. *Blastomyces dermatitidis* in a non-pathogenic mycelial form are cysteine prototrophs but lose the ability to synthesise cysteine in their pathogenic yeast form (Jastrzebowska and Gabriel, 2015). Additional experiments, e.g. transcriptomic analysis would be necessary to support any suggestion whether the whole pathway may be downregulated in the C5 mutant.

As described earlier, the isolates for the present analysis were selected based on the presence or absence of known mutations in genes 1654 and 3558, predicted to encode methylmalonate semialdehyde dehydrogenase and 2–oxoisovalarate dehydrogenase subunit alpha, respectively. The C5 isolate that showed significant change to its AA profile bore mutations in both genes whereas the C11 and C4 isolates had a mutation in either 1654 or 3558, respectively. This however is not enough to ascribe the phenotype to these mutations as multiple other mutations are present. The main interest in the 1654 and 3558 gene mutations was to see whether these affect BCAA synthesis and consequently impact the BCAA content in the AA profile of the mutant. Methylmalonate semialdehyde dehydrogenase (1654) was shown, among other functions to have role in cell growth and regulation BCAA catabolism

and synthesis in *Magnaporthe oryzae* and 2–oxoisovalarate dehydrogenase subunit alpha (3558) was shown to be essential for BCAA catabolism in *Aspergillus nidulans* (Norvienyeku et al., 2017; Maggio-Hall et al., 2008). However, BCAA levels in the mutants were not significantly altered. Analysis of both hydrolysate and free AA profiles of more C variant isolates could help to establish any general trends of change to AA profiles in these mutants. C-variant rich biomass is currently not used as a source of mycoprotein but plans exist to utilise it e.g. as a pet food where sensory component of the product is not that important (Johnson, R. pers. comms.) – in this case however the AA profile of C-variants needs to be monitored to ensure continued high nutritional value. Additionally, morphological growth and virulence in fungi are interconnected with activity of AA metabolic pathways. The understanding the changes to expression of major pathways in C-variant might give valuable clues as to what underlying change drives the formation of C-variant morphologies (Jastrzebowska and Gabriel, 2015; Beremand et al., 1988; Subramaniam et al., 2015).

3.5.2 Presence of taurine in *F. venenatum*

Taurine is one of the most abundant AAs found in humans and other eukaryotes, but it is not used in protein synthesis. Nevertheless, it is considered conditionally essential in humans and an essential amino acid in cats. In humans it can be synthesized from cysteine but a lot of taurine is obtained through the diet (Redmond et al., 1998), being present in high concentrations in mussels, clams, shellfish, turkey and dark chicken meat (Spitze et al., 2003). Taurine is increasingly thought to have important cellular roles in humans and animals, e.g., antioxidant properties, cell membrane stabilisation and a role in the production of bile acids (Ripps and Shen, 2012; Bae et al., 2022), and is generally considered beneficial in human nutrition (Lourenço and Camilo, 2002). Taurine deficiencies are linked to a variety of disorders, such as obesity, hypertension, defects in neurotransmission and development. A recent study also identified taurine deficiency as a driver of ageing in worms, mice and monkeys (Singh et al., 2023b).

The presence of taurine in *F. venenatum* was previously not known (T Ingmire, Marlow Foods Ltd., pers. comms.) so its discovery in the free AA profile of *F. venenatum* may be considered a factor adding to the nutritional quality of the mycoprotein. The levels of taurine detected here in wild type *F. venenatum* are comparable to meats rich in taurine (7.23 vs 7.77 g/kg taurine for *F. venenatum* vs ground turkey meat fried with juices) and higher than others (0.61 g taurine per kg of raw boneless skinless chicken breast) (Spitze et al., 2003). As a free AA, a lot of taurine can be lost from meat depending on the cooking process, e.g., boiling of meat causes leakage of taurine into the water (e.g. leakage of ~50 % of taurine in case of boiled vs raw chicken breast) (Spitze et al., 2003). After extraction from the airlift fermenter *F. venenatum* biomass is briefly heated up to 68 ^{o}C to lower the levels of nucleic acids in the mycelium (Whittaker et al., 2020). Such heating results in leakage of free amino acids out of the mycelium and, therefore, is likely to reduce the level of taurine in the final product (Finnigan et al., 2017b). Nevertheless, the presence of taurine in the centrate – a term used to describe the broth left over after the mycoprotein heating step – could increase its value as a nutrient rich waste stream that currently is discarded but which is being considered for its potential uses (T. Ingmire, pers. comm.).

Seemingly not much research has been done on taurine synthesis in fungi with some sources claiming no known taurine synthesis pathways in fungi (Tevatia et al., 2015). Three distinct pathways of taurine metabolism are known in biology: synthesis from methionine/cysteine in animals, synthesis from serine/sulphate in chick embryos and microalgae, and breakdown of

taurine into acetate and acetyl-CoA in bacteria (Tevatia et al., 2015). A publication by (Hébert et al., 2013) reports finding for the first time evidence of taurine and hypotaurine synthesis in a yeast, *Yarrowia lipolytica*. Since hypotaurine is a precursor to synthesis of taurine in the methionine/cysteine pathway, and the work noted increased levels of taurine and hypotaurine in the yeasts that were fed high levels of methionine, it is likely that the taurine synthesis pathway in *Y. lipolytica* may be similar to the methionine/cysteine pathway of animals. In the *F. venenatum* C5 variant, AA profile data weakly hinted at a possibility that the transsulphuration pathway is downregulated which could suggest a possibility that taurine in *F. venenatum* is synthesised by a pathway similar to animals and *Y. lipolytica*. Further investigation into the synthesis and role of taurine in *F. venenatum* and other fungi is needed. This includes alternative methods for validating its presence (e.g., NMR) and characterisation of the relevant biosynthetic pathway(s) and gene functions. A biological role of taurine in fungi aside from general antioxidant and antifreezing functions is unclear (Hébert et al., 2013). Understanding the role of this AA in the wider transsulphuration pathway could help to better understand mechanisms that drive the formation of C variants in *F. venenatum*. In other fungi the transsupluration pathway was shown to be essential for pathogenicity in both plant and human hosts (Traynor et al., 2019; Saint-Macary et al., 2015). Such broader understating may also help pave a way to more efficient large- scale production of this nutritionally valuable AA.

4 Chapter 4 – Targeting translation as means of amino acid profile manipulation

4.1 Introduction

The AA composition of proteins is determined by the information encoded in organisms' genomes. During protein synthesis, the relevant DNA sequence is first transcribed into mRNA, which serves as a template for ribosomes to link individual AAs that are carried by tRNA molecules. Each tRNA molecule has an anticodon that matches a codon sequence on the mRNA strand to an AA-specific for that anticodon **(Figure 4.1**). However, this process of mRNA translation is not error free, creating potential for some variability in the AA composition of synthesised proteins. Translation errors arise primarily during either tRNA aminoacylation, where an AA may associate with the incorrect tRNA molecule resulting in a tRNA loaded with an AA that is not encoded by the anticodon on the tRNA, or polypeptide chain formation where an mRNA-codon: tRNA-anticodon mismatch is accepted by the ribosome (Berg et al., 2017; Wong et al., 2018; Ou et al., 2019).

Erroneous changes to the AA chain during translation can have a range of effects on the final protein, from benign through affecting the structure and function of the protein to causing toxicity and/or loss of function, e.g., errors in tRNA aminoacylation were linked to multiple neurological disorders in humans (Kapur and Ackerman, 2018). Another study has shown that limiting the rate of errors via limiting the speed of translation can lead to a longer lifespan in cells (Xie et al., 2019). Despite these negative consequences of mistranslation, the rate of error during translation is orders of magnitude higher (10^{-2}-10^{-5}) than during DNA replication (10^{-9}-10^{11}) or mRNA transcription (10^{-4}-10^{-5}) (Fijalkowska et al., 2012; Imashimizu et al., 2013; Ribas de Pouplana et al., 2014; Ellis and Gallant, 1982).

In fact, some organisms have evolved high rates of certain mistranslation events, e.g., the yeast *Candida. albicans* can misincorporate leucine in place of serine at rates up to 28%, with beneficial consequences for its fungus-host interactions by masking the fungal cell molecule β-glucan that is normally recognised by the host immune system (Miranda et al., 2013). Whereas such high levels of serine to leucine mistranslation are a result of a unique CUG codon in *C. albicans*, methionine misacylation is reported as more universal phenomenon. Methionine misacylation is mediated by a fully functional methionyl-tRNA synthetase and appears to be present in all domains of life. For example, in mammalian cells under optimal conditions approximately 1% of all tRNAs were misacylated with methionine, while this effect was reported to increase 10 fold under stress (Netzer et al., 2009). A similar phenomenon was also documented in yeast and bacteria (Jones et al., 2011; Wiltrout et al., 2012). Overall, higher global levels of mistranslation were linked to adaptability in stressful environments through increased phenotypic variability and fitness, resulting in improved survivability (Samhita et al., 2020; Samhita et al., 2021).

While specific types of mistranslation such as these can be positively selected, organisms may also actively suppress stop codon misreading to limit nonsense errors. Codon usage can also play a role, with rarer codons having lower rates of mistranslation and often being found in highly conserved critical areas of proteins which results in lower translational error rates in these important regions (Sun and Zhang, 2022).

The examples above paint a picture in which some organisms have evolved a variety of tools to mitigate the potential for negative effects from mistranslation but also to better tolerate or

even benefit from increases in the levels of these errors. This phenomenon where organisms show increased levels of translational errors under conditions (e.g. stress) where such a response may be beneficial is referred to as adaptive mistranslation (Mohler and Ibba, 2017). Although mistranslation may help organisms actively adapt to stressful environments, resultant changes to the proteome are not a consequence of altered genotype of the organism and therefore are not expected to be heritable. Nevertheless, mistranslation was shown to affect the dynamics of evolution by changing the adaptive landscape (a relationship between genotypes and reproductive success), in a variety of ways, e.g., by increasing the evolution of fitness on rugged landscape (adaptive landscape containing multiple fitness peaks), or increasing the probability of fixation of mutations (Schmutzer and Wagner, 2023).

The patterns of mistranslation are not random. In examples such as mistranslation linked to deficiency of a particular AA, another near cognate – that is AAs encoded by codons that differ by only one or two bases compared to the mistranslated codon – are preferentially misincorporated (Wong et al., 2018). Higher levels of mistranslation can also be induced chemically. Paromomycin is an aminoglycoside drug that is a known promoter of mistranslation, impairing the cells' abilities to correctly translate protein by binding to the 16S ribosomal RNA, which switches the ribosome into a high-affinity conformation regardless of whether cognate or non-cognate -tRNA is bound to the A site of the ribosome (Gromadski and Rodnina, 2004). This mistranslation inducing effect was documented in both prokaryotic and eukaryotic organisms including bacteria (Kramer and Farabaugh, 2007), yeast (von der Haar et al., 2017; Holland et al., 2007) and human cell lines (Wilhelm et al., 1978). Exposing *E. coli* and yeast cells even to sublethal levels of paromomycin modifies i.e., changes the types of misincorporation errors and elevates the overall number of translational errors (Mordret et al., 2019).

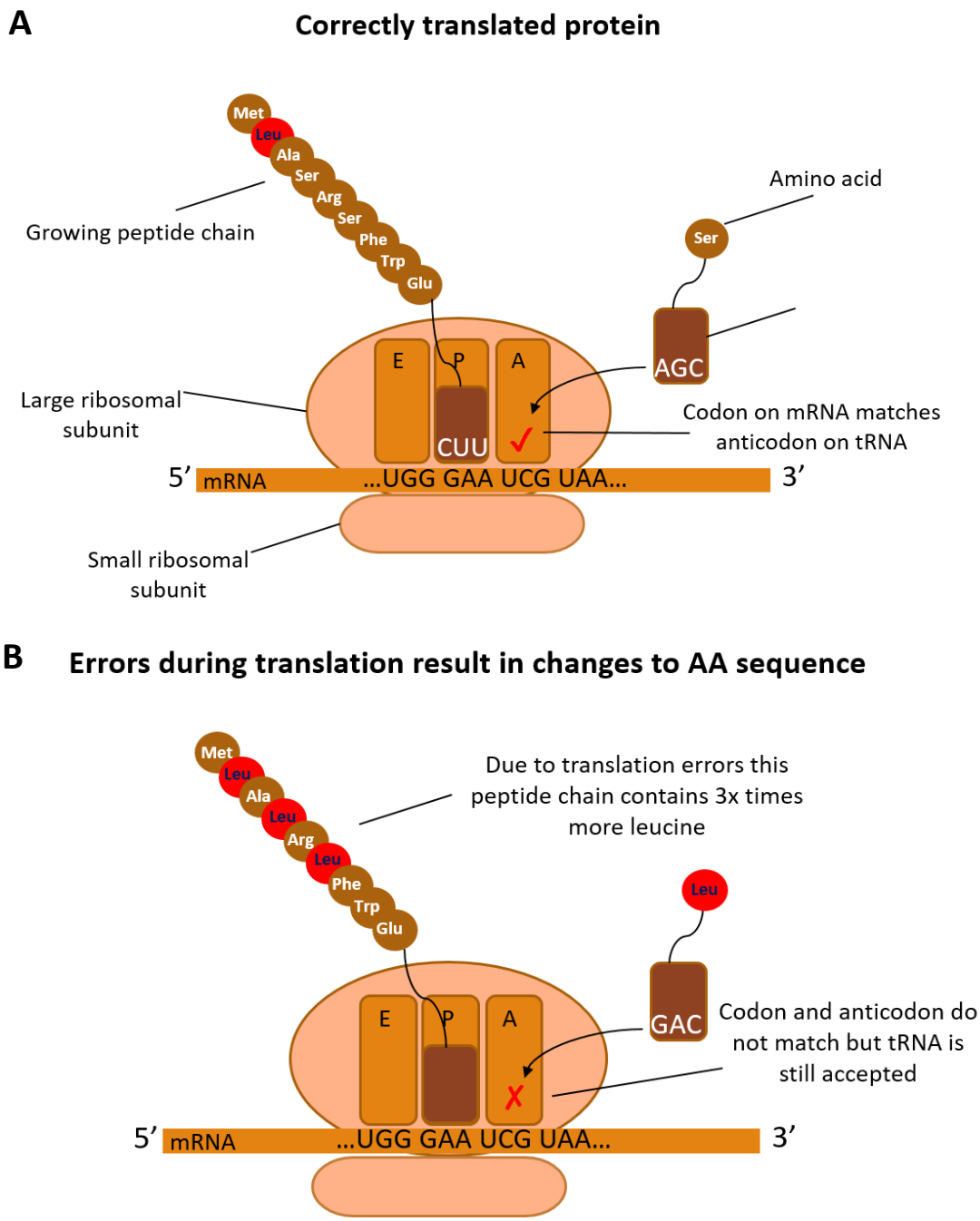

Figure 4.1 A simplified schematic illustrating the process of translation and mistranslation. A) When protein is translated correctly it contains amino acids corresponding to the codons contained in the mRNA sequence. B) When codon and anticodon pair are mismatched, or tRNA carries an amino acid not matching to the tRNA anticodon, an amino acid not encoded by the mRNA can be incorporated into the peptide chain resulting in mistranslation.

4.2 Chapter Aims

As outlined above, organisms can sometimes tolerate mistranslation to a remarkable level. One of the goals of this project was to explore the possibility of using mistranslation as a tool for deliberately changing the AA composition of *Fusarium venenatum*. The specific aims are:

a) Explore the effect of chemically induced mistranslation on the AA profile of *F. venenatum*.
b) Design a medium for promoting the misincorporation of branch chained amino acids (BCAAs) in *F. venenatum.*
c) Use adaptive evolution to try increasing the BCAA content of *F. venenatum*.

4.3 Materials and Methods

4.3.1 Media preparation

The growth medium was prepared as standard RHM medium, described in (**2.3.6**), except where stated the level of NH_4Cl was lowered or removed completely and replaced with one or more BCAAs.

2 mM BCAAs selection medium was prepared by dissolving in 1 l of RHM without NH_4Cl medium 0.087 g leucine, 0.087 g isoleucine and 0.078 g valine.
41.1 mM BCAAs selection medium was prepared as described above but dissolving 1.8 g leucine, 1.8 g isoleucine, 1.6 g valine.

4.3.2 Chemicals

500 mg of paromomycin sulphate was dissolved in of dH_2O up to 1 ml total volume, filter sterilised and kept at -20 ^oC to serve as stock solution to be diluted as needed.

30 % (9.8 M) H_2O_2 solution was stored at 4 ^oC and diluted as needed with sterile dH_2O.

4.3.3 Tube race setup and protocol

Tube race experiments were conducted in either liquid or solid (agar) medium. A tube race was prepared by drawing 25 ml of medium into a sterile 50 ml serological pipette (Greiner Bio-One Ltd, UK). The tube was placed horizontally and blocked with a sterile rubber cap at the inlet and blocked with tape on the other end. Inoculation and extraction points (**Figure 4.5)** were created with a needle pre-heated over a Bunsen burner. 100 µl of a 10 000 spore/ml *F. venenatum* spore solution prepared as described in section (**2.3.2**) was introduced with a syringe via the inoculation point and an empty syringe was inserted at the extraction point. The tubes were incubated statically at 28 ^oC. For the tube containing liquid medium, medium containing fragments of fungal hyphae was extracted through the extraction point after the tube was fully colonised (usually 72 h) and reinjected to a new race tube. This was repeated two times following the initial inoculation, after which the mycelium was cultured on a petri dish with potato dextrose agar until sporulation. Afterwards the spores from the

petri dish were used to repeat the cycle. For tube races using agar medium, after the tube was fully colonised (usually ~ 3 weeks) the spores at the extraction point were harvested and used to inoculate a new tube.

All other Methods used in this Chapter are described earlier in the thesis.

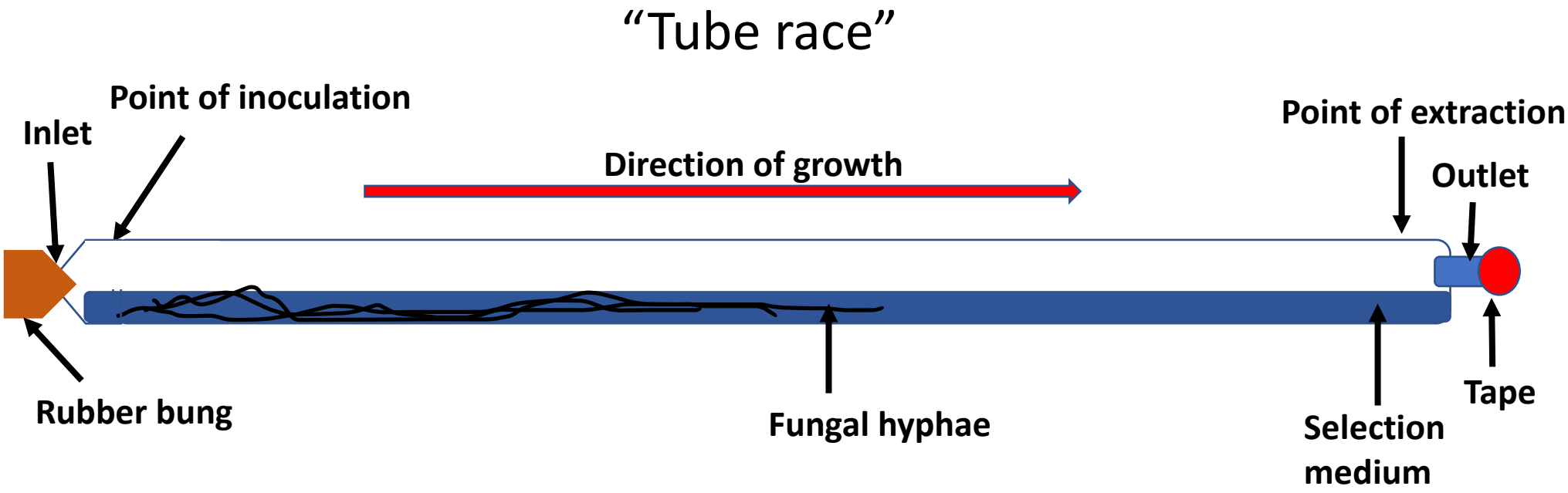

Figure 4.2 Diagram outlining the setup of the "tube race" adaptive evolution experiment. *F. venenatum* spores are injected at the point of the inoculation into the selection medium. The tube is then incubated at 28°C allowing fungal hyphae to develop and colonise the tube in the direction of the outlet. The hyphae that arrive towards the end point first are extracted and used to reinoculate a new tube/or cultured on agar until sporulation.

4.4 Results

4.4.1 Identification of subinhibitory concentration of paromomycin for *F. venenatum* in plate reader cultures

For investigating effects of paromomycin on the AA profile of *F. venenatum*, first subinhibitory (non-growth slowing) concentrations were determined. The use of subinhibitory concentrations was because growth inhibition would lead to more general effects and response in the *F. venenatum* cells, which may not be specific to the action of the aminoglycoside drug but reflective of downstream general consequences of growth perturbation.

F. venenatum was cultured in in microwells in RHM medium supplemented with a range of paromomycin concentrations (**Figure 4.3)**. The effect on growth was measured by comparing the doubling times during exponential growth between 16 and 24 h. Concentrations up to 50 µg/ml showed no effect, with calculated doubling times of 5.48, 5.25 and 5.42 h at 0, 25, 50 µg/ml paromomycin, respectively. In samples treated with 100 and 200 µg/ml of paromomycin the average doubling times were increased to 7.45 and 6.40 h respectively ($p = 0.0351$).

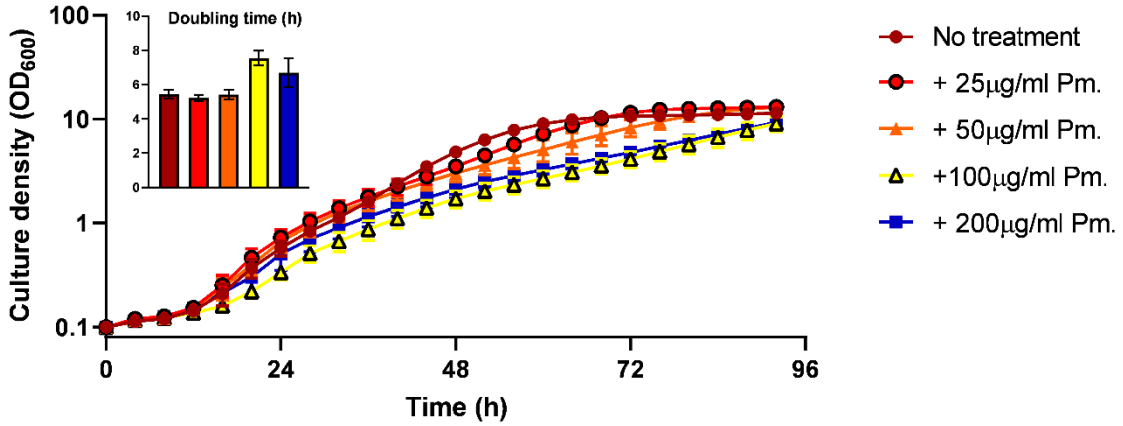

Figure 4.3 Growth curve of *F. venenatum* in microplate culture with paromomycin. RHM medium was inoculated with 10,000 spores/ml and 300 ul of the suspension was aliquoted into wells, supplemented or not with paromomycin and incubated statically at 28° C for 96 h with OD measurements taken every 1 h. Data points indicate means ± SD, n = 3 (biological replicates). The calculated doubling times were compared with Kruskal-Wallis test ($H = 8.771$, $df = 4$, $p = 0.0351$).

4.4.2 Identification of subinhibitory concentration of paromomycin with *F. venenatum* in flask cultures

The experiment described above was repeated in flask cultures, using a similar range of paromomycin concentrations as a starting point. In this case, samples from cultures in RHM medium supplemented or not with paromomycin were extracted after 30 h of incubation and the total dry biomass was compared. In flask culture, *F. venenatum* showed less sensitivity to paromomycin compared to microplate reader experiment (**Table 4.1**). Cultures at up to 200 µg/ml of paromomycin showed no decline in biomass yield after 30 h, higher concentrations resulted in some cases lowering of biomass indicating growth inhibition. There was some variability between replicates, especially at 300 µg/ml paromomycin.

Table 4.1 Growth of *F. venenatum* in flask cultures treated with paromomycin. The biomass from samples was extracted after 30 h of growth in baffled flasks. The total biomass was freeze dried and weighed to look for indication of growth inhibition. All the masses are expressed as mg of dry weight per 1 ml of liquid culture.

	Mass (mg/ml)	
	Sample 1	Sample 2
Control	2.74	3.07
+ 100 µg/ml Pm	2.61	3.07
+ 200 µg/ml Pm	2.70	2.90
+ 300 µg/ml Pm	0.94	2.70
+ 400 µg/ml Pm	0.74	2.14

4.4.3 Measurements of effect of paromomycin treatment on the AA profile of *F. venenatum*

Next, amino acid profiles of 30 h *F. venenatum* hydrolysate were compared after culture with or without subinhibitory levels of paromomycin. Additionally, to investigate the hypothesis that availability of free AA might enhance misincorporation of that AA into the organism's proteome, some cultures were supplemented with 2 mM leucine alongside paromomycin treatment.

The analysis of the PC1-3 via One-Way ANOVA revealed no statistically significant difference in the total amount of the AAs or their relative levels between the treatments ($p = 0.60$, $p = 0.11$, $p = 0.25$, for PC1-3 respectively) **(Table 4.2)**. Examination of the absolute and relative AA profiles (**Table 4.2**, **Appendix Table 16**, **Figure 4.4**) did not show an indication of a change to AA profile specific to the presence of paromomycin or paromomycin + leucine in the medium. One change specific to sample treated with 300 µg/ml paromomycin was a decrease in relative valine to 5.4 % versus 6-7 % in the other samples.

To further investigate the potential effect of paromomycin on the AA profile of *F. venenatum* hydrolysate, a higher concentration (500 µg/ml) that was partially inhibitory to growth was used. The biomass treated with paromomycin showed visual signs of stress (orange reddish colour and changed texture of the culture) and treated samples had lower total biomass

compared to untreated cultures – although not significant (**Appendix Table 9)**. This was to assess whether certain effects noted above, e.g., small decrease in relative valine content with paromomycin, would be accentuated at a higher paromomycin concentration. *F. venenatum* biomass after culture with 500 µg/ml paromomycin with or without additional leucine was extracted for AA profiling at 30 and 36 h. The addition of 500 µg/ml of paromomycin resulted in a visible signs of stress in the culture – change of colour and texture, as well as a decrease in total biomass extracted at 36 h timepoint compared to no treatment control ($p = 0.0001$) (**Appendix Table 9**).

Comparison of the by One-Way ANOVA of the PC1-3 from the 30 h dataset revealed no significant differences in the total amount of AAs or the relative AA levels ($p = 0.53$, $p = 0.06$, $p = 0.08$, respectively for PC1-3) (**Table 4.3)**. Similarly, no differences were detected after analysis of PC1-3 from the 36 h dataset ($p = 0.82$, $p = 0.95$, $p = 0.71$). At both timepoints, the profile did not show an indication of the decrease in valine with paromomycin, as had been noted earlier (**Figure 4.5, Table 4.3**). In general, the AA profiles looked similar (**Table 4.3)**. To help further identify any effects of the treatment on AA profile of *F. venenatum*, levels of individual AAs from the 36 h extracted cultures were normalised to the means of the corresponding AAs in the control (**Figure 4.5**). Here, besides differences in alanine and glutamate, relative levels of methionine, serine and threonine appeared potentially to be lowered in both treated samples compared to the control. These changes, however, were small and not statistically significant. No additional effect of leucine addition in the medium over and above of that of paromomycin treatment was observed.

Table 4.2 Comparison of hydrolysate amino acid profiles from *F. venenatum* cultures grown for 30 h in RHM in the absence and presence of paromomycin and/or leucine. Values indicate amounts of AA in g/kg biomass ± SD. The bottom three rows indicate the principal component values ± SD. The PC1-3 from different treatments were compared by One-Way ANOVA (F = 0.7607, df = 5, p = 0.6032; F = 2.6439, df = 5, p = 0.1067; F = 1.6474, df = 5, p = 0.2524) respectively. Pm – paromomycin, L – leucine.

	Control 30 h (n = 4)	+ 50 µg/ml Pm (n = 2)	+ 100 µg/ml Pm (n = 2)	+ 300 µg/ml Pm (n = 2)	+ 2 mM L (n = 2)	+ 2 mM L + 100 µg/ml Pm (n = 2)
Ala	36.74 ± 4.91	32.74 ± 12.01	36.03 ± 3.53	30.13 ± 2.04	36.02 ± 3.54	32.75 ± 1.13
Arg	29.07 ± 2.28	27.59 ± 8.81	32.45 ± 4.19	29.40 ± 2.01	29.50 ± 1.59	28.01 ± 1.13
Asp	35.56 ± 3.58	30.14 ± 6.07	33.61 ± 2.74	40.44 ± 3.02	35.34 ± 0.01	30.47 ± 0.31
Cys	2.98 ± 0.31	2.31 ± 0.52	2.73 ± 0.29	3.30 ± 0.42	2.81 ± 0.37	2.26 ± 0.09
Glu	79.88 ± 13.70	62.14 ± 14.50	63.78 ± 3.32	81.87 ± 9.57	68.73 ± 6.27	65.04 ± 2.51
Gly	18.92 ± 1.74	15.76 ± 3.88	18.27 ± 1.78	21.11 ± 4.33	18.12 ± 1.12	17.14 ± 0.22
His	9.92 ± 1.02	9.00 ± 2.74	10.36 ± 1.33	9.38 ± 0.79	10.38 ± 0.23	9.53 ± 0.50
Ile	19.12 ± 2.84	18.01 ± 5.30	21.14 ± 2.14	17.90 ± 0.85	21.24 ± 1.21	18.71 ± 0.78
Leu	31.06 ± 3.71	25.42 ± 6.50	31.82 ± 4.93	31.52 ± 1.89	34.22 ± 3.34	29.13 ± 1.52
Lys	34.25 ± 3.10	30.40 ± 9.38	35.14 ± 4.01	33.84 ± 0.73	35.29 ± 1.87	31.39 ± 1.34
Met	11.36 ± 2.15	8.30 ± 2.52	10.25 ± 1.60	12.50 ± 1.40	10.33 ± 0.77	8.38 ± 0.83
Phe	18.75 ± 1.77	16.25 ± 4.93	19.14 ± 2.61	17.84 ± 0.56	19.00 ± 0.98	16.57 ± 0.48
Pro	17.96 ± 1.46	15.31 ± 4.08	17.83 ± 1.97	17.74 ± 0.79	18.12 ± 1.18	15.75 ± 0.78
Ser	16.83 ± 1.97	14.32 ± 3.82	16.40 ± 1.15	17.06 ± 0.93	16.39 ± 0.82	14.29 ± 0.69
Thr	21.25 ± 2.34	17.65 ± 4.46	19.73 ± 1.89	20.29 ± 1.61	20.92 ± 0.96	18.73 ± 0.57
Tyr	9.98 ± 1.55	7.67 ± 2.06	8.82 ± 1.22	10.73 ± 0.33	9.23 ± 0.33	7.75 ± 0.12
Val	36.74 ± 3.63	24.41 ± 7.63	28.85 ± 3.10	22.76 ± 4.15	28.59 ± 2.52	25.46 ± 1.39
Total	418.85 ± 37.34	357.42 ± 99.19	406.34 ± 35.17	417.81 ± 29.44	414.22 ± 27.08	371.35 ± 14.41
PC1	0.1 ± 1.7	- 2.42 ± 4.1	- 0.45 ± 1.3	0.15 ± 1.2	0.09 ± 1.0	- 1.89 ± 0.7
PC2	0.56 ± 0.6	- 0.67 ± 1.0	- 0.2 ± 0.3	0.85 ± 0.45	- 0.03 ± 0.4	- 0.58 ± 0.1
PC3	1.41 ± 0.4	0.75 ± 0.6	1.04 ± 0.2	1.39 ± 0.4	1.11 ± 0.4	0.62 ± 0.2

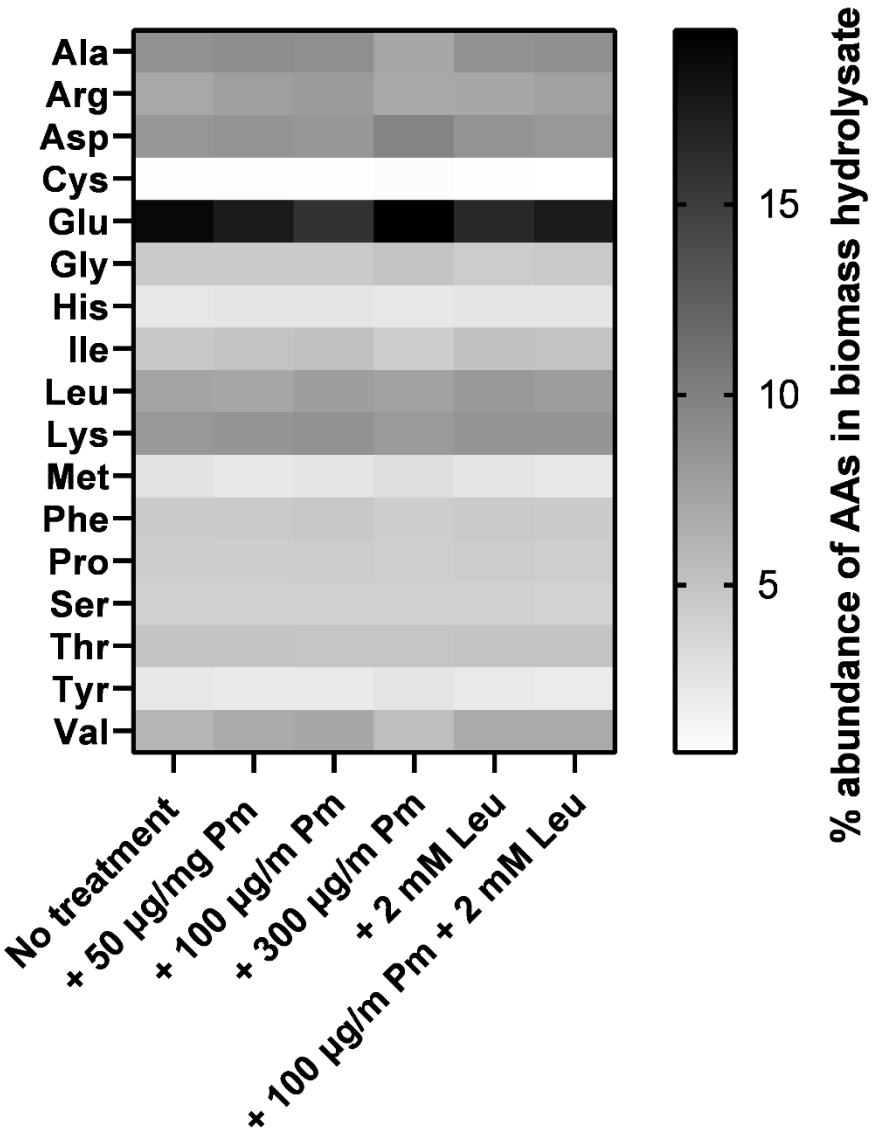

Figure 4.4 Heat map illustration of relative amino acid abundance within *F. venenatum* samples grown for 30 h in RHM medium treated with paromomycin and/or leucine. The values from **Appendix Table 16** (converted to heatmap according to right side scale) are normalised to the total amino acid amount from their respective treatments. N = 4 for control and N = 2 for remaining treatments.

Table 4.3. Comparison of hydrolysate amino acid profiles of biomass samples of *F. venenatum* cultured in RHM with 500 µg/ml paromomycin (Pm) or 500 µg/ml paromomycin and 2 mM leucine (Leu). The values are expressed as g/kg biomass ± SD. Samples extracted at 30 and 36 h were compared separately. The bottom three rows indicate the principal component values ± SD. The PC1-3 compared by One-Way ANOVA (F = 0.6969, df = 2, p = 0.5339; F = 4.6933, df = 2, p = 0.0593; F = 3.993, df = 2, p = 0.0790) respectively for 30 h dataset and (F = 0.2098, df = 2, p = 0.8165; F = 0.0462, df = 2, p = 0.9552; F = 0.3646, df = 2, p = 0.7088) respectively for 36 h dataset. n = 3.

	30 h			36 h		
	Wt	**Pm**	**Pm + Leu**	**Wt**	**Pm**	**Pm + Leu**
Ala	**34.10 ± 1.80**	**28.50 ± 1.15**	**29.48 ± 4.67**	**26.40 ± 4.07**	**25.98 ± 3.38**	**33.68 ± 4.77**
Arg	**25.21 ± 0.97**	**27.23 ± 1.04**	**25.08 ± 2.98**	**26.11 ± 2.95**	**27.21 ± 2.14**	**23.54 ± 0.87**
Asp	**42.72 ± 2.86**	**40.91 ± 4.67**	**42.36 ± 1.74**	**42.43 ± 4.69**	**40.72 ± 4.98**	**39.73 ± 3.11**
Cys	**1.93 ± 0.21**	**1.78 ± 0.33**	**2.43 ± 0.21**	**2.16 ± 0.14**	**2.23 ± 0.32**	**2.20 ± 0.10**
Glu	**59.52 ± 2.60**	**59.04 ± 2.39**	**63.67 ± 8.18**	**52.64 ± 5.75**	**62.83 ± 1.42**	**57.11 ± 2.58**
Gly	**23.40 ± 1.63**	**21.81 ± 0.85**	**23.84 ± 3.03**	**21.55 ± 1.61**	**22.39 ± 2.65**	**21.44 ± 2.03**
His	**8.93 ± 0.46**	**9.36 ± 1.00**	**9.40 ± 1.54**	**9.67 ± 1.04**	**9.29 ± 0.73**	**9.91 ± 1.47**
Ile	**18.30 ± 1.22**	**17.07 ± 1.42**	**17.98 ± 2.12**	**18.18 ± 2.18**	**17.06 ± 0.92**	**17.85 ± 1.53**
Leu	**20.30 ± 0.64**	**18.83 ± 1.33**	**20.45 ± 2.92**	**20.84 ± 2.09**	**19.86 ± 0.80**	**20.60 ± 1.80**
Lys	**28.30 ± 1.06**	**27.89 ± 2.59**	**27.83 ± 2.40**	**29.83 ± 2.65**	**28.17 ± 1.58**	**30.47 ± 2.35**
Met	**8.01 ± 0.04**	**7.31 ± 0.43**	**7.57 ± 0.66**	**8.06 ± 0.84**	**7.29 ± 0.97**	**7.03 ± 0.18**
Phe	**14.31 ±0.35**	**13.11 ± 0.68**	**14.57 ± 1.62**	**15.06 ± 1.81**	**14.28 ± 0.92**	**14.37 ± 1.26**
Pro	**14.27 ± 0.48**	**13.22 ± 0.66**	**14.41 ± 1.42**	**15.03 ± 1.80**	**14.19 ± 0.96**	**14.21 ± 1.24**
Ser	**13.70 ± 1.27**	**11.82 ± 1.17**	**13.20 ± 1.96**	**15.34 ± 1.80**	**13.79 ± 0.73**	**13.30 ± 1.51**
Thr	**15.33 ± 0.76**	**13.61 ± 0.88**	**15.50 ± 1.62**	**15.86 ± 2.69**	**14.70 ± 1.13**	**14.58 ± 0.99**
Tyr	**8.00 ± 0.22**	**7.62 ± 1.12**	**7.66 ± 1.23**	**8.29 ± 1.18**	**8.13 ± 0.55**	**8.14 ± 0.96**
Val	**16.68 ± 0.83**	**15.46 ± 0.58**	**18.00 ± 2.58**	**17.27 ± 1.95**	**16.87 ± 0.67**	**17.17 ± 2.58**
Total	**353.01 ± 8.71**	**334.56 ± 17.65**	**353.44 ± 34.34**	**344.73 ± 37.44**	**345.00 ± 20.23**	**345.33 ± 22.63**
PC1	**-3.22 ± 0.3**	**- 3.94 ± 0.7**	**- 3.22 ± 1.3**	**-2.88 ± 1.6**	**- 3.32 ± 0.8**	**- 3.46 ± 0.9**
PC2	**0.22 ± 0.2**	**- 0.37 ± 0.1**	**0.13 ± 0.4**	**- 0.27 ± 0.5**	**- 0.22 ± 0.5**	**- 0.17 ± 0.1**
PC3	**-0.72 ± 0.2**	**- 0.80 ± 0.2**	**- 0.44 ± 0.1**	**- 0.38 ± 2**	**- 0.41 ± 0.1**	**- 0.51 ± 0.3**

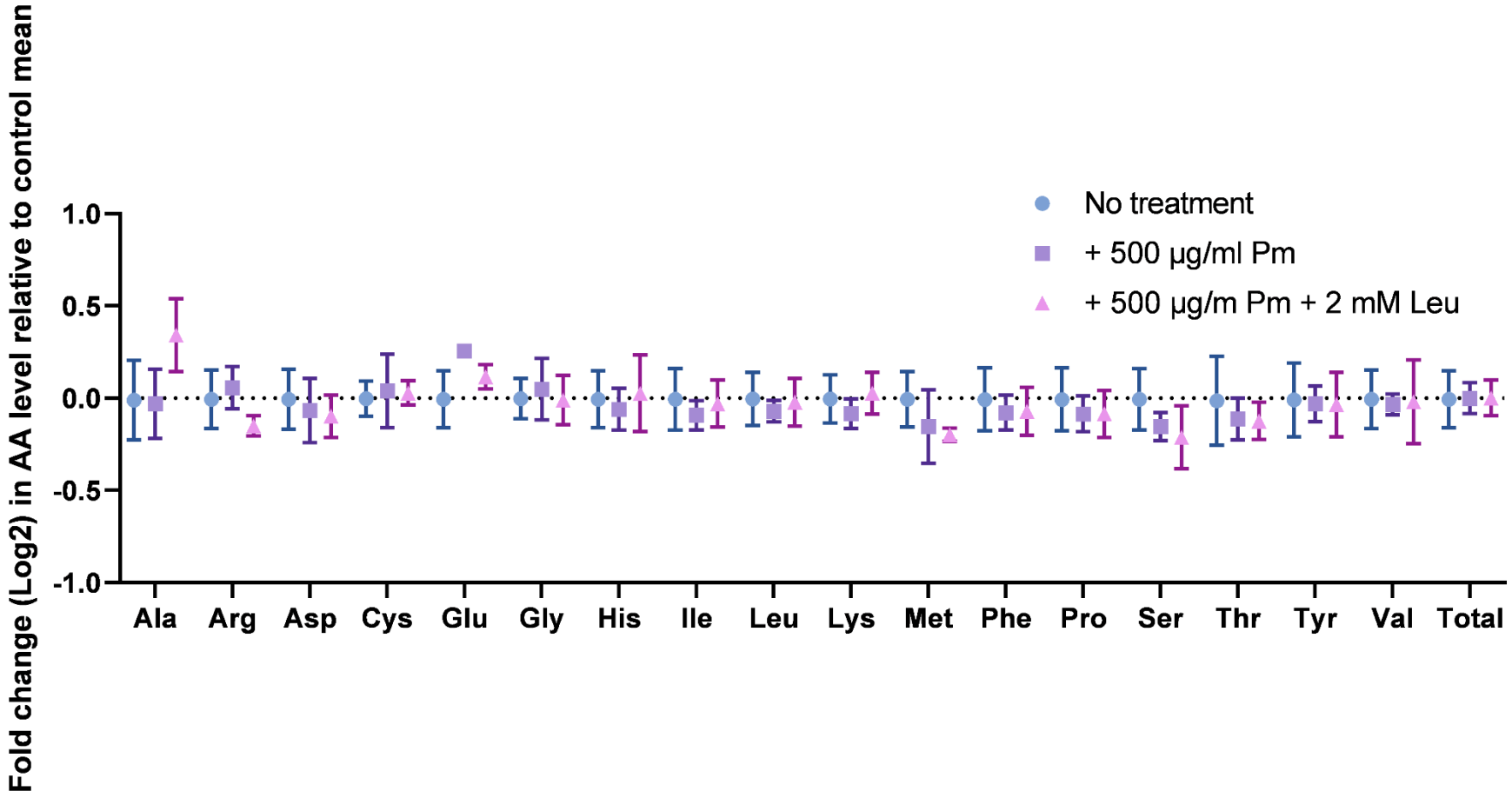

Figure 4.5 Change to the amino acid profile in *F. venenatum* samples extracted after 36 h growth from medium supplemented with paromomycin or paromomycin + leucine. The points on the graph are the level of each amino acid normalised against the relevant amino acid level from the control sample (**Table 4.3**)

4.4.4 Identification of subinhibitory H_2O_2 concentrations against *F. venenatum* growth in microplate cultures

As discussed in **section 4.1** methionine misacylation is a well conserved stress response. One function that methionine residues have in proteins is antioxidant properties (Levine et al., 1996). Accordingly, increased levels of oxidative stress have been shown to promote methionine misincorporation (Wang and Pan, 2016). H_2O_2 has been long characterised as an oxidative stress inducer (Ward et al., 1987). As an alternative to paromomycin and AA supplementation, here H_2O_2 was considered for its potential to the abundance of methionine in the AA profile of *F. venenatum*.

To determine the subinhibitory concentration, *F. venenatum* was cultured with a range of H_2O_2 concentrations (**Figure 4.6**). Concentrations of 2 mM or above were fully inhibitory over the first 40 h of incubation and were therefore excluded from further analysis. Doubling times were calculated using the ODs between 16 and 24 h of growth. At 1 mM there was a significant increase in doubling time to 9.71 h, from 5.18 h in control ($p = 0.0064$). Treatment with 0.5 mM H_2O_2 did not significantly change the average doubling time compared to the control ($p > 0.9999$).

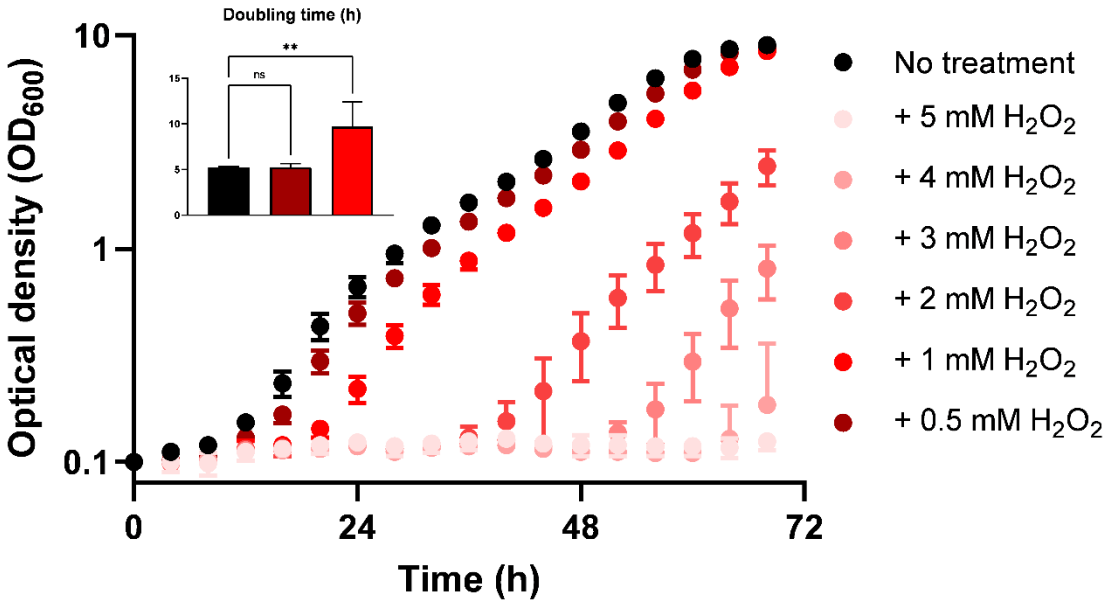

Figure 4.6 Growth of *F. venenatum* in microplate culture treated with H_2O_2. RHM medium was inoculated with 10 000 spores/ml and 300 µl of the suspension was aliquoted into wells, supplemented or not with H_2O_2 and incubated statically at 28° C for 72 h with OD measurements taken every 1 h. Data points indicate means ± SD, n = 6. The calculated doubling times were compared with Kruskall-Wallis test: ($H = 11.39$, $df = 2$, $p = 0.0005$).

4.4.5 Growth curve with H_2O_2 in in flasks

After identifying subinhibitory concentrations in the microplate reader setup, the experiment was repeated in flask cultures, using the range of subinhibitory concentrations from microplate cultures as a frame of reference. Considering the corresponding growth assays with paromomycin (outset of this Results section), where transition from microplate to flask cultures yielded decreased sensitivity, the growth in flasks was initially carried out using 2- 4 mM treatment of H_2O_2 **(Appendix Figure 4**). In flask cultures *F. venenatum* appeared to be more sensitive to H_2O_2 than in microplate cultures. Next the *F. venenatum* was treated with a lower 0.5 - 1 mM range of H_2O_2 and the biomass was extracted after 36 h of incubation (**Appendix Table 10**). The decrease in total dry biomass in all the cultures grown with H_2O_2 showed that ≥0.5 mM H_2O_2 was sufficient to inhibit the growth of *F. venenatum* in flask culture.

4.4.6 Effects of H_2O_2 on AA profile

Growth of *F. venenatum* cultures in flasks in presence of 0.5-0.75 mM H_2O_2 did not statistically affect the overall AA profile of the hydrolysate as evidenced by comparison of the PC1 by One-Way ANOVA ($p = 0.22$) (**Table 4.4**). Similarly, no apparent difference to the relative abundance of individual AAs was discovered by comparison of PC2-3 ($p = 0.17$, $p = 0.26$, respectively) and the levels of individual AAs varied significantly only in the cases of glutamate and alanine as determined by multiple comparisons analysis. The total level of AAs in the samples from cultures supplemented with 0.5 mM H_2O_2 (but not 0.75 mM H_2O_2) appeared lower than for the minus-H_2O_2 control. However, it is worth noting that with the small sample size ($n = 3$) this may be due to apparent increase in variability (reflected by large error values) in the total AA level in the hydrolysate of samples treated with H_2O_2 giving a false indication of difference due to increase in noise of the data. The absolute level of methionine appeared to be lower in the sample treated with 0.5 mM H_2O_2 vs control, but this likely reflected the lower overall AA content as supported by the fact that the relative methionine profile did not show a change due to H_2O_2 treatment **(Figure 4.7, Appendix Table 18).**

Table 4.4 Comparison of hydrolysate amino acid profiles of *F. venenatum* samples cultured in RHM with 0.5-0.75 mM H_2O_2. The values are expressed as g/kg biomass ± SD. The bottom three rows indicate the principal component values ± SD. The PC1-3 from different treatments were compared by One-Way ANOVA (F = 2.1161, df = 2, p = 0.2159; F = 2.6306, df = 2, p = 0.1657; F = 1.7629, df = 2, p = 0.2634)

	Control (n = 3)	+ 0.5 mM H_2O_2 (n = 3)	+ 0.75 mM H_2O_2 (n = 2)
Ala	45.73 ± 7.08 [A]	31.83 ± 6.90 [B]	37.37 ± 0.57 [A]
Arg	31.21 ± 0.64	25.15 ± 4.31	28.12 ± 4.30
Asp	45.41 ± 1.18	37.88 ± 11.26	40.03 ± 7.04
Cys	2.20 ± 0.36	1.41 ± 0.86	1.55 ± 0.21
Glu	75.54 ± 1.48	60.75 ± 13.97	72.30 ± 10.34
Gly	18.78 ± 0.75	15.48 ± 2.44	17.00 ± 1.80
His	9.95 ± 0.32	7.76 ± 1.44	8.39 ± 1.10
Ile	23.09 ± 0.74	17.69 ± 3.30	19.92 ± 3.23
Leu	33.99 ± 0.22	26.13 ± 4.72	29.52 ± 4.82
Lys	35.23 ± 0.70	29.07 ± 4.62	32.12 ± 3.95
Met	11.29 ± 1.03	8.86 ± 2.00	10.20 ± 1.98
Phe	19.10 ± 0.65	15.66 ± 2.95	17.76 ± 2.45
Pro	19.04 ± 0.60	15.37 ± 2.75	16.76 ± 2.80
Ser	16.30 ± 0.42	13.64 ± 2.63	14.87 ± 2.83
Thr	21.01 ± 1.54	16.82 ± 3.30	18.34 ± 2.05
Tyr	12.21 ± 0.50	10.88 ± 1.72	11.78 ± 1.40
Val	31.46 ± 1.19	25.27 ± 5.53	27.96 ± 4.85
Total	451.54 ± 4.43	359.64 ± 73.49	403.94 ± 54.15
PC1	1.0 ± 0.3	- 2.46 ± 2.8	- 0.8 ± 2.4
PC2	0.52 ± 0.1	- 0.75 ± 1.0	- 0.23 ± 0.4
PC3	0.46 ± 0.4	- 0.18 ± 0.5	0.04 ± 0.1

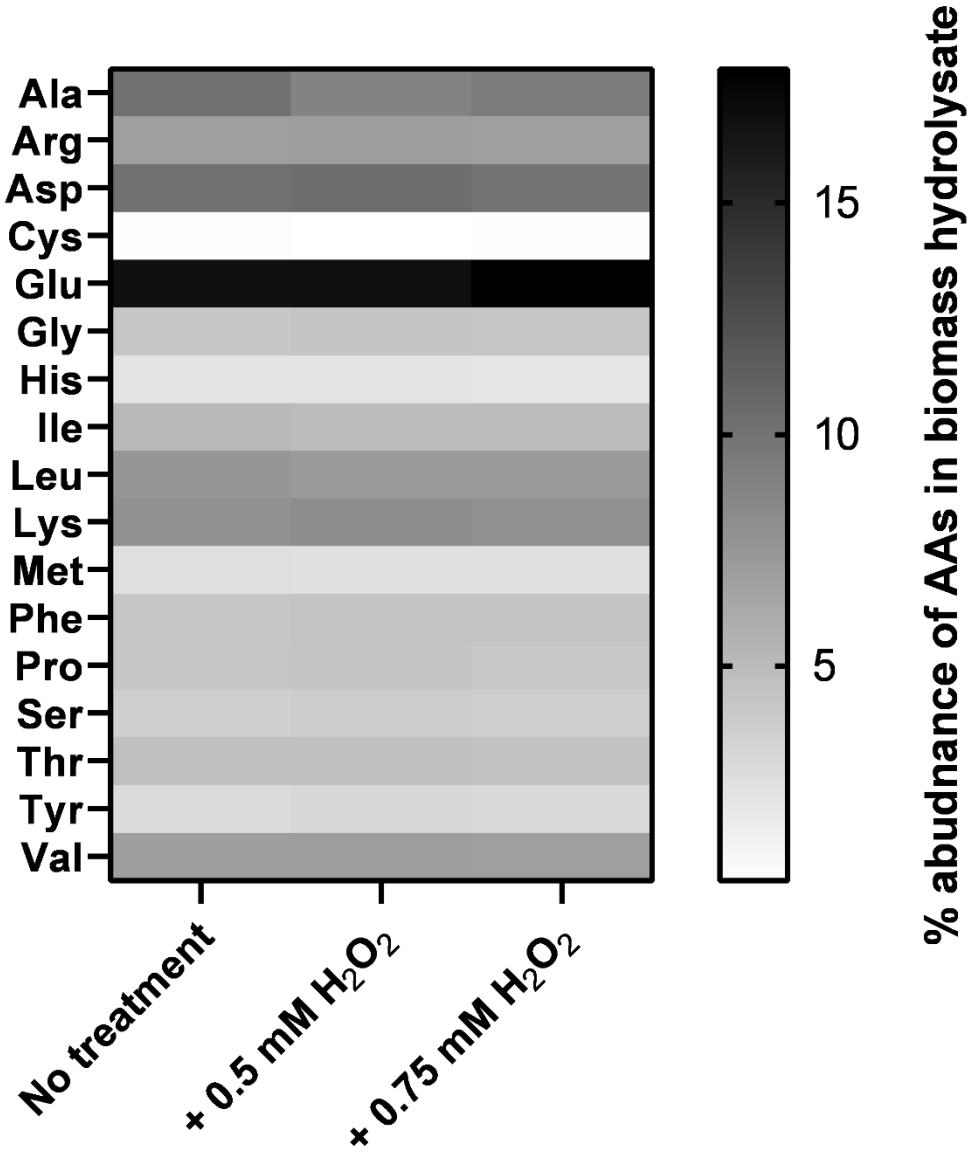

Figure 4.7 Heat map illustration of relative amino acid abundance within the hydrolysate of *F. venenatum* samples from RHM treated with 0.5 or 0.75 mM H_2O_2. The values from **Appendix Table 18**. (converted to heatmap according to right side scale) are normalised to the total amino acid levels for the same treatments. n = 2 for the + 0.75 mM H_2O_2 treatment; for the other treatments, n = 3 (biological replicates).

4.4.7 Adaptive mistranslation setup rationale

As effects on AA profile were very limited with the treatments attempted above, an adaptive-evolution experiment was designed to encourage misincorporation specifically of branch chained amino acids (BCAAs). The tube race setup is described in **section 4.3.2,** based on a well-established method for selection of fitness traits in filamentous fungi (Zhang et al., 2015; Casselton and Zolan, 2002). As mentioned before, culturing cells in medium lacking some essential AAs but abundant in other AAs can cause misincorporation of these more abundant AAs in place of the limiting AAs (Wong et al., 2018). As *F. venenatum* is prototrophic for all the AAs, a different approach to create AA scarcity may be needed. To achieve this, it was hypothesised that limiting the source of inorganic nitrogen in the medium and replacing it with excess BCAAs could be a route to increasing BCAA content of the fungus. To produce all of the AAs the fungus would need to metabolise the in-excess BCAAs to obtain nitrogen necessary to synthesise other AAs, but higher levels of misincorporation of these readily available BCAAs could in principle allow the organism to grow faster, if use of exogenous BCAA decreases the energy demand for *de novo* AA biosynthesis. It was reasoned that such selection over many generations may have the effect of fixing enhanced BCAA incorporation, as a beneficial trait in these conditions.

4.4.8 Growth with low nitrogen (N)

To create conditions in which *F. venenatum* experiences nitrogen starvation, initially the amount of available inorganic nitrogen in the medium was limited by reducing the amount of added NH_4Cl (the principal source of nitrogen in RHM medium). In plate reader experiments, even a 100-fold reduction in NH_4Cl did not affect the initial growth rate, but the final yield was decreased due to a shortened exponential phase presumably coincident with depletion of the available N (**Appendix Figure *5***) To exert pressure on the initial growth rate, the inorganic N source was completely removed and replaced with varying amounts of a BCAA mix (**Figure 4.8**). In the presence of BCAAs, growth was partially recovered compared to culture in the absence of any N source. The cell doubling time (calculated between 16–24 h for control and 20–28 h for growth without NH_4Cl, due to an elongated lag phase in the latter) was 4.97 h in standard RHM medium, whereas the shortest doubling time for growth in NH_4Cl-free medium supplemented with BCAAs (0.5, 1 or 2 mM) was 7.62 h.

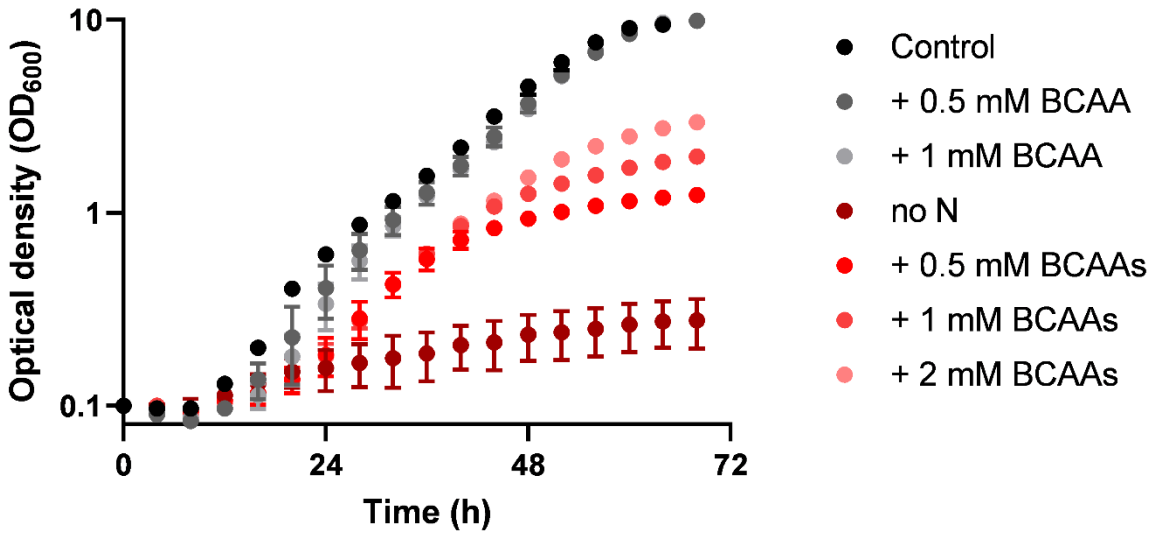

Figure 4.8 Growth curve of *F. venenatum* in nitrogen deficient RHM medium with BCAA supplementation in microplate culture. Standard or nitrogen deficient RHM medium was inoculated with 10,000/ml of spores and 300 µl of the suspension was deposited into wells and incubated statically at 28ºC for 72 h with OD measurements taken every 1 h for 72 h. Data points indicate mean average, ± SD, n = 3.

4.4.9 Effect of high BCAAs medium on biomass

Next the culture conditions were progressed to flask cultures. The concentration of the branch chained AAs was changed from the total of ~ 2 mM (0.667 mM each of leucine, isoleucine and valine) to the total of 40 mM (13.33 mM each of leucine, isoleucine and valine) to support biomass build-up. Similar to microplate reader results, in flask cultures the growth in RHM medium supplemented with BCAAs but without NH_4Cl was slower than in unaltered RHM medium (**Figure 4.9**). The cultures with added BCAAs generally grew to lower yield than in normal RHM medium though there was variability between replicates in the former case. This meant that at 30 h timepoint the amount of biomass in the +BCAA cultures was very low and likely not in exponential growth, leaving the 36 h timepoint as a point of extraction for AA analysis.

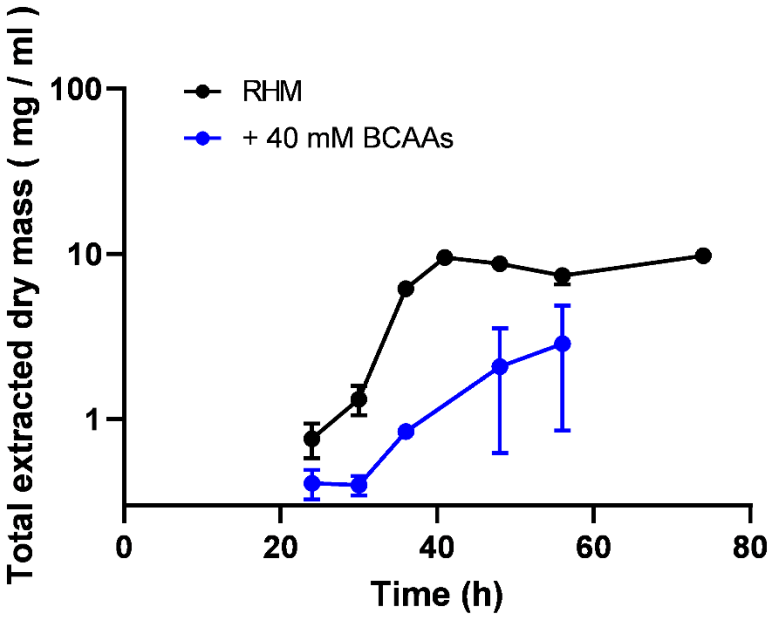

Figure 4.9 Growth curve of *F. venenatum* in flask cultures grown in modified RHM medium. Modified RHM medium where inorganic nitrogen was replaced with a 40 mM mix of BCAAs was inoculated with 10,000/ml spores and 50 ml of the suspension was deposited into 250 ml baffled flask and incubated statically at 28°C with shaking (150 rev/min). The biomass was extracted at 24, 30, 48, 56 h. Data points indicate mean average, ± SD, n = 3. For reference the growth curve was plotted alongside flask culture growth curve of F. *venenatum* grown in standard RHM medium from **Figure 2.3.**

4.4.10 Effect of high BCAA medium on AA profile

Next the AA profile of exponential growth phase *F. venenatum* biomass cultivated in the BCAAs selection medium was analysed to see whether growth in the medium can enrich the AA profile in BCAAs. Samples from flask cultures were extracted and prepared for analysis after 36 h of growth.

Analysis of PCA1 by One-Way ANOVA revealed a significant difference between the treatments ($p = 0.0009$), and subsequent Tukey's multiple comparisons showed that the differences are between the control vs 40 mM BCAA ($p = 0.005$), and control vs 80 mM BCAA ($p = 0.0008$) treatment. The values of PCA1 for both BCAA treated samples are lower than control indicating an overall decrease in AA content which is in line with the absolute AA data presented in **Table 4.5**. Comparison of PC2 revealed a significant difference in the relative AA levels ($p < 0.0001$) and Tukey's multiple comparisons showed that again BCAA treated samples were different to the control ($p < 0.0001$, for both). Lower values of PC2 seen in BCAA samples (**Table 4.5**) indicate a relative increase in the relative levels of Val and His group and decrease in Ala, Asp, Gly and Pro. Both the absolute (**Table 4.5**) and relative (**Figure 4.10**, **Appendix Table 19**) values indicate that BCAA treated samples do indeed show an increase in relative Val abundance and a decrease in Ala. Lastly there were no significant differences revealed by the comparison of the PC3 ($p = 0.09$).

Table 4.5 Comparison of hydrolysate amino acid profiles of *F. venenatum* samples grown in RHM lacking NH_4Cl and supplemented with a mix of branch chained amino acids. The values are expressed as g/kg biomass ± SD. The values are expressed as g/kg biomass ± SD. The bottom three rows indicate the principal component values ± SD. The PC1-3 from different treatments were compared by One-Way ANOVA (F = 28.441, df = 2, p = 0.0009; F = 237.84, df = 2, p < 0.0001; F = 3.8222, df = 2, p = 0.085). Different letters in superscript in the last three rows indicate statistically significant difference between values derived from One-Way-ANOVA with Tukey's multiple comparisons. Lack of any superscript letters indicates lack of significant difference within the relevant part of a row. n = 3.

	Control	BCAAS 40mM	BCAAS 80mM
Ala	**45.73 ± 7.08**	**24.81 ± 0.85**	**23.47 ± 2.85**
Arg	**31.21 ± 0.64**	**25.31 ± 1.25**	**22.58 ± 1.48**
Asp	**45.41 ± 1.18**	**35.19 ± 3.96**	**31.79 ± 2.16**
Cys	**2.20 ± 0.36**	**1.07 ± 0.48**	**0.97 ± 0.60**
Glu	**75.54 ± 1.48**	**56.12 ± 1.46**	**49.55 ± 3.63**
Gly	**18.78 ± 0.75**	**15.11 ± 0.48**	**15.18 ± 4.14**
His	**9.95 ± 0.32**	**8.07 ± 0.63**	**7.08 ± 0.05**
Ile	**23.09 ± 0.74**	**17.60 ± 0.26**	**16.69 ± 2.11**
Leu	**33.99 ± 0.22**	**25.96 ± 0.87**	**25.10 ± 3.96**
Lys	**35.23 ± 0.70**	**29.34 ± 0.98**	**25.40 ± 1.19**
Met	**11.29 ± 1.03**	**8.92 ± 0.41**	**8.21 ± 0.44**
Phe	**19.10 ± 0.65**	**15.88 ± 0.86**	**14.19 ± 1.50**
Pro	**19.04 ± 0.60**	**15.27 ± 0.31**	**13.66 ± 1.07**
Ser	**16.30 ± 0.42**	**14.01 ± 1.34**	**12.16 ± 1.42**
Thr	**21.01 ± 1.54**	**17.44 ± 0.81**	**15.78 ± 1.36**
Tyr	**12.21 ± 0.50**	**11.32 ± 1.18**	**10.05 ± 1.88**
Val	**31.46 ± 1.19**	**33.20 ± 0.93**	**34.53 ± 3.70**
Total	**451.54 ± 4.43**	**354.61 ± 4.78**	**326.38 ± 30.54**
PC1	**1.00 ± 0.3 [A]**	**- 2.26 ± 0.3 [B]**	**- 3.57 ± 1.3 [B]**
PC2	**0.52 ± 0.1 [A]**	**- 1.59 ± 0.1 [B]**	**- 1.95 ± 0.2 [B]**
PC3	**0.46 ± 0.4**	**- 0.32 ± 0.4**	**- 0.57 ± 0.6**

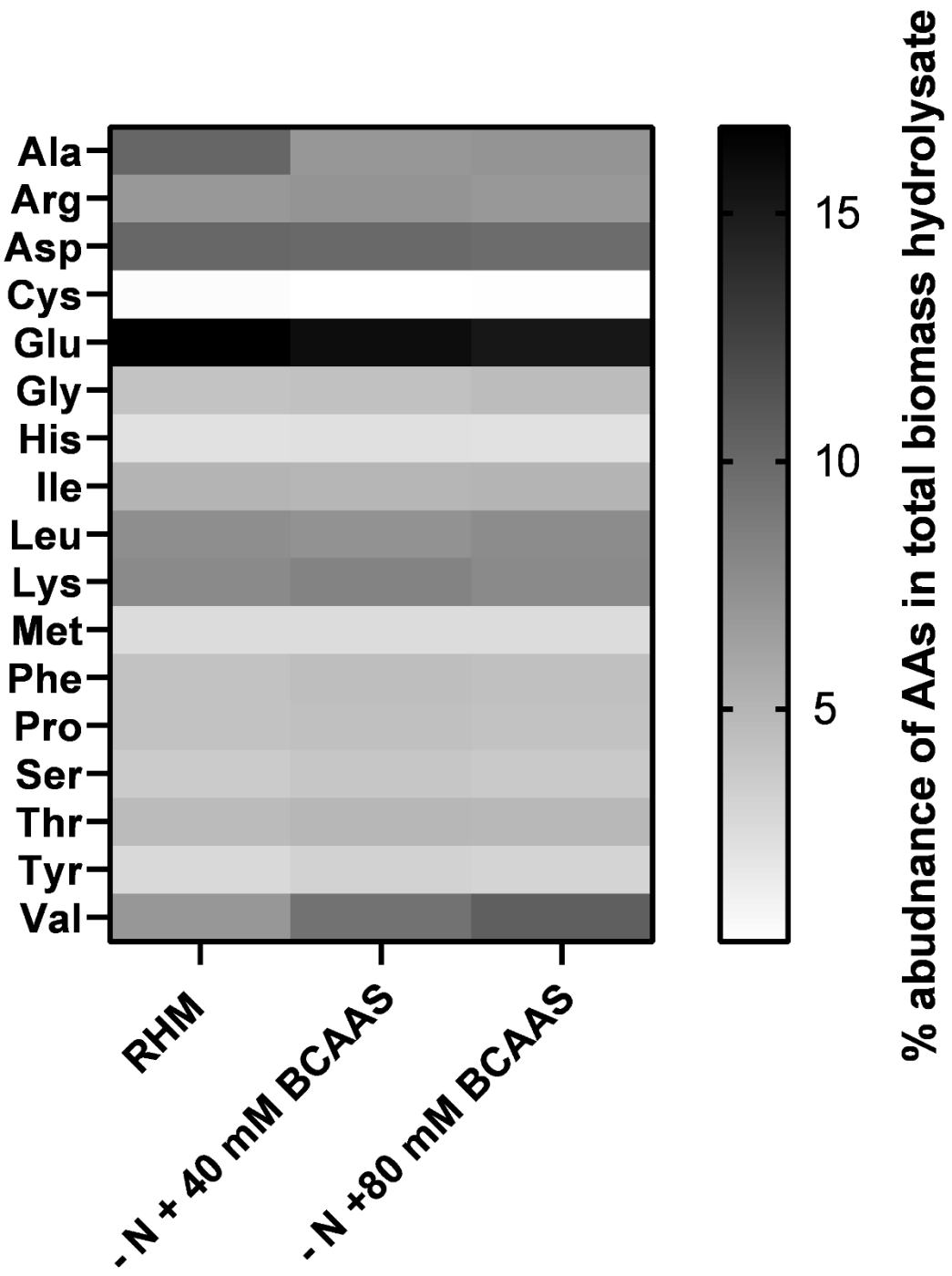

Figure 4.10 Heat map illustration of relative amino acid composition within *F. venenatum* samples grown in BCAAs-modified RHM medium. The values from **(**converted to heatmap according to right side scale) are normalised to the total amino acid amount from their respective treatments (**Appendix Table 19**). n = 3 (biological replicates).

4.4.11 The effect of removal of valine from the BCAA mix in selection medium.

Next three variations of the selection medium were prepared, containing 40 mM BCAA but excluding valine (that is, containing: 40 mM of leucine or 40 mM isoleucine or mix of 20 mM isoleucine and 20 mM leucine). This was done to assay whether exclusion of the BCAA that was comparatively enriched in the preceding experiment, i.e., valine, may help facilitate biomass enrichment with the other BCAAs. When valine was absent, the total AA content of cells cultivated in selection media was similar to that of unaltered RHM medium, unlike in the case of growth with added valine (**section 4.4.10)**. Overall, although biomass accumulation in the BCAA-minus-valine media was still lower than in standard RHM medium, the growth was faster than in the BCAA medium with valine (**section 4.4.9)** which allowed for exponential-phase biomass extracts at both 30 h (**Table 4.6**) and 36 h (**Appendix Table 11**) to be assessed.

Two experiments (designated 1 and 2) are distinguished in **Table 4.6** and because respective results come from samples grown, processed and analysed by LCMSMS in different runs. For cells from the Leu- and Leu + Ile-modified media, comparison of PC1 and 2 by One-Way ANOVA showed no significant effect ($p = 0.85$, $p = 0.06$, respectively), indicating no change to overall AA abundance and change in the levels of AAs described by PC2 **Table 4.6**. PC3 has shown a borderline significant effect ($p = 0.052$), Tukey multiple comparisons analysis indicated that the difference was between control and sample grown in Leu modified medium ($p = 0.053$). PC3 value is low in this sample which indicates an enrichment in leucine where the absolute amount of Leu and Asp is ~10 and g higher compared to control (**Table 4.6**). Similarly, the relative abundance of Leu in cells grown in Leu modified medium has increased from 7.9 to 9.7 % , and for Asp from 10.8 to 13.9 % compared to control (**Figure 4.11**, **Appendix Table 20**). Due to p-value for PC2 analysis being close to 0.05 threshold it is worth noting that the level of Ala has also dropped from 9.4 to 3.6 % compared to control. Overall, cells cultivated in the medium containing leucine and isoleucine did not show any changes to the absolute profile compared to control. However, cells from medium containing 40 mM Leu did significantly impact the AA profile of hydrolysate including a ~25 % increase in Leu content in absolute terms.

In cells extracted after 36 h growth in the same conditions (**Appendix Table 11)**, the overall AA abundance was not significantly affected by the treatment (PC1 – $p = 0.078$) alongside no significant difference in PC3 ($p = 0.2$). However, analysis of PC2 showed significant difference ($p = 0.046$), but Tukey's multiple comparison analysis did not indicate a significant difference between control and Leu and Leu + Ile treatments ($p = 0.06$, $p = 0.07$, respectively). In the relative % profile at 36 h (**Appendix Table 21**), relative level of Asp changed from 11.9 to 11.0 % in the control vs +Leu media. Relative alanine levels did not show a change.

In a second experiment, cells were tested in RHM medium lacking NH_4Cl and supplemented only with isoleucine. This was to determine whether removal of both valine and leucine (i.e. the two BCAAs showing enrichment in certain conditions above) could facilitate enrichment with isoleucine as the only BCAA supplement. After 30 h, in the culture with the added isoleucine analysis of PC1 indicated no change to the overall AA abundance compared to

control (p = 0.44), similarly no difference was found in PC3 (p = 0.47) (**Table 4.6**). Comparison of PC2 indicated a significant difference (p = 0.005) compared to control with lower absolute and relative levels of alanine and aspartate (**Table 4.6**, **Figure 4.11**, **Appendix Table 20**). It is worth noting that although not described by the PCs in this analysis, the relative (6.9 vs 5.2 %,), and absolute (~25 % increase) of isoleucine was also higher than in the control (**Table 4.6, Figure 4.11**, **Appendix Table 20**).

In cells extracted after 36 h analysis of PC1 and 2 did not indicate a significant change (p = 0.68, p = 0.73 respectively), but analysis of PC3 did (p = 0.034). The absolute level of Ile (indicated by more negative value of PC3) was ~35 % higher compared to control, levels of Asp, were also changed between the two conditions **Appendix Table 11**). In relative terms at 36 h isoleucine level was higher in cells grown in isoleucine medium vs control (6.6 vs 5.3 %, p = < 0.0001). The relative level of Asp, Ile varied between control and cells grown in isoleucine medium (**Appendix Table 21**).

Collectively the results showed that culture in RHM lacking NH_4Cl but supplemented either with all BCAAs, Leu + Ile, or Ile alone gave successful enrichment of cells with Val, Leu or Ile, respectively.

Table 4.6 Comparison of amino acid profiles of *F. venenatum* hydrolysate grown in BCAA-modified RHM medium for 30 h. The values are expressed as g/kg biomass ± SD. Experiment 1 and 2 were performed and analysed separately. The bottom three rows indicate the principal component values ± SD. The PC1-3 from different treatments were compared by One-Way ANOVA (F = 0.1566, df = 2, p = 0.8584; F = 4.5348, df = 2, p = 0.0631; F = 5.0464, df = 2, p = 0.0518) for experiment 1 and (F = 0.0734, df = 1, p = 0.44; F = 32.322, df = 1, p = 0.0047; F = 0.6118, df = 1, p = 0.4778) for experiment 2 . Different letters in superscript in the last three rows indicate statistically significant difference between values derived from One-Way-ANOVA with Tukey's multiple comparisons. Lack of any superscript letters indicates lack of significant difference within the relevant part of a row. n = 3 (biological replicates).

	Experiment 1			Experiment 2	
	Control, n = 3	Leu + Ile, n = 3	Leu, n = 3	Control, n = 3	Ile, n = 3
Ala	48.88 ± 4.94	33.98 ± 1.19	17.14 ± 9.77	34.10 ± 1.80	27.44 ± 2.57
Arg	36.19 ± 1.24	35.28 ± 2.05	29.93 ± 0.34	25.21 ± 0.97	27.54 ± 0.86
Asp	56.12 ± 1.85	54.33 ± 2.09	68.79 ± 18.36	42.72 ± 2.86	37.97 ± 0.89
Cys	2.33 ± 0.47	1.83 ± 0.15	1.53 ± 0.54	1.93 ± 0.21	1.83 ± 0.21
Glu	95.94 ± 3.20	88.21 ± 3.33	78.60 ± 2.17	59.52 ± 2.60	55.54 ± 5.42
Gly	23.04 ± 1.12	21.39 ± 1.32	34.06 ± 11.24	23.40 ±1.63	21.43 ± 0.82
His	12.80 ± 0.45	12.86 ± 0.65	13.46 ± 1.87	8.93 ± 0.46	9.33 ± 1.00
Ile	22.80 ± 0.28	26.23 ± 1.42	20.34 ± 1.65	18.30 ± 1.22	23.02 ± 0.80
Leu	37.92 ± 1.24	37.50 ± 0.75	47.96 ± 7.09	20.30 ± 0.64	22.67 ± 1.59
Lys	41.54 ± 1.55	39.86 ± 0.18	39.63 ± 3.67	28.30 ± 1.06	27.90 ± 3.17
Met	12.61 ±0.36	11.16 ± 0.58	12.20 ± 2.01	8.01 ± 0.04	6.85 ± 0.30
Phe	21.71 ± 0.51	20.88 ± 0.27	20.59 ± 1.76	14.31 ± 0.35	12.92 ± 1.06
Pro	21.79 ± 0.95	21.46 ± 0.13	20.39 ± 1.17	14.27 ± 0.48	13.20 ± 0.81
Ser	17.44 ± 0.71	16.84 ± 0.70	19.65 ± 4.69	13.70 ± 1.27	12.13 ± 2.19
Thr	27.09 ± 0.87	26.21 ± 0.37	25.83 ± 1.62	15.33 ± 0.76	13.77 ± 1.44
Tyr	12.66 ± 0.60	12.32 ± 0.88	11.44 ± 0.62	8.00 ± 0.22	7.27 ± 0.53
Val	28.97 ± 1.24	29.12 ± 0.38	29.63 ± 2.41	16.68 ± 0.83	15.54 ± 1.29
Total	519.82 ± 21.57	489.48 ± 16.43	491.14 ± 71.01	353.01 ± 8.71	336.36 ± 14.86
PC1	3.46 ± 0.5	3.10 ± 2.2	2.87 ± 0.4	- 3.22 ± 0.3	- 3.58 ± 0.7
PC2	1.87 ± 0.3	1.25 ± 0.8	0.62 ± 0.3	0.22 ± 0.2 ^{A}	- 0.80 ± 0.2 ^{B}
PC3	0.49 ± 0.5 ^{A}	- 1.85 ± 1.6 ^{A}	- 0.02 ± 0.1 ^{B}	- 0.72 ± 0.2	- 0.85 ± 0.2

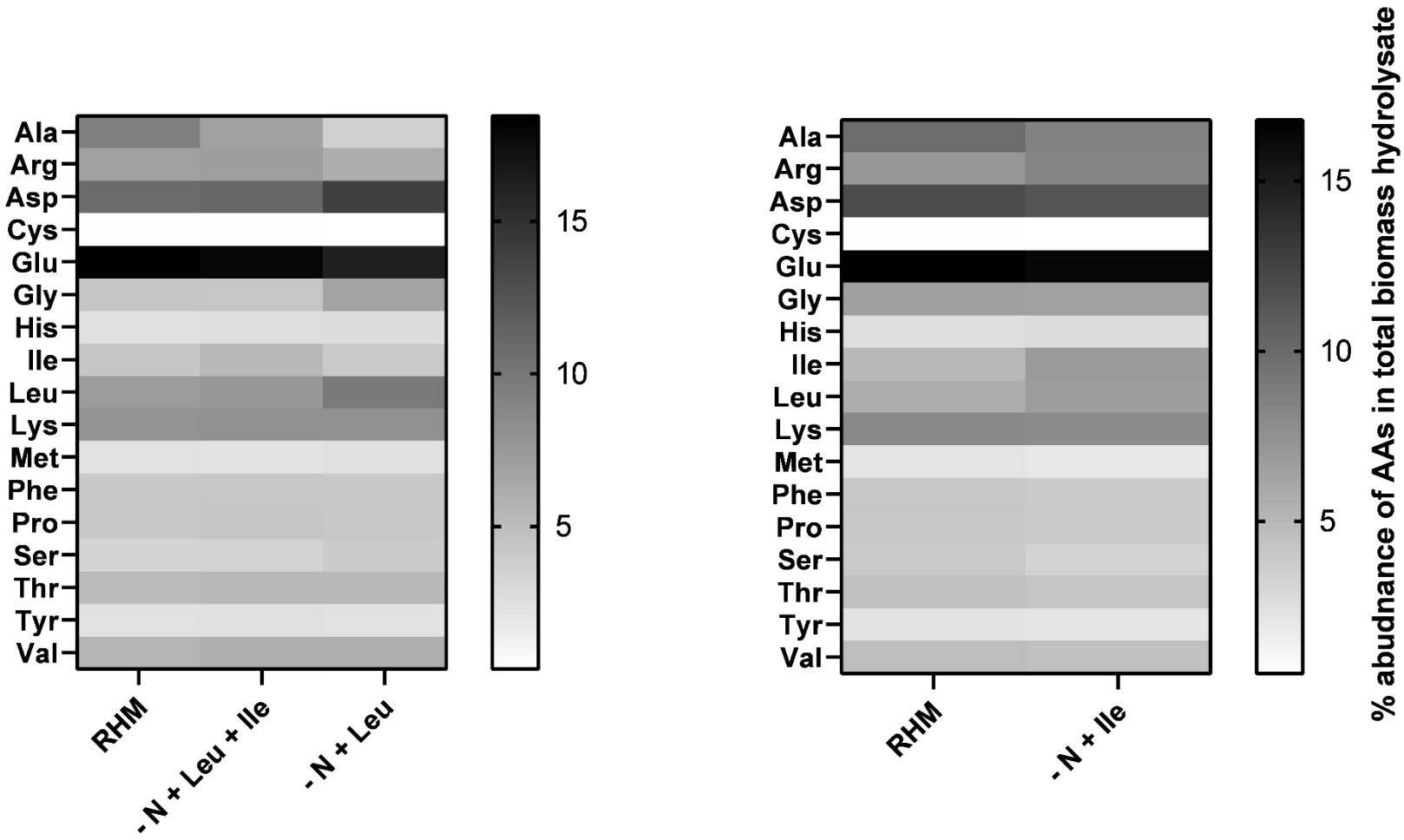

Figure 4.11 Heat map illustration of relative amino acid abundance in F. venenatum grown for 30 h in RHM medium modified or not with leucine, isoleucine, or both. The values from **Table 4.6** (converted to heatmap according to right side scale) are normalised to the total amino acid amount from their respective treatments - **Appendix Table 20**. n = 3 (biological replicates).

4.4.12 The effect of tube race selection in liquid medium on the AA hydrolysate composition of *F. venenatum*

To test whether adaptive evolution on selective medium (RHM medium lacking NH_4Cl but with added BCAAs: RHMBCAA) can result in BCAA enrichment in *F. venenatum*, a series of race tube experiments were conducted. A tube race is an adaptive evolution experimental method that helps to select the fittest individual in a given selection medium by consecutively inoculating fungi at one end of the tube, allowing the most adapted organisms to reach the end of the tube first and selecting them for subsequent round of selection in another tube race (**4.3.3**). Here the race tube experiment was carried out by selection in liquid medium for 10 generations (each generation was defined as 3 passages through the tube, then subsequent growth on agar and sporulation, before re-inoculation of race tube for the next generation). The experiment was carried out in triplicate parallel tubes throughout. After 10 consecutive generations, three isolates from each race tube were grown for 36 h in standard RHM medium or in BCAA selection medium before assay of hydrolysate AA composition.

First, the total dry weights of the flask culture samples after 36 h of culturing were compared to see whether the selection under the tube race affected the growth rate of *F. venenatum* isolates **(Figure 4.12**). Statistical analysis by Kruskal-Wallis test revealed no significant difference in the growth yield of wild type versus 10th-generation isolates either on RHM ($p = 0.1606$) (**Figure 4.12 A**) or on BCAA modified RHM medium ($p = 0.0502$) (**Figure 4.12 B**).

The AA hydrolysates of WT and tube race isolates grown in standard RHM medium were compared. Analysis of the PC1-3 by One-Way ANOVA did not indicate any significant differences between the AA hydrolysate profiles of the control and tube race isolates ($p = 0.95$, $p = 0.65$, $p = 0.23$) respectively (**Table 4.7**, **Figure 4.13**, **Appendix Table 22**).

Next the hydrolysate of biomass from wild type and the tube race isolates of *F. venenatum* were compared after culturing in the RHMBCAA medium. There was no significant effect on the overall AA abundance between control and the tested isolates (PC1 – $p = 0.41$) **Table 4.8**. Analysis of PC2-3 revealed significant changes to the relative AA composition ($p = 0.048$, $p = 0.049$, respectively). Tukey's multiple comparisons only revealed a significant difference in PC2 only between T1 and T3. T3 isolate has shown a decrease in Ala and Asp content and increase in His content, alongside other AAs (**Table 4.8**, **Figure 4.14**, **Appendix Table 23**). This result though is debatable due to lower sample size and very low biomass at the harvested which was previously shown in this thesis to correlate with higher overall protein content (**2.4.4**).

Overall, the isolates from the tube races in liquid medium did not show statistically significant changes to their absolute hydrolysate profiles. There were some specific changes in relative composition for certain AAs and certain isolates of organisms grown in RHMBCAA medium, but these were in Ala and Asp rather than in BCAA content on which the prior selection had been based.

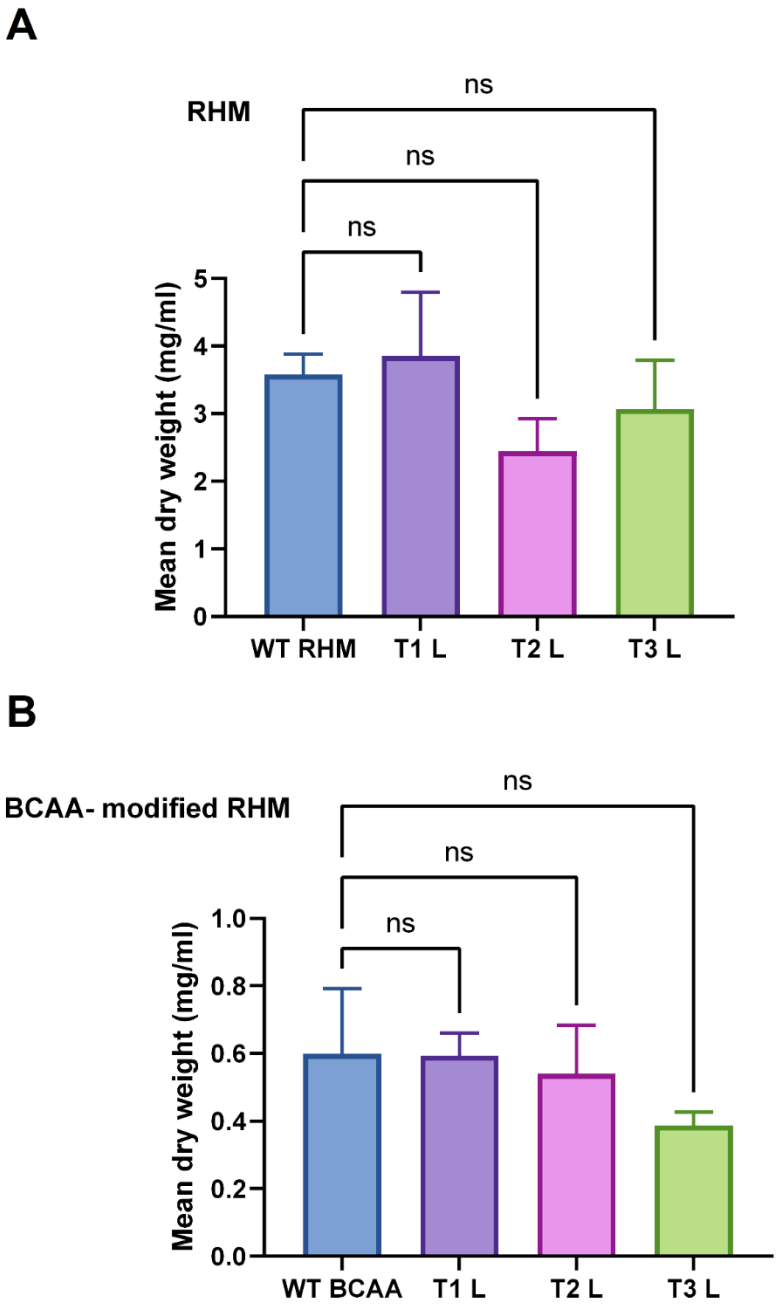

Figure 4.12 Mean dry weight of *F. venenatum* wild type and tube race isolates (T1-T3) after 36 h cultivation in flask cultures. A – isolates and WT were cultivated in normal RHM medium. **B** – isolates and WT were cultured in a modified RHM medium (NH_4Cl replaced with a mix of 13.33 mM each of leucine, isoleucine and valine). The cultures were grown with orbital shaking at 150 rev/min at 28 ºC. The values on the graphs represent mean of total dry mass extracted from flask cultures expressed as mg of dry mass per ml of culture (n = 3, biological replicates). The means were compared using Kruskall-Wallis test with Dunn's multiple comparisons, for A: H = 5.205, df = 3, p = 0.1606); for B: H = 6.897, df = 3, p = 0.0502

Table 4.7 Hydrolysate amino acid profiles of *F. venenatum* wild type and isolates obtained from tube race experiments, following subsequent growth on RHM medium in flask cultures. The values are expressed as g/kg biomass ±SD. The bottom three rows indicate the principal component values ± SD. The PC1-3 from different treatments were compared by One-Way ANOVA (F = 0.101, df = 3, p = 0.9572; F = 0.5668, df = 3, p = 0.6522; F = 1.7468, df = 3, p = 0.2348) respectively. n = 3

	WT	Tube race 1	Tube race 2	Tube race 3
Ala	**28.49 ± 6.30**	**33.81 ± 3.44**	**34.85 ± 1.42**	**33.85 ± 0.27**
Arg	**31.43 ± 3.57**	**32.89 ± 1.35**	**32.24 ± 6.39**	**32.94 ± 0.25**
Asp	**50.14 ± 10.37**	**50.39 ± 0.95**	**47.46 ± 15.00**	**46.19 ± 4.77**
Cys	**1.31 ± 0.41**	**2.49 ± 1.14**	**2.10 ± 0.38 (n = 2)**	**2.10 ± 0.19**
Glu	**79.67 ± 6.32**	**87.95 ± 5.42**	**87.70 ± 15.64**	**92.47 ± 2.80**
Gly	**20.64 ± 2.25**	**21.88 ± 1.30**	**22.37 ± 6.31**	**22.60 ± 0.83**
His	**13.29 ± 1.37**	**13.33 ± 1.13**	**13.26 ± 2.28**	**13.17 ± 0.53**
Ile	**21.33 ± 1.23**	**22.40 ± 1.15**	**25.56 ± 5.95**	**24.75 ± 1.53**
Leu	**34.64 ± 3.20**	**36.05 ± 1.74**	**36.06 ± 7.98**	**37.97 ± 1.78**
Lys	**35.20 ± 3.37**	**36.67 ± 2.06**	**36.51 ± 6.87**	**36.59 ± 0.74**
Met	**8.86 ± 1.00**	**9.27 ± 0.1**	**9.35 ± 1.56**	**8.97 ± 0.22**
Phe	**20.44 ± 2.28**	**21.05 ± 065**	**21.02 ± 4.00**	**21.13 ± 0.53**
Pro	**17.10 ± 2.57**	**17.61 ± 0.91**	**16.64 ± 3.73**	**17.89 ± 0.93**
Ser	**18.34 ± 1.04**	**18.96 ± 1.03**	**18.68 ± 3.93**	**18.55 ± 2.83**
Thr	**20.01 ± 4.52**	**20.34 ± 2.52**	**18.82 ± 2.60**	**18.53 ± 2.10**
Tyr	**13.71 ± 1.15**	**13.94 ± 0.68**	**14.34 ± 2.54**	**14.30 ± 0.89**
Val	**26.21 ± 3.70**	**27.89 ± 0.39**	**27.32 ± 5.88**	**27.27 ± 2.03**
Total	**440.81 ± 49.38**	**466.93 ± 19.01**	**463.58 ± 91.61**	**468.42 ± 18.32**
PC1	**0.95 ± 1.9**	**1.71 ± 0.7**	**1.66 ± 3.6**	**1.79 ± 0.8**
PC2	**- 0.52 ± 0.7**	**0.09 ± 0.3**	**-0.26 ± 0.8**	**- 0.30 ± 0.1**
PC3	**- 0.92 ± 0.3**	**- 0.09 ± 0.7**	**- 0.47 ± 0.6**	**- 0.96 ± 0.3**

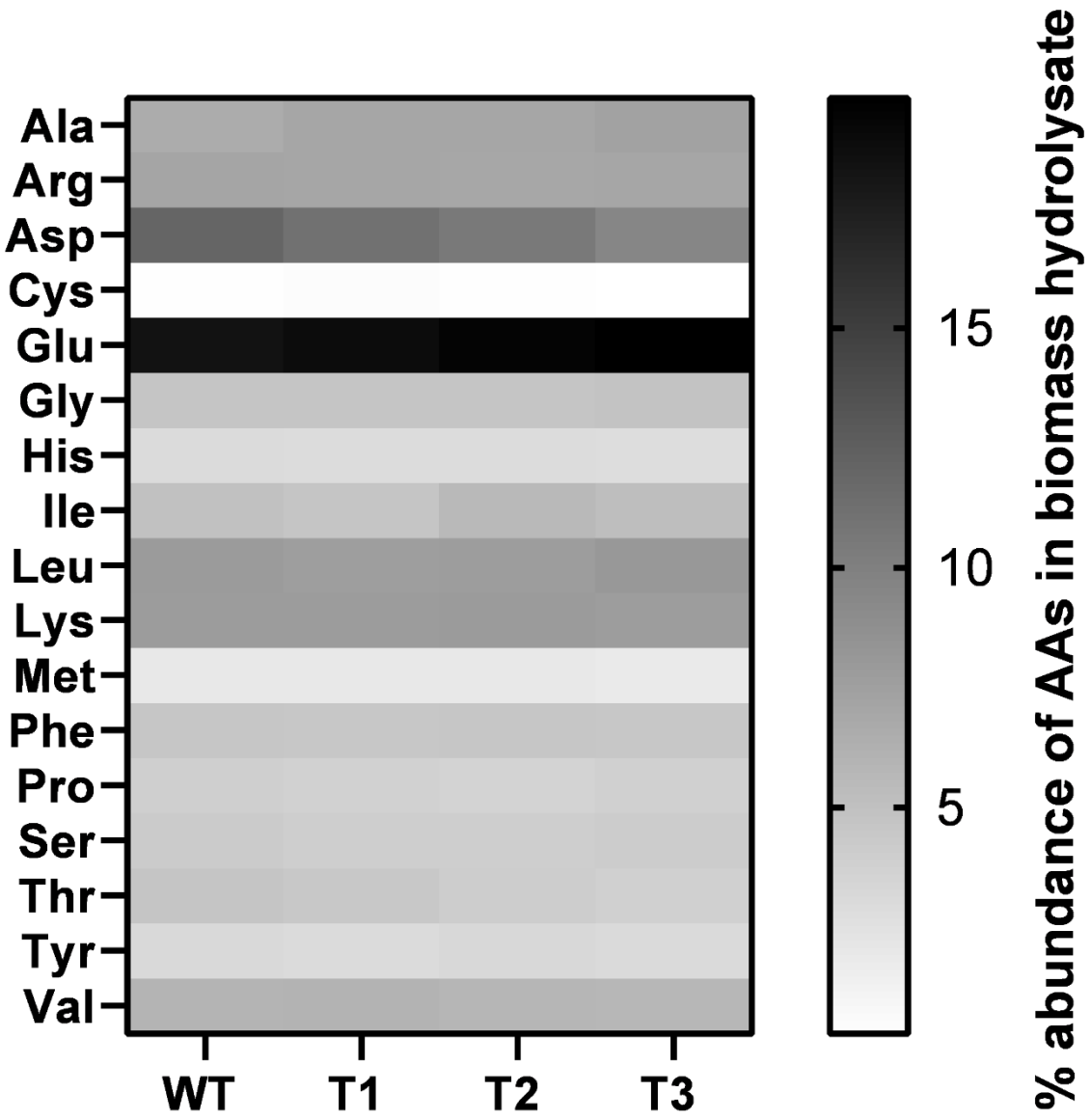

Figure 4.13 Heat map illustration of relative amino acid composition within hydrolysate of *F. venenatum* wild type and isolates from tube race experiment, following subsequent growth on RHM medium in flask. The values from **Table 4.7 (**converted to heatmap according to the right-side scale) are normalised to the total amino acid amount from their respective treatments (**Appendix Table 22**). n = 3

Table 4.8 Hydrolysate amino acid profiles of *F. venenatum* wild type and tube isolates obtained from tube race, following subsequent growth on RHMBCAA medium in flask cultures. The values are expressed as g/kg biomass ± SD. The bottom three rows indicate the principal component values ± SD. The PC1-3 from different treatments were compared by One-Way ANOVA (F = 1.0948, df = 3, p = 0.4123; F = 4.4476, df = 3, p = 0.0479; F = 4.4476, df = 3, p = 0.0493) respectively. Different letters in superscript in the last three rows indicate statistically significant difference between values derived from One-Way-ANOVA with Tukey's multiple comparisons. Lack of any superscript letters indicates lack of significant difference within the relevant part of a row. n = 3 (unless indicated otherwise) N/Q – not quantifiable.

	WT	Tube race 1	Tube race 2	Tube race 3 (n = 2)
Ala	9.58 ± 3.52	18.47 ± 3.30	19.90 ± 15.38	3.75 ± 5.30
Arg	36.17 ± 6.52	30.39 ± 0.35	38.01 ± 17.40	52.48 ± 14.13
Asp	40.03 ± 4.90	36.68 ± 2.33	36.96 ± 6.15	24.71 ± 16.32
Cys	1.42 (n = 1)	1.28 ± 0.97	2.78 ± 0.88 (n = 2)	N/Q
Glu	64.20 ± 5.89	67.90 ± 3.34	74.75 ± 18.86	78.49 ± 2.99
Gly	17.04 ± 5.29	15.77 ± 2.92	15.55 ± 6.39	23.19 ± 12.11
His	19.49 ± 4.48	14.08 ± 0.52	20.87 ± 12.18	33.33 ± 14.62
Ile	28.56 ± 8.03	19.50 ± 1.17	26.23 ± 11.89	41.56 ± 11.35
Leu	42.11 ± 6.67	31.66 ± 2.73	42.82 ± 16.65	46.40 ± 10.99
Lys	40.06 ± 6.92	33.40 ± 2.05	42.45 ± 21.36	57.95 ± 17.76
Met	9.76 ± 1.74	8.01 ± 0.49	10.44 ± 4.63	13.04 ± 3.14
Phe	23.69 ± 4.87	18.63 ± 0.12	25.37 ± 13.55	38.13 ± 13.27
Pro	15.09 ± 2.33	14.47 ± 2.30	16.80 ± 7.86	12.48 ± 5.74
Ser	19.66 ± 4.51	17.48 ± 1.20	17.55 ± 8.20	16.87± 1.83
Thr	20.87 ± 2.99	18.81 ± 0.97	22.01 ± 5.27	25.18 ± 5.10
Tyr	16.45 ± 3.44	13.58 ± 0.37	18.66 ± 10.75	29.04 ± 11.34
Val	49.84 ± 6.42	43.22 ± 1.39	52.06 ± 19.75	64.27 ± 15.81
Total	453.06 ± 59.60	403.37 ± 19.38	482.28 ± 158.84	560.89 ± 118.56
PC1	3.20 ± 3.3	- 0.04 ± 0.7	3.99 ± 8.9	9.52 ± 7.4
PC2	- 3.95 ± 0.7 $^{A, B}$	- 2.72 ± 0.6 ^{A}	- 3.52 ± 2.1 $^{A, B}$	- 6.92 ± 1.3 ^{B}
PC3	- 0.39 ± 0.4	-0.52 ± 0.4	0.54 ± 0.5	- 0.62 ± 0.3

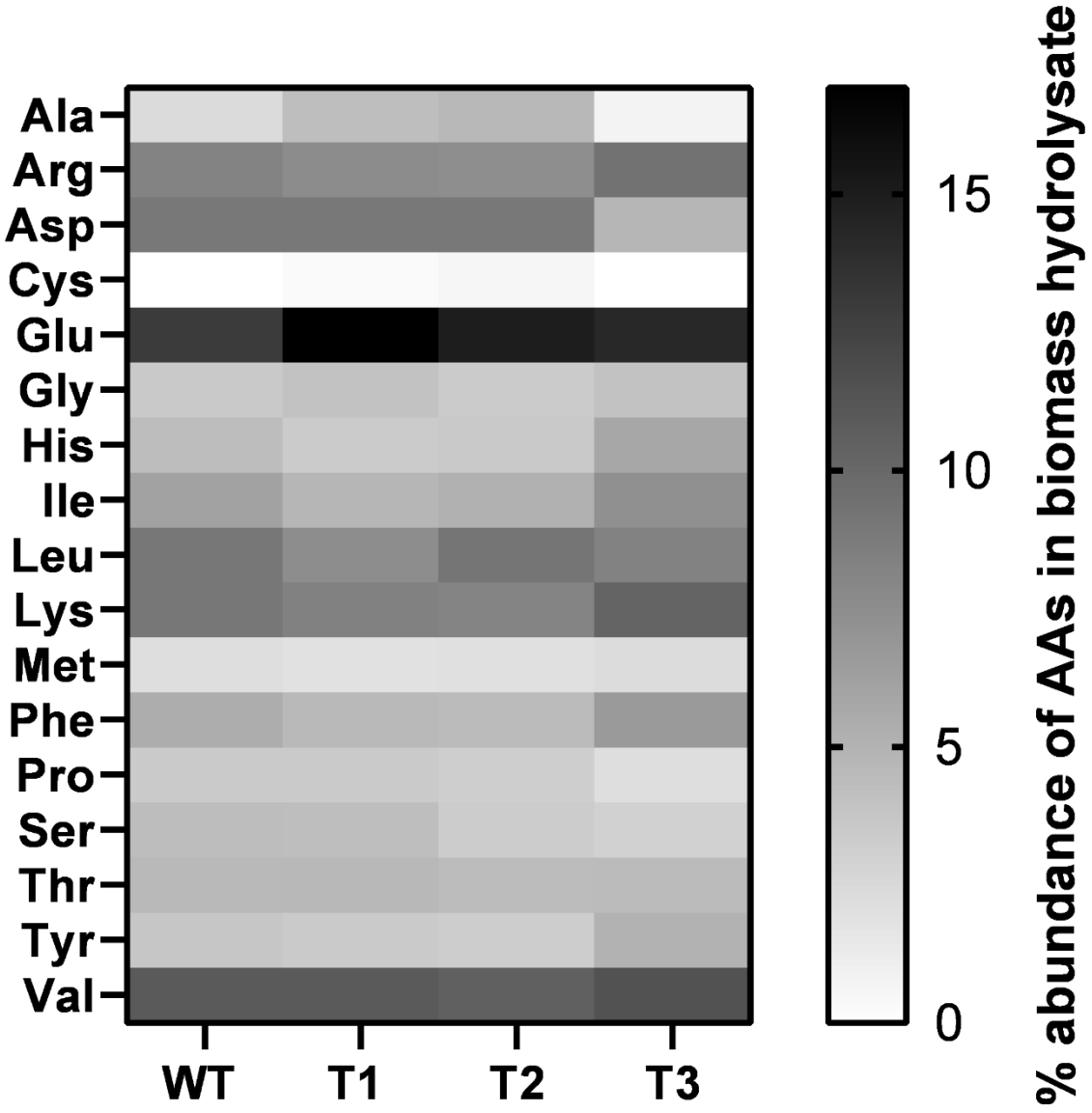

Figure 4.14 Heat map illustration of relative amino acid composition within hydrolysate of F. venenatum wild type and isolates from tube race experiment, following subsequent growth on BCAARHM medium in flask. The values from **Table 4.8 (**converted to heatmap according to right side scale) are normalised to the total amino acid amount from their respective treatments (**Appendix Table 23**). n = 3 (biological replicates).

4.4.13 The effect of tube race selection in agar medium on the AA hydrolysate composition of *F. venenatum*

In parallel to the above experiment, the tube race was carried out on an agar version of the RHMBCAA selective medium. This was done because the race-tube colonisation proceeds more slowly on agar (~3 weeks per passage compared to 2-3 days on liquid medium) and it was reasoned that this may increase the opportunity for development and selection of relevant mutations. After (~10 weeks of selection through consecutive tube races, isolates were cultured in regular or BCAA-modified RHM (BCAARHM) medium, hydrolysed and the AA profiles compared to that of the WT hydrolysate.

First, the dry weights of the samples from flasks after 36 h of culturing were compared to see whether the selection in the agar-based tube race had affected the growth rate of *F. venenatum* isolates (**Figure 4.4.15**). Analysis of the means by Kruskal-Wallis test revealed a significant difference between the growth yields of all compared strains ($p = 0.0006$) with Dunn's multiple comparisons test corroborating a very marked decrease in biomass yield of the T3 isolate compared to WT ($p = 0.0067$) during culture in the RHM medium (**Figure 4.4.15 A)**. In the RHMBCAA medium, Kruskal-Wallis test revealed no significant differences in the growth yields between the growth yields of all compared strains ($p = 0.0502$) (**Figure 4.4.15 B)**.

First, the AA hydrolysates of WT and tube race isolates grown in standard RHM medium were compared. Comparison of the PC1 by One-Way ANOVA revealed no change to the overall AA abundance in tested hydrolysates ($p = 0.47$) (**Table 4.9**). Analysis of PC2 and 3 indicated a significant change to the relative AA levels ($p = 0.06$, $p = 0.044$, respectively). Tukey's multiple comparison analysis of PC3 revealed a significant difference between control and T2 isolate ($p < 0.034$). Higher values in PC3 indicate enrichment in Cys in the T2 (**Table 4.9**), and increase in relative Cys content (0.67% vs 0.29% in control) (**Figure 4.16 Appendix Table *24***). It is worth noting that this change in cysteine content can be observed in all three isolates.

Next hydrolysates of the biomass from WT and tube race isolates of *F. venenatum* were compared after culturing in the RHMBCAA medium. For this comparison isolate 3 was not included in the analysis as at 36 h the samples did not accumulate sufficient biomass to permit LCMSMS analysis (**Figure 4.4.15 B**). Analysis of PC1 by One-Way ANOVA revealed no significant difference in the total AA abundance of the control and tube race isolates ($p = 0.26$) (**Table 4.10**). There were also no differences between PC3 ($p = 0.49$), but significant difference in PC2 values was found ($p = 0.049$). Tukey's multiple comparisons indicated that the difference in PC2 was between the control and T1 isolate ($p = 0.044$). Higher PC2 value in T1 isolate indicates an increase in relative Ala, Asp and Gly abundance and decrease in Leu and His which can be seen in both absolute (**Table 4.10**) and relative values (1.3, 2.4, 0.84 % increase, and 1.32, 0.53 % decrease in T1 respectively) (**Figure 4.17**, **Appendix Table 25**) .

Overall, the tube races on agar did noticeably change some properties of the isolates. First, isolate T3 showed an undesirable decrease in the ability to grow in flask culture. Furthermore, the agar tube-race selected isolates did show some significant changes to AA composition compared to the wild type. However consistently increased AAs were not the BCAAs.

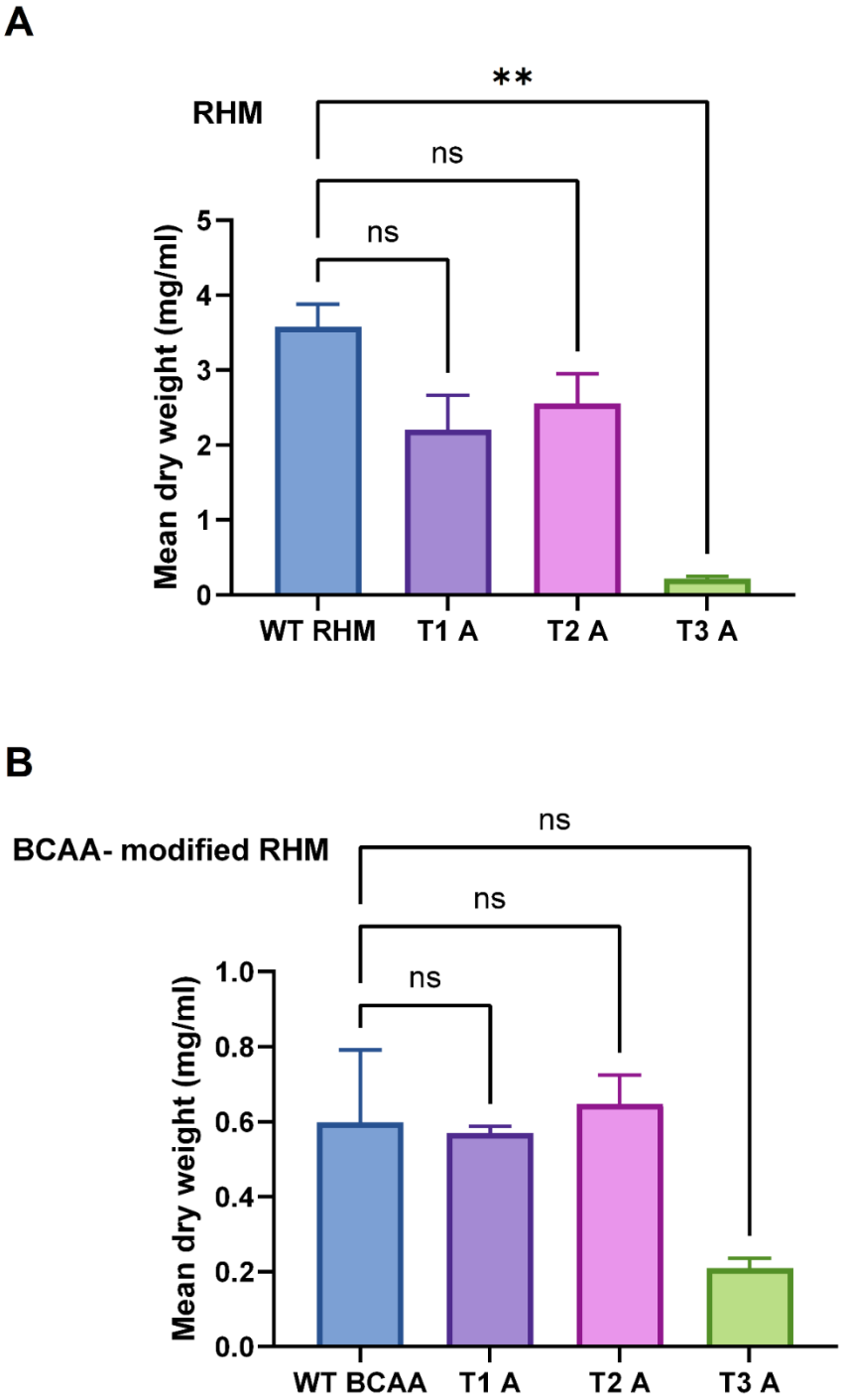

Figure 4.4.15 Mean dry weight of *F. venenatum* wild type and agar tube race isolates (A1-A3) after 36 h cultivation in flask cultures. A – isolates and WT were cultivated in normal RHM medium, B – isolates and WT were cultured in a modified RHM medium (NH_4Cl replaced with a mix of 13.33 mM each of leucine, isoleucine and valine). The cultures were grown with orbital shaking at 150 rev/min at 28 ^{o}C. The values on the graphs represent mean of total dry mass extracted from flask cultures expressed as mg of dry mass per ml of culture (n = 3 biological replicates). The means were compared using Kruskall-Wallis test, for A: H = 9.667, df = 3, p = 0.0006) with Dunn's multiple comparisons (WT vs T3, p = 0.0067); for B: H = 6.897, df = 3, p = 0.0502.

Table 4.9 Comparison of hydrolysate amino acid profiles of *F. venenatum* isolates obtained from tube race experiments in agar medium grown flask cultures in RHM medium. The values are expressed as g/kg biomass ±SD. The bottom three rows indicate the principal component values ± SD. The PC1-3 from different treatments were compared by One-Way ANOVA (F = 0.9325, df = 3, p = 0.4685; F = 3.7108, df = 3, p = 0.0612; F = 4.291, df = 3, p = 0.0442) respectively. Different letters in superscript in the last three rows indicate statistically significant difference between values derived from One-Way-ANOVA with Tukey's multiple comparisons. Lack of any superscript letters indicates lack of significant difference within the relevant part of a row. n = 3.

	WT	Tube race 1	Tube race 2	Tube race 3
Ala	**28.49 ± 6.3**	**27.16 ± 3.40**	**28.44 ± 1.58**	**41.75 ± 1.78**
Arg	**31.43 ± 3.57**	**33.01 ± 0.68**	**32.84 ± 0.92**	**34.34 ± 1.25**
Asp	**50.14 ± 10.37**	**50.76 ± 3.11**	**50.66 ± 2.42**	**51.55 ± 0.58**
Cys	**1.31 ± 0.41**	**3.25 ± 0.40**	**3.18 ± 0.92**	**2.75 ± 0.21**
Glu	**79.67 ± 6.32**	**95.47 ± 5.60**	**97.48 ± 6.69**	**87.49 ± 2.82**
Gly	**20.64 ± 2.25**	**27.58 ± 3.41**	**24.29 ± 4.08**	**23.40 ± 1.22**
His	**13.29 ± 1.37**	**13.73 ± 0.56**	**13.91 ± 0.61**	**13.75 ± 0.43**
Ile	**21.33 ± 1.23**	**23.31 ± 1.00**	**23.16 ± 1.02**	**24.67 ± 1.59**
Leu	**34.64 ± 3.20**	**36.78 ± 0.70**	**35.07 ± 0.91**	**37.84 ± 3.28**
Lys	**35.20 ± 3.37**	**38.15 ± 0.53**	**38.21 ± 0.64**	**39.02 ± 1.46**
Met	**8.86 ± 1.00**	**9.10 ± 0.21**	**9.36 ± 0.17**	**10.05 ± 0.09**
Phe	**20.44 ± 2.28**	**21.74 ± 0.27**	**21.46 ± 0.32**	**21.58 ± 0.75**
Pro	**17.10 ± 2.57**	**18.90 ± 0.18**	**18.58 ± 2.06**	**17.76 ± 1.22**
Ser	**18.34 ± 1.04**	**18.04 ± 2.52**	**17.99 ± 1.93**	**16.66 ± 0.35**
Thr	**20.01 ± 4.52**	**19.53 ± 0.46**	**23.62 ± 1.79**	**19.07 ± 1.91**
Tyr	**13.71 ± 1.15**	**12.82 ± 0.13**	**13.01 ± 0.37**	**13.17 ± 1.06**
Val	**26.21 ± 3.70**	**28.53 ± 0.79**	**27.19 ± 1.29**	**28.72 ± 0.67**
Total	**440.81 ± 49.36**	**477.86 ± 9.49**	**478.49 ± 11.26**	**483.56 ± 10.47**
PC1	**0.95 ± 1.9**	**2.07 ± 0.1**	**2.18 ± 0.6**	**2.01 ± 0.5**
PC2	**- 0.52 ± 0.7**	**0.44 ± 0.4**	**0.48 ± 0.2**	**0.39 ± 0.2**
PC3	**- 0.92 ± 0.3**	**0.02 ± 0.1**	**0.39 ± 0.8**	**- 0.09 ± 0.2**

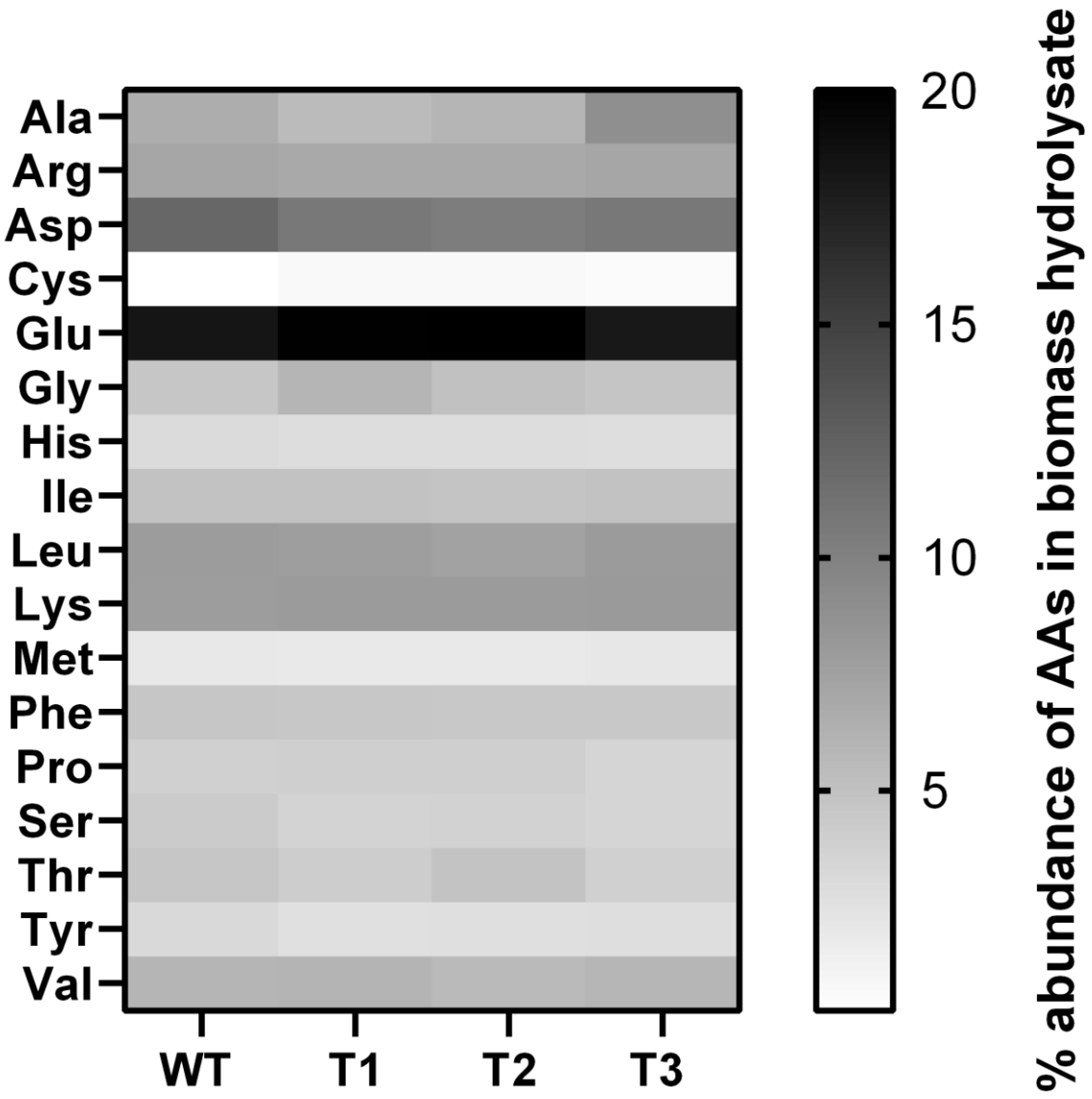

Figure 4.16 Heat map illustration of relative amino acid composition within hydrolysate of *F. venenatum* isolates from tube race experiment in liquid medium grown in RHM medium. The values from **Table 4.9** (converted to heatmap according to right side scale) are normalised to the total amino acid amount from their respective treatments (**Appendix Table *24***). n = 3 (biological replicates)

Table 4.10. Comparison of the hydrolysates of the amino acid profiles of *F. venenatum* isolates obtained from tube race experiments on agar, grown in flask cultures in RHM medium lacking NH_4Cl and supplemented with a mix of branch chained amino acids. The values are expressed as g/kg biomass ±SD. The bottom three rows indicate the principal component values ± SD. The PC1-3 from different treatments were compared by One-Way ANOVA (F = 1.677, df = 2, p = 0.2639; F = 5.1873, df = 2, p = 0.0492; F = 0.7903, df = 2, p = 0.4959) respectively. Different letters in superscript in the last three rows indicate statistically significant difference between values derived from One-Way-ANOVA with Tukey's multiple comparisons. Lack of any superscript letters indicates lack of significant difference within the relevant part of a row. n = 3 (unless indicated otherwise).

	WT	Tube race 1	Tube race 2 (n =2)
Ala	9.58 ± 3.52	14.49 ± 7.26	10.44 ± 7.02
Arg	36.17 ± 6.52	31.75 ± 2.13	29.55 ± 3.27
Asp	40.03 ± 4.90	47.12 ± 8.03	36.49 ± 2.23
Cys	1.31 ± 0.41	0.98 ± 0.89 (n =2)	N/Q
Glu	64.20 ± 5.89	68.31 ± 5.15	61.33 ± 8.12
Gly	17.04 ± 5.29	19.13 ± 2.03	14.78 ± 2.00
His	19.49 ± 4.48	15.63 ± 2.06	15.89 ± 2.25
Ile	28.56 ± 8.03	22.85 ± 3.08	24.68 ± 4.43
Leu	42.11 ± 6.67	33.34 ± 3.19	31.82 ± 4.62
Lys	40.06 ± 6.92	33.70 ± 2.45	32.28 ± 3.72
Met	9.76 ± 1.74	8.48 ± 0.92	8.14 ± 1.06
Phe	23.69 ± 4.87	19.19 ± 2.10	19.00 ± 2.60
Pro	15.09 ± 2.33	14.63 ± 1.63	13.68 ± 1.25
Ser	19.66 ± 4.51	15.83 ± 0.11	13.38 ± 1.53
Thr	20.87 ± 2.99	21.69 ± 2.63	21.18 ± 2.18
Tyr	16.45 ± 3.44	12.07 ± 2.04	12.41 ± 1.78
Val	49.84 ± 6.42	40.49 ± 2.04	42.23 ± 2.51
Total	453.06 ± 59.60	419.35 ± 34.30	387.28 ± 38.58
PC1	3.18 ± 3.3	0.53 ± 1.5	- 0.24 ± 2.0
PC2	- 4.07 ± 0.8	- 2.35 ± 0.6	- 3.50 ± 0.5
PC3	- 0.82 ± 0.2	-1.01 ± 0.4	- 0.44 ± 0.9

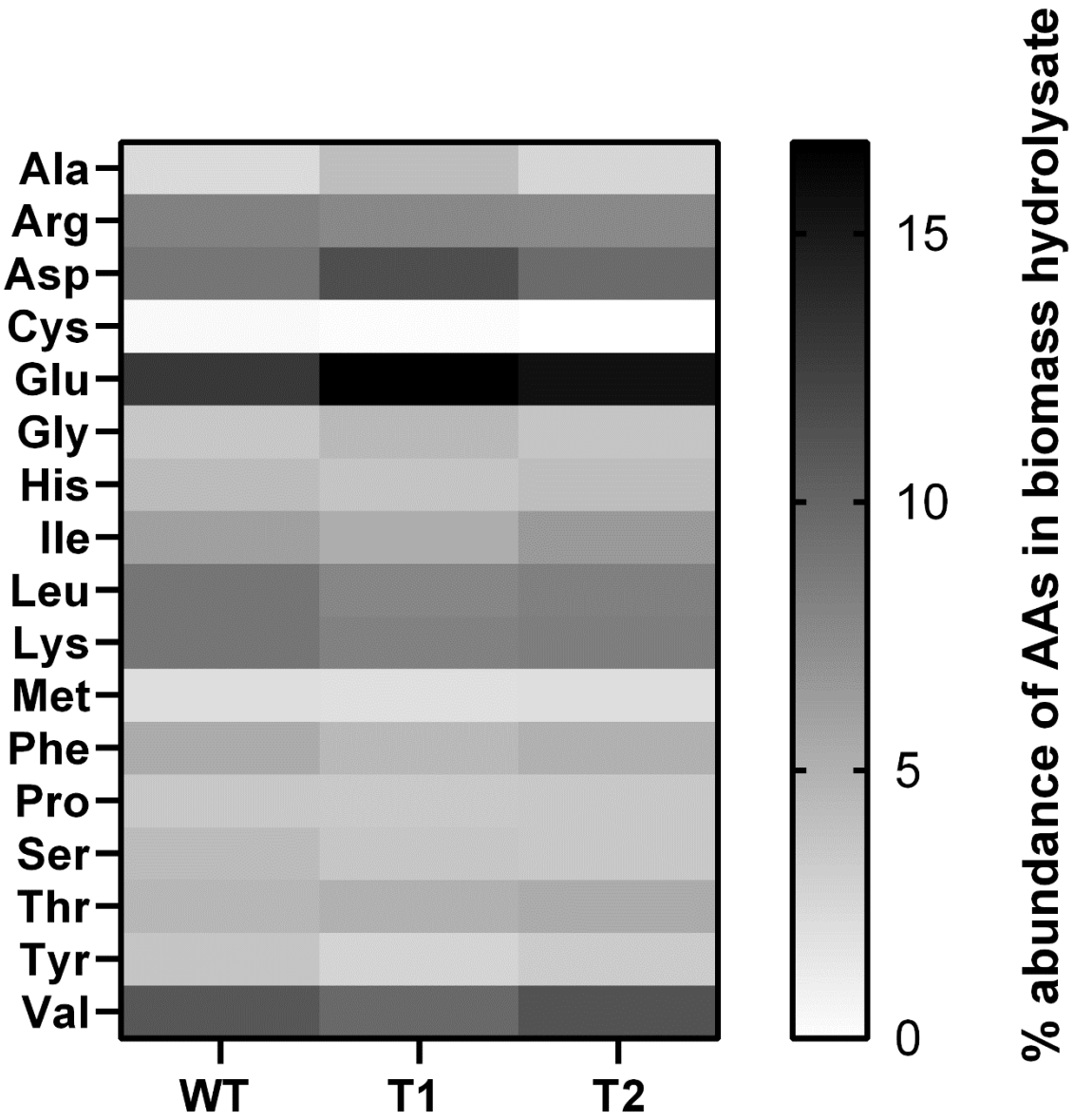

Figure 4.17. Heat map illustration of relative amino acid composition within hydrolysate of F. venenatum isolates from tube race experiment in liquid medium grown in RHM medium lacking NH_4Cl and supplemented with a mix of branch chained amino acids. The values from **Table 4.10 (**converted to heatmap according to right side scale) are normalised to the total amino acid amount from their respective treatments (**Appendix Table 25**). n = 3 (biological replicates)

4.5 Discussion

4.5.1 Chemically induced mistranslation

Addition of the aminoglycoside drugs did not have a clear effect on the AA profile. Despite significant effect of the treatment on the AA profile in samples treated with a growth-slowing level of paromomycin combined with leucine, only levels of alanine and glutamate differed significantly between the control and experimental treatments, but these two AAs are prone to fluctuation in control treatments as discussed in **Chapter 2**. Comparison of fold changes versus control values revealed very modest variation in the levels of individual AAs. Likewise, the addition of leucine to the medium did not affect leucine in the AA profile.

Aminoglycosides have been shown to increase the mistranslation rate prokaryotes like *E. coli* (Kohanski et al., 2008*)* in eukaryotes like yeast (Fan-Minogue and Bedwell, 2008) and humans (Keeling et al., 2014) so it is likely that the effect is similar in *F. venenatum*, although mistranslation wasn't specifically assayed here, e.g., with mistranslation reporters (Altamura et al., 2016) (Chen et al., 2020).

Lack of clear effect on the AA profile could also be due to the specific mechanism in which paromomycin induces mistranslation. Although aminoglycosides including paromomycin have been reported to increase the levels of mistranslation several fold, more recent studies revealed the mechanisms in which aminoglycosides cause the mistranslation which rather than increasing the levels of errors throughout the whole protein causes clusters of errors that are more likely to completely disrupt protein function (Wohlgemuth et al., 2021). Alternatively, even a 2- or 3-fold increase in mistranslation rate at only certain amino acid residues (Holland et al., 2010) is likely insufficient to have a substantial impact on overall measurable AA composition, given that the starting, background mistranslation rates are typically very low (Kramer and Farabaugh, 2007).

Another reason for lack of measured change may be the fact that misincorporation of non-cognate AAs would have to happen out of the pool of AAs already present within the fungus – which are a part of the hydrolysate. This could be corrected for by subtracting the free AA pool from the hydrolysate result to look for a change to the in-protein AAs only, between the control and paromomycin treated samples. However, in *F. venenatum* the pool predominantly consists of alanine and glutamine. Other free AAs making up a very small proportion of their respective AAs as free AAs meaning that for most of the other AAs misincorporation of the available free pool would make a very small change to the overall amounts of AAs in protein. This concern was partly addressed by supplementing growth medium with additional leucine alongside paromomycin but resulted in no additional change to the hydrolysate AA profile. This could be because the organism did not uptake the free leucine in sufficient amounts. Alternative way of increasing the abundance of available free AAs within *F. venenatum* cells could be by e.g., upregulating relevant biosynthesis pathways.

Similar to experiments with paromomycin, attempts to increase the incorporation of methionine in *F. venenatum* through induction of oxidative stress with H_2O_2 did not yield significant changes to the overall methionine content. The lack of measurable change could be for similar reasons as discussed above for paromomycin, including the low levels of free methionine naturally present in the fungus as shown in **Chapter 2** of this thesis. Alternatively, a recent overview of use of H_2O_2 as oxidative stress model revealed a problem with the use of H_2O_2 as oxidative stress agent. The study shows that using catalase enzyme

cells are able to break most or all the H_2O_2 within a few minutes of treatment releasing high amounts of O_2 and postulates that the observed results are due to only transient effect of H_2O_2 and/or various possible effects of elevated O_2 (Ransy et al., 2020). Perhaps in the present study, the inhibitory effect that H_2O_2 had on *F. venenatum* was not due to the oxidative stress caused by H_2O_2 but rather oxygen toxicity effects of which are not very well understood (Bai et al., 2003).Oxygen or ROS toxicity could explain higher growth inhibition in baffled flask cultures, which oxygenate the medium much more effectively than via static cultivation in 96 well plates (McDaniel and Bailey, 1969). The effect of oxidative stress rather than oxygen toxicity on the AA profile could be tested by using another well-established oxidative stress inducer, e.g., redox-active metal ions (Stohs and Bagchi, 1995) or superoxide generators like paraquat (Cochemé and Murphy, 2008).

4.5.2 Effects of BCAA selection media on *F. venenatum* hydrolysate AA profile

The growth in modified RHM medium with the inorganic nitrogen source replaced by one or more BCAAs changed the *F. venenatum* AA profile in variety of ways. First, the medium containing leucine, isoleucine and valine not only increased the relative valine composition but also significantly affected the total levels of AAs. The relative amount of leucine and isoleucine (which were also present in the medium) was not changed compared to the WT. One relevant effect here could be the potential toxicity of valine, where valine acts as an inhibitor of isoleucine synthesis causing accumulation of α-ketobutyrate (Reitzer, 2014). The present inclusion of high isoleucine levels in the same selection medium here indicate that isoleucine limitation was not a likely limiting factor for growth of *F. venenatum*. Consistent with this, accumulation of α-ketobutyrate was previously shown to cause toxicity (LaRossa et al., 1987) and similar could explain the poorer growth of *F. venenatum* in this BCAAs-modified medium. Accordingly, inclusion only of leucine and isoleucine (not valine) in the selection medium here gave improvement to the AA abundance compared to when valine was also present. Some common changes were evident in all the tested selection media, like a decrease in levels of glutamate and alanine and increase in aspartate. The lower levels of glutamate and alanine could be due to depletion of free AA stores although this would need to be tested by comparing the free AA pools of cells cultivated in selection media. Removal of valine from the selection medium seems to limit the toxicity as the protein content of tested samples from the other media was comparable to the WT.

Because experiments in this chapter were conducted with an intent to find a suitable selection medium for adaptive evolution, formulations containing NH_4Cl were disregarded due to lack of pressure on growth – even small amounts of NH_4Cl present in the medium allowed *F. venenatum* to grow at a rate comparable to unaltered medium (**Appendix Figure 5)**. However, it would be interesting to see whether cultivation with excess AAs and small amounts of inorganic nitrogen can result in similar changes to the AA profile. This is because such formulation would allow for immediate modification of the AA profile with smaller/or no effect to the growth rate e.g. to produce mycoprotein for commercial or research purposes. Testing the effect of formulations with other AAs as a sole/main source of nitrogen on the AA profile would also be of interest because it could lead to opportunities to both enrich other AAs of interest and identify potential undesirable changes to the AA profile. The knowledge of how high abundances of different AAs can affect the AA profile of *F. venenatum* is useful in the context of ambitions to use waste/side streams as substrates for fungal growth, e.g., waste products from food processing for cultivation of the fungus; these

waste products such e.g. waste from processing crops or animals are already rich in AAs or peptides (Arun et al., 2020).

4.5.3 The effect of tube race selection

Unfortunately, the tube race selection was not successful in producing isolates with increased BCAA contents (**as hypothesised in section 4.4.7**). The tube race in liquid medium did not significantly change the absolute AA profile of the isolates compared to WT (when subsequently grown in RHM or RHMBCAA medium). The tube race in agar RHM medium did cause a significant change but this was not BCAA specific (significant increases were in glutamate and glycine levels).

Isolates from the agar-based tube race subsequently grown in RHMBCAA medium had significantly lower levels of valine and leucine. This could reflect an adaptation resulting, for example, in a more efficient catabolism of the BCAAs that were the only source of nitrogen in the selection medium. Similar phenomenon was showcased when e.g. *E. coli* cells subject to adaptive laboratory evolution in glucose medium evolve 1.6 times faster growth rates due to reshaping of their metabolism (Long and Antoniewicz, 2018). However, it isn't clear whether this difference between isolates and the wild type may arise from changes to the cellular protein profile, free AA pool or both, and investigating this e.g., by comparing the free AA profiles, or proteomic analysis could help to better inform future investigations.

Overall, the selection on agar proved more effective in producing change to the AA profile, but it also had an unintended, but not unexpected consequence in one of the isolates, which exhibited markedly decreased growth in liquid medium (**Figure 4.4.15**). Thus, repeated selections on agar made the isolate less fit for growth in liquid medium, an established phenomenon (Lin et al., 2014; Riquelme et al., 2018). This undesirable effect could be potentially overcome by running the adaptation experiment in continuous culture or using a microfluidics based selection system (Zoheir et al., 2021). The advantage of such method over tube race in liquid medium would be longer selection times and better control of influx of fresh selection medium in both alternatives. In these experiments the idea was to capitalise on the concept of adaptive mistranslation by promoting misincorporation of AAs abundant in medium otherwise lacking other nitrogen sources to increase their overall presence in the AA profile (Wong et al., 2018). The idea behind this approach is that over consecutive generations the organism may evolve to use more of the desired AAs in its proteome leading to fixation of the enriched phenotype when transferred back in regular growth conditions. Nevertheless, other methods like random mutagenesis that might add could be incorporated into the selection regimes to help accelerate the speed and outcomes of adaptation (Zhang et al., 2015; Casselton and Zolan, 2002). In this study the adaptive evolution experiments were carried out using only one of the four tested formulations of selection medium (containing valine, leucine and isoleucine, leucine and isoleucine, only leucine and only isoleucine) (**4.4.10, 4.4.11**), but it would be worth investigating whether selection in all media tends to lead to similar outcomes in terms of AA profile.

5 Chapter 5 Targeting leucine biosynthesis as a means of altering the amino acid profile of *F. venenatum*.

5.1 Introduction

Organisms can obtain amino acids (AA) used to produce proteins either by direct uptake of required AAs from the environment, breakdown of AAs and other complex organic molecules to synthesise the required AAs or biosynthesis of the required AAs from inorganic compounds. In humans, essential AAs (those that cannot be synthesised in sufficient amounts or at all) must be obtained from the diet (WHO, 2007). For example, high dietary levels of essential branch-chained AAs (BCAAs) (L-leucine, L-isoleucine, L-valine) are linked to increased muscle health (Blomstrand et al., 2006). This means that generally increasing the amount of available BCAAs in food protein is desirable from the perspective of improving the health of populations through good nutrition. Sufficient amounts of leucine in particular are necessary to trigger the muscle synthesis pathway in humans, with higher amounts needed in the elderly, making this BCAA of especial interest in nutrition and muscle health (Drummond and Rasmussen, 2008; Rondanelli et al., 2021).

Many microbial organisms unlike humans and other animals are AA prototrophs, meaning that they can synthesize all proteinogenic AAs from simple organic substrates and inorganic nitrogen sources. For example, RHM medium used to cultivate *F. venenatum* contains only one source of nitrogen in the form of the inorganic salt NH_4Cl, so all the proteinogenic AAs have to be synthesised by the fungus using the inorganic nitrogen from the medium. This is possible due to the presence of metabolic pathways for AA biosynthetis that exist in fungi, bacteria and plants but were lost in animals. For example the metabolic pathways used to synthesise BCAAs are ancient and highly conserved as evidenced by functional homology of the enzymes in the pathway between archaeal, prokaryotic, and eukaryotic cells (Xing and Whitman, 1991).

In fungi, L-isoleucine is synthesised from L-threonine and only the four last steps of the pathway are unique to L-isoleucine (Jastrzebowska and Gabriel, 2015). The four last steps of L-isoleucine synthesis and initial steps of L-leucine and L-valine synthesis are catalysed by a common group of enzymes that act on different substrates. The valine and leucine synthesis pathways split after the common intermediate α-ketoisovalarate, which can be converted to valine or to α-isopropylmalate and continue down leucine synthesis pathway (**Figure 5.1**) (Takagi et al., 2015). The leucine biosynthesis pathway is interesting because of its wider role and complexity as a transcription regulator and e.g., modulator of virulence in fungi (Kohlhaw, 2003; Jastrzebowska and Gabriel, 2015). The metabolic bottleneck and main self-regulatory step of the pathway is conversion of α-ketoisovalarate to α-isopropylmalate by isopropylmalate synthase (IPMS). The activity of IPMS is inhibited by binding of leucine (the end product of the pathway) or reversibly inactivated by CoA in the presence of Zn^{2+} ions (Kohlhaw, 2003). In *S. cerevisiae* the IPMS enzyme is encoded by two paralogous genes (*LEU4* and *LEU9*), with *LEU4* accounting for about ~80% of cellular IPMS activity. *LEU4* can be expressed as either a full length protein or as shorter versions of the enzyme which are located in either the mitochondrial matrix or cytoplasm respectively (Beltzer et al., 1988).

The aforementioned leucine feedback inhibition can be mimicked by 5’5’5-trifluoro-DL-leucine (TFL). TFL is a non-metabolizable analogue of leucine that binds to the IPMS enzyme and, in *S. cerevisiae*, inhibits leucine synthesis leading to halted growth if in the

absence of exogenous leucine (Cavalieri et al., 1999). Previously TFL was used to select *S. cerevisiae* with IPMS desensitised to leucine-mediated feedback inhibition and for characterising the mutated enzymes (Oba et al., 2005; Cavalieri et al., 1999). In *S. cerevisiae* this deregulation of the pathway was desirable due to the potential for improved production of isoamyl alcohol, a product of the pathway (**Figure 5.1**) and a flavour component in sake. Analysis of the mutations in the deregulated, TFL-resistant *S. cerevisiae* isolates revealed Asp578Tyr as one of the key mutations in IPMS required for bypassing the feedback inhibition by leucine. Isolates with this mutation retained ~65% IPMS activity in the presence of leucine but were still affected by CoA + Zn^{2+}-mediated inhibition (Oba et al., 2005). Subsequent transcriptomic analysis of one of the TFL resistant mutants revealed an increased expression of the *LEU1*, *LEU2* and *BAT1* genes (Oba et al., 2006).

In other work, virulence and toxin production have been linked to BCAA metabolism in pathogenic fungi. For example, the dihydroxyacid dehydratase Ilv3p was shown to be essential for full virulence of the human pathogenic fungus *Aspergillus fumigatus* (Oliver et al., 2012). The virulence of *Candida albicans* in a murine infection model was reduced in mutants lacking genes involved in isoleucine synthesis (Kingsbury and McCusker, 2010). In the major crop pathogen *Fusarium graminearum* the BCAA synthesis pathway was implicated in the regulation of trichothecene mycotoxins and disruption of the leucine metabolic pathway significantly reduced the organism's virulence (Subramaniam et al., 2015). Elsewhere it was demonstrated that in *Fusarium sporotrichioides,* leucine auxotrophy leads to underproduction of T-2 mycotoxins but induces overproduction of T-2 toxin analogues (Beremand et al., 1988). Since *F. venenatum* belongs to the same genus and is capable of producing mycotoxins in specific conditions (Miller and MacKenzie, 2000; Whittaker, 2022), it is a concern for potential food use that deregulation of leucine synthesis pathway could trigger mycotoxin production.

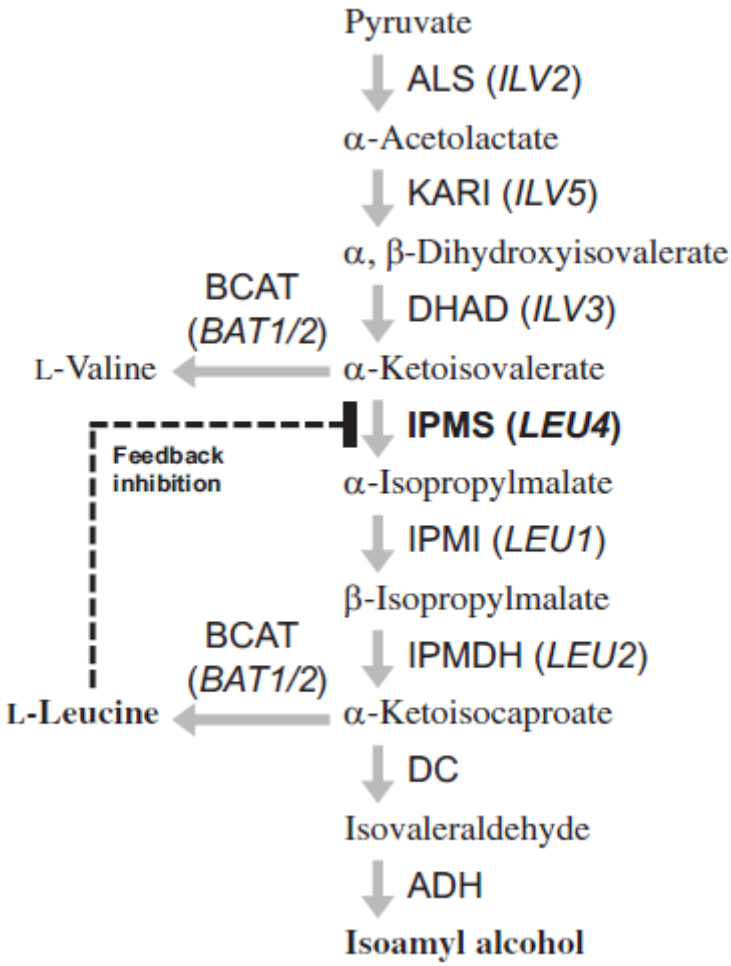

Figure 5.1 Biosynthetic pathway of leucine and isoamyl alcohol in *Saccharomyces cerevisiae*. The genes encoding the different enzymes are shown in parentheses. Protein names: ALS, acetolactate synthase catalytic subunit; KARI, ketol-acid reductoisomerase; DHAD, dihydroxy acid dehydratase; IPMS, α-isopropylmalate synthase; DC, α-keto acid decarboxylase; ADH, alcohol dehydrogenase; BCAT, branched-chain amino acid aminotransferase. IPMS activity is regulated by L-leucine feedback inhibition. Figure taken from Takagi et al. (2015).

5.2 Chapter Aims

As explained above leucine is a nutritionally relevant BCAA that could increase the nutritional value of mycoprotein if more abundant. A highly conserved synthesis pathway means that *F. venenatum* leucine synthesis is regulated similarly to other studied organisms and that supports the potential for selection of variants insensitive to feedback inhibition using TFL. However, the innate potential for mycotoxin production in *F. venenatum* and the links between BCAA metabolism and virulence in other fungi could be an obstacle for enriching leucine in the mycoprotein by upregulation of leucine synthesis. For the work described in this this chapter the aims were:

a) To design and optimise a screen for mutants insensitive to feedback inhibition in leucine biosynthesis
b) To investigate the properties of the isolates including mycotoxin production
c) To characterise the mutations producing the observed phenotypes

5.3 Materials and Methods

All the chemicals are obtained from Sigma-Aldricht (UK), unless indiciated otherwise.

5.3.1 Chemicals

Polymerase chain reaction (PCR) consumables: all the PCR reactions were carried out using a M0530L Phusion® kit (NEB, USA) containing Phusion® High-Fidelity DNA Polymerase, DMSO, and Phusion® HF Buffer and dNTPs mix. Reference DNA ladders **(**100 bp and 1 kB) were purchased from (NEB, USA).

Ethidium bromide stock (10 mg/ml) was prepared by dissolving a 100 mg ethidium bromide tablet in 10 ml of distilled H_2O.

Ampicillin and **Carbenicillin:** A 1000x (100 mg/ml) stock was prepared by dissolving 1 g of ampicillin sodium salt or carbenicillin disodium salt respectively in 10 ml dH_2O. The solutions were aliquoted into Eppendorf tubes and stored at – 20 ^oC

5'5'5-Trifluoro-DL-leucine (TFL) stock (at 500 mg/ml) was prepared by dissolving 500 mg of TFL powder in 0.1 M NaOH and making up the volume to 1 ml. After dissolving, the solution was filter sterilised using a 22 µm filter and stored at -20 ^oC. If precipitate was present in the solution after thawing, it was heated to 80 ^oC in a heat block and vortexed periodically until clear prior to use.

5.3.2 Buffers

Tris-acetate-EDTA (TAE) buffer: a 50X solution was prepared by mixing 242 g of Tris, 57.1 ml of glacial acetic acid and 100 ml of 0.5 M EDTA and made up to a 1 l volume with deionised water.

Tris-EDTA (TE) buffer was prepared by mixing 10 ml of 1 M Tris pH 7.5 solution, 2 ml of 0.5 M EDTA solution and 988 ml of dH_2O.

Colony PCR cell lysis buffer was prepared by dissolving 1 ml of Triton X-100 in 1 l of TE buffer.

5.3.3 Culture media

Lysogeny broth (LB) medium was prepared by dissolving 10 g tryptone, 5 g yeast extract and 10 g NaCl in dH_2O, adjusting to pH 7 with NaOH and made up to volume of 1 l with dH_2O.

Lysogeny agar (LA) medium was produced as above but with the addition of 15 g agar per 1 l of medium.

Yeast extract, peptone, glucose (YEPD) medium was prepared by dissolving 20 g of bacteriological peptone 10 g of yeast extract per 900 ml of dH_2O. After autoclaving, 100 ml of 20 % sterile glucose solution was added to result in a final concentration of 2 % glucose.

YEPD agar was made in the same way but with the addition 15 g of agar per 1 l of medium. Here the 20% glucose solution was added directly to molten agar prior to setting.

5.3.4 Culture conditions

5.3.4.1 Culture of *Kluyveromyces marxianus* GK1005

Cells from the main stock stored at – 80 ^{o}C cells were streaked on 9 cm YEPD agar plates and incubated at 30 ^{o}C overnight. A single colony from the agar plate was picked using a sterile pipette tip and used to inoculate 10 ml of YEPD medium in a 50 ml conical flask before incubation overnight at 37 ^{o}C, 150 rev/min.

5.3.4.2 Culture of *Escherichia coli BL21(DE3)*

Cells from the main stock stored at – 80 ^{o}C were streaked on 9 cm LA plates containing 100 µg/ml ampicillin (if needed) and incubated at 37 ^{o}C overnight. A single colony from the plate was used to inoculate 5 ml of LB medium (supplemented if needed with 5 µl of 1000X ampicillin stock) in a 30 ml universal tube. The tubes were incubated overnight at 37 ^{o}C with shaking at 150 rev/min.

5.3.5 Molecular cloning

5.3.5.1 Preparation of chemically competent cells

An aliquot (2 ml) of overnight *E. coli* BL21(DE3) culture was diluted into 100 ml of LB broth in a 250 ml conical flask and grown at 37 ^{o}C with shaking at 150 rev/min until OD_{600} ~0.6. Next 25 ml of the culture was harvested by centrifugation at 4000x g for 10 min at 4 ^{o}C, the supernatant was discarded, and pellet resuspended in 5 ml of ice cold 100 mM $CaCl_2$. This washing step was repeated, followed by 30 min incubation on ice. The cells were re-harvested by centrifugation, resuspended in 1 ml of ice-cold 100 mM $CaCl_2$ and maintained on ice. Samples (100 µl) of the cell suspension were aliquoted into Eppendorf tubes containing 20 µl of 50 % glycerol, flash frozen in liquid nitrogen and stored at -80 ^{o}C.

5.3.5.2 Plasmid purification

Plasmid DNA was purified using a NuceloSpin® plasmid kit (Machary-Nagel, Germany). An aliquot (5 ml) of overnight culture of *E. coli* containing the relevant plasmid was centrifuged at 11,000x *g* for 1 min. The supernatant was discarded, and cells resuspended in 250 µl of A1 buffer from the kit, followed by addition of 250 µl of lysis buffer A2. The contents were gently mixed by inverting tubes and incubated at room temperature for up to 5 min or until the lysate became clear. An aliquot (300 µl) of neutralising buffer A3 was added and contents were mixed by inverting the tube until the lysis buffer A2 was neutralised (colour of the solution changed from blue to white). The mixture was then centrifuged at 11,000x *g* for 5 min. The supernatant was loaded onto a NuceloSpin® Plasmid column and centrifuged at 11,000x *g* for 1 min to bind the plasmid to the column membrane. Flow through was discarded and column was washed with 500 µl of AW buffer pre-heated to 50 ^{o}C before centrifugation at 11000x g for 1 min, a wash with 600 µl of A4 buffer and centrifugation again at 11,000x *g* for 1 min. Then the column membrane was dried by centrifugation for 2 min at 11,000x *g*. The plasmid DNA was eluted by adding 50 µl of AE buffer to the column, incubating at room temperature for 1 min followed by centrifugation for 1 min at 11,000x *g*. The DNA concentration and purity was then measured using a nanodrop spectrophotometer (DS-11FX+, DeNovix, Wilmington, USA).

5.3.5.3 PCR cleanup

The DNA from PCR reactions (described in **5.3.5.11**) was purified using a NucleoSpin® Gel and PCR-cleanup kit (Machary-Nagel, Germany). Briefly, the PCR reaction was mixed with 2x volume of NTI buffer and loaded onto a NucleoSpin® Gel and PCR cleanup column before centrifugation at 11000 *g* for 30 s to bind the DNA to the column membrane. The flow through was discarded. This was followed by two washes of the column with 700 µl NT3 buffer and centrifugation for 30 s at 11,000x *g*. The column membrane was then centrifuged at 11000x *g* for 1 min and then incubated for 5 min at 70 ^{o}C to remove residual ethanol from the NT3 buffer. The DNA in the column was eluted by adding 30 µl of NE buffer, incubation at room temperature for 1 min and then centrifugation at 11,000x *g* for 1 min. The DNA concentration and purity was measured using a Nanodrop spectrophotometer (DS-11FX+, DeNovix, Wilmington, USA).

5.3.5.4 Gel cleanup

After loading PCR (**5.3.5.11**) reaction products on gels and performing electrophoresis (**5.3.5.12**) a UV transilluminator was used to identify the DNA band(s) and a sterile scalpel used to excise the band(s) and transfer it to pre-weighed Eppendorf tube(s). The DNA was extracted from the gel using a NucleoSpin® Gel and PCR-cleanup kit (Machary-Nagel, Germany). An aliquot (2 µl) of NTI buffer (from the kit) was added per 1 mg of gel, before incubation for 10 min at 50 ^{o}C to dissolve the gel. The resulting mixture was loaded onto a NucleoSpin® Gel and PCR cleanup column and centrifuged at 11,000x *g* for 30 s to bind the DNA to the column membrane. The following steps were the same as in **5.3.5.3**.

5.3.5.5 Restriction digestion

Restriction enzymes BamHI-Hf, XhoI and 10x CutSmart™ buffer were from NEB (Salisbury, UK). Per reaction volume (20 µl) 1 µg of DNA was mixed with 2 µl of 10x Cutsmart™ buffer and 1 µl of relevant restriction enzyme, then made up to volume (20 µl)

using dH_2O. The reaction mixes were incubated at 37°C for 2 h and purified either by PCR cleanup **(5.3.5.3)** or by gel electrophoresis and gel cleanup **(5.3.5.4)**.

5.3.5.6 Gibson assembly

For Gibson assembly reactions, 100 ng of the relevant vector (described in **5.3.5.10**) with 2-3-fold molar excesses of each insert were mixed with 10 µl of Gibson Assembly Master Mix (NEB, USA) and adjusted to 20 µl with dH_2O. The mixture was then incubated at 50 °C for 15 min and stored at –20 °C or used immediately for transformation (**5.3.5.7**).

5.3.5.7 Transformation

A 100 µl aliquot of chemically competent *E. coli* BL21 (DE3) cells prepared as described in **section 5.3.5.1** was mixed with 2 µl of Gibson assembly reaction (**5.3.5.6**) and incubated on ice for 5 min followed by 90 s heat shock at 42 °C. Afterwards 1 ml of LB medium pre heated to 37 °C was added to the Gibson reaction and cell mix and incubated with shaking at 150 rev/min for 60 min. The cells were centrifugated at 3000x *g* for 3 min, supernatant was discarded and cells were resuspended in 150 µl of LB medium. The cells were then spread to LA plates supplemented with 100 µg/ml carbenicillin and incubated at 37 °C overnight.

5.3.5.8 Colony PCR protocol

Samples of single colonies from a transformation plate were picked with sterile pipette tips and each stirred into an Eppendorf tube containing 20 µl of colony PCR lysis buffer (**5.3.2**). The tubes were heated for 8 min at 100 °C. Afterwards 1 µl of each solution was used in a PCR reaction (**5.3.5.11)**.

5.3.5.9 Genomic DNA extraction

Genomic DNA of *F. venenatum* was extracted using a DNeasy® Plant Pro Kit (Qiagen, Venlo, Netherlands). A sample (100 mg) of freeze-dried powdered *F. venenatum* biomass was mixed with 500 µl of solution CD1 (from the kit) and vortexed until homogeneous, followed by centrifugation at 12,000x *g* for 2 min. The supernatant was transferred to a fresh tube and mixed with 250 µl of solution CD2 and centrifuged at 12,000x *g* for 1 min. The supernatant was transferred to a fresh tube, mixed with 500 µl of APP buffer and vortexed. The mixture was loaded onto a MB spin column and centrifuged at 12,000x *g* for 1 min. Supernatant was discarded and the column was washed with 650 µl of buffer AW1 then AW2 with each followed by centrifugation at 12000 g for 1 min. The column was then centrifuged at 16,000x *g* for 2 min to dry the membrane, followed by addition of 100 µl of EB buffer to elute the DNA and centrifugation for 1 min at 12,000x *g*. The DNA quantity and quality was determined using a nanodrop instrument (DS-11FX+, DeNovix, Wilmington, USA).

5.3.5.10 Primer and plasmid design

Properties of the primers designed in this study were researched using SNAPGene software (GSL Biotech LLC, Boston, USA). All primers were ordered from Sigma-Aldrich (Missouri, USA) as DNA salts. These were diluted with dH_2O according to the manufacturer's instructions and stored at -20 °C. The primers were designed based on genomic DNA

sequence of *F. venenatum* from BLAST searches and validated with independent genomic sequencing of *F. venenatum* A3/5 produced by NIAB (Cambridge, UK). Forward and reverse primers for Gibson assembly were designed using the NEBuilder™ Assembly Tool (NEB, Salisbury, UK), with primers were designed to insert between BamHI and XhoI sites.

The empty pET-19b plasmid vector (**Figure 5.2**) was purchased from GenScript (Oxford, UK) as 0.5 µg of dry DNA, diluted according to manufacturer instructions and transformed into *E. coli* Bl21 (DE3) for further propagation. The Gibson assembly primers were designed to allow insertion into the multiple cloning site of the plasmid; the plasmid was linearised using BamHI and XhoI restriction enzymes (**Table 5.1**).

Primers were designed using SNAPGene (GLS Biotech LLC, Boston USA), protein structures were predicted and compared using Swissprot (Expasy, Switzerland) and ChimeraX (RBVI, USA) software.

Table 5.1 Table of primers used in this study. The primers were all designed using SNAPGene (GLS Biotech LLC, Boston USA) and ordered from Sigma-Aldrich (Missouri, USA). For Gibson primers lowercase letters indicate region of homology with the vector and UPPERCASE letters homology with the target gene. **Fw – forward primer (3’ -> 5’) Rv – reverse primer**

Primer ID	**Primer sequence**
Fw GIBSON genomic DNA	tcgggctttgttagcagccgATGACCATGTGAGCTGCGA
Rv GIBSON genomic DNA	cgacgacgacaagcatatgcTTACATATCCTCTGCCTTCTG
Fw_Sequencing_1	ATCGTCATCCTCGGCACCGTCA
Fw_Sequencing_2	CTCCAAGAAATACAAGCCTTTC
Fw_Sequencing_3	CTGCAACAACATTGGAGACAGA
Fw_Sequencing_4	AATGGTCCCATTTCCAGCATGG
Fw_Sequencing_5	AATGAGGTTAAGGGACTGGATG
Rv_Sequencing	ATCATCACAGCAGCGGCCATAT

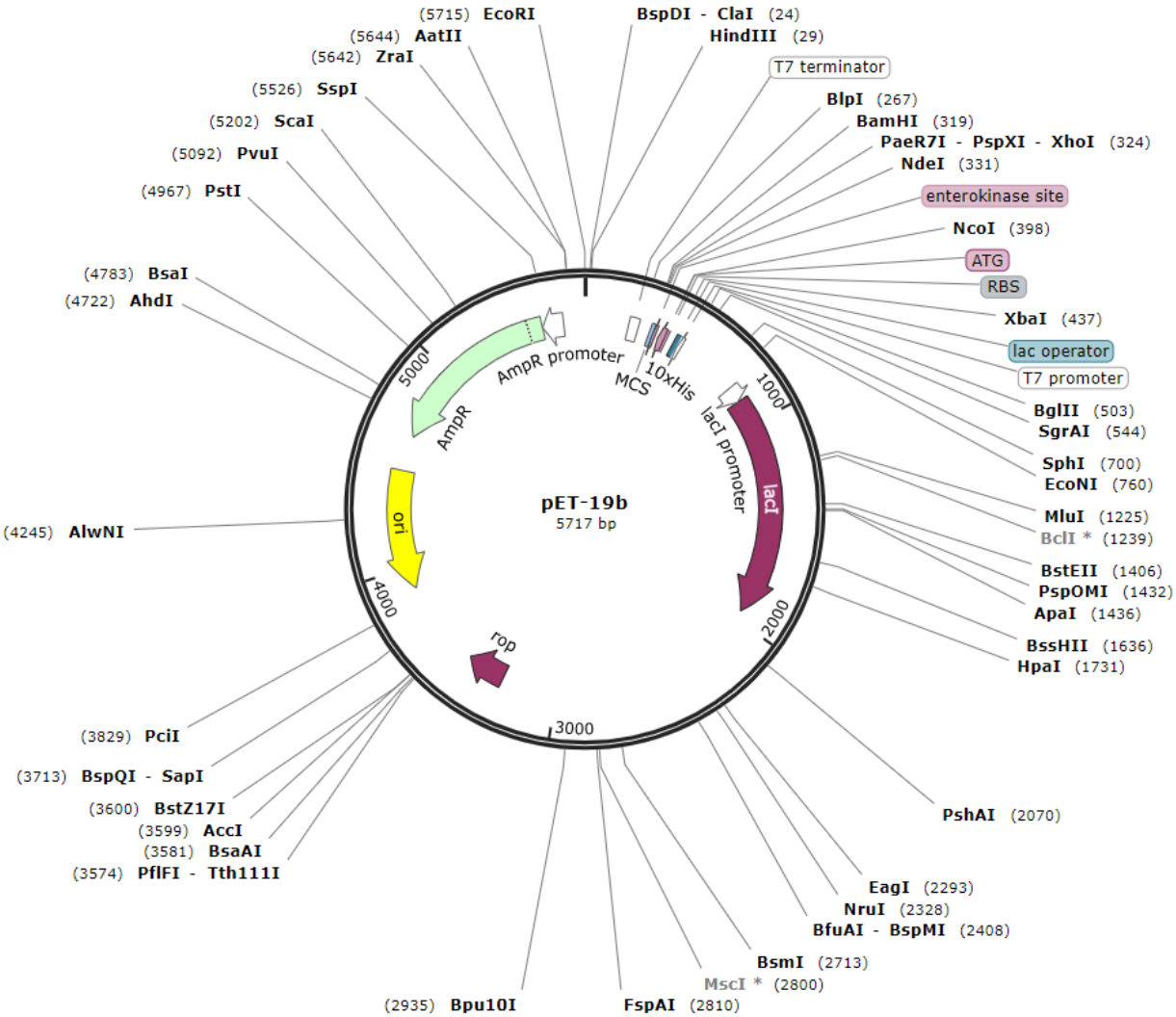

Figure 5.2 Map of pET-19b plasmid – sequence information and plasmid map were obtained from https://www.snapgene.com/plasmids/pet_and_duet_vectors_(novagen)/pET-19b .

5.3.5.11 Polymerase chain reaction (PCR)

PCR tubes of 0.2 ml volume (Starlab, Milton Keynes, UK) were used for all the reactions. The standard PCR mix was formulated as described in **Table 5.2**. The PCR reactions were carried out using a TC-512 thermocycler (Bio-Techne, USA). The samples were denatured for 5 min at 98 ^{o}C followed by denaturation for 30 s at 98 ^{o}C, annealing for 30 s at 42 ^{o}C and extension for 2 min at 70 ^{o}C repeated in 30 cycles, with final extension at 70 ^{o}C for 10 min.

The lid was heated at 120 °C throughout the PCR programme to prevent condensation at the top of the tube. After the programme was finished samples were stored at 4 °C for later use.

Table 5.2. List of reagents and amounts (µl) in a typical polymerase chain reaction (PCR) in this study.

Reagent	Amount
Phusion®	0.5 µl
DMSO	1.5 µl
Phusion® HF Buffer	10 µl
dNTPs mix	1 µl
Reverse primer	2.5 µl
Forward primer	2.5 µl
DNA template	250 ng
DNAse free H_2O	Up to 50 µl

5.3.5.12 DNA gel preparation, DNA loading and gel electrophoresis

Agarose gels (1.5 % w/v) were generally prepared by mixing 0.6 g of agarose powder with 40 ml of TBE buffer (**5.3.2**) and microwaved until the agarose was fully dissolved. Two microlitres of a 10 mg/ml ethidium bromide solution was added to the mixture and and the mixture was poured onto a 15x10 cm gel tray (150 ml volume) and left to set with a well comb. After setting, the gel tray was transferred to a gel tank filled with TBE buffer. The DNA samples were loaded (5-40 µl) into wells after mixing with 6x purple loading dye (NEB, USA). A 1 kb or 100 bp (or both) (NEB, USA) DNA marker(s) were also loaded. The electrophoresis was usually run for 35 min at 100 V and 400 mA. The gels were imaged in GelDoc™ XR+ with ImageLab 6.1 software (Bio Rad, UK) using the ethidium bromide mode.

5.3.5.13 DNA sequencing

For sequencing, 100 ng/µl of pET-19b plasmids with inserts were premixed with 2 µl of a 10 pmol/µl solution of relevant sequencing primer and adjusted to a total volume of 17 µl with dH_2O. The mixtures were sent to a sequencing service arranged by Sanger sequencing (Eurofins, Luxembourg). The obtained DNA reads were then assembled using SnapGene software (GSL Biotech LLC, Boston, USA).

5.3.6 Pre-germination of *F. venenatum* spores

Flasks containing RHM medium with 10,000,000 *F. venenatum* spores/ml (**Chapter 2, 2.3.3**) were incubated with shaking at 150 rev/min at 28 °C. Between 4-6 h a sample of the contents of the flasks was examined using light microscopy. When most of the spores in the field of view showed signs of germination (presence of at least one germ tube) the suspension was deemed ready for downstream use.

5.3.7 UV mutagenesis conditions

A Sylvania G15T8 germicidal UV-C source emitting at wavelength 254 nm was used to induce mutagenesis. The intensity of UV exposure was determined using a J-225 Blak-Ray

UV Meter from Ultra-Violet Products (San Gabriel, USA). A Petri dish with spore suspension in 0.1 % TWEEN was placed 22 cm away from the UV source and, at intervals during UV irradiation, spores samples were spread on RHM agar selection plates containing 200 µg/ml TFL and incubated at 28 ºC in the dark for 2-5 days.

5.3.8 Mycotoxin assay

The assay was performed by treating a culture of *K. marxianus* yeast with the supernatant from a *F. venenatum* culture (Whittaker, 2022). The *F. venenatum* cultures were first grown in RHM medium with glucose or sucrose as carbon source for 96 h. The supernatant was passed through a 20 µm filter and 20 µl of filtered supernatant were added to a 130 µl of exponentially growing *K. marxianus* culture (**5.3.4.1**). The sample of culture with sucrose was treated as a positive mycotoxin control. For a negative control, 20 µl of water were added instead of the supernatant. The plates were incubated with shaking for 48 h at 37 ºC with optical density readings at 600 nm every 30 min.

5.4 Results

5.4.1 Prediction of a potential gene target enabling selection for increased leucine synthesis in *F. venenatum*

As described in the Introduction, mutants insensitive to feedback-inhibition by leucine of its biosynthesis pathway have previously been successfully selected in yeast, according to a high level of TFL resistance (Oba et al., 2005). In the filamentous fungus *Neurospora crassa* leucine synthesis is controlled in a similar way to *S. cerevisiae*, with gene *leu-4* encoding a 625 AA long 2-isopropylmalate synthase (IPMS) enzyme (Kohlhaw, 2003). Like *Neurospora* spp, *Fusarium* spp. belong to the class *Sordariomycetes*. To identify a corresponding protein in *F. venenatum*, the predicated AA sequence of *N. crassa* IPMS (EC number: EC:2.3.3.13) was used to search by BLAST for homologies in *F. venenatum*. An uncharacterised protein (FVRRES_11338 ID: XP_025581042.1) 616 AA long and sharing 68.95 % identity with the *N. crassa* protein was found. Analysis of the AA sequence in UniProt predicted it to be an *F. venenatum* IPMS (inferred by homology), with an annotation score 2/5 (higher score means better annotated entry). Given that leucine synthesis in *N. crassa* is reported to be regulated by a feedback inhibition system similar to that of *S. cerevisiae* (Kohlhaw, 2003) and that key residues for feedback inhibition identified in the previous study with *S. cerevisiae* (Oba et al., 2005) are conserved in *F. venenatum*, it was reasoned that selection for TFL resistance may yield mutants desensitized to feedback inhibition by leucine also in *F. venenatum*. Accordingly, such deregulated mutants of *F. venenatum* could exhibit increased production of leucine.

5.4.2 The effect of TFL on growth of *F. venenatum*

First, in order to find appropriate TFL concentrations for selecting mutants of interest, the effects of various concentrations of TFL on growth of *F. venenatum* were assessed. *F. venenatum* spores were cultured in microplate cultures supplemented with TFL and leucine concentrations (**Figure 5.3**). In yeast, TFL in concentrations between 75-175 µg/ml fully inhibited growth (**Appendix Figure 6**), but in *F. venenatum* spore outgrowth at 200 µg/ml TFL was inhibited only for ~24 h after which growth progressed nearly normally (**Figure**

5.3). When *F. venenatum* spores were spread on RHM agar supplemented with 100-500 µg/ml TFL, colonies still appeared albeit smaller than on regular RHM agar (data not shown). This was problematic for the envisioned TFL selection screen as the fact that *F. venenatum* could still grow in the presence of relatively high TFL concentrations would only allow a small number of cells to be spread per plate (to avoid colony overlap) and a need to pick potential TFL resistant mutants based on relative colony size rather than colony presence versus absence.

Another question investigated was whether TFL has any mechanism of action on *F. venenatum* other than leucine synthesis inhibition. Such an action would be expected to affect *F. venenatum* growth at high TFL concentrations even when leucine was added. However, addition of leucine fully rescued the TFL growth inhibition effect (**Figure 5.3**), corroborating that the growth inhibitory action of TFL is due to its reported inhibition of leucine biosynthesis.

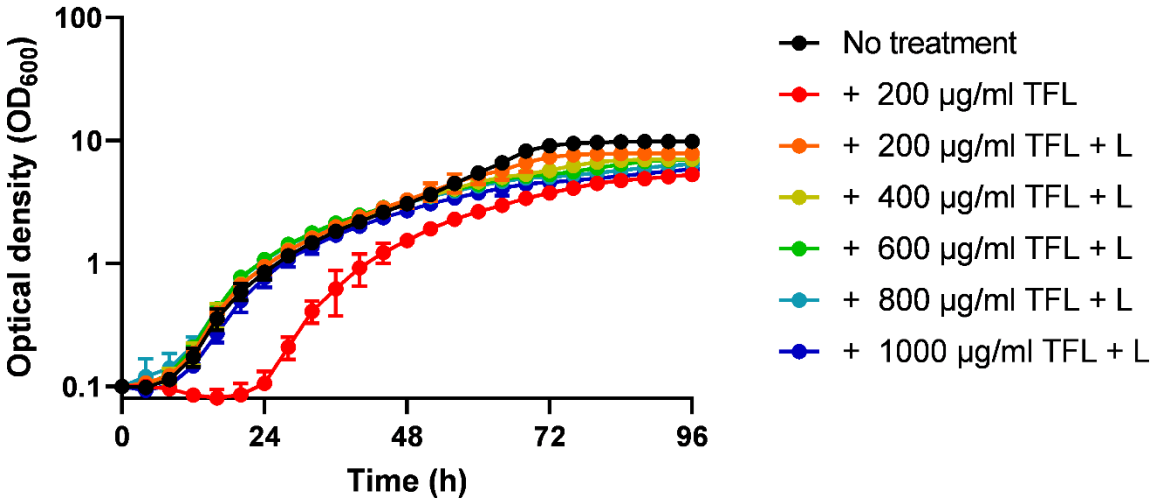

Figure 5.3 Growth of *F. venenatum* in microplate culture with TFL and leucine. Outgrowth from an inoculum of 10,000 spores/ml was monitored during static incubation at 28 ºC for 96 h in RHM medium supplemented with 5'5'5'–Trifluoro-DL-leucine (TFL) ± 2 mM leucine (L). Data points indicate means ± SD, n = 6 (biological replicates).

5.4.3 Pre-germinated *F. venenatum* spores can be fully inhibited by TFL.

It was not clear why *F. venenatum* spores were able to overcome TFL inhibition after 24 h. One explanation could be that the leucine synthesis pathway in this fungus is already leaky to inhibition by TFL. This would complicate TFL-based selection for high-Leu mutants, while the use of direct genetic manipulation to achieve increased Leu would be undesirable from a commercial perspective owing to GM concerns. Another possible explanation could be that *F. venenatum* adapts to TFL during the initial phases of spore germination (Huang and Hull, 2017). To test the latter hypothesis, *F. venenatum* spores were pre-germinated for 4-6 h in RHM medium before being inoculated to medium supplemented with TFL or TFL + leucine. Unlike the ungerminated 'fresh' spores (FS) already reported above, the growth of pre-germinated spores (GS) was fully inhibited when incubated with TFL (**Figure 5.4**). Furthermore, as with fresh spores, the presence of leucine fully suppressed this growth

inhibitory effect. This result suggests that *F. venenatum* spores are able to adapt to TFL during initiation of germination, but not if introduced to TFL only after germination has progressed. In relation to the TFL selection screen this outcome allowed for a high-throughput screen based on a clearer phenotype, as only pre-germinated (mutant) spores that had some innate resistance to TFL would be expected to form colonies.

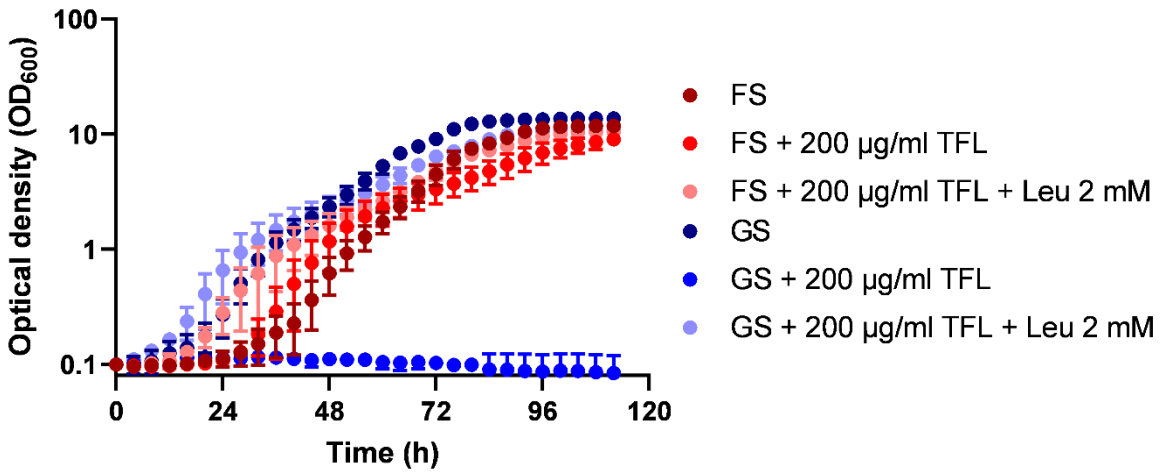

Figure 5.4. Growth of fresh and pre-germinated *F. venenatum* spores in microplate culture with TFL. Outgrowth from an inoculum of 10,000 spores/ml of freshly harvested (FS) or pre-germinated spores (GS) (**section 5.3.6**) was monitored during static incubation at 28 °C for 114 h in RHM medium supplemented with 5'5'5'–Trifluoro-DL-leucine (TFL) or TFL and 2 mM of leucine (L). Data points indicate means ± SD, n = 6 (biological replicates).

5.4.4 Determining the appropriate UV irradiation time of pre-germinated *F. venenatum* spores

Next, to find appropriate conditions for UV-induced mutagenesis in the planned TFL selection screen, the colony-forming ability (viability) of pre-germinated spores was determined at intervals during irradiation for up to 45 s. The colonies were counted to determine the survival % of the spores from consecutive samples. Viability declined with time of exposure and after 45 s only ~50 % of the pre-germinated spores were able to form colonies (**Figure 5.5**). This was selected as irradiation time for the TFL screen as in previous studies in fungi and bacteria it was concluded that achieving 50 % kill rate through UV exposure equates to a near optimal mutation to survival rate for mutant-selection via random mutagenesis screens (Tillich et al., 2012; Barsoum et al., 2020).

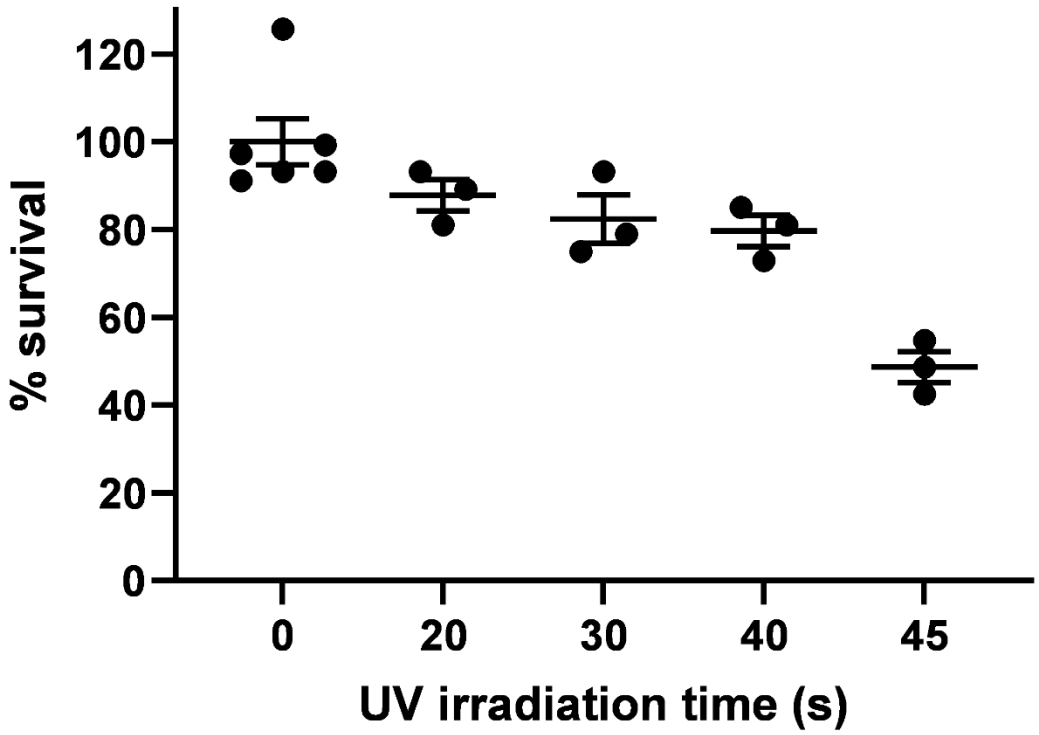

Figure 5.5. Viability of pre-germinated *F. venenatum* spores during UV treatment. A suspension of 1,000,000 pre-germinated spores per ml (**section 5.3.6**) were UV irradiated for up to 45 s in the conditions outlined in **5.3.7**. After irradiation the spore solution was serially diluted and ~30 spores spread per RHM agar plate. Colonies were enumerated after incubation in the dark at 28 ^{o}C for 2-5 days and these were normalised as a percentage against the average colony formation at 0 time before UV exposure. Data points indicate means ± SD, each black dot on a graph represents a single biological replicate.

5.4.5 TFL selection screen and validation of gain of TFL resistance

To select for any *F. venenatum* isolates that could resist TFL inhibition, pre-germinated TFL spores were UV irradiated for 45 s and 10,000 spores per plate were spread on three RHM agar plates containing 200 µg/ml TFL. Pregerminated spores that were not UV irradiated served as a negative control. There were no colonies apparent after incubation on the control plates, but five colonies in total emerged across the three plates inoculated with UV irradiated spores. These isolates were named (Iso 1-5). The screen was then repeated and this yielded another six isolates named (Iso I-VI). Iso 3-5 from the first screen proved to exhibit poor growth in liquid RHM medium and were not included in further analysis. The remaining isolates were cultivated until sporulation (2.3.2). To corroborate acquisition of TFL resistance, spores from each isolate were pre-germinated and grown in microplate culture in RHM medium supplemented with TFL. As in the screen, all the isolates exhibited a degree of resistance to the TFL treatment (**Figure 5.6**) (data not shown for isolates 1-2) supplemented with TFL.

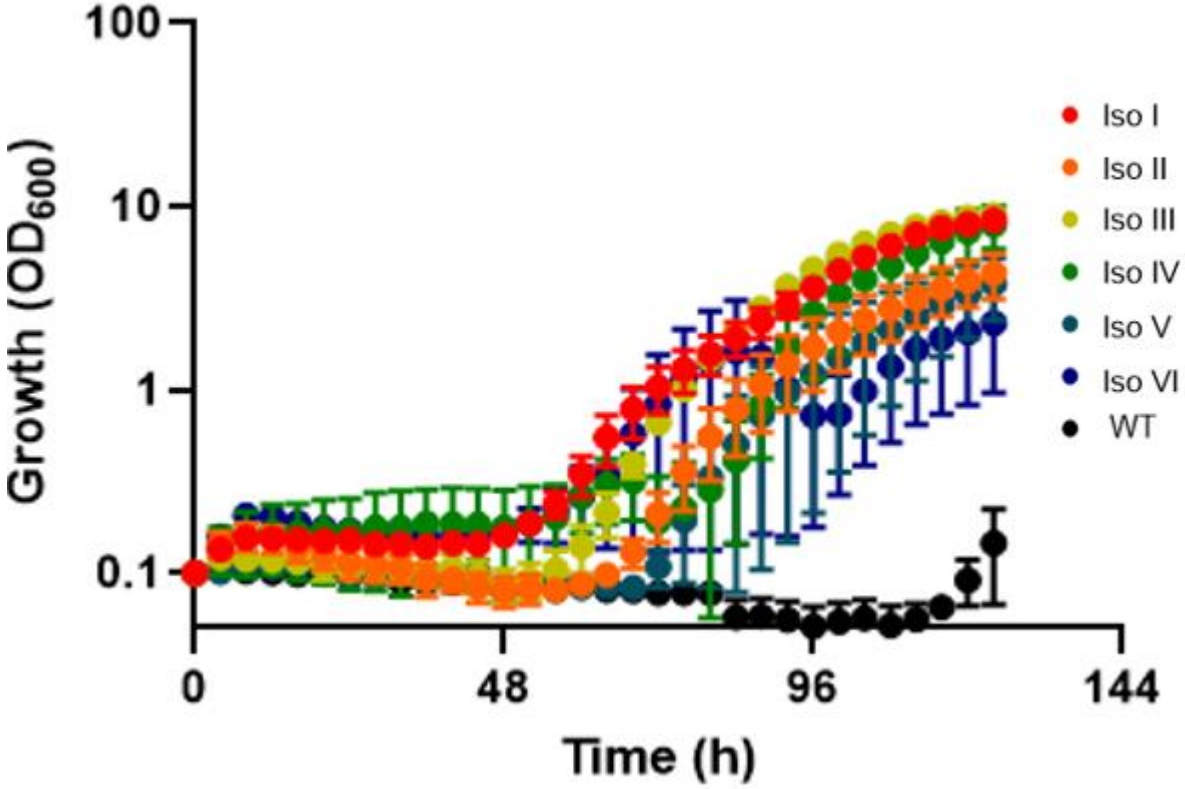

Figure 5.6 Growth of *F. venenatum* isolates of interest in microplate culture with TFL. RHM medium supplemented with 200 µg/ml TFL was inoculated with 10,000 spores/ml pre-germinated spores of the wild type and isolates of interest from the first screen of UV-mutagenised *F. venenatum.* Microplates were incubated statically at 28 ºC, with OD determined every 1 h. Data points indicate means ± SD n = 6 (biological replicates).

5.4.6 Free-AA analysis of the TFL screen isolates

After corroborating the TFL resistance of isolates 1, 2 and I-IV, these isolates were examined for their free-AA composition (as described in **3.3.4).** Due to the differences in times it took different isolates to sporulate and spore yields of the isolates as well as the number of isolates to study, these extractions and free-AA analyses were conducted in independent batches (**Table 5.3**, **Table 5.4**, **Table *5.5***). First the means of free AAs from profiles of WT, Iso 1 and 2 were compared (**Table 5.3**). Tukey's multiple comparisons analysis revealed a significant difference between the levels of free AAs in WT Iso 2 samples. The most dramatic change in Iso 2 was a large increase in the amount of free leucine compared to WT (1.14 vs 0.09 g/kg, $p < 0.0001$, respectively) – a target outcome of the TFL selection screen. To investigate further, the free AA profiles were normalised to the mean value of each AA from the WT free AA profile (**Figure 5.7 A, Appendix Table 26)** The values of the means were compared by One-Way ANOVA with Tukey's multiple comparisons and revealed a significant increase in the significant increase in the absolute amounts of free Leu (11.15-fold, $p < 0.0001$) and free Lys (1.73-fold, $p = 0.015$) in isolate 2 compared with the WT.

Next, free AA profiles of new samples of WT Iso 2 and Iso II were prepared, analysed by LCMSMS and the means of the free AAs from the hydrolysate profiles were compared by One-Way ANOVA (**Table 5.4**). Tukey's multiple comparisons analysis showed a significant

difference in the levels of various free AAs between the WT and both Iso 2 and Iso II. With Leu being higher than in WT in both the TLF strains ($p < 0.0001$ and $p = 0.046$ for WT vs Iso2 and WT vs Iso II respectively). Next the free AA profiles were normalised to the mean values of the individual AAs from the WT free AA profile (**Figure 5.7 B**, **Appendix Table 27**). The values were compared by 1-Way ANOVA with Tukey's multiple comparisons, showing a significant increase in the absolute levels of free leucine in Iso II and Iso 2 compared to WT (1.32- and 5.58-fold increases, $p = 0.046$, $p < 0.0001$, respectively). Additionally, a significant increase in the absolute levels of free isoleucine was observed in both Iso II and Iso 2 (1.31 and 1.49-fold) $p = 0.017$, $p = 0.002$ respectively), as well as other minor changes in other free AAs (**Appendix Table 27**).

Next, free AA profiles from extracts of isolates I, III-VI were measured by LCMSMS (**Table 5.5**). Comparison of the means of AAs from the hydrolysate profile by One-Way ANOVA revealed significant differences between various free AA levels of the WT and tested isolates. Tukey's multiple comparison analysis revealed a significant decrease in glutamate and the total levels in Iso IV compared to WT ($p = 0.047$, $p = 0.002$, respectively).Next the free AA profiles were normalised to the mean values of individual AAs from the free AA profile of the WT and compared using One-Way ANOVA (**Figure 5.8**, **Appendix Table 28**). Tukey's multiple comparisons revealed significant changes to the relative levels of several free AAs (mostly decreases relative to WT), but no changes specific to the level of free leucine. Notably Iso III exhibited increases in the relative levels of Phe and Trp (1.51, 1.68-fold respectively, $p = 0.014$, $p = 0.007$).

In summary only two (isolates 2 and II) of the eight tested isolates (1-2, I-VI) exhibited the sought-after phenotype of increased Leu production, with Iso II showing a modest ~1.4-fold increase in measured free Leu and Iso 2 an increase between 5- and 11-fold increase as measured in two independent experiments. Iso III exhibited increases in free Trp and Phe, but it remains unclear whether these phenotypes of increased Trp and Phe are specifically linked to TFL resistance or are a result of other independent mutations acquired during UV irradiation.

Table 5.3 Comparison of the free amino acid profiles of *F. venenatum* isolates 1 and 2 obtained from UV mutagenesis and the TFL selection screen. The values are expressed as g/kg biomass ± SD (n=3, biological replicates). The means of the rows were compared using One-Way ANOVA with Tukey's multiple comparisons. Different letters in superscript between values in the same row indicate statistically significant difference according to One-Way ANOVA with Tukey's multiple comparisons ($p < 0.05$). A lack of any superscript letters indicates lack of significant difference within a row.

	WT	Iso 1	Iso 2
Ala	**11.29 ± 4.60**	**10.20 ± 3.29**	**13.28 ± 1.66**
Arg	**0.93 ± 0.26 $^{A, B}$**	**0.74 ± 0.10 ^{A}**	**1.39 ± 0.33 ^{B}**
Asp	**1.41 ± 1.22**	**2.00 ± 0.61**	**1.82 ± 0.35**
Cys	**0.01 ± 0.00**	**0.01 ± 0.00**	**0.01 ± 0.00**
Glu	**19.12 ± 6.06**	**16.40 ± 5.65**	**26.32 ± 4.85**
Gly	**0.37 ± 0.10**	**0.35 ± 0.07**	**0.53 ± 0.06**
His	**0.26 ± 0.05 ^{A}**	**0.25 ± 0.04 ^{A}**	**0.40 ± 0.07 ^{B}**
Ile	**0.09 ± 0.02**	**0.10 ± 0.03**	**0.12 ± 0.02**
Leu	**0.09 ± 0.02 ^{A}**	**0.11 ± 0.02 ^{A}**	**1.04 ± 0.14 ^{B}**
Lys	**0.32 ± 0.08 ^{A}**	**0.32 ± 0.06 ^{A}**	**0.55 ± 0.06 ^{B}**
Met	**0.06 ± 0.02**	**0.08 ± 0.03**	**0.09 ± 0.02**
Phe	**0.05 ± 0.01**	**0.06 ± 0.01**	**0.06 ± 0.01**
Pro	**0.22 ± 0.03**	**0.23 ± 0.06**	**0.27 ± 0.03**
Ser	**0.79 ± 0.23**	**0.69 ± 0.10**	**1.01 ± 0.24**
Thr	**1.35 ± 0.21 $^{A, B}$**	**1.11 ± 0.23 ^{A}**	**1.83 ± 0.23 ^{B}**
Tyr	**0.04 ± 0.01**	**0.05 ± 0.01**	**0.05 ± 0.01**
Trp	**0.04 ± 0.01**	**0.04 ± 0.00**	**0.04 ± 0.00**
Val	**0.67 ± 0.27**	**0.51 ± 0.13**	**0.76 ± 0.13**
Total	**37.10 ± 10.54**	**33.24 ± 9.51**	**49.58 ± 8.12**

Table 5.4 Comparison of the free amino acid profiles of *F. venenatum* isolates 2 and II obtained from UV mutagenesis and the TFL selection screen. The values are expressed as g/kg biomass ± SD (n = 3, biological replicates). The means of the rows were compared using One-Way ANOVA with Tukey's multiple comparisons. Different letters in superscript between values in the same row indicate statistically significant difference according to One-Way ANOVA with Tukey's multiple comparisons ($p < 0.05$). A lack of any superscript letters indicates lack of significant difference within a row. N/Q – not quantifiable.

	WT	Iso 2	Iso II
Ala	**12.62 ± 1.24 ^{A}**	**17.06 ± 1.60 ^{B}**	**15.81 ± 1.02 ^{B}**
Arg	**1.06 ± 0.07 ^{A}**	**1.19 ± 0.05 ^{B}**	**0.89 ± 0.02 ^{C}**
Asp	**2.41 ± 0.59**	**2.99 ± 0.28**	**3.36 ± 1.39**
Cys	**N/Q**	**N/Q**	**N/Q**
Glu	**19.75 ± 1.75**	**22.91 ± 2.43**	**22.53 ± 2.02**
Gly	**0.52 ± 0.06**	**0.58 ± 0.05**	**0.64 ± 0.06**
His	**0.30 ± 0.03 $^{A, B}$**	**0.33 ± 0.02 ^{A}**	**0.26 ± 0.01 ^{B}**
Ile	**0.06 ± 0.00 ^{A}**	**0.10 ± 0.01 ^{B}**	**0.09 ± 0.00 ^{B}**
Leu	**0.07 ± 0.01 ^{A}**	**0.42 ± 0.01 ^{B}**	**0.10 ± 0.01 ^{C}**
Lys	**0.29 ± 0.01 ^{A}**	**0.43 ± 0.03 ^{B}**	**0.29 ± 0.02 ^{A}**
Met	**N/Q**	**N/Q**	**N/Q**
Phe	**0.05 ± 0.00 ^{A}**	**0.06 ± 0.00 ^{B}**	**0.06 ± 0.00 ^{B}**
Pro	**0.26 ± 0.01 ^{A}**	**0.23 ± 0.01 ^{B}**	**0.25 ± 0.00 ^{A}**
Ser	**0.73 ± 0.03 ^{A}**	**0.80 ± 0.01 ^{B}**	**0.82 ± 0.01 ^{B}**
Thr	**0.61 ± 0.05 ^{A}**	**0.75 ± 0.03 ^{B}**	**0.75 ± 0.03 ^{B}**
Tyr	**0.04 ± 0.00 ^{A}**	**0.05 ± 0.00 ^{B}**	**0.05 ± 0.00 ^{B}**
Trp	**0.04 ± 0.00**	**0.05 ± 0.00**	**0.05 ± 0.08**
Val	**1.16 ± 0.11 ^{A}**	**1.18 ± 0.09 ^{A}**	**1.42 ± 0.00 ^{B}**
Total	**39.96 ± 3.73 ^{A}**	**49.10 ± 3.82 ^{B}**	**47.35 ± 1.76 $^{A, B}$**

Table 5.5 Comparison of the free amino acid profiles of *F. venenatum* isolates I and III-VI obtained from UV mutagenesis and the TFL selection screen. The values are expressed as g/kg biomass ± SD (n = 3, biological replicates). The means of the rows were compared using One-Way ANOVA with Tukey's multiple comparisons. Different letters in superscript between values in the same row indicate statistically significant difference according to One-Way ANOVA with Tukey's multiple comparisons ($p < 0.05$). A lack of any superscript letters indicates lack of significant difference within a row.

	WT	Iso I	Iso III	Iso IV	Iso V	Iso VI
Ala	4.97 ± 0.55	4.64 ± 0.70	4.41 ± 0.78	4.21 ± 0.95	5.07 ± 0.13	5.63 ± 0.18
Arg	2.35 ± 0.03 ^{A}	1.84 ± 0.07 ^{B}	1.75 ± 0.03 ^{B}	2.38 ± 0.42 ^{A}	1.78 ± 0.22 ^{B}	1.50 ± 0.12 ^{B}
Asx	0.51 ± 0.01 $^{A, C}$	0.42 ± 0.08 $^{A, C}$	0.25 ± 0.04 ^{B}	0.28 ± 0.09 $^{B, C}$	0.38 ± 0.03 $^{B, C}$	0.34 ± 0.07 $^{B, C}$
Asp	2.28 ± 0.17	1.85 ± 0.44	1.98 ± 0.96	0.97 ± 0.06	1.64 ± 0.20	1.08 ± 0.37
Cys	0.06 ± 0.01	0.06 ± 0.01	0.06 ± 0.05	0.02 ± 0.03	0.06 ± 0.00	0.05 ± 0.01
Glu	31.34 ± 2.10 ^{A}	30.31 ± 1.05 $^{A, B}$	24.60 ± 1.21 ^{B}	24.19 ± 2.81 ^{B}	31.51 ± 4.70 ^{A}	33.09 ± 1.7 ^{A}
Glx	0.14 ± 0.03 $^{A, B}$	0.17 ± 0.04 ^{A}	0.08 ± 0.00 ^{B}	0.09 ± 0.05 $^{A, B}$	0.15 ± 0.02 $^{A, B}$	0.12 ± 0.05 ^{A,B}
Gly	0.82 ± 0.04	0.89 ± 0.26	0.41 ± 0.15	0.39 ± 0.19	0.57 ± 0.20	0.77 ± 0.31
His	0.70 ± 0.10 ^{A}	0.52 ± 0.05 ^{B}	0.50 ± 0.01 ^{B}	0.55 ± 0.04 $^{A, B}$	0.59 ± 0.09 $^{A, B}$	0.49 ± 0.04 ^{B}
Ile	0.19 ± 0.02	0.21 ± 0.02	0.24 ± 0.01	0.20 ± 0.03	0.23 ± 0.01	0.21 ± 0.01
Leu	0.22 ± 0.02	0.24 ± 0.05	0.23 ± 0.06	0.20 ± 0.06	0.23 ± 0.03	0.22 ± 0.00
Lys	0.69 ± 0.04	0.68 ± 0.12	0.67 ± 0.11	0.81 ± 0.09	0.63 ± 0.07	0.58 ± 0.14
Met	0.34 ± 0.01	0.31 ± 0.03	0.32 ±0.03	0.27 ± 0.01	0.29 ± 0.04	0.32 ± 0.03
Phe	0.32 ± 0.02 ^{A}	0.32 ± 0.02 ^{A}	0.48 ± 0.05 ^{B}	0.38 ± 0.10 $^{A, B}$	0.34 ± 0.01 ^{A}	0.31 ± 0.02 ^{A}
Pro	0.61 ± 0.02 ^{A}	0.60 ± 0.00 ^{A}	0.49 ± 0.06 ^{B}	0.51 ± 0.04 $^{A, B}$	0.51 ± 0.05 $^{A, B}$	0.50 ± 0.03 $^{A, B}$
Ser	1.61 ± 0.05 $^{A, B}$	1.73 ± 0.03 ^{A}	1.59 ± 0.12 $^{A, B}$	1.45 ± 0.05 ^{B}	1.75 ± 0.09 ^{A}	1.75 ± 0.13 ^{A}
Thr	1.97 ± 0.06	1.75 ± 0.11	1.80 ± 0.13	1.61 ± 0.10	1.97 ± 0.17	1.94 ± 0.18
Trp	0.12 ± 0.01 ^{A}	0.12 ± 0.01 ^{A}	0.21 ± 0.02 ^{B}	0.16 ± 0.05 $^{A, B}$	0.13 ± 0.01 ^{A}	0.11 ± 0.01 ^{A}
Tyr	0.15 ± 0.00	0.15 ± 0.01	0.17 ± 0.01	0.15 ± 0.02	0.16 ± 0.01	0.16 ± 0.00
Val	0.90 ± 0.06	1.02 ± 0.06	0.98 ± 0.14	0.85 ± 0.05	1.04 ± 0.07	0.97 ± 0.06
Total	62.15 ± 2.56 ^{A}	56.55 ± 1.63 $^{A, B}$	51.86 ± 1.83 ^{B}	47.99 ± 3.35 ^{B}	59.20 ± 5.94 ^{A,}	59.54 ± 2.33 ^{A}

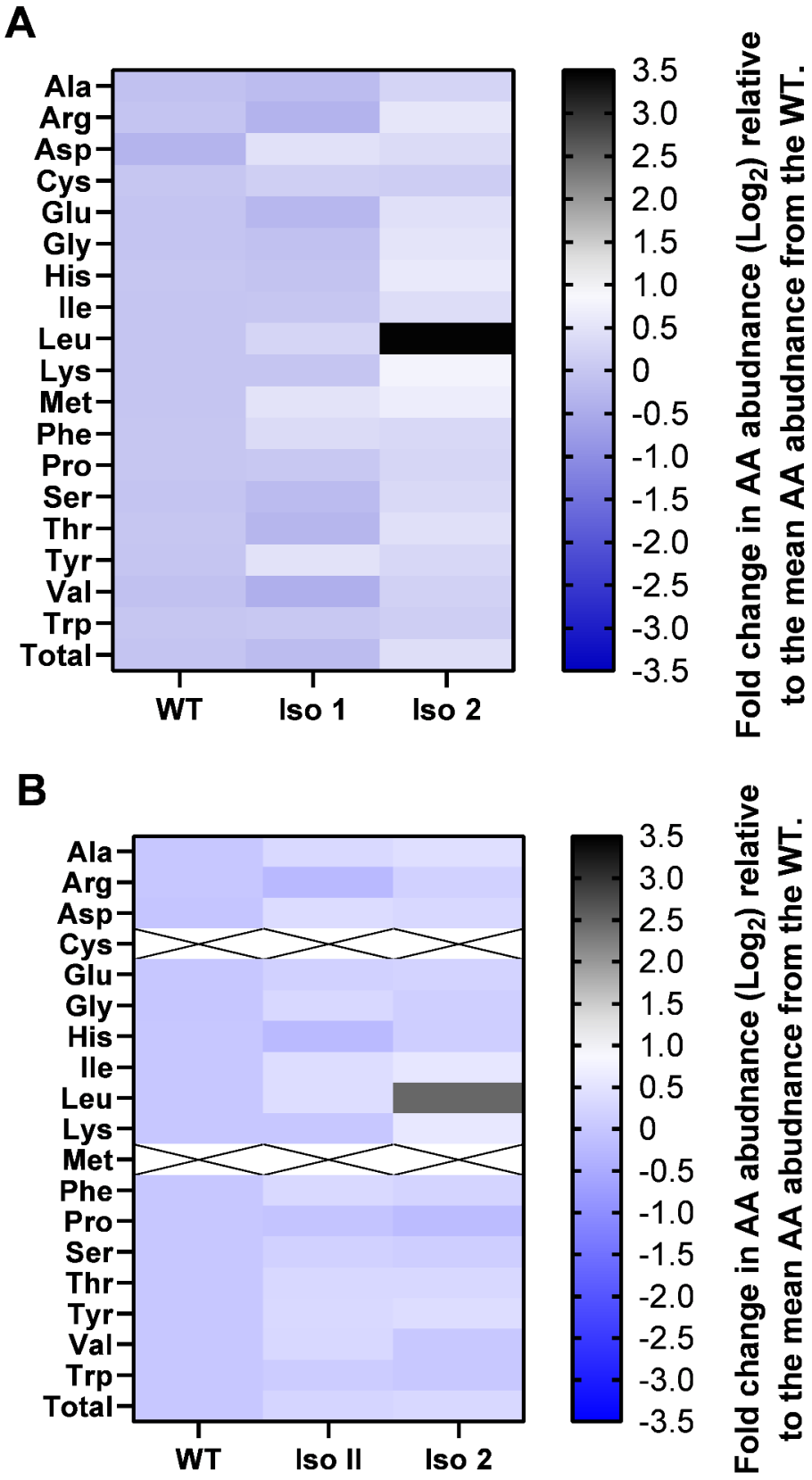

Figure 5.7 A heat map illustrating the fold change in the level of each free AA in Iso 1 and 2 (A) and Iso 2 and II (B) relative to the WT. The data are expressed as a Log_2 of the values from **Appendix Table 26** for **A** and **Appendix Table 27** for **B**. n = 3.

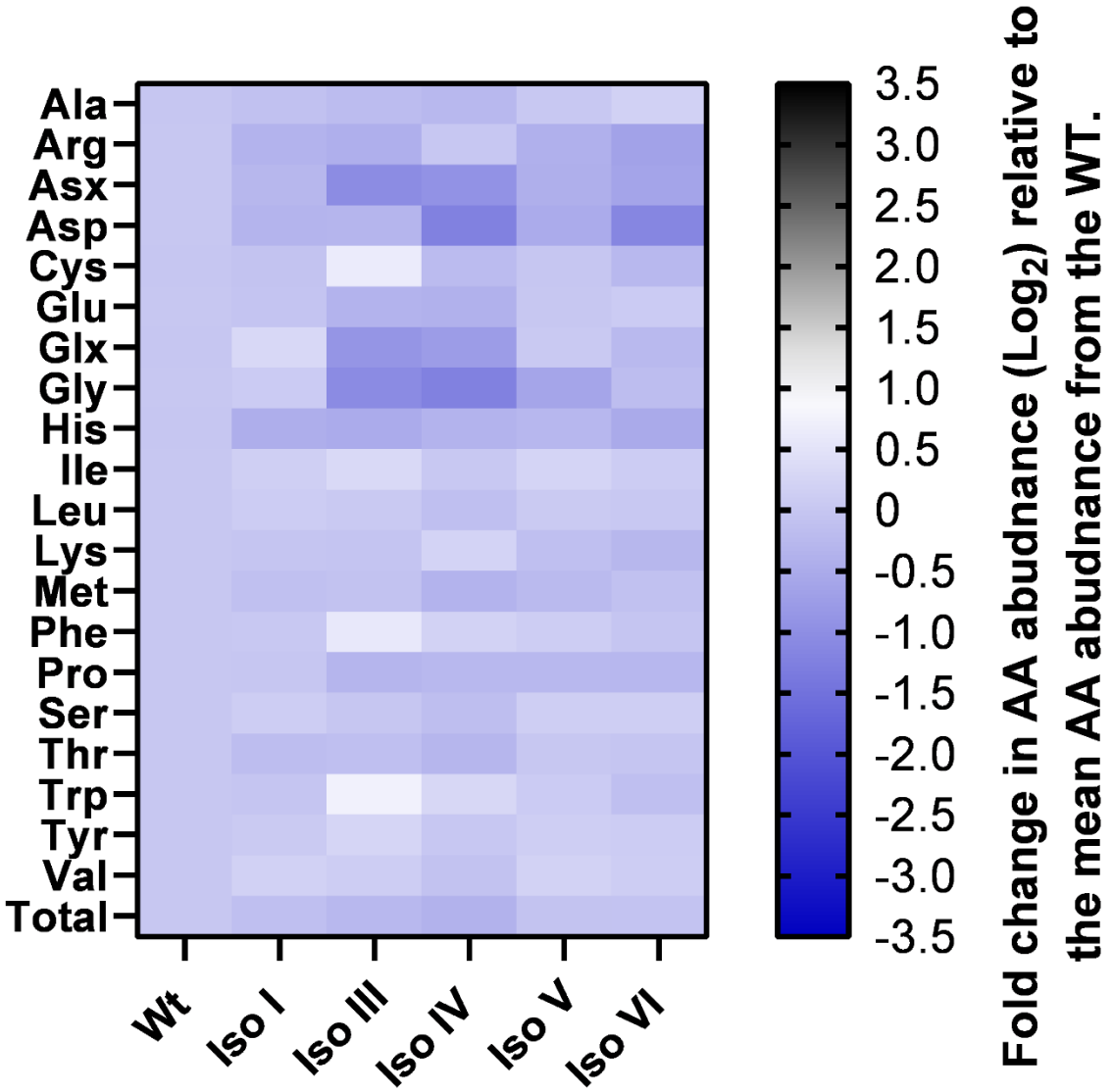

Figure 5.8 A heat map illustrating the fold change in the level of each free AA in Iso I and III-VI relative to the WT. The data are expressed as a Log_2 of the values from **Appendix Table 28**. n = 3.

5.4.7 Comparison of AA profile of Iso2 and WT hydrolysates

To test whether putative mutations leading to increased free-leucine content in Iso 2 are reflected in the protein hydrolysate composition of the organism, WT, and Iso 2 *F. venenatum* cultures were grown in shake-flask cultures and sampled after 30 or 36 h of growth. The biomass samples were freeze-dried, powdered, and hydrolysed. The hydrolysate was analysed using LCMSMS and the quantitative data compared independently in the 30 and 36 h datasets. For the 30 h dataset analysis of PC1 and 2 by One-Way ANOVA did not indicate a significant difference in the total AA abundance or change in AA levels measured by PC2 ($p = 0.13$, $p = 0.11$, respectively) (**Table 5.6**). Analysis of PC3, however showed a significant difference between the WT and Iso2 hydrolysate profiles ($p = 0.006$). A lower PC3 value in the Iso2 indicates an increase in Asp, His, Leu and Ile (**Table 5.6**), these

changes seems miniscule though in terms of relative abundance of the named AAs with highest increase being in Asp (0.63 %) (**Figure 5.9, Appendix Table 29**).

Comparison of the PC1 of the hydrolysate profiles from the 36 h dataset revealed no change to the overall AA abundance ($p = 0.55$) (**Table 5.6**). Similarly, no significant statistically differences were identified in the analysis of PC2-3 ($p = 0.055$, $p = 0.75$, respectively). Because p-value for the PC2 comparison approached significance threshold it was determined it may be worth investigating possible change to the relevant AA levels, which in this case would be elevated Ala and decreased Leu in Iso2 compared to control (**Table 5.6**), 1.2 % increase and 0.57 % decrease respectively in relative terms (**Figure 5.9, Appendix Table 29)**.

In summary in the leucine overproducing Iso 2 strain there is an indication of a change in the hydrolysate AA composition profile but that is limited to increased total levels of Asp, His and Leu, Ile (measured at 30 h) or of Ala (measured at 36 h). Therefore, the high leucine content in the free-AA pool of the Iso2 strain was strongly reflected in its protein hydrolysate.

Table 5.6 Comparison of the amino acid profiles from protein hydrolysates of *F. venenatum* WT and Iso 2 obtained from UV mutagenesis and the TFL selection screen. The values are expressed as g/kg biomass ±SD (n = 3, biological replicates). The 30 and 36 h sets were analysed separately. The PC1-3 from different treatments were compared by One-Way ANOVA (F = 4.3327, df = 1, p = 0.1288; F = 5.2189, df = 1, p = 0.1065; F = 45.315, df = 1, p = 0.0067) for 30 h (F = 0.4213, df = 1, p = 0.5517; F = 7.1646, df = 1, p = 0.0554; F = 0.1174, df = 1, p = 0.7491) for 36 h cultivation respectively. Different letters in superscript in the last three rows indicate statistically significant difference between values derived from One-Way-ANOVA. Lack of any superscript letters indicates lack of significant difference within the relevant part of a row.

	30 h		36 h	
	WT	**Iso 2**	**WT**	**Iso 2**
Ala	**41.17 ± 1.58**	**38.76 ± 1.17**	**35.08 ± 0.95**	**41.14 ± 2.69**
Arg	**33.73 ± 0.03**	**36.21 ± 1.72**	**33.79 ± 0.27**	**33.79 ± 1.89**
Asp	**49.43 ± 0.9**	**55.18 ± 2.78**	**47.88 ± 0.48**	**46.00 ± 1.61**
Cys	**2.75 ± 0.07**	**2.67 ± 0.12**	**3.17 ± 0.15**	**2.73 ± 0.45**
Glu	**82.65 ± 0.38**	**87.64 ± 2.44**	**75.70 ± 3.63**	**88.62 ± 3.06**
Gly	**23.21 ± 0.45**	**27.58 ± 1.66**	**23.13 ± 0.73**	**22.14 ± 1.67**
His	**11.24 ± 0.90**	**12.80 ± 0.38**	**12.27 ± 0.17**	**11.26 ± 1.16**
Ile	**22.13 ± 0.50**	**23.95 ± 1.72**	**23.29 ± 0.66**	**23.06 ± 1.89**
Leu	**33.44 ± 2.01**	**36.09 ± 0.19**	**35.55 ± 1.45**	**33.29 ± 2.77**
Lys	**36.85 ± 0.94**	**37.94 ± 1.66**	**39.08 ± 1.08**	**37.49 ± 1.15**
Met	**9.80 ± 0.35**	**11.12 ± 0.52**	**10.40 ± 0.52**	**10.40 ± 0.41**
Phe	**20.79 ± 0.13**	**21.12 ± 1.02**	**21.66 ± 0.81**	**20.63 ± 0.90**
Pro	**19.84 ± 0.37**	**20.28 ± 0.88**	**20.38 ± 0.59**	**19.91 ± 0.84**
Ser	**19.48 ± 0.24**	**20.64 ± 0.52**	**20.19 ± 0.72**	**19.71 ± 0.97**
Thr	**22.65 ± 0.53**	**24.87 ± 1.34**	**23.01 ± 0.83**	**22.49 ± 1.18**
Tyr	**13.75 ± 0.51**	**14.60 ± 1.30**	**14.60 ± 0.19**	**13.09 ± 0.51**
Val	**27.48 ± 0.10**	**27.47 ± 1.01**	**26.61 ± 0.80**	**25.29 ± 1.34**
Total	**470.39 ± 2.46**	**498.95 ± 18.67**	**465.75 ± 11.06**	**471.06 ± 22.67**
PC1	**1.88 ± 0.1**	**3.14 ± 0.8**	**2.37 ± 0.4**	**1.98 ± 0.9**
PC2	**0.94 ± 0.0** ^{A}	**1.31 ± 0.2** ^{B}	**0.56 ± 0.2**	**1.01 ± 0.2**
PC3	**0.41 ± 0.0**	**0.03 ± 0.1**	**0.74 ± 0.1**	**0.70 ± 0.2**

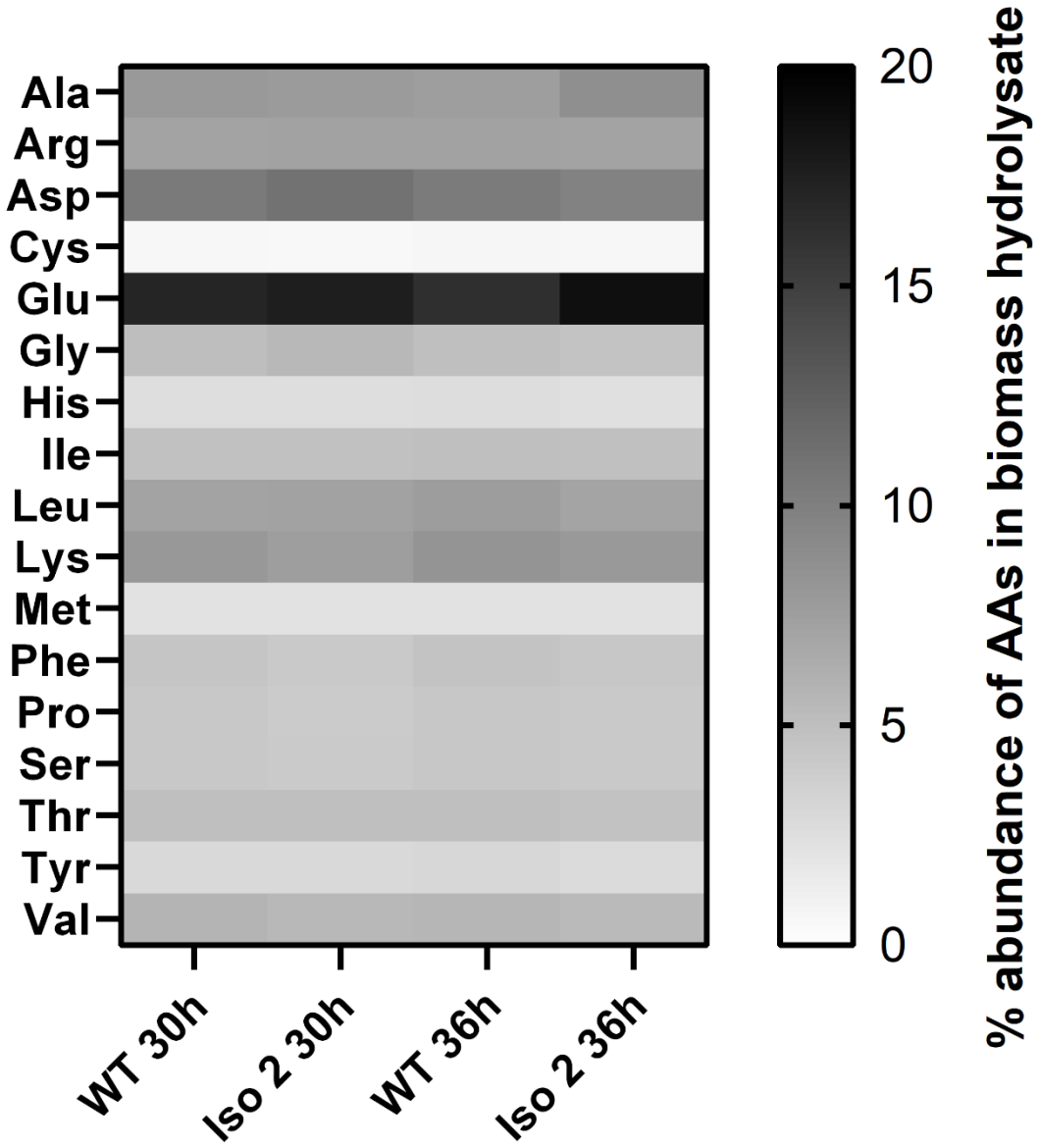

Figure 5.9 Heat map illustration of relative amino acid composition in hydrolysates of *F. venenatum* from WT and Iso 2 strains extracted at 30 and 36 h. The values from **Table 5.6** (converted to heatmap according to the right side scale) are normalised to the total amino acid content of the same sample type (**Appendix Table 29**). n = 3 for all samples except WT at 30 h (n = 2).

5.4.8 Amplification and sequencing of IPMS from TFL isolates

To assess whether the observed phenotype of interest in Iso II and Iso 2 may be due to mutations in IPMS-encoding DNA, as hypothesised at the beginning of this work, the sequence of the predicted *LEU4* gene encoding IPMS was compared between the WT, Iso 2 and Iso II strains. Genomic DNA was extracted from each strain and used as a template for amplification of the predicted *LEU4* gene from *F. venenatum*, using forward and reverse primers designed to amplify between the start codon and TAA STOP codon ending at 2117 bp (see section **5.4.1**). PCR products were examined by agarose gel electrophoresis to corroborate the anticipated fragment length of 2.1 kb. Purified PCR products and the DNA

vector (pET-19b, **5.3.5.10**) were digested with restriction enzymes (BamHI-Hf and XhoI) and used to conduct three independent Gibson assembly reactions for vector-insertion of putative *LEU4* amplified from the WT, Iso 2 and Iso II strains. Reaction products were then transformed into *E. coli* and cells plated on LA agar containing 100 µg/ml carbenicillin. 10 transformant colonies per Gibson assembly transformation were subjected to colony PCR and, of these, between 2 and 7 were found to contain the 2.1 kB insert between the bp 128 and 352 of the pET19-b plasmid backbone . Plasmid DNA was purified from clones containing putative *LEU4* from each of the three *F. venenatum* strains and sent for sequencing. Resultant sequences were compared with those for the predicted IPMS-encoding sequence available on the NCBI blast database and from sequence information for *F. venenatum* A3/5 available for this project from NIAB (see section **5.3.5.10**). The cloned DNA derived from WT *F. venenatum* showed 100% identity with the database sequence for the predicted IPMS encoding sequence. In contrast, the Iso II sequence contained a single SNP A to G at 1694 that would cause a Asp565 to Gly substitution. Iso 2 contained two mutations: (i) an A deletion at 1588 that would cause a frameshift and result in a premature stop codon at AA 570; (ii) a SNP - A to G at 1693 that would result in Met565 to Val substitution (**Figure 5.9**). Predicted structures of the IPMS proteins of the three strains were generated using Swissprot software and overlayed using Chimera X software (**Figure 5.11 A)**. Comparison of the structures predicted the protein product from Iso2 would lack two alpha helices from its C- terminal end. Comparison of the Iso2 IPMS with the crystal structure for the IPMS enzyme from *Mycobacterium tuberculosis* indicated that the structure of the predicted truncated protein from Iso2 would resemble the bacterial enzyme (**Figure 5.11 B**).

A

```
WT     1551 taaggagatcaacatcgaattcgacgtcaacgactacaaggagcacgcta   1600
            |||||||||||||||||||||||||||||||||||| |||||||||||
Iso 2  1551 taaggagatcaacatcgaattcgacgtcaacgactac-aggagcacgcta   1599

       1601 ttggtgagggacgtggcgtcaaggctgcttcatacatcgagtgcaagcct   1650
            ||||||||||||||||||||||||||||||||||||||||||||||||||
       1600 ttggtgagggacgtggcgtcaaggctgcttcatacatcgagtgcaagcct   1649

       1651 gttggcagcaagaactctgtgtggggtgttggtatccacgaggatgttgt   1700
            |||||||||||||||||||||||||||||||||||||||||.||||||
       1650 gttggcagcaagaactctgtgtggggtgttggtatccacgagggtgttgt   1699
```

B

```
WT     1651 gttggcagcaagaactctgtgtggggtgttggtatccacgaggatgttgt   1700
            |||||||||||||||||||||||||||||||||||||||||.||||||
Iso II 1651 gttggcagcaagaactctgtgtggggtgttggtatccacgagggtgttgt   1700
```

Figure 5.10 Diagram summarising mutations found in sequence of putative LEU4 gene from *F. venenatum* isolate 2 and II. The cDNA sequences of putative LEU4 gene encoding predicted α-isopropylmalate synthase (IPMS) from two UV mutagenesis TFL screen isolates were compared to the cDNA of the putative LEU4 sequence of WT *F. venenatum* using EMBOSS pairwise comparison NEEDLE tool (https://www.ebi.ac.uk/Tools/psa/emboss_needle/). Only fragments of the sequence containing differences to WT are shown. A) Isolate 2 compared to WT B) Isolate II compared to WT. A vertical line between the two sequences signifies a base pair match, a lack of line indicates a deletion, a dot indicates a mismatch.

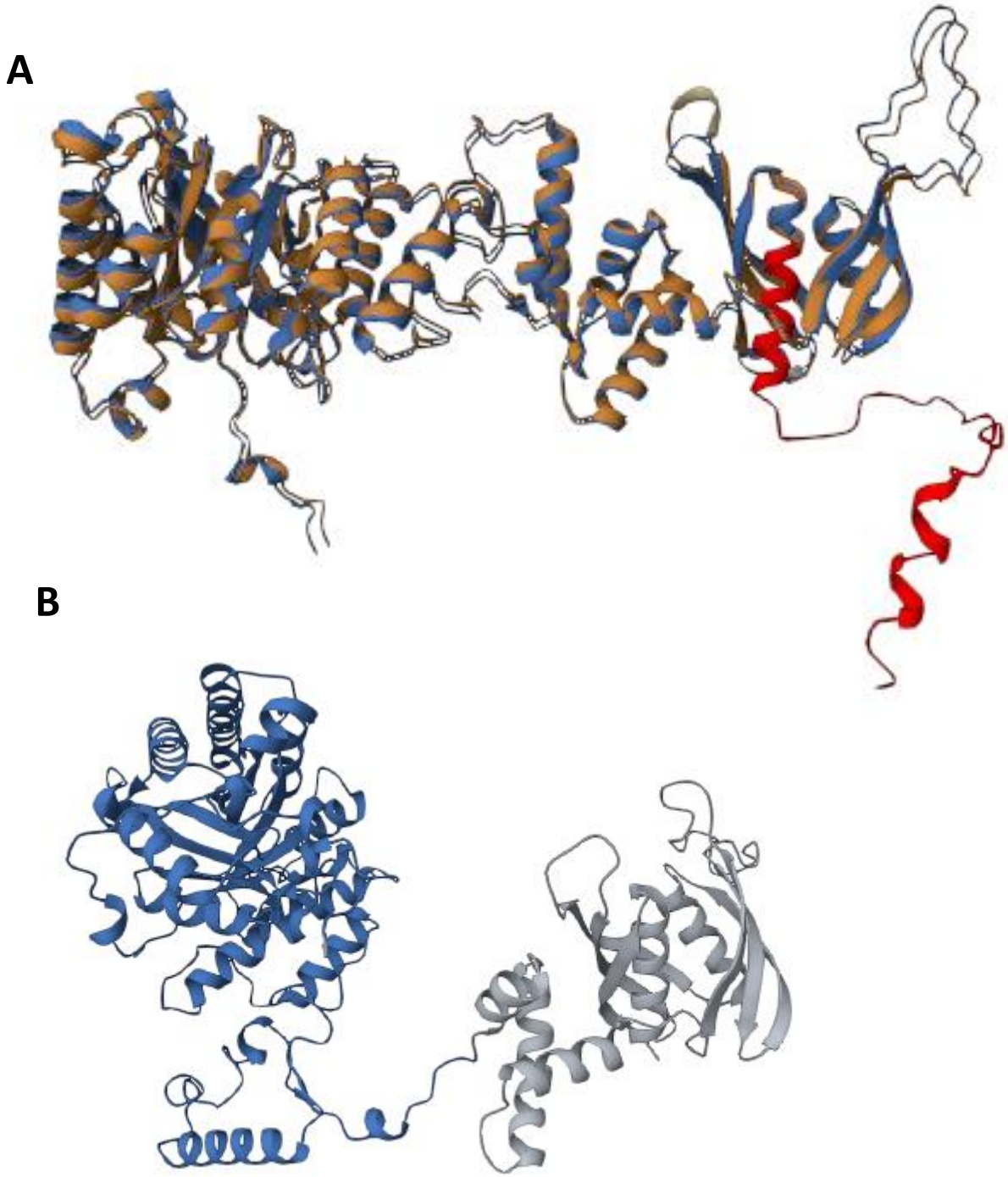

Figure 5.11 In silica comparison of IPMS from *F. venenatum* WT and Iso 2. A: predicted structure of *F. venenatum* IMPS. The sequence of WT (blue) and Iso2 (orange) IPMS were overlayed, the part that is missing in Iso2 IPMS is shown in red. B: diagram of crystal structure of IPMS from *Mycobacterium tuberculosis*.

5.4.9 Bioassay for mycotoxin production by the high free-leucine Iso 2 isolate

As mentioned in the Introduction of this chapter, the BCAA synthesis pathway in *Fusarium* species has been linked to the regulation of mycotoxin production (Subramaniam et al., 2015; Beremand et al., 1988). To test whether selection for high-leucine in the Iso2 isolate may also have altered mycotoxin production, supernatants were taken from WT and Iso2 *F. venenatum*

flask cultures in RHM medium and used to treat cultures of *K. marxianus* GK1005, an organism highly sensitive to various types of mycotoxin (Engler et al., 1999; Whittaker, 2022). Supernatant from *F. venenatum* cultured with sucrose was used as a positive control as sucrose is known to induce mycotoxin production (Whittaker, 2022). The growth of *K. marxianus* supplemented with supernatant from either WT or Iso2 on glucose was very similar to that with no supernatant and there was no significant difference in cell doubling time between these conditions (Mann-Whitney test: two-tailed p = 0.3) (**Figure 5.12**). This suggested that the mutations to IPMS in Iso2 did not induce detectable mycoprotein production, whereas the positive control (with sucrose) validated the sensitivity of the assay.

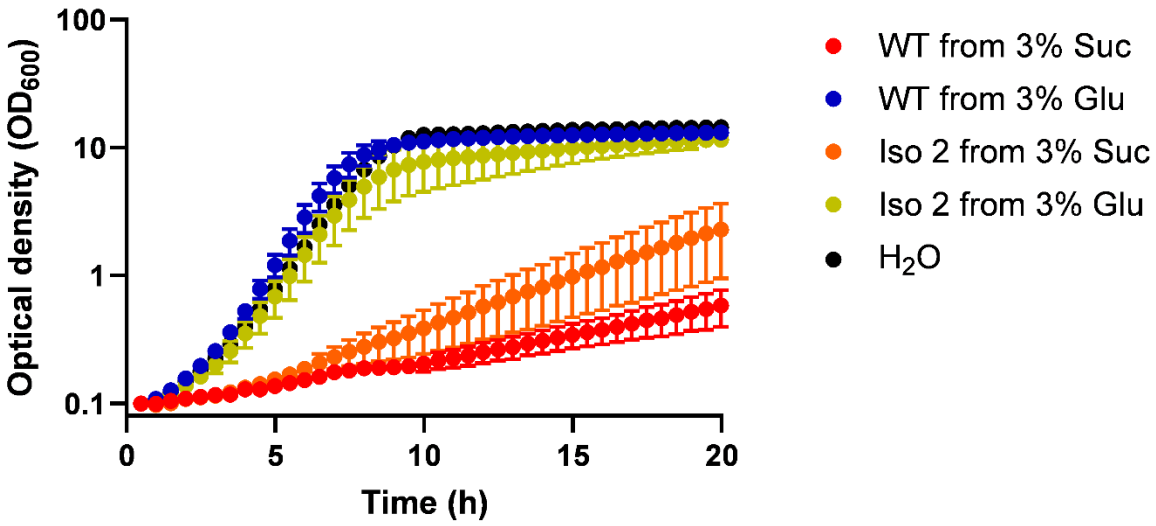

Figure 5.12. Microplate culture of *K. marxianus* in YEPD medium supplemented with supernatant from *F. venenatum* flask cultures. Aliquots (20 µl) of filtered supernatant from cultures of either WT or Iso 2 *F. venenatum* grown for 96 h in RHM medium supplemented with either 3 % glucose or 3 % sucrose was added to wells containing 130 µl of YEPD medium inoculated to a starting OD_{600} 0.01 of exponentially growing *K. marxianus* cells. The plates were incubated with shaking for 20 h at 37 °C with OD readings at 600 nm every 30 min. (n=3, biological replicates)

5.4.10 The extent of loss of free leucine (and other AAs) during the RNA lowering step of mycoprotein production

As mentioned in the **Chapter 1 (1.3.3)** when *F. venenatum* mycelium is being extracted from the airlift fermenter at the production plant it is heated at 68 °C for about 10-15 minutes to reduce the levels of RNAs present in the cells to levels that are safe for human consumption. It is likely that in the process free AAs and some proteins may also leak out of the cells (Whittaker et al., 2020). To see whether any of the extra free leucine produced in Iso 2 remains in the cells after the heating step, mycelium of WT and Iso 2 was heated in water bath at 68 °C for 10 minutes. Then mycelium samples from both WT and Iso 2, heated or unheated were freeze dried, powdered, and free AA extracts were prepared. The free AA extracts were analysed by LCMSMS (**Table 5.7**). No statistical analysis was carried out on these data due a large high number of values for AAs that could not be quantified reliably either due too low or too high levels. However, it is clear that the 68 °C incubation resulted in

the loss of most the free AAs. Free leucine is also among the AAs that leaked out of the mycelium during the heating step meaning that any extra free leucine synthesised by Iso 2 would not end up in the final mycelium product in a routine production setup.

Table 5.7 Comparison of the free amino acid profiles of *F. venenatum* WT and isolate 2 after heat treatment. The values are expressed as g/kg biomass ± SD (n = 3, biological replicates). O/S – oversaturated, N/D not detected.

	WT	WT heated	Iso 2	Iso 2 heated
Ala	2.20 ± 0.10	0.14 ± 0.00	3.10 ± 0.94	N/D
Arg	O/S	0.27 ± 0.09	O/S	0.16 ± 0.03
Asp	2.43 ± 0.53	0.27 ± 0.06	3.48 ± 2.20	0.28 ± 0.03
Glu	14.57 ± 3.02	0.01 ± 0.01	24.00 ± 1.21	0.03 ± 0.02
Gly	0.86 ± 0.37	0.32 ± 0.09	0.70 ± 0.19	N/D
His	O/S	N/D	O/S	N/D
Ile	O/S	0.13 ± 0.05	O/S	0.05 ± 0.01
Leu	O/S	0.04 ± 0.04	O/S	0.03 ± 0.00
Lys	O/S	0.18 ± 0.04	O/S	0.11 ± 0.02
Met	0.25 ± 0.02	0.18 ± 0.07	0.32 ± 0.04	0.11 ± 0.03
Phe	0.25 ± 0.02	0.24 ± 0.08	0.31 ± 0.02	0.14 ± 0.04
Pro	0.46 ± 0.06	N/D	0.56 ± 0.04	N/D
Ser	1.33 ± 0.03	0.30 ± 0.09	1.70 ± 0.19	0.20 ± 0.03
Thr	O/S	0.16 ± 0.06	O/S	0.10 ± 0.02
Trp	0.13 ± 0.03	0.18 ± 0.07	0.14 ± 0.01	0.11 ± 0.03
Tyr	0.26 ± 0.04	0.24 ± 0.09	0.29 ± 0.04	0.13 ± 0.02
Val	O/S	0.24 ± 0.09	O/S	0.15 ± 0.02

5.5 Discussion

The use of TFL as means of selection of leucine feedback insensitive isolates of *F. venenatum* proved successful yielding in particular two isolates (named 2 and II) that had measurably increased levels of free leucine by ~1.5 and ~ 5-10-fold respectively. A common mutation A to G at 1694 in the DNA sequence of the putative *LEU4* gene was identified for both isolates and additional frameshift causing single base pair deletion was identified in Iso 2 at 1588. The frameshift resulted in premature stop codon introduction and truncation of the IPMS protein.

5.5.1 The resistance to TFL in *F. venenatum* spores.

Pre-germination of *F. venenatum* spores proved effective in dramatically sensitizing the organism to TFL and therefore improving the efficacy of the TFL screen. Nevertheless, it remains unclear how ungerminated *F. venenatum* spores could escape inhibition by TFL during germination outgrowth. The process of spore germination is complex and specific to that part of the life cycle of the fungus. In the plant pathogen *Corynespora cassiicola*, transcriptomes of germinating spores revealed a total of 3288 differentially expressed genes compared to mature hyphae, many involved in i.a. metabolism, and environmental information processing (Gao et al., 2020). Comparison of the transcriptomes of *F. venenatum* spores and germlings with and without TFL should give clues to whether the ability to grow with TFL is a result of specific window of response in ungerminated spores or in very early germination, that the pre-germination in the present study was sufficiently long-duration to miss. It is even feasible to consider comparing individual spores (as germination is not perfectly synchronous), given that transcriptomics is possible for single spores of fungi (Geoghegan et al., 2020). Understanding the mechanisms by which *F. venenatum* spores can grow in the presence of TFL might also give some new insight to how fungal pathogens might gain resistance to anti-fungal treatments more broadly, especially in the case of antifungal approaches that target BCAA metabolism (Jastrzebowska and Gabriel, 2015).

5.5.2 Changes to IPMS in Iso2

In *F. venenatum* Iso2 the identified 1588A deletion should result in a frameshift and introduce a premature stop codon, so truncating the protein from 616 to 570 AA in length. Comparison of the predicted structure of the Iso2 IPMS with the crystal structure of the corresponding protein of *Mycobactetrium tuberculosis* revealed that the predicted structure of Iso2 IPMS is more similar to the IPMS of *M. tuberculosis* than to WT *F. venenatum* IPMS. In another study, valine synthesis was upregulated by relocating the relevant pathway from mitochondrial matrix to cytosol in *S. cerevisiae* (Brat et al., 2012). This was achieved by constructing shortened versions of the enzymes Ilv2, Ilv3 and Ilv5 which lacked the mitochondrial binding sequences. One additional possible explanation for the observed increase in leucine synthesis in the Iso2 isolate would be relocation of the IPMS enzyme from the mitochondrial matrix to cytosol as a result of truncation of the protein C terminus. As mentioned before different isoforms of IPMS are present in *S. cerevisiae* that are located in different places in the cells with shorter versions of IPMS present in the cytosol, the cytosol version in fact reportedly lacks the final 30 AAs from the C terminus which contain the mitochondrial binding sequence (Kohlhaw, 2003). To reveal whether this is similar in *F. venenatum*, assays of the localization of IPMS isoforms could be used to determine any such differences occur between the WT and Iso 2 strains.

Elsewhere it was shown that Asp578 is a key residue for (in)sensitivity to leucine feedback inhibition in *S. cerevisiae* (Oba et al., 2005). Here in *F. venenatum* both Iso 2 and Iso II had the same predicted A to G mutation at 1693/1694 bp in putative *LEU4* respectively (the 1 bp difference is due to an upstream 1 bp present in Iso II but absent in Iso 2). Therefore, this mutation could appear to be important for bypassing feedback inhibition in *F. venenatum*. However, because of the upstream frameshift mutation in Iso2, the mutation did not result in the same AA substitutions in the two isolates. To further investigate whether mutation at 1694 is a prerequisite for leucine feedback insensitive IPMS, the relevant site-directed

modification could be introduced to the wild type and/or the variant protein versions purified and assayed for *in vitro* IPMS activity with/without leucine additions.

Another question relevant to the altered free-leucine levels of the isolates is whether the mutation of IPMS may regulate other enzymes in the pathway. In *S. cerevisiae*, the feedback insensitive mutant was shown to have upregulated expression of *LEU1*, *LEU2* and *BAT1* genes of the BCAA synthesis pathway (Oba et al., 2006). Analyses of transcript levels could be used to reveal whether expression of other genes in the BCAA pathway changes in Iso II and Iso 2. Additionally, because the isolates were generated by UV mutagenesis, it is possible that mutations arising elsewhere in the genome had an impact on the leucine synthesis. One way of checking whether mutations affecting other enzymes in the pathway may be having an effect on leucine synthesis would be to compare directly the activities and levels of sensitivity to leucine inhibition of WT and mutated IPMS by *in vitro* assay (Ulm et al., 1972). This would help to indicate whether the activity of the mutated enzyme reflects the observed phenotype and inform whether mutations elsewhere in the genome may also have an effect vs WT. This could be followed up by measuring free AA profiles of WT with mutated IPMS inserted via molecular cloning, then any change to leucine levels in WT carrying the mutated IPMS vs the original isolate that is a source of this mutated IPMS would indicate role of other mutations in the genome.

5.5.3 The utility of Iso2 and other potential isolates

Overall, the Iso 2 isolate did not show evidence of mycotoxin production nor marked changes to growth rate. However, these strains' increased free-leucine levels were not reflected in their protein (hydrolysate) AA profiles. The increase in free leucine synthesis on its own was not expected to change the AA profile of the proteins, but the wider association of BCAA metabolism with mycotoxin production and virulence in *Fusarium* spp. could have changed protein expression in *F. venenatum* consequently altering the AA hydrolysate profile (Subramaniam et al., 2015). Unfortunately, during the heating up step designed to reduce the amount RNA to levels that are safe for human consumption (Whittaker et al., 2020), most of the free AAs of *F. venenatum* for Quorn production leak out of the cells as well. This includes the extra leucine from Iso 2 cells (**5.4.10**). The mixture of nutrients leaked out of *F. venenatum* mycelium during this heating step is referred to as the centrate and is currently discarded, despite general interest in finding a use for it (T. Ingmire, pers. comm.). Nevertheless, increased leucine content in the centrate would increase its nutritional value as a component of growth medium for other SCP operations or even as a source of AAs for operations such as laboratory grown meat (Specht, 2020). Alternatively, mycoprotein not intended for human consumption would not need to go through this heating process as non-primate animals possess the enzyme uricase that allows them to degrade the higher levels of nucleic acids found in mycoprotein. This would also mean that the extra leucine in Iso 2 could be utilised in this type of feed. Additionally, isolates with increased synthesis of other AAs could be generated in a similar way, where the relevant AA synthesis pathway is regulatable by a compound that can be used for appropriate selection of mutants. The isolates with increased AA synthesis could also be used in different experimental regimes, e.g., adaptive evolution experiments conducted in **Chapter 4** of this thesis, with the idea that increased intracellular leucine concentration could promote more leucine misincorporation into protein under favourable conditions.

6 General discussion

As outlined in the introduction of this thesis, the use of microbial derived proteins is on the rise, but fundamental knowledge is still lagging behind when compared to livestock and crops. The diversity and versatility of the microbes is enormous and so is the variety of ideas regarding the application, and to address current problems. The progress in, molecular diagnostic techniques combined with fast generation times of the microbes provides ample opportunities for innovation.

This thesis aimed at establishing a background for monitoring the changes to AA profile of *Fusarium venenatum* A3/5 on a lab scale that can be used as a proxy prediction of change when the conditions of growth are changed. In the second part of the thesis the aim was to explore of the possibility of manipulating the AA profile of *F. venenatum* with focus on targeting translation and AA synthesis whilst avoiding methods that would be classed as genetic modification

6.1 The stability of *F. venenatum* amino acid profile

In **Chapter 2** of this thesis a framework for experimental scale assessment of changes to the AA profile of *F. venenatum* was proposed and validated. The results have revealed that the AA profile of *F. venenatum* exponentially growing in a flask culture is like the AA profile of the mycelium from industrial production (**2.4.5**). The AA profile was shown not to change when the fungus was grown in the exponential phase in different fungal growth media or in sucrose (**2.4.8** and **2.4.9**). Chapter **3** continued to investigate the changes to AA profile of the morphological mutant C-variants that emerge during industrial production of mycoprotein. Even the changes to the AA profiles of C-variant morphological mutants were not dramatic i.e., the content of essential amino acids – crucial determinant of nutritional value of a protein remained unchanged (**3.4.3**). At the same time these results contradict previous claims that the AA profile of C-variant is completely unchanged compared to WT (Trinci, 1994). This could be due to the nature of the specific mutants tested in the other study, because as shown (**3.4.3**) the changes to the AA profile very from mutant to mutant, this is also true about the specific mutation load in each C-variant.

Overall, these experiments revealed that the AA profile of *F. venenatum* is reasonably stable and likely considerable premediated effort needs to be taken to change it. This can be seen as a positive from two perspectives. Firstly, the stability of the profile opens potential possibility of changing the composition of the growth medium e.g., by supplementing with nutrients from waste streams (Hashempour-Baltork et al., 2020). Secondly, when the AA profile changes due to change in the medium it should be relatively easy to identify the component responsible. This is beneficial as the price and availability of particular components of the medium may change overtime e.g., sucrose that was seen as a cheaper alternative to the use of glucose in the mycoprotein industrial process (Whittaker, 2022), is no longer seen as a worthwhile alternative due to change in economic circumstances (I. Geoghegan pers. comms.). Nevertheless, composition of the AA profile is not the only factor worthy of consideration. Different treatments during this thesis were able to change e.g. the colour or smell of the culture (author's unpublished data). These factors might be detrimental to the mycoprotein as a product and would be disqualifying from use in industrial production even if the AA profile is improved/unchanged (R. Johnsons pers. comms.). In the future, a framework of steps in order of priority should be developed to be able to identify promising

approaches more quickly whilst discarding others that although may outperform in some criteria, fail in other aspects that are non-negotiable (like texture or smell) from the mycoprotein product perspective. The focus of this thesis was on protein content (specifically AA profile) but other factors e.g. B-vitamins, micro and macronutrients are of interest from nutritional perspective of SCPs and not considered in this thesis, which does not mean that they remained unchanged in tested conditions. Overall, any change introduced to the organism would have to be viewed in context of all these parameters to accurately assess the potential benefit/drawback balance.

An interesting aspect that was observed during the testing of the protein content of *F. venenatum* across exponential growth was that the lower biomass was associated with higher protein content. This is interesting as in bacteria the higher protein content was associated with higher growth rate (Belliveau et al., 2021). Future research projects could investigate this phenomenon in *F. venenatum* and other filamentous species as knowing how growth rate can modulate protein content could have applications for optimising the protein content of a filamentous fungus SCP by adjusting the growth rate.

6.2 The translation focused amino acid profile manipulation approach

The attempt to change the AA profile and increase the amount of branched chained amino acid was of debatable success. Firstly, the use of chemical inducers of mistranslation did not change the AA profile of the hydrolysates (**4.4.3** and **4.4.6**) . A different approach might have been better for these experiments to e.g. use of mistranslation reporters to see what mistranslation patterns exist and how often are caused by given drugs and conditions (Cvetesic et al., 2016; Wohlgemuth et al., 2021; Altamura et al., 2016). In general use of such reporters would be beneficial for preliminary experiments in all the experiments conducted in **Chapter 4**, including confirming increased incorporation/changed protein expression in the *F. venenatum* grown in the branch chained AA selection media (**4.4.10** and **4.4.11**). Additionally, in recent years a lot of groundbreaking work was done in the area of monitoring mistranslation in biological systems that could radically change future approaches to tackling questions presented in Chapter **4**. This includes novel methods to monitor mRNA translation in real time (Livingston et al., 2023). Increasing understanding of the role of mistranslation in adaptation and evolution and consequently its function and limitations. The fact that mistranslation patterns can be more species or even strain specific than initially thought adds complexity but also might promise unique solutions in specific organisms (Schmutzer and Wagner, 2023). Mapping of specific preferences for mistranslation in different codons on a proteomic level and distinguishing deleterious vs non-deleterious forms of substitutions on proteomic level can inform of best practice to achieve desired changes to proteome via misincorporation (Mordret et al., 2019; Rodriguez-Mias et al., 2022). Or measuring the effects of mistranslation on proteome by use of tRNA variants from different organisms or even engineered ones (Schuntermann et al., 2023; Cozma et al., 2023). Considering the examples of research presented here it is likely that fundamental research into the responses and relationship of *F. venenatum* with mistranslation would be a necessary first step. This could be then followed by identification of properties of *F. venenatum* translational system to design potential approaches to capitalise on parts of the mistranslation that happens in *F. venenatum*.

Specifically regarding the adaptive evolution experiments attempted in this thesis (**4.4.12** and **4.4.13**) the utilisation of the mutated tRNA variants that incorporate a different AA than

dictated by tRNA anticodon and were shown to be deleterious for growth due to toxic impacts of mistranslation could be considered to evaluate the ability of *F. venenatum* to adapt to such artificially increased levels of mistranslation in an experimental evolution setup (Cozma et al., 2023). Of course, organism like this could still not be used directly for food production due to genetic modification status, but it would inform about the level of mistranslation that *F. venenatum* can adapt to and potentially the maximum enrichment of the proteome with the AA of interest.

The leucine overproducing variant selected on TFL had a significantly increased leucine production, however as it is the use would be limited because 1) even 10 fold increase in free leucine (**5.4.6**) represents relatively low increase (~3%) in overall leucine locked in the protein, 2) the free leucine leaks out of the cells during the mycelium heating step applied during industrial production process (**5.4.10**). The method for selection of increased leucine as shown here is quite simple due to the way the leucine synthesis pathway regulates itself by leucine inhibition of the key enzyme α-isopropylmalate in the pathway (Kohlhaw, 2003). However, to increase the synthesis of other AAs without the use of genetic engineering would be more challenging but could potentially done e.g., using specifically engineered auxotrophic bacteria for identification of mutants excreting elevated amounts of desired AAs (Hernandez-Valdes et al., 2020). Overall, though, with the current way *F. venenatum* is produced, increasing the free AA content will only likely increase abundance of these AAs in the centrate limiting the potential of this approach. However, a leucine overproducing isolate tested here did not exhibit any obvious disadvantages meaning that if centrate was to be used as e.g. an ingredient for a growth medium for other applications the amount of free AAs (and therefore value) could be increased without impacting the main biomass production process.

6.3 Concluding remarks

This PhD project has built on existing knowledge of the application of *F. venenatum* as a SCP organism by assessing the changes the AA profile in in a variety of growth conditions. It also explored some methods that aimed to manipulate the AA profile of the fungus, these however had limited success with potential for further exploration for the adaptive evolution selection approach. This work has also generated *F. venenatum* isolates that in principle should be usable in industrial production as no change to growth rate or toxicity was measured. Without further work however, these would be providing the same product with addition of extra free leucine that would enrich the centrate left over from the production process. Overall, this thesis added current body of knowledge by providing some background on the behaviour of the AA profile of *F. venenatum* and highlighted obstacles in attempts to modify the AA composition, that can be extrapolated to other fungal SCP candidates.

7 Appendix

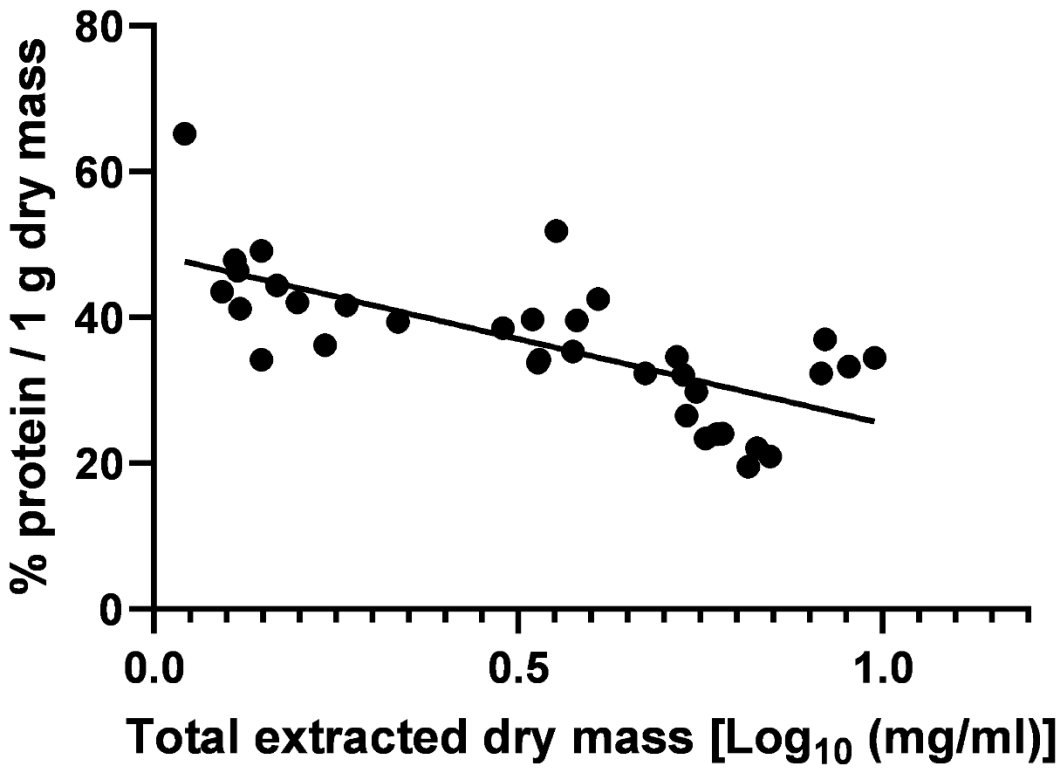

Appendix Figure 1. The relationship between total dry mass at the point of extraction and the protein content in *F. venenatum* samples grown in flask cultures. The protein content and mass of individual samples from **Figure 2.5, Figure 2.9, Figure 2.10** were plotted on x and y axis respectively. There was a negative correlation between the protein content an increasing extracted dry mass of the samples; Pearson r (68) = -0.7150, $p < 0.0001$.

.

Appendix Table 1. Comparison of relative AA profiles of *F. venenatum* biomass hydrolysate extracted from flask cultures at 30 h and airlift fermenter. The values for each AA represent % abundance relative to the AA total of the sample. n = 3

AA g/kg	Flask	Airlift Q5	Airlift Q3
Ala	9.23 ± 1.25	10.14 ± 0.61	10.22 ± 1.20
Arg	6.93 ± 0.20	7.46 ± 0.35	7.88 ± 0.59
Asp	8.28 ± 0.24	8.19 ± 0.14	8.35 ± 0.22
Cys	0.71 ± 0.03	0.73 ± 0.03	0.70 ± 0.06
Glu	18.66 ± 2.68[A]	16.67 ± 0.28[B]	15.56 ± 0.32[C]
Gly	4.40 ± 0.07	4.10 ± 0.10	4.14 ± 0.02
His	2.39 ± 0.19	2.60 ± 0.07	2.53 ± 0.06
Ile	4.82 ± 0.49	5.00 ± 0.19	5.18 ± 0.34
Leu	7.41 ± 0.49	7.40 ± 0.14	7.82 ± 0.29
Lys	8.08 ± 0.20	8.45 ± 0.16	8.26 ± 0.26
Met	2.64 ± 0.39	2.57 ± 0.20	2.51 ± 0.13
Phe	4.49 ± 0.11	4.43 ± 0.13	4.48 ± 0.12
Pro	4.29 ± 0.09	4.57 ± 0.05	4.53 ± 0.12
Ser	4.06 ± 0.14	3.87 ± 0.11	3.99 ± 0.10
Thr	5.07 ± 0.15	5.03 ± 0.04	5.08 ± 0.11
Tyr	2.30 ± 0.24	2.14 ± 0.05	2.20 ± 0.06
Val	6.23 ± 0.91	6.64 ± 0.07	6.56 ± 0.22

Appendix Table 2. Absolute AA values from analysis of hydrolysate from *F. venenatum* biomass grown in flask cultures. The values are expressed as mg AA per kg of dry biomass. The bottom three rows indicate the principal component values ± SD. The PC1-3 from different treatments were compared by One-Way ANOVA (F = 0.1265, df = 1, p = 0.741; F = 2.9317, df = 1, p = 0.162; F = 0.36, df = 1, p = 0.5809) for replica 1, and (F = 1.1184, df = 1, p = 0.3499; F = 9.7705, df = 1, p = 0.0353; F = 5.6981, df = 1, p = 0.0754) for replica 2. Different letters in superscript in the last three rows indicate statistically significant difference between values derived from One-Way-ANOVA with Tukey's multiple comparisons. Lack of any superscript letters indicates lack of significant difference within the relevant part of a row ± SD. n = 3.

	Replica 1		**Replica 2**	
	30h	**36h**	**30h**	**36h**
Ala	**48.88 ± 4.94**	**32.99 ± 3.19**	**34.10 ± 1.80**	**23.98 ± 0.57**
Arg	**36.19 ± 1.24**	**33.62 ± 3.14**	**25.21 ± 0.97**	**24.57 ± 0.44**
Asp	**56.12 ± 1.85**	**59.57 ± 3.48**	**42.72 ± 2.86**	**41.33 ± 3.43**
Cys	**2.33 ± 0.47**	**2.77 ± 0.23**	**1.93 ± 0.21**	**2.16 ± 0.14**
Glu	**95.94 ± 3.20**	**93.43 ± 13.25**	**59.52 ± 2.60**	**49.65 ± 1.51**
Gly	**23.04 ± 1.12**	**24.23 ± 1.40**	**23.40 ± 1.63**	**21.06 ± 1.53**
His	**12.80 ± 0.45**	**12.67 ± 1.11**	**8.93 ± 0.46**	**9.16 ± 0.46**
Ile	**22.80 ± 0.28**	**22.44 ± 1.75**	**18.30 ± 1.22**	**16.81 ± 0.29**
Leu	**37.92 ± 1.24**	**38.46 ± 3.38**	**20.30 ± 0.64**	**20.09 ± 1.09**
Lys	**41.54 ± 1.55**	**40.25 ± 2.03**	**28.30 ± 1.06**	**29.77 ± 2.56**
Met	**12.61 ± 0.36**	**11.18 ± 0.61**	**8.01 ± 0.04**	**7.75 ± 0.45**
Phe	**21.71 ± 0.51**	**21.64 ± 1.98**	**14.31 ± 0.35**	**14.33 ± 0.77**
Pro	**21.79 ± 0.95**	**21.54 ± 1.78**	**14.27 ± 0.48**	**14.19 ± 0.60**
Ser	**17.44 ± 0.71**	**17.51 ± 1.11**	**13.70 ± 1.27**	**14.49 ± 0.50**
Thr	**27.09 ± 0.87**	**27.66 ± 0.94**	**15.33 ± 0.76**	**14.24 ± 0.92**
Tyr	**12.66 ± 0.60**	**13.22 ± 0.84**	**8.00 ± 0.22**	**7.73 ± 0.37**
Val	**28.97 ± 1.24**	**30.35 ± 2.12**	**16.68 ± 0.83**	**16.21 ± 0.32**
Total	**519.82 ± 14.13**	**503.54 ± 40.21**	**353.01 ± 8.71**	**327.50 ± 13.81**
PC1	**3.46 ± 0.5**	**3.15 ± 1.4**	**- 3.22 ± 0.3**	**- 3.31 ± 1.0**
PC2	**1.87 ± 0.3**	**1.30 ± 0.5**	**0.22 ± 0.2 [A]**	**- 0.56 ± 0.3 [B]**
PC3	**0.49 ± 0.5**	**0.32 ± 0.2**	**- 0.72 ± 0.2**	**- 0.65 ± 0.1**

Appendix Table 3. Absolute AA values from y biomass grown in flask cultures. The values for each AA represent % abundance relative to the AA total of the sample n = 3.

	Replica 1		Replica 2	
	30h	**36h**	**30h**	**36h**
Ala	**9.39 ± 0.76**	**6.55 ± 0.12**	**9.66 ± 0.59**	**7.33 ± 0.21**
Arg	**6.96 ± 0.08**	**6.67 ± 0.14**	**7.15 ± 0.36**	**7.51 ± 0.41**
Asp	**10.81 ± 0.65**	**11.85 ± 0.30**	**12.10 ± 0.61**	**12.60 ± 0.54**
Cys	**0.45 ± 0.08**	**0.55 ± 0.00**	**0.55 ± 0.05**	**0.66 ± 0.02**
Glu	**18.45 ± 0.14**	**18.49 ± 1.21**	**16.86 ± 0.41**	**15.17 ± 0.20**
Gly	**4.43 ± 0.11**	**4.82 ± 0.21**	**6.63 ± 0.38**	**6.43 ± 0.27**
His	**2.46 ± 0.09**	**2.52 ± 0.02**	**2.53 ± 0.16**	**2.80 ± 0.04**
Ile	**4.39 ± 0.07**	**4.46 ± 0.08**	**5.18 ± 0.32**	**5.14 ± 0.31**
Leu	**7.30 ± 0.38**	**7.65 ± 0.58**	**5.75 ± 0.05**	**6.13 ± 0.09**
Lys	**7.99 ± 0.08**	**8.01 ± 0.26**	**8.02 ± 0.41**	**9.08 ± 0.47**
Met	**2.43 ± 0.07**	**2.22 ± 0.07**	**2.27 ± 0.06**	**2.37 ± 0.04**
Phe	**4.18 ± 0.03**	**4.29 ± 0.05**	**4.05 ± 0.04**	**4.37 ± 0.06**
Pro	**4.19 ± 0.08**	**4.28 ± 0.09**	**4.04 ± 0.06**	**4.33 ± 0.01**
Ser	**3.35 ± 0.08**	**3.48 ± 0.07**	**3.88 ± 0.28**	**4.43 ± 0.05**
Thr	**5.21 ± 0.10**	**5.51 ± 0.28**	**4.34 ± 0.20**	**4.35 ± 0.18**
Tyr	**2.43 ± 0.07**	**2.63 ± 0.12**	**2.27 ± 0.07**	**2.36 ± 0.01**
Val	**5.57 ± 0.09**	**6.03 ± 0.07**	**4.72 ± 0.15**	**4.95 ± 0.11**

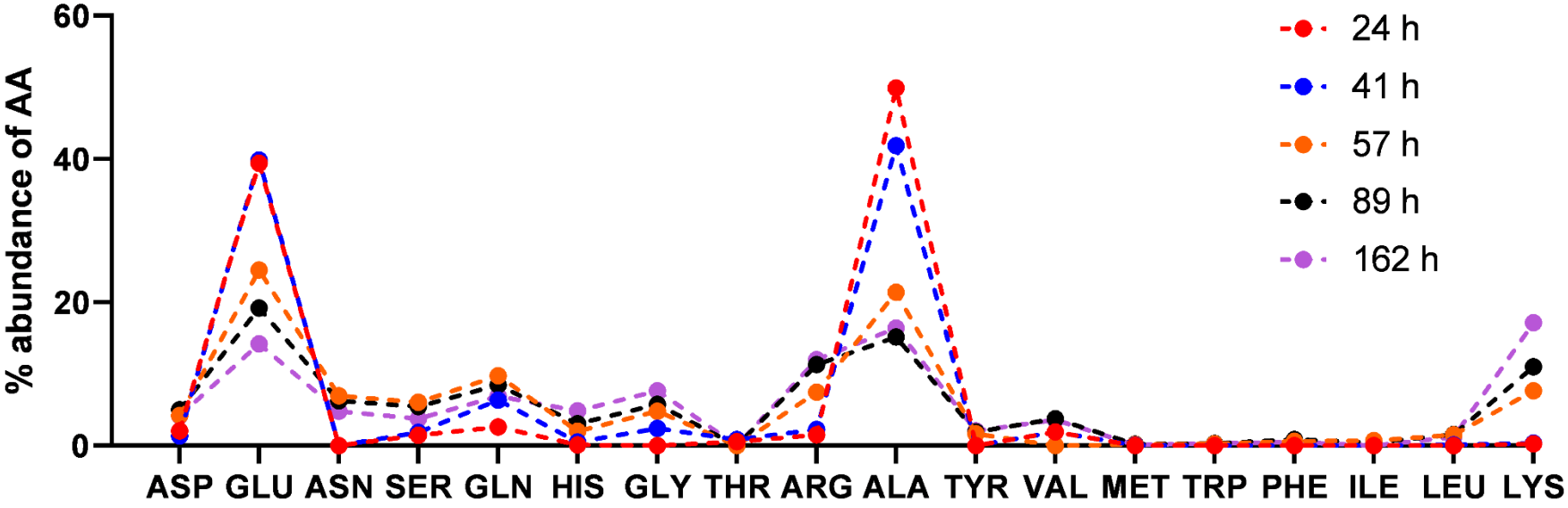

Appendix Figure 2. Relative free AA levels in *F. venenatum* biomass at different timepoints. The free AA levels were measured by HPLC and expressed as parts of the total pool within one sample. The free AAs were extracted as described in (**2.3.10**), n = 3.

Appendix Table 4. Comparison of relative AA profiles of *F. venenatum* biomass hydrolysate extracted at 30 or 41 h from flaks cultures grown in RHM, ACM or AMM medium. The values for each AA represent % abundance relative to the AA total of the sample.

AA g/kg	30h growth			41h growth		
	RHM (n=4)	AMM (n=4)	ACM (n=4)	RHM (n=4)	AMM (n=4)	ACM (n=4)
Ala	8.81 ± 1.32	10.31 ± 0.80	7.60 ± 0.55	7.46 ± 0.67	9.79 ± 1.88	8.14 ± 0.45
Arg	6.95 ± 0.17	6.50 ± 0.22	6.91 ± 0.11	7.38 ± 1.27	9.26 ± 2.86	8.67 ± 2.03
Asp	8.49 ± 0.46	8.62 ± 0.36	9.17 ± 0.19	11.36 ± 0.85	10.18 ± 0.25	10.60 ± 1.03
Cys	0.71 ± 0.02	0.97 ± 0.22	0.92 ± 0.15	1.25 ± 0.20	1.17 ± 0.10	1.20 ± 0.11
Glu	19.02 ± 2.31	17.90 ± 1.31	18.04 ± 1.36	17.50 ± 1.36	18.30 ± 1.53 [A]	16.08 ± 1.92
Gly	4.52 ± 0.24	4.78 ± 0.20	4.88 ± 0.28	5.46 ± 0.64	5.11 ± 0.11	5.38 ± 0.34
His	2.37 ± 0.16	2.27 ± 0.18	2.41 ± 0.09	1.68 ± 0.81	1.55 ± 0.98	1.60 ± 0.88
Ile	4.57 ± 0.63	4.72 ± 0.31	4.54 ± 0.39	4.44 ± 0.20	4.16 ± 0.12	4.58 ± 0.40
Leu	7.41 ± 0.40	7.54 ± 0.12	7.29 ± 0.28	7.19 ± 0.30	6.78 ± 0.49	7.23 ± 0.47
Lys	8.18 ± 0.25	7.98 ± 0.33	9.07 ± 0.83	7.19 ± 1.11	6.25 ± 1.15	7.64 ± 1.55
Met	2.70 ± 0.34	2.54 ± 0.38	2.65 ± 0.37	2.38 ± 0.54	2.26 ± 0.47	2.56 ± 0.54
Phe	4.48 ± 0.09	4.26 ± 0.18	4.35 ± 0.05	4.22 ± 0.13	4.00 ± 0.18	4.32 ± 0.18
Pro	4.29 ± 0.07	4.49 ± 0.02	4.52 ± 0.10	4.75 ± 0.47	4.45 ± 0.10	4.53 ± 0.04
Ser	4.01 ± 0.15	3.96 ± 0.18	4.06 ± 0.04	4.20 ± 0.20	3.98 ± 0.39	4.13 ± 0.05
Thr	5.07 ± 0.12	4.88 ± 0.15	5.06 ± 0.17	5.22 ± 0.12	4.80 ± 0.16	5.00 ± 0.15
Tyr	2.37 ± 0.24	2.25 ± 0.14	2.28 ± 0.27	2.49 ± 0.22	2.40 ± 0.13	2.56 ± 0.10
Val	6.06 ± 0.82	6.01 ± 0.84	6.24 ± 0.35	5.82 ± 0.19	5.57 ± 0.37	5.77 ± 0.63

Appendix Table 5. Extracted dry biomass from samples grown with different carbon sources. R – replica, G – glucose, S – sucrose.

	Mass (mg/ml)		
	R1	R2	R3
3 % G 30 h	1.75	2.23	1.56
3 % S 30 h	1.47	1.51	0.73
1.5/1.5 % G/S 30 h	3.13	3.27	2.28
3 % G 36 h	6.20	6.73	5.46
3 % S 36 h	7.31	2.29	6.50
1.5/1.5 % G/S 36 h	1.86	2.27	5.51

Appendix Table 6. Comparison of relative AA profiles of *F. venenatum* biomass hydrolysate extracted after 30 or 36 h from flask cultures grown in RHM with glucose, sucrose or 50/50 glucose sucrose mix as a carbon source. The values for each AA represent % abundance relative to the AA total of the sample.

	30 h			36 h		
AA g/kg	Glucose 3% (n=3)	Sucrose 3% (n=2)	Glucose/Sucrose 1.5/1.5 % (n=3)	Glucose 3% (n=3)	Sucrose 3% (n=3)	Glucose/Sucrose 1.5/1.5 % (n=3)
Ala	10.76 ± 1.55	11.18 ± 1.12	9.50 ± 015	9.05 ± 0.35	10.32 ± 1.02	9.17 ± 0.99
Arg	5.98 ± 0.56	5.26 ± 0.41	6.01 ± 0.26	5.68 ± 0.51	5.90 ± 0.34	6.03 ± 0.45
Asp	14.51 ± 2.62	17.85 ± 1.50	14.85 ± 0.86	16.88 ± 3.08	15.46 ± 1.58	14.42 ± 1.69
Cys	0.33 ± 0.11	0.23 ± 0.00	0.31 ± 0.05	0.34 ± 0.06	0.29 ± 0.07	0.33 ± 0.01
Glu	17.29 ± 1.92	15.70 ± 1.57	17.32 ± 0.34	14.94 ± 1.23	15.18 ± 1.24	16.62 ± 0.64
Gly	6.29 ± 1.27	7.62 ± 0.62	6.55 ± 0.53	7.19 ± 0.99	7.58 ± 2.30	6.26 ± 0.96
His	2.00 ± 0.18	1.74 ± 0.13	2.02 ± 0.08	2.02 ± 0.14	2.09 ± 0.26	2.17 ± 0.12
Ile	4.39 ± 0.36	3.85 ± 0.26	4.39 ± 0.22	4.57 ± 0.37	4.18 ± 0.37	4.67 ± 0.40
Leu	6.94 ± 0.26	7.55 ± 0.54	7.19 ± 0.47	7.40 ± 0.19	7.28 ± 0.45	7.41 ± 0.10
Lys	7.26 ± 0.70	6.48 ± 0.04	7.34 ± 0.33	6.84 ± 0.46	6.96 ± 0.59	7.62 ± 0.46
Met	1.98 ± 0.21	1.81 ± 0.14	2.04 ± 0.09	2.06 ± 0.21	2.08 ± 0.23	2.11 ± 0.22
Phe	3.79 ± 0.33	3.41 ± 0.28	3.80 ± 0.15	3.80 ± 0.30	3.79 ± 0.20	4.02 ± 0.31
Pro	3.74 ± 0.31	3.27 ± 0.21	3.72 ± 0.14	3.73 ± 0.34	3.67 ± 0.26	3.91 ± 0.27
Ser	3.30 ± 0.44	3.25 ± 0.28	3.46 ± 0.07	3.50 ± 0.21	3.47 ± 0.31	3.50 ± 0.17
Thr	4.28 ± 0.49	3.68 ± 0.52	4.27 ± 0.04	4.39 ± 0.33	4.47 ± 0.38	4.59 ± 0.44
Tyr	2.18 ± 0.02	2.13 ± 0.04	2.21 ± 0.02	2.34 ± 0.15	2.26 ± 0.04	2.32 ± 0.17
Val	4.98 ± 0.09	4.99 ± 0.11	5.01 ± 0.07	5.26 ±0.04	5.04 ± 0.12	4.84 ± 0.04

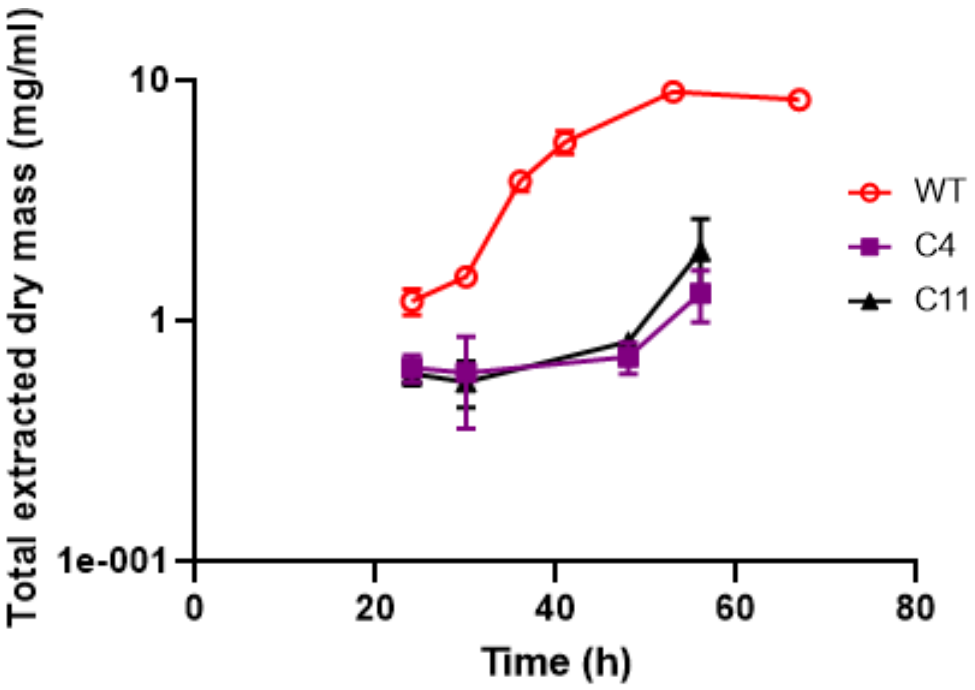

Appendix Figure 3. Growth curve of *F. venenatum* C variant mutants in flask cultures with 1 % glucose. RHM medium was inoculated with 10 000/ml of spores and 50 ml of the suspension was deposited into 250 ml baffled flasks and incubated statically at 28° C with shaking (150 rev/min). The biomass was extracted at 24, 30, 36, 41, 48, 56 and 74 h. Data points indicate mean average, ± SD, n = 3.

Appendix Table 7. Absolute values from free AA extracts from *F. venenatum* C5 isolate. The samples were harvested from flask cultures at 30 h, n = 3 N/I – not included, N/D- not detected

	WT	C5
Ala	**N/I**	**N/I**
Arg	**52.80 ± 3.70**	**74.70 ± 8.00**
Asp	**120.68 ± 29.67**	**62.55 ± 18.31**
Cys	**0.06 ± 0.02**	**N/D**
Glu	**N/I**	**N/I**
Gly	**25.91 ± 3.21**	**24.90 ± 0.86**
His	**15.09 ± 1.52**	**14.40 ± 0.51**
Ile	**3.22 ± 0.15**	**3.13 ± 0.16**
Leu	**3.73 ± 0.26**	**3.66 ± 0.18**
Lys	**14.36 ± 0.38**	**14.24 ± 0.78**
Met	**0.34 ± 0.01**	**0.33 ± 0.02**
Phe	**2.37 ± 0.02**	**2.05 ± 0.05**
Pro	**12.88 ± 0.40**	**20.17 ± 0.29**
Ser	**36.33 ± 1.47**	**29.96 ± 1.56**
Thr	**30.31 ± 2.74**	**36.00 ± 2.33**
Tyr	**1.89 ± 0.01**	**1.57 ± 0.08**
Val	**57.75 ± 5.34**	**85.98 ± 0.64**
Trp	**2.22 ± 0.16**	**2.17 ± 0.11**

Appendix Table 8. The relative AA profiles of hydrolysates from C-variant mutants. All the samples were produced by growth in flask cultures and extracted 36 h from inoculation. The values for each AA represent % abundance relative to the AA total of the sample.

	Set 1		Set 2		
	WT (n = 3)	**C5 (n = 3)**	**WT (n = 3)**	**C4 (n = 3)**	**C11 (n = 2)**
Ala	**10.12 ± 1.48**	**8.73 ± 0.62**	**7.81 ± 0.22**	**7.57 ± 1.79**	**7.41 ± 0.01**
Arg	**6.91 ± 0.21**	**6.80 ± 0.07**	**7.03 ± 0.11**	**7.17 ± 0.19**	**7.13 ± 0.06**
Asp	**10.06 ± 0.35**	**11.15 ± 0.95**	**10.87 ± 0.38**	**12.27 ± 1.04**	**11.18 ± 0.56**
Cys	**0.49 ± 0.07**	**0.35 ± 0.09**	**0.62 ± 0.01**	**0.45 ± 0.04**	**0.42 ± 0.02**
Glu	**16.73 ± 0.30**	**15.76 ± 0.61**	**16.74 ± 0.46**	**14.54 ± 1.38**	**16.57 ± 0.89**
Gly	**4.16 ± 0.13**	**4.67 ± 0.34**	**4.61 ± 0.21**	**6.60 ± 1.54**	**5.70 ± 0.66**
His	**2.20 ± 0.08**	**2.04 ± 0.17**	**2.73 ± 0.02**	**2.64 ± 0.10**	**2.54 ± 0.01**
Ile	**5.11 ± 0.16**	**4.98 ± 0.23**	**4.75 ± 0.13**	**4.54 ± 0.10**	**5.04 ± 0.25**
Leu	**7.53 ± 0.06**	**7.55 ± 0.15**	**7.54 ± 0.17**	**8.02 ± 0.25**	**8.36 ± 0.18**
Lys	**7.80 ± 0.20**	**8.01 ± 0.16**	**8.48 ± 0.01**	**8.41 ± 0.38**	**8.04 ± 0.10**
Met	**2.50 ± 0.25**	**2.41 ± 0.04**	**2.47 ± 0.11**	**2.67 ± 0.24**	**2.47 ± 0.00**
Phe	**4.23 ± 0.16**	**4.37 ± 0.16**	**4.36 ± 0.08**	**3.98 ± 0.08**	**4.05 ± 0.03**
Pro	**4.22 ± 0.14**	**4.49 ± 0.21**	**4.35 ± 0.03**	**4.08 ± 0.24**	**4.24 ± 0.14**
Ser	**3.61 ± 0.09**	**3.88 ± 0.17**	**3.46 ± 0.10**	**3.56 ± 0.29**	**3.47 ± 0.20**
Thr	**4.65 ± 0.38**	**4.65 ± 0.08**	**6.35 ± 0.12**	**6.13 ± 0.49**	**5.54 ± 0.15**
Tyr	**2.70 ± 0.11**	**2.85 ± 0.05**	**2.28 ± 0.02**	**2.15 ± 0.05**	**2.28 ± 0.05**
Val	**6.97 ± 0.20**	**7.31 ± 0.31**	**5.55 ± 0.05**	**5.24 ± 0.30**	**5.54 ± 0.12**

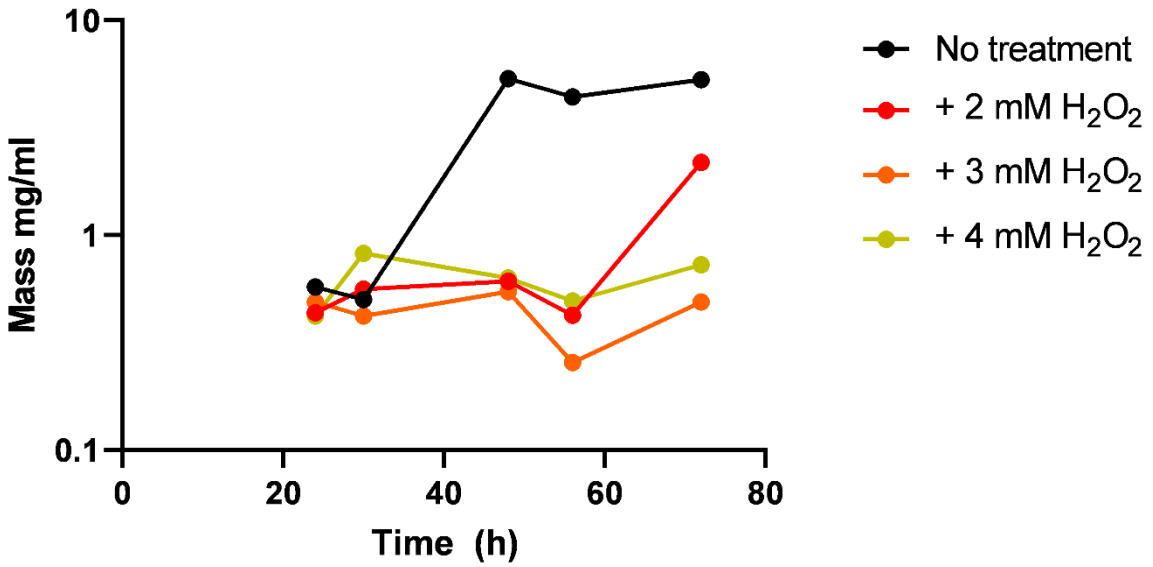

Appendix Figure 4 Growth of *F. venenatum* in flask cultures in presence of H_2O_2. Flasks with RHM medium treated or not with H_2O_2 were inoculated with 10 000 spores per ml. The biomass was extracted at indicated times, lyophilised, and weighed, the values are expressed as mg of biomass per ml of medium, n = 1.

Appendix Table 9. Growth of *F. venenatum* in flask cultures treated with 500 µg/ml paromomycin. The flask cultures of *F. venantum* were treated or not with 500 µg/ml paromomycin and extracted after 30 or 36 h of growth. Extracted biomass was freeze dried and weighed. The differences between means of masses of samples extracted at the same timepoint were analysed using Welch's t-test: 30h (t = 1.520, df = 3.870 two-tailed p = 0.2032); 36 h (t = 17.88, df = 3.581 two tailed p = 0.0001). The values in the table are expressed as mg of dry mass per ml of liquid culture. n = 3.

	Mass (mg/ml)
Control 30 h	3.28 ± 0.59
+ 500 µg/ml Pm 30 h	2.47 ± 0.71
Control 36 h	6.49 ± 0.10
+ 500 µg/ml Pm 36 h	5.23 ± 0.07

Appendix Table 10. Growth of *F. venenatum* in flask cultures when treated with H_2O_2. The flask cultures of *F. venantum* were treated or not with 0.5, 0.75 and 1 mM H_2O_2 and extracted after 30 h of growth. Extracted biomass was freeze dried and weighed. Brown-Forsythe ANOVA test (F* (DFn, DFd) = 10.63 (3.000, 6.480) with multiple comparisons was used to compare the means of extracted biomass from samples treated with H_2O_2 with control. "*" at the treatment row indicates significant difference between that treatment and control as derived from the multiple comparison analysis. The mass is expressed as mg of dry biomass per ml of liquid culture. n=4.

Treatment	Mass (mg/ml)
Control	4.31 ± 1.42
+ 0.5 mM H_2O_2	2.26 ± 1.17
+ 0.75 mM H_2O_2 *	1.32 ± 0.44
+ 1 mM H_2O_2 *	0.81 ± 0.12

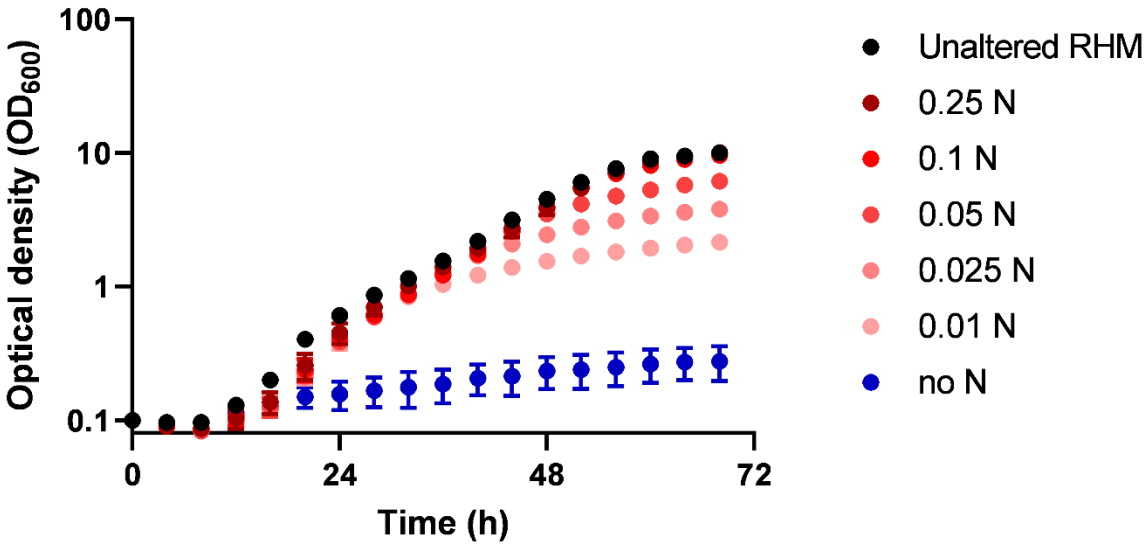

Appendix Figure 5. Growth curve of *F. venenatum* in RHM medium with limited nitrogen source in microplate culture. Standard or nitrogen deficient RHM medium was inoculated with 10,000/ml of spores and 300 µl of the suspension was deposited into wells and incubated statically at 28°C for 72 h with OD measurements taken every 1 h for 72 h. Data points indicate mean average, ± SD, n = 3.

Appendix Table 11. Comparison of amino acid profiles of *F. venenatum* hydrolysate grown in BCAA-modified RHM medium for 36 h. The values are expressed as g/kg biomass ± SD. Experiment 1 and 2 were performed and analysed separately. n = 3 (biological replicates). The bottom three rows indicate the principal component values ± SD. The PC1-3 from different treatments were compared by One-Way ANOVA (F = 4.0245, df = 2, p = 0.0779; F = 5.359, df = 2, p = 0.0462; F = 2.0844, df = 2, p = 0.2054) for experiment 1, and (F = 0.1924, df = 1, p = 0.6835; F = 0.1341, df = 1, p = 0.7327; F = 10.077, df = 1, p = 0.0034) for experiment 2. Different letters in superscript in the last three rows indicate statistically significant difference between values derived from One-Way-ANOVA with Tukey's multiple comparisons. Lack of any superscript letters indicates lack of significant difference within the relevant part of a row.

	Experiment 1			Experiment 2	
	Control	**Leu+ Ile**	**Leu**	**Control**	**Ile**
Ala	32.99 ± 3.19	30.66 ± 2.77	30.71 ± 1.82	23.98 ± 0.57	28.29 ± 1.83
Arg	33.62 ± 3.14	32.53 ± 0.64	30.30 ± 0.84	24.57 ± 0.44	27.96 ± 1.40
Asp	59.57 ± 3.48	51.44 ± 0.36	48.76 ± 3.18	41.33 ± 3.43	39.07 ± 2.13
Cys	2.77 ± 0.23	2.36 ± 0.19	2.43 ± 0.06	2.16 ± 0.14	2.07 ± 0.06
Glu	93.43 ± 13.25	79.92 ± 0.80	76.46 ± 1.30	49.65 ± 1.51	57.02 ± 3.88
Gly	24.23 ± 1.40	22.20 ± 0.45	20.03 ± 1.09	21.06 ± 1.53	22.01 ± 2.07
His	12.67 ± 1.11	12.47 ± 0.25	12.44 ± 0.76	9.16 ± 0.46	9.74 ± 1.39
Ile	22.44 ± 1.75	22.95 ± 2.42	20.24 ± 1.32	16.81 ± 0.29	22.69 ± 2.00
Leu	38.46 ± 3.38	37.31 ± 2.90	38.03 ± 2.43	20.09 ± 1.09	22.71 ± 2.95
Lys	40.25 ± 2.03	37.88 ± 0.39	36.23 ± 0.72	29.77 ± 2.56	28.02 ± 1.38
Met	11.18 ± 0.61	10.91 ± 0.29	10.80 ± 0.47	7.75 ± 0.45	7.32 ± 0.39
Phe	21.64 ± 1.98	20.16 ± 0.31	19.22 ± 0.29	14.33 ± 0.77	13.18 ± 1.10
Pro	21.54 ± 1.78	20.80 ± 0.17	19.95 ± 0.82	14.19 ± 0.60	13.72 ± 1.13
Ser	17.51 ± 1.11	15.80 ± 0.43	15.31 ± 0.40	14.49 ± 0.50	12.49 ± 1.08
Thr	27.66 ± 0.94	25.34 ± 0.64	25.28 ± 1.72	14.24 ± 0.92	14.22 ± 1.56
Tyr	13.22 ± 0.84	12.08 ± 0.31	10.84 ± 0.58	7.73 ± 0.37	7.01 ± 0.74
Val	30.35 ± 2.12	28.90 ± 0.57	27.32 ± 0.85	16.21 ± 0.32	16.12 ± 1.58
Total	503.54 ± 40.21	463.71 ± 5.54	444.34 ± 12.57	327.50 ± 13.81	343.63 ± 23.47
PC1	3.15 ± 1.4	1.15 ± 0.4	1.95 ± 0.2	- 3.60 ± 0.5	- 3.31 ± 1.0
PC2	1.30 ± 0.5	0.47 ± 0.3	0.52 ± 0.2	- 0.46 ± 0.3	- 0.56 ± 0.3
PC3	0.32 ± 0.2	0.47 ± 0.0	0.24 ± 0.1	- 0.45 ± 0.0 [A]	- 0.65 ± 0.1 [B]

Appendix Table 12. Comparison of relative AA profiles of *F. venenatum* biomass hydrolysate extracted from flask cultures at 30 h and airlift fermenter. Values indicate % of total AAs. n = 3.

	Flask	Q5 fermenter	Q3 Fermenter
Ala	**10.22 ± 1.20**	**10.14 ± 0.61**	**9.23 ± 1.25**
Arg	**7.88 ± 0.59**	**7.46 ± 0.35**	**6.93 ± 0.20**
Asp	**8.35 ± 0.22**	**8.19 ± 0.14**	**8.28 ± 0.24**
Cys	**0.70 ± 0.06**	**0.73 ± 0.03**	**0.71 ± 0.03**
Glu	**15.56 ± 0.32**	**16.67 ± 0.28**	**18.66 ± 2.68**
Gly	**4.14 ± 0.02**	**4.10 ± 0.10**	**4.40 ± 0.07**
His	**2.53 ± 0.06**	**2.60 ± 0.07**	**2.39 ± 0.19**
Ile	**5.18 ± 0.34**	**5.00 ± 0.19**	**4.82 ± 0.49**
Leu	**7.82 ± 0.29**	**7.40 ± 0.14**	**7.41 ± 0.49**
Lys	**8.26 ± 0.26**	**8.45 ± 0.16**	**8.08 ± 0.20**
Met	**2.51 ± 0.13**	**2.57 ± 0.20**	**2.64 ± 0.39**
Phe	**4.48 ± 0.12**	**4.43 ± 0.13**	**4.49 ± 0.11**
Pro	**4.53 ± 0.12**	**4.57 ± 0.05**	**4.29 ± 0.09**
Ser	**3.99 ± 0.10**	**3.87 ± 0.11**	**4.06 ± 0.14**
Thr	**5.08 ± 0.11**	**5.03 ± 0.04**	**5.07 ± 0.15**
Tyr	**2.20 ± 0.06**	**2.14 ± 0.05**	**2.30 ± 0.24**
Val	**6.56 ± 0.22**	**6.64 ± 0.07**	**6.23 ± 0.91**

Appendix Table 13. Relative AA profiles of *F. venenatum* biomass hydrolysate in different media after growth for 30 h and 41 h. Values represent % of the total AAs. Statistical analysis was carried out separately for data from 30 and 41h time points.

	30 h growth			41 h growth		
	RHM	**AMM**	**ACM**	**RHM**	**AMM**	**ACM**
Ala	**8.82 ± 1.32**	**10.31 ± 0.80**	**7.60 ± 0.55**	**7.46 ± 0.67**	**9.79 ± 1.88**	**8.14 ± 0.45**
Arg	**6.95 ± 0.17**	**6.51 ± 0.21**	**6.91 ± 0.11**	**7.38 ± 1.27**	**9.26 ± 2.86**	**8.67 ± 2.03**
Asp	**8.49 ± 0.46**	**8.62 ± 0.36**	**9.17 ± 0.20**	**11.36 ± 0.85**	**10.18 ± 0.25**	**10.60 ± 1.03**
Cys	**0.71 ± 0.02**	**0.97 ± 0.22**	**0.92 ± 0.14**	**1.25 ± 0.20**	**1.17 ± 0.11**	**1.19 ± 0.11**
Glu	**19.02 ± 2.31**	**17.91 ± 1.32**	**18.04 ± 1.36**	**17.50 ± 1.36**	**18.30 ± 1.54**	**16.08 ± 1.92**
Gly	**4.52 ± 0.24**	**4.78 ± 0.20**	**4.89 ± 0.29**	**5.46 ± 0.64**	**5.11 ± 0.11**	**5.38 ± 0.34**
His	**2.37 ± 0.16**	**2.26 ± 0.19**	**2.40 ± 0.09**	**1.68 ± 0.81**	**1.55 ± 0.98**	**1.60 ± 0.88**
Ile	**4.57 ± 0.63**	**4.72 ± 0.31**	**4.55 ± 0.39**	**4.44 ± 0.20**	**4.16 ± 0.12**	**4.58 ± 0.40**
Leu	**7.41 ± 0.40**	**7.54 ± 0.12**	**7.29 ± 0.29**	**7.19 ± 0.30**	**6.78 ± 0.49**	**7.24 ± 0.47**
Lys	**8.18 ± 0.25**	**7.98 ± 0.33**	**9.07 ± 0.83**	**7.19 ± 1.11**	**6.25 ± 1.15**	**7.64 ± 1.56**
Met	**2.70 ± 0.34**	**2.54 ± 0.37**	**2.66 ± 0.37**	**2.38 ± 0.54**	**2.26 ± 0.47**	**2.56 ± 0.54**
Phe	**4.47 ± 0.09**	**4.27 ± 0.17**	**4.35 ± 0.05**	**4.22 ± 0.13**	**4.00 ± 0.18**	**4.32 ± 0.18**
Pro	**4.29 ± 0.07**	**4.49 ± 0.03**	**4.52 ± 0.11**	**4.75 ± 0.47**	**4.45 ± 0.10**	**4.53 ± 0.03**
Ser	**4.01 ± 0.15**	**3.96 ± 0.19**	**4.06 ± 0.04**	**4.20 ± 0.20**	**3.98 ± 0.39**	**4.13 ± 0.04**
Thr	**5.06 ± 0.12**	**4.89 ± 0.15**	**5.06 ± 0.17**	**5.22 ± 0.12**	**4.80 ± 0.16**	**5.00 ± 0.15**
Tyr	**2.38 ± 0.24**	**2.25 ± 0.14**	**2.28 ± 0.27**	**2.49 ± 0.22**	**2.40 ± 0.13**	**2.56 ± 0.10**
Val	**6.06 ± 0.82**	**6.01 ± 0.84**	**6.25 ± 0.34**	**5.82 ± 0.19**	**5.57 ± 0.37**	**5.77 ± 0.63**

Appendix Table 14. Relative AA profiles of *F. venenatum* biomass hydrolysate from samples grown on different carbon sources. The values in the table represent % of the total AAs.

	30 h growth			36 h growth		
	Glucose 3% (n=3)	Sucrose 3% (n=2)	Glucose/Sucrose 1.5/1.5% (n=3)	Glucose 3% (n=3)	Sucrose 3% (n=3)	Glucose/Sucrose 1.5/1.5% (n=3)
Ala	10.76 ± 1.55	11.18 ± 1.12	9.50 ± 0.15	9.05 ± 0.35	10.32 ± 1.02	9.17 ± 0.99
Arg	5.98 ± 0.56	5.26 ± 0.41	6.01 ± 0.26	5.68 ± 0.51	5.90 ± 0.34	6.03 ± 0.45
Asp	14.51 ± 2.62	17.85 ± 1.50	14.85 ± 0.86	16.88 ± 3.08	15.46 ± 1.58	14.42 ± 1.69
Cys	0.33 ± 0.11	0.23 ± 0.00	0.31 ± 0.05	0.34 ± 0.06	0.29 ± 0.07	0.33 ± 0.01
Glu	17.29 ± 1.92	15.70 ± 1.57	17.32 ± 0.34	14.94 ± 1.23	15.18 ± 1.24	16.62 ± 0.64
Gly	6.29 ± 1.27	7.62 ± 0.62	6.55 ± 0.53	7.19 ± 0.99	7.58 ± 2.30	6.26 ± 0.96
His	2.00 ± 0.18	1.74 ± 0.13	2.02 ± 0.08	2.02 ± 0.14	2.09 ± 0.26	2.17 ± 0.12
Ile	4.39 ± 0.36	3.85 ± 0.26	4.39 ± 0.22	4.57 ± 0.37	4.18 ± 0.37	4.67 ± 0.40
Leu	6.94 ± 0.26	7.55 ± 0.54	7.19 ± 0.47	7.40 ± 0.19	7.28 ± 0.45	7.41 ± 0.10
Lys	7.26 ± 0.70	6.48 ± 0.04	7.34 ± 0.33	6.84 ± 0.46	6.96 ± 0.59	7.62 ± 0.46
Met	1.98 ± 0.21	1.81 ± 0.14	2.04 ± 0.09	2.06 ± 0.21	2.08 ± 0.23	2.11 ± 0.22
Phe	3.79 ± 0.33	3.41 ± 0.28	3.80 ± 0.15	3.80 ± 0.30	3.79 ± 0.20	4.02 ± 0.31
Pro	3.74 ± 0.31	3.27 ± 0.21	3.72 ± 0.14	3.73 ± 0.34	3.67 ± 0.26	3.91 ± 0.27
Ser	3.30 ± 0.44	3.25 ± 0.28	3.46 ± 0.07	3.50 ± 0.21	3.47 ± 0.31	3.50 ± 0.17
Thr	4.28 ± 0.49	3.68 ± 0.52	4.27 ± 0.04	4.39 ± 0.33	4.47 ± 0.38	4.59 ± 0.44
Tyr	2.18 ± 0.02	2.13 ± 0.04	2.21 ± 0.02	2.34 ± 0.15	2.26 ± 0.04	2.32 ± 0.17
Val	4.98 ± 0.09	4.99 ± 0.11	5.01 ± 0.07	5.26 ± 0.04	5.04 ± 0.12	4.84 ± 0.04

Appendix Table 15. The relative AA profiles of hydrolysates from C-variant mutants. All the samples were produced by growth in flask cultures and extracted 36 h from inoculation. The values in the table represent % of the total AAs.

	Set 1		Set 2	
	WT (n=3)	**C4 (n=3)**	**WT (n=3)**	**C5 (n=3)**
Ala	**7.81 ± 0.22**	**7.57 ± 1.79**	**10.12 ± 1.48^{A}**	**8.73 ± 0.62^{B}**
Arg	**7.03 ± 0.11**	**7.17 ± 0.19**	**6.91 ± 0.21**	**6.80 ± 0.07**
Asp	**10.87 ±0.38^{A}**	**12.27 ± 1.04^{B}**	**10.06 ± 0.35^{A}**	**11.15 ± 0.95^{B}**
Cys	**0.62 ± 0.01**	**0.45 ± 0.04**	**0.49 ± 0.07**	**0.35 ± 0.09**
Glu	**16.74 ± 0.46^{A}**	**14.54 ± 1.38^{B}**	**16.73 ± 0.30^{A}**	**15.76 ± 0.61^{B}**
Gly	**4.61 ± 0.21^{A}**	**6.60 ± 1.54^{B}**	**4.16 ± 0.13**	**4.67 ± 0.34**
His	**2.73 ± 0.02**	**2.64 ± 0.10**	**2.20 ± 0.08**	**2.04 ± 0.17**
Ile	**4.75 ± 0.13**	**4.54 ± 0.10**	**5.11 ± 0.16**	**4.98 ± 0.23**
Leu	**7.54 ± 0.17**	**8.02 ± 0.25**	**7.53 ± 0.06**	**7.55 ± 0.15**
Lys	**8.48 ± 0.01**	**8.41 ± 0.38**	**7.80 ± 0.20**	**8.01 ± 0.16**
Met	**2.47 ± 0.11**	**2.67 ± 0.24**	**2.50 ± 0.25**	**2.41 ± 0.04**
Phe	**4.36 ± 0.08**	**3.98 ± 0.08**	**4.23 ± 0.16**	**4.37 ± 0.16**
Pro	**4.35 ± 0.03**	**4.08 ± 0.24**	**4.22 ± 0.14**	**4.49 ± 0.21**
Ser	**3.46 ± 0.10**	**3.56 ± 0.29**	**3.61 ± 0.09**	**3.88 ± 0.17**
Thr	**6.35 ± 0.12**	**6.13 ± 0.49**	**4.65 ± 0.38**	**4.65 ± 0.08**
Tyr	**2.28 ± 0.02**	**2.15 ± 0.05**	**2.70 ± 0.11**	**2.85 ± 0.05**
Val	**5.55 ± 0.05**	**5.24 ± 0.30**	**6.97 ± 0.20**	**7.31 ± 0.31**

Appendix Table 16. Comparison of relative hydrolysate amino acid profiles from *F. venenatum* cultures grown in the absence and presence of paromomycin and/or leucine. Values indicate the % amount relative to the AA total. Pm – paromomycin, L – leucine.

	Control	+ 50 µg/mg Pm	+ 100 µg/mg Pm	+ 300 µg/mg Pm	+ 2 mM Leu	+ 100 µg/mg Pm + 2 mM Leu
Ala	8.82 ± 1.32 [A]	9.04 ± 0.85 [A]	8.86 ± 0.10 [A]	7.21 ± 0.02 [B]	8.69 ± 0.29	8.82 ± 0.04
Arg	6.95 ± 0.17	7.67 ± 0.34	7.97 ± 0.34	7.04 ± 0.01	7.12 ± 0.08	7.54 ± 0.01
Asp	8.49 ± 0.46	8.52 ± 0.67	8.27 ± 0.04	9.73 ± 1.41	8.55 ± 0.56	8.21 ± 0.24
Cys	0.71 ± 0.02	0.65 ± 0.04	0.67 ± 0.01	0.79 ± 0.06	0.68 ± 0.05	0.61 ± 0.00
Glu	19.02 ± 2.31	17.50 ± 0.80	15.79 ± 2.18	19.56 ± 0.91	16.58 ± 0.43	17.52 ± 0.00
Gly	4.52 ± 0.24	4.43 ± 0.15	4.49 ± 0.05	5.03 ± 0.68	4.37 ± 0.01	4.62 ± 0.12
His	2.37 ± 0.16	2.51 ± 0.07	2.55 ± 0.11	2.24 ± 0.03	2.51 ± 0.11	2.57 ± 0.04
Ile	4.57 ± 0.63	5.03 ± 0.09	5.20 ± 0.08	4.29 ± 0.10	5.13 ± 0.04	5.04 ± 0.02
Leu	7.41 ± 0.40	7.13 ± 0.16	7.81 ± 0.54	7.55 ± 0.08	8.25 ± 0.27	7.84 ± 0.10
Lys	8.18 ± 0.25	8.47 ± 0.27	8.64 ± 0.24	8.11 ± 0.40	8.52 ± 0.11	8.45 ± 0.03
Met	2.70 ± 0.34	2.31 ± 0.06	2.51 ± 0.18	2.99 ± 0.13	2.49 ± 0.02	2.25 ± 0.14
Phe	4.47 ± 0.09	4.53 ± 0.12	4.70 ± 0.23	4.28 ± 0.17	4.59 ± 0.06	4.46 ± 0.04
Pro	4.29 ± 0.07	4.29 ± 0.05	4.38 ± 0.10	4.25 ± 0.11	4.37 ± 0.00	4.24 ± 0.05
Ser	4.01 ± 0.15	4.01 ± 0.05	4.04 ± 0.07	4.09 ± 0.06	3.96 ± 0.06	3.85 ± 0.04
Thr	5.06 ± 0.12	4.96 ± 0.13	4.85 ± 0.04	4.86 ± 0.04	5.05 ± 0.10	5.04 ± 0.04
Tyr	2.38 ± 0.24	2.15 ± 0.02	2.16 ± 0.10	2.57 ± 0.10	2.23 ± 0.07	2.09 ± 0.05
Val	6.06 ± 0.82	6.80 ± 0.25	7.09 ± 0.61	5.42 ± 0.61	6.90 ± 0.16	6.85 ± 0.11

Appendix Table 17. Comparison of relative hydrolysate amino acid profiles of biomass samples of *F. venenatum* cultured with 500 µg/ml paromomycin (Pm) or 500 µg/ml paromomycin and 2mM leucine (Leu). The values are expressed as % of the total AAs. Samples extracted at 30 and 36 h were compared separately.

	30 h			36 h		
	Control	+ 500 µg/mg Pm	+ 500 µg/mg Pm + 2 mM Leu	Control	+ 500 µg/mg Pm	+ 500 µg/mg Pm + 2 mM Leu
Ala	9.66 ± 0.59	8.52 ± 0.12	8.31 ± 0.56	8.10 ± 0.26	7.53 ± 0.92	9.76 ± 1.27
Arg	7.14 ± 0.36	8.15 ± 0.41	7.12 ± 0.79	7.89 ± 0.26	7.88 ± 0.19	6.84 ± 0.59
Asp	12.09 ± 0.61	12.20 ± 0.75	12.03 ± 0.78	9.50 ± 0.52	11.77 ± 0.74	11.50 ± 0.24
Cys	0.55 ± 0.05	0.53 ± 0.10	0.68 ± 0.04	0.65 ± 0.01	0.65 ± 0.06	0.65 ± 0.08
Glu	16.86 ± 0.41	17.66 ± 0.66	17.98 ± 0.63	15.63 ± 0.20	18.24 ± 0.66	16.55 ± 0.47
Gly	6.63 ± 0.38	6.54 ± 0.58	6.76 ± 0.73	5.46 ± 0.27	6.48 ± 0.49	6.21 ± 0.51
His	2.53 ± 0.16	2.79 ± 0.16	2.65 ± 0.26	2.84 ± 0.02	2.69 ± 0.06	2.87 ± 0.32
Ile	5.18 ± 0.32	5.10 ± 0.18	5.09 ± 0.34	6.55 ± 0.05	4.96 ± 0.42	5.16 ± 0.13
Leu	5.75 ± 0.05	5.63 ± 0.18	5.78 ± 0.43	6.40 ± 0.13	5.76 ± 0.21	5.96 ± 0.19
Lys	8.02 ± 0.41	8.33 ± 0.37	7.89 ± 0.38	8.84 ± 0.29	8.17 ± 0.37	8.82 ± 0.12
Met	2.27 ± 0.06	2.19 ± 0.09	2.15 ± 0.27	2.38 ± 0.02	2.11 ± 0.18	2.04 ± 0.17
Phe	4.05 ± 0.04	3.92 ± 0.07	4.12 ± 0.15	4.48 ± 0.04	4.14 ± 0.07	4.16 ± 0.10
Pro	4.04 ± 0.06	3.95 ± 0.02	4.08 ± 0.06	4.47 ± 0.03	4.11 ± 0.04	4.11 ± 0.11
Ser	3.88 ± 0.28	3.54 ± 0.33	3.73 ± 0.27	4.49 ± 0.01	4.00 ± 0.02	3.84 ± 0.19
Thr	4.34 ± 0.20	4.07 ± 0.17	4.39 ± 0.23	4.68 ± 0.27	4.26 ± 0.14	4.22 ± 0.03
Tyr	2.27 ± 0.07	2.27 ± 0.22	2.16 ± 0.16	2.49 ± 0.05	2.36 ± 0.03	2.35 ± 0.13
Val	4.72 ± 0.15	4.62 ± 0.17	5.08 ± 0.35	5.15 ± 0.09	4.90 ± 0.16	4.95 ± 0.44

Appendix Table 18. Comparison of relative hydrolysate amino acid profiles of *F. venenatum* samples cultured with 0.5-0.75 mM H_2O_2. The values are expressed as g/kg biomass ± SD. n = 3 except for 0.75 mM H_2O_2 where n = 2.

	Control	+ 0.5 mM H_2O_2	+ 0.75 mM H_2O_2
Ala	**10.12 ± 1.48**	**8.86 ± 0.66**	**9.34 ± 1.39**
Arg	**6.91 ± 0.21**	**7.03 ± 0.27**	**6.95 ± 0.13**
Asp	**10.06 ± 0.35**	**10.39 ± 1.41**	**9.88 ± 0.42**
Cys	**0.49 ± 0.07**	**0.36 ± 0.18**	**0.38 ± 0.11**
Glu	**16.73 ± 0.30**	**16.84 ± 0.47**	**17.89 ± 0.16**
Gly	**4.16 ± 0.13**	**4.33 ± 0.21**	**4.22 ± 0.12**
His	**2.20 ± 0.08**	**2.16 ± 0.13**	**2.08 ± 0.01**
Ile	**5.11 ± 0.16**	**4.93 ± 0.11**	**4.92 ± 0.14**
Leu	**7.53 ± 0.06**	**7.29 ± 0.23**	**7.29 ± 0.22**
Lys	**7.80 ± 0.20**	**8.15 ± 0.56**	**7.96 ± 0.09**
Met	**2.50 ± 0.25**	**2.46 ± 0.09**	**2.51 ± 0.15**
Phe	**4.23 ± 0.16**	**4.36 ± 0.12**	**4.40 ± 0.02**
Pro	**4.22 ± 0.14**	**4.29 ± 0.11**	**4.14 ± 0.14**
Ser	**3.61 ± 0.09**	**3.80 ± 0.05**	**3.67 ± 0.21**
Thr	**4.65 ± 0.38**	**4.68 ± 0.05**	**4.55 ± 0.10**
Tyr	**2.70 ± 0.11**	**3.05 ± 0.17**	**2.92 ± 0.04**
Val	**6.97 ± 0.20**	**7.02 ± 0.12**	**6.90 ± 0.27**

Appendix Table 19. Comparison of relative hydrolysate amino acid profiles of *F. venenatum* samples grown in RHM lacking NH_4Cl and supplemented with a mix an equimolar mix of branch chained amino acids (Leu, Ile, Val). The values are expressed as % of the total AAs. n =3.

	Control	- N + 40 mM BCAAS	- N +80 mM BCAAS
Ala	**10.12 ± 1.48**	**7.00 ± 0.33**	**7.19 ± 0.51**
Arg	**6.91 ± 0.21**	**7.14 ± 0.34**	**6.93 ± 0.23**
Asp	**10.06 ± 0.35**	**9.91 ± 0.98**	**9.76 ± 0.57**
Cys	**0.49 ± 0.07**	**0.30 ± 0.14**	**0.30 ± 0.18**
Glu	**16.73 ± 0.30**	**15.83 ± 0.51**	**15.20 ± 0.42**
Gly	**4.16 ± 0.13**	**4.26 ± 0.14**	**4.60 ± 0.81**
His	**2.20 ± 0.08**	**2.28 ± 0.21**	**2.18 ± 0.20**
Ile	**5.11 ± 0.16**	**4.96 ± 0.13**	**5.10 ± 0.23**
Leu	**7.53 ± 0.06**	**7.32 ± 0.23**	**7.66 ± 0.48**
Lys	**7.80 ± 0.20**	**8.28 ± 0.34**	**7.80 ± 0.36**
Met	**2.50 ± 0.25**	**2.52 ± 0.14**	**2.52 ± 0.15**
Phe	**4.23 ± 0.16**	**4.48 ± 0.19**	**4.35 ± 0.05**
Pro	**4.22 ± 0.14**	**4.31 ± 0.09**	**4.19 ± 0.06**
Ser	**3.61 ± 0.09**	**3.95 ± 0.32**	**3.72 ± 0.20**
Thr	**4.65 ± 0.38**	**4.92 ± 0.19**	**4.84 ± 0.07**
Tyr	**2.70 ± 0.11**	**3.19 ± 0.29**	**3.06 ± 0.28**
Val	**6.97 ± 0.20**	**9.37 ± 0.37**	**10.57 ± 0.51**

Appendix Table 20. Comparison of relative hydrolysate amino acid profiles of *F. venenatum* samples grown in modified RHM (lacking NH_4Cl and replaced with 40 mM in total of Leu, Ile or equimolar mix of both) medium for 30 h. The values are expressed as % of the total AA content within the sample. Experiment 1 and 2 were analysed separately. n = 3.

	Experiment 1			Experiment 2	
	Control	**Leu+ Ile**	**Leu**	**Control**	**Ile**
Ala	**9.39 ± 0.76**	**6.95 ± 0.36**	**3.64 ± 2.36**	**9.66 ± 0.59**	**8.15 ± 0.51**
Arg	**6.96 ± 0.08**	**7.20 ± 0.32**	**6.13 ± 0.60**	**7.14 ± 0.36**	**8.20 ± 0.53**
Asp	**10.81 ± 0.65**	**11.10 ± 0.29**	**13.85 ± 2.48**	**12.09 ± 0.61**	**11.31 ± 0.64**
Cys	**0.45 ± 0.08**	**0.37 ± 0.02**	**0.32 ± 0.14**	**0.55 ± 0.05**	**0.54 ± 0.07**
Glu	**18.45 ± 0.14**	**18.02 ± 0.60**	**16.11 ± 1.71**	**16.86 ± 0.41**	**16.49 ± 0.88**
Gly	**4.43 ± 0.11**	**4.37 ± 0.20**	**6.83 ± 1.68**	**6.63 ± 0.38**	**6.38 ± 0.46**
His	**2.46 ± 0.09**	**2.63 ± 0.12**	**2.73 ± 0.13**	**2.53 ± 0.16**	**2.77 ± 0.28**
Ile	**4.39 ± 0.07**	**5.36 ± 0.27**	**4.15 ± 0.07**	**5.18 ± 0.32**	**6.85 ± 0.06**
Leu	**7.30 ± 0.38**	**7.66 ± 0.25**	**9.73 ± 0.53**	**5.75 ± 0.05**	**6.74 ± 0.18**
Lys	**7.99 ± 0.08**	**8.15 ± 0.09**	**8.07 ± 0.07**	**8.02 ± 0.41**	**8.32 ± 1.17**
Met	**2.43 ± 0.07**	**2.28 ± 0.08**	**2.47 ± 0.18**	**2.27 ± 0.06**	**2.04 ± 0.09**
Phe	**4.18 ± 0.03**	**4.27 ± 0.04**	**4.19 ± 0.05**	**4.05 ± 0.04**	**3.84 ± 0.15**
Pro	**4.19 ± 0.08**	**4.39 ± 0.09**	**4.17 ± 0.25**	**4.04 ± 0.06**	**3.92 ± 0.08**
Ser	**3.35 ± 0.08**	**3.44 ± 0.09**	**3.96 ± 0.60**	**3.88 ± 0.28**	**3.59 ± 0.48**
Thr	**5.21 ± 0.10**	**5.35 ± 0.05**	**5.28 ± 0.30**	**4.34 ± 0.20**	**4.09 ± 0.29**
Tyr	**2.43 ± 0.07**	**2.52 ± 0.19**	**2.34 ± 0.10**	**2.27 ± 0.07**	**2.16 ± 0.09**
Val	**5.57 ± 0.09**	**5.95 ± 0.03**	**6.04 ± 0.14**	**4.72 ± 0.15**	**4.62 ± 0.18**

Appendix Table 21. Comparison of relative hydrolysate amino acid profiles of *F. venenatum* samples grown in modified RHM medium for 36 h. The values are expressed as % of the total AA content within the sample. Experiment 1 and 2 were analysed separately. n = 3.

	Experiment 1			Experiment 2	
	Control	**Leu+ Ile**	**Leu**	**Control**	**Ile**
Ala	**6.55 ± 0.12**	**6.22 ± 0.24**	**6.91 ± 0.29**	**7.64 ± 0.39**	**8.24 ± 0.40**
Arg	**6.67 ± 0.14**	**7.17 ± 0.05**	**6.82 ± 0.04**	**7.58 ± 0.41**	**8.15 ± 0.36**
Asp	**11.84 ± 0.30**	**11.28 ± 0.20**	**10.97 ± 0.41**	**12.31 ± 0.47**	**11.38 ± 0.18**
Cys	**0.55 ± 0.01**	**0.51 ± 0.04**	**0.55 ± 0.02**	**0.63 ± 0.05**	**0.61 ± 0.03**
Glu	**18.49 ± 1.21**	**17.43 ± 0.05**	**17.21 ± 0.28**	**15.27 ± 0.16**	**16.60 ± 0.40**
Gly	**4.82 ± 0.21**	**4.85 ± 0.11**	**4.51 ± 0.17**	**6.27 ± 0.49**	**6.41 ± 0.46**
His	**2.51 ± 0.02**	**2.69 ± 0.03**	**2.80 ± 0.10**	**2.80 ± 0.03**	**2.83 ± 0.27**
Ile	**4.46 ± 0.08**	**4.88 ± 0.55**	**4.56 ± 0.43**	**5.28 ± 0.28**	**6.60 ± 0.34**
Leu	**7.65 ± 0.58**	**7.84 ± 0.34**	**8.55 ± 0.33**	**6.05 ± 0.08**	**6.59 ± 0.41**
Lys	**8.01 ± 0.26**	**8.29 ± 0.04**	**8.16 ± 0.40**	**8.67 ± 0.34**	**8.17 ± 0.50**
Met	**2.22 ± 0.07**	**2.35 ± 0.04**	**2.43 ± 0.06**	**2.34 ± 0.04**	**2.13 ± 0.03**
Phe	**4.29 ± 0.05**	**4.33 ± 0.03**	**4.33 ± 0.11**	**4.37 ± 0.05**	**3.83 ± 0.08**
Pro	**4.28 ± 0.09**	**4.52 ± 0.04**	**4.49 ± 0.06**	**4.36 ± 0.05**	**3.99 ± 0.06**
Ser	**3.48 ± 0.07**	**3.39 ± 0.05**	**3.45 ± 0.07**	**4.45 ± 0.07**	**3.64 ± 0.11**
Thr	**5.51 ± 0.28**	**5.49 ± 0.13**	**5.69 ± 0.27**	**4.58 ± 0.27**	**4.13 ± 0.20**
Tyr	**2.63 ± 0.12**	**2.61 ± 0.07**	**2.44 ± 0.07**	**2.40 ± 0.08**	**2.04 ± 0.07**
Val	**6.03 ± 6.14**	**6.14 ± 0.11**	**6.15 ± 0.12**	**5.01 ± 0.11**	**4.69 ± 0.14**

Appendix Table 22. Comparison of relative hydrolysate amino acid profiles of *F. venenatum* isolates obtained from tube race experiments in liquid medium grown flask cultures in RHM medium. The values are expressed as % of the total AAs. n =3.

	WT	Tube race 1	Tube race 2	Tube race 3
Ala	**6.46 ± 1.23**	**7.23 ± 0.43**	**7.70 ± 1.37**	**7.23 ± 0.28**
Arg	**7.13 ± 0.13**	**7.04 ± 0.05**	**6.96 ± 0.10**	**7.04 ± 0.22**
Asp	**11.33 ± 1.59**	**10.81 ± 0.60**	**10.06 ± 1.48**	**9.85 ± 0.63**
Cys	**0.29 ± 0.06**	**0.54 ± 0.25**	**0.27 ± 0.24**	**0.27 ± 0.05**
Glu	**18.11 ± 0.56**	**18.83 ± 0.45**	**18.99 ± 0.90**	**19.75 ± 0.66**
Gly	**4.69 ± 0.15**	**4.68 ± 0.09**	**4.77 ± 0.51**	**4.83 ± 0.03**
His	**3.02 ± 0.04**	**2.85 ± 0.17**	**2.87 ± 0.12**	**2.81 ± 0.03**
Ile	**4.86 ± 0.25**	**4.81 ± 0.37**	**5.48 ± 0.23**	**5.28 ± 0.22**
Leu	**7.87 ± 0.17**	**7.72 ± 0.24**	**7.75 ± 0.24**	**8.10 ± 0.06**
Lys	**8.00 ± 0.28**	**7.85 ± 0.12**	**7.89 ± 0.09**	**7.82 ± 0.18**
Met	**2.01 ± 0.05**	**1.99 ± 0.06**	**2.03 ± 0.07**	**1.92 ± 0.08**
Phe	**4.64 ± 0.01**	**4.51 ± 0.06**	**4.54 ± 0.14**	**4.51 ± 0.07**
Pro	**3.87 ± 0.16**	**3.77 ± 0.04**	**3.58 ± 0.12**	**3.82 ± 0.24**
Ser	**4.18 ± 0.23**	**4.06 ± 0.25**	**4.02 ± 0.13**	**3.95 ± 0.53**
Thr	**4.51 ± 0.58**	**4.35 ± 0.38**	**4.10 ± 0.36**	**3.95 ± 0.29**
Tyr	**3.12 ± 0.09**	**2.99 ± 0.03**	**3.11 ± 0.22**	**3.05 ± 0.07**
Val	**5.94 ± 0.19**	**5.98 ± 0.17**	**5.88 ± 0.29**	**5.82 ± 0.23**

Appendix Table 23. Comparison of relative hydrolysate amino acid profiles of *F. venenatum* isolates obtained from tube race experiments in liquid medium grown flask cultures in RHM medium lacking NH_4Cl and supplemented with a mix of branch chained amino acids (40 mM equimolar mix of Leu, Ile and Val). The values are expressed as % of the total AAs. n = 3 (unless stated otherwise).

	WT	Tube race 1	Tube race 2	Tube race 3 (n=2)
Ala	**2.15 ± 0.87**	**4.56 ± 0.62**	**4.76 ± 3.87**	**0.79 ± 1.11**
Arg	**7.95 ± 0.44**	**7.54 ± 0.31**	**7.69 ± 0.99**	**9.30 ± 0.55**
Asp	**8.85 ± 0.37**	**9.09 ± 0.41**	**8.19 ± 2.70**	**4.82 ± 3.93**
Cys	**0.12 ± 0.21**	**0.31 ± 0.24**	**0.47 ± 0.42**	**0.00**
Glu	**14.40 ± 2.96**	**16.85 ± 0.81**	**15.79 ± 1.79**	**14.26 ± 2.48**
Gly	**3.73 ± 0.77**	**3.89 ± 0.54**	**3.19 ± 0.51**	**4.00 ± 1.32**
His	**4.26 ± 0.44**	**3.50 ± 0.21**	**4.11 ± 1.00**	**5.80 ± 1.38**
Ile	**6.24 ± 1.26**	**4.83 ± 0.10**	**5.31 ± 0.64**	**7.36 ± 0.47**
Leu	**9.28 ± 0.63**	**7.85 ± 0.56**	**8.80 ± 0.78**	**8.25 ± 0.22**
Lys	**8.81 ± 0.44**	**8.28 ± 0.12**	**8.52 ± 1.46**	**10.23 ± 1.00**
Met	**2.15 ± 0.10**	**1.99 ± 0.04**	**2.12 ± 0.23**	**2.32 ± 0.07**
Phe	**5.19 ± 0.43**	**4.63 ± 0.20**	**5.05 ± 0.98**	**6.70 ± 0.95**
Pro	**3.35 ± 0.54**	**3.58 ± 0.43**	**3.39 ± 0.41**	**2.17 ± 0.57**
Ser	**4.30 ± 0.44**	**4.33 ± 0.09**	**3.54 ± 0.46**	**3.04 ± 0.32**
Thr	**4.60 ± 0.13**	**4.67 ± 0.25**	**4.69 ± 1.00**	**4.49 ± 0.04**
Tyr	**3.60 ± 0.34**	**3.37 ± 0.18**	**3.69 ± 0.87**	**5.08 ± 0.95**
Val	**11.01 ± 0.53**	**10.72 ± 0.42**	**10.69 ± 0.52**	**11.42 ± 0.41**

Appendix Table 24. Comparison of relative hydrolysate amino acid profiles of *F. venenatum* isolates obtained from tube race experiments on agar medium grown flask cultures in RHM medium. The values are expressed as % of the total AAs. n =3.

	WT	Tube race 1	Tube race 2	Tube race 3
Ala	**6.46 ± 1.23**	**5.68 ± 0.63**	**5.94 ± 0.30**	**8.64 ± 0.54**
Arg	**7.13 ± 0.13**	**6.91 ± 0.05**	**6.86 ± 0.18**	**7.10 ± 0.17**
Asp	**11.33 ± 1.59**	**10.63 ± 0.81**	**10.60 ± 0.75**	**10.66 ± 0.14**
Cys	**0.29 ± 0.06**	**0.68 ± 0.07**	**0.67 ± 0.20**	**0.57 ± 0.05**
Glu	**18.11 ± 0.56**	**19.97 ± 0.83**	**20.37 ± 1.07**	**18.09 ± 0.43**
Gly	**4.69 ± 0.15**	**5.76 ± 0.61**	**5.08 ± 0.82**	**4.84 ± 0.26**
His	**3.02 ± 0.04**	**2.87 ± 0.12**	**2.91 ± 0.07**	**2.84 ± 0.10**
Ile	**4.86 ± 0.25**	**4.88 ± 0.22**	**4.84 ± 0.12**	**5.10 ± 0.22**
Leu	**7.87 ± 0.17**	**7.70 ± 0.19**	**7.33 ± 0.19**	**7.82 ± 0.56**
Lys	**8.00 ± 0.28**	**7.98 ± 0.05**	**7.99 ± 0.29**	**8.07 ± 0.14**
Met	**2.01 ± 0.05**	**1.90 ± 0.05**	**1.96 ± 0.01**	**2.08 ± 0.06**
Phe	**4.64 ± 0.01**	**4.55 ± 0.11**	**4.49 ± 0.04**	**4.46 ± 0.11**
Pro	**3.87 ± 0.16**	**3.96 ± 0.04**	**3.88 ± 0.34**	**3.67 ± 0.27**
Ser	**4.18 ± 0.23**	**3.78 ± 0.60**	**3.76 ± 0.36**	**3.45 ± 0.15**
Thr	**4.51 ± 0.58**	**4.09 ± 0.09**	**4.94 ± 0.36** [A]	**3.94 ± 0.31**
Tyr	**3.12 ± 0.09**	**2.68 ± 0.03**	**2.72 ± 0.06**	**2.72 ± 0.17**
Val	**5.94 ± 0.19**	**5.97 ± 0.16**	**5.68 ± 0.31**	**5.94 ± 0.10**

Appendix Table 25. Comparison of relative hydrolysate amino acid profiles of *F. venenatum* isolates obtained from tube race experiments on agar medium grown flask cultures in RHM medium. The values are expressed as % of the total AAs. n =3.

	WT	Tube race 1	Tube race 2
Ala	**2.15 ± 0.87**	**3.48 ± 1.71**	**2.77 ± 2.05**
Arg	**7.93 ± 0.43**	**7.58 ± 0.23**	**7.62 ± 0.12**
Asp	**8.83 ± 0.38**	**11.18 ± 1.09**	**9.45 ± 0.40**
Cys	**0.29 ± 0.07**	**0.15 ± 0.19**	**0.00**
Glu	**14.38 ± 2.99**	**16.32 ± 1.03**	**15.80 ± 0.58**
Gly	**3.72 ± 0.77**	**4.56 ± 0.13**	**3.82 ± 0.49**
His	**4.26 ± 0.43**	**3.73 ± 0.44**	**4.09 ± 0.20**
Ile	**6.23 ± 1.25**	**5.44 ± 0.40**	**6.34 ± 0.64**
Leu	**9.27 ± 0.63**	**7.95 ± 0.22**	**8.19 ± 0.38**
Lys	**8.79 ± 0.42**	**8.04 ± 0.30**	**8.33 ± 0.19**
Met	**2.14 ± 0.10**	**2.02 ± 0.13**	**2.10 ± 0.07**
Phe	**5.18 ± 0.42**	**4.58 ± 0.32**	**4.89 ± 0.20**
Pro	**3.35 ± 0.54**	**3.48 ± 0.12**	**3.53 ± 0.10**
Ser	**4.29 ± 0.43**	**3.79 ± 0.35**	**3.45 ± 0.07**
Thr	**4.60 ± 0.13**	**5.17 ± 0.42**	**5.47 ± 0.13**
Tyr	**3.60 ± 0.33**	**2.88 ± 0.39**	**3.19 ± 0.17**
Val	**10.99 ± 0.53**	**9.66 ± 0.21**	**10.94 ± 0.53**

Appendix Table 26. Free amino acid profiles of *F. venenatum* isolates 1 and 2 obtained from UV mutagenesis TFL selection screen normalised to the mean the free AA profile of the WT. The value of each AA was normalised to the mean of that same AA from WT dataset ± SD. All the values are derived from **Table 5.3**. The means of the rows were compared using One-Way ANOVA with Tukey's multiple comparisons. Different letters in superscript between values in the same row indicate statistically significant difference according to One-Way ANOVA with Tukey's multiple comparisons ($p < 0.05$). A lack of any superscript letters indicates lack of significant difference within a row. n = 3.

	WT	Iso 1	Iso 2
Ala	**1.00 ± 0.41**	**0.90 ± 0.29**	**1.18 ± 0.15**
Arg	**1.00 ± 0.28 ^{A,B}**	**0.79 ± 0.10 ^{A}**	**1.49 ± 0.36 ^{B}**
Asp	**1.00 ± 0.86**	**1.41 ± 0.43**	**1.29 ± 0.25**
Cys	**1.00 ± 0.14**	**1.12 ± 0.28**	**1.08 ± 0.12**
Glu	**1.00 ± 0.32**	**0.86 ± 0.30**	**1.37 ± 0.25**
Gly	**1.00 ± 0.27**	**0.95 ± 0.20**	**1.44 ± 0.17**
His	**1.00 ± 0.19 ^{B}**	**0.96 ± 0.14 ^{B}**	**1.54 ± 0.27 ^{B}**
Ile	**1.00 ± 0.23**	**1.02 ± 0.29**	**1.32 ± 0.19**
Leu	**1.00 ± 0.24 ^{A}**	**1.20 ± 0.22 ^{A}**	**11.15 ± 1.53 ^{B}**
Lys	**1.00 ± 0.26 ^{A}**	**0.99 ± 0.20 ^{A}**	**1.73 ± 0.20 ^{B}**
Met	**1.00 ± 0.30**	**1.48 ± 0.58**	**1.61 ± 0.32**
Phe	**1.00 ± 0.17**	**1.30 ± 0.25**	**1.24 ± 0.13**
Pro	**1.00 ± 0.14**	**1.03 ± 0.25**	**1.20 ± 0.15**
Ser	**1.00 ± 0.29**	**0.87 ± 0.13**	**1.28 ± 0.30**
Thr	**1.00 ± 0.15 ^{A,B}**	**0.82 ± 0.17 ^{A}**	**1.36 ± 0.18 ^{B}**
Tyr	**1.00 ± 0.24**	**1.43 ± 0.31**	**1.23 ± 0.13**
Trp	**1.00 ± 0.40**	**0.76 ± 0.19**	**1.14 ± 0.19**
Val	**1.00 ± 0.20**	**1.02 ± 0.11**	**1.10 ± 0.09**
Total	**1.00 ± 0.28**	**0.90 ± 0.26**	**1.34 ± 0.22**

Appendix Table 27. Free amino acid profiles of *F. venenatum* isolates II and 2 obtained from UV mutagenesis TFL selection screen normalised to the mean the free AA profile of the WT. The value of each AA was normalised to the mean of that same AA from WT dataset ± SD. All the values are derived from **Table 5.4**. The means of the rows were compared using One-Way ANOVA with Tukey's multiple comparisons. Different letters in superscript between values in the same row indicate statistically significant difference according to One-Way ANOVA with Tukey's multiple comparisons ($p < 0.05$). A lack of any superscript letters indicates lack of significant difference within a row. n = 3.

	WT	Iso II	Iso 2
Ala	**1.00 ± 0.10 ^{A}**	**1.25 ± 0.08 $^{A, B}$**	**1.35 ± 0.13 ^{B}**
Arg	**1.00 ± 0.07 ^{A}**	**0.85 ± 0.02 ^{B}**	**1.13 ± 0.05 ^{C}**
Asp	**1.00 ± 0.25**	**1.39 ± 0.58**	**1.24 ± 0.11**
Cys	**N/Q**	**N/Q**	**N/Q**
Glu	**1.00 ± 0.09**	**1.14 ± 0.10**	**1.16 ± 0.12**
Gly	**1.00 ± 0.12**	**1.23 ± 0.11**	**1.11 ± 0.09**
His	**1.00 ± 0.10 $^{A, B}$**	**0.85 ± 0.04 ^{A}**	**1.09 ± 0.06 ^{B}**
Ile	**1.00 ± 0.05 ^{A}**	**1.31 ± 0.07 ^{B}**	**1.49 ± 0.15 ^{B}**
Leu	**1.00 ± 0.07 ^{A}**	**1.32 ± 0.11 ^{B}**	**5.58 ± 0.17 ^{C}**
Lys	**1.00 ± 0.03 ^{A}**	**1.00 ± 0.08 ^{A}**	**1.50 ± 0.09 ^{B}**
Met	**N/Q**	**N/Q**	**N/Q**
Phe	**1.00 ± 0.01 ^{A}**	**1.25 ± 0.06 ^{B}**	**1.18 ± 0.03 ^{B}**
Pro	**1.00 ± 0.03 ^{A}**	**0.96 ± 0.00 ^{A}**	**0.88 ± 0.02 ^{B}**
Ser	**1.00 ± 0.04 ^{A}**	**1.13 ± 0.01 ^{B}**	**1.09 ± 0.01 ^{B}**
Thr	**1.00 ± 0.09 ^{A}**	**1.24 ± 0.05 ^{B}**	**1.24 ± 0.06 ^{B}**
Tyr	**1.00 ± 0.00 ^{A}**	**1.25 ± 0.09 ^{B}**	**1.32 ± 0.03 ^{B}**
Trp	**1.00 ± 0.09**	**1.23 ± 0.07**	**1.02 ± 0.08**
Val	**1.00 ± 0.07 ^{A}**	**1.06 ± 0.02 ^{B}**	**1.02 ± 0.02 ^{A}**
Total	**1.00 ± 0.09 ^{A}**	**1.19 ± 0.04 $^{A, B}$**	**1.23 ± 0.10 ^{B}**

Appendix Table 28. Free amino acid profiles of *F. venenatum* isolates I and III-VI obtained from UV mutagenesis TFL selection screen normalised to the mean the free AA profile of the WT. The value of each AA was normalised to the mean of that same AA from WT dataset ± SD. All the values are derived from **Table 5.5**. The means of the rows were compared using One-Way ANOVA with Tukey's multiple comparisons. Different letters in superscript between values in the same row indicate statistically significant difference according to One-Way ANOVA with Tukey's multiple comparisons ($p < 0.05$). A lack of any superscript letters indicates lack of significant difference within a row. n = 3, unless indicated otherwise.

	WT	Iso I	Iso III	Iso IV	Iso V	Iso VI
Ala	1.00 ± 0.11	0.93 ± 0.15	0.89 ± 0.16	0.85 ± 0.19	1.02 ± 0.03	1.13 ± 0.04
Arg	1.00 ± 0.01 ^{A}	0.78 ± 0.03 $^{A, B}$	0.74 ± 0.02 ^{B}	1.02 ± 0.18 ^{A}	0.76 ± 0.09 ^{B}	0.64 ± 0.05 ^{B}
Asx	1.00 ± 0.02 ^{A}	0.83 ± 0.16 $^{A, C}$	0.49 ± 0.09 ^{B}	0.55 ± 0.19 ^{B,}	0.74 ± 0.05	0.66 ± 0.14 ^{B}
Asp	1.00 ± 0.07 ^{A}	0.81 ± 0.20 ^{A}	0.87 ± 0.42 ^{B}	0.42 ± 0.03 ^{B}	0.72 ± 0.09 ^{A}	0.47 ± 0.16 ^{B}
Cys	1.00 ± 0.21	0.95 ± 0.13	1.57 ± 0.02 (n = 2)	0.87 (n = 1)	0.99 ± 0.02	0.84 ± 0.10
Glu	1.00 ± 0.07 $^{A, C}$	0.97 ± 0.03 $^{A, C}$	0.79 ± 0.04 $^{B, C}$	0.77 ± 0.09 ^{B}	1.01 ± 0.15 $^{A, C}$	1.06 ± 0.06 ^{A}
Glx	1.00 ± 0.18 $^{A, B}$	1.25 ± 0.26 ^{A}	0.55 ± 0.03 ^{B}	0.64 ± 0.33 $^{A, B}$	1.04 ± 0.15 $^{A, B}$	0.88 ± 0.32 $^{A, B}$
Gly	1.00 ± 0.04	1.08 ± 0.32	0.50 ± 0.17	0.47 ± 0.23	0.69 ± 0.25	0.94 ± 0.38
His	1.00 ± 0.14 ^{A}	0.74 ± 0.07 ^{B}	0.71 ± 0.02 ^{B}	0.79 ± 0.06 $^{A, B}$	0.83 ± 0.14 $^{A, B}$	0.71 ± 0.06 ^{B}
Ile	1.00 ± 0.09	1.11 ± 0.12	1.25 ± 0.07	1.02 ± 0.17	1.18 ± 0.08	1.07 ± 0.07
Leu	1.00 ± 0.11	1.08 ± 0.21	1.05 ± 0.28	0.94 ± 0.29	1.05 ± 0.13	1.02 ± 0.02
Lys	1.00 ± 0.06	0.99 ± 0.18	0.97 ± 0.17	1.17 ± 0.12	0.91 ± 0.11	0.84 ± 0.20
Met	1.00 ± 0.03	0.92 ± 0.08	0.94 ± 0.10	0.78 ± 0.01	0.86 ± 0.13	0.93 ± 0.09
Phe	1.00 ± 0.06 ^{A}	1.01 ± 0.08 ^{A}	1.51 ± 0.15 ^{B}	1.18 ± 0.32 ^{A}	1.07 ± 0.05 ^{A}	0.98 ± 0.06 ^{A}
Pro	1.00 ± 0.03 ^{A}	0.99 ± 0.01 ^{A}	0.81 ± 0.10 ^{B}	0.83 ± 0.06 $^{A, B}$	0.83 ± 0.08 $^{A, B}$	0.83 ± 0.05 $^{A, B}$
Ser	1.00 ± 0.03 $^{A, B}$	1.08 ± 0.02 ^{B}	0.98 ± 0.07 $^{A, B}$	0.90 ± 0.03 ^{A}	1.09 ± 0.06 ^{B}	1.09 ± 0.08 ^{B}
Thr	1.00 ± 0.03	0.89 ± 0.06	0.92 ± 0.07	0.82 ± 0.05	1.00 ± 0.09	0.99 ± 0.09
Trp	1.00 ± 0.09 ^{A}	0.98 ± 0.11 ^{A}	1.68 ± 0.17 ^{B}	1.26 ± 0.37 $^{A, B}$	1.06 ± 0.06 ^{A}	0.91 ± 0.12 ^{A}
Tyr	1.00 ± 0.02	1.04 ± 0.06	1.19 ± 0.09	1.01 ± 0.15	1.09 ± 0.03	1.07 ± 0.03
Val	1.00 ± 0.06	1.13 ± 0.07	1.08 ± 0.15	0.94 ± 0.06	1.15 ± 0.08	1.08 ± 0.07
Total	1.00 ± 0.04 ^{A}	0.91 ± 0.03 $^{A, B, C}$	0.84 ± 0.03 ^{C}	0.77 ± 0.05 ^{B}	0.95 ± 0.09 $^{A, C}$	0.96 ± 0.04 $^{A, C}$

Appendix Table 29. Comparison of relative hydrolysate amino acid profiles of WT and Iso 2 *F. venenatum* strains. The values are expressed as % of the total AAs. The 30 h and 36 h datasets were analysed separately. n = 3, unless stated otherwise.

	30 h		36 h	
	WT (n = 2)	**Iso 2**	**WT**	**Iso 2**
Ala	**7.98 ± 0.80**	**7.77 ± 0.17**	**7.53 ± 0.11**	**8.73 ± 0.40**
Arg	**7.15 ± 0.05**	**7.26 ± 0.13**	**7.26 ± 0.16**	**7.17 ± 0.13**
Asp	**10.43 ± 0.29**	**11.06 ± 0.16**	**10.28 ± 0.15**	**9.77 ± 0.22**
Cys	**0.61 ± 0.02**	**0.54 ± 0.02**	**0.68 ± 0.04**	**0.58 ± 0.08**
Glu	**17.02 ± 0.95**	**17.57 ± 0.26**	**16.25 ± 0.41**	**18.82 ± 0.26**
Gly	**5.05 ± 0.04**	**5.52 ± 0.14**	**4.97 ± 0.13**	**4.70 ± 0.13**
His	**2.55 ± 0.02**	**2.57 ± 0.04**	**2.64 ± 0.09**	**2.39 ± 0.13**
Ile	**4.81 ± 0.23**	**4.80 ± 0.23**	**5.00 ± 0.04**	**4.89 ± 0.16**
Leu	**7.18 ± 0.49**	**7.24 ± 0.31**	**7.63 ± 0.18**	**7.06 ± 0.28**
Lys	**8.03 ± 0.44**	**7.60 ± 0.14**	**8.39 ± 0.07**	**7.96 ± 0.15**
Met	**2.24 ± 0.13**	**2.23 ± 0.03**	**2.23 ± 0.09**	**2.21 ± 0.02**
Phe	**4.54 ± 0.18**	**4.23 ± 0.07**	**4.65 ± 0.07**	**4.38 ± 0.03**
Pro	**4.29 ± 0.16**	**4.06 ± 0.03**	**4.38 ± 0.03**	**4.23 ± 0.03**
Ser	**4.31 ± 0.17**	**4.14 ± 0.09**	**4.33 ± 0.08**	**4.19 ± 0.10**
Thr	**4.99 ± 0.10**	**4.98 ± 0.09**	**4.94 ± 0.20**	**4.77 ± 0.15**
Tyr	**2.96 ± 0.15**	**2.92 ± 0.16**	**3.14 ± 0.07**	**2.78 ± 0.07**
Val	**5.86 ± 0.03**	**5.51 ± 0.09**	**5.71 ± 0.15**	**5.37 ± 0.11**

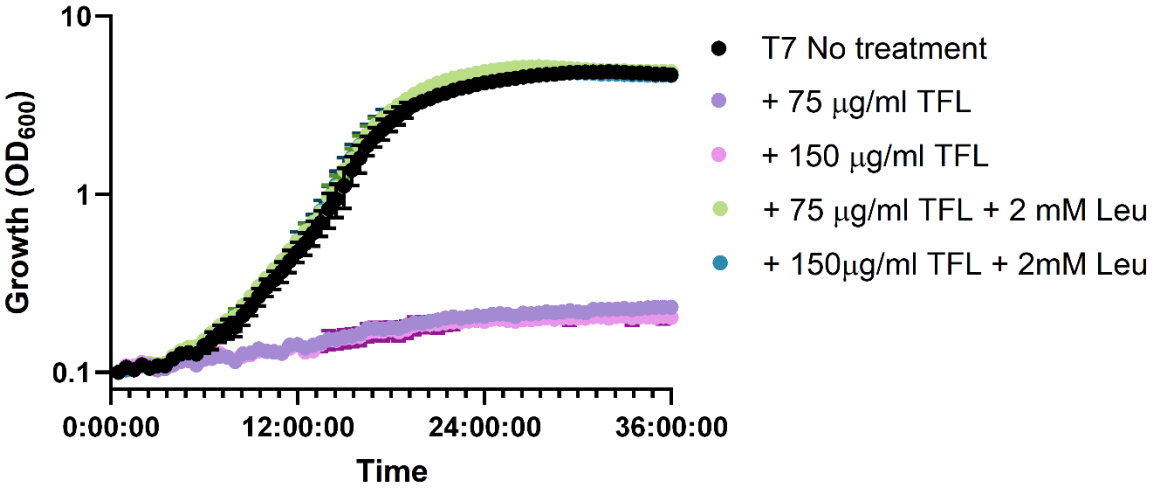

Appendix Figure 6. Growth of *Saccharomyces cerevisiae* cells in YNB medium containing 2 % glucose with 5'5'5 - Tri-fluoro – DL – leucine (TFL). Exponentially growing cells were inoculated into microplate wells containing YNB medium with or without 75/150 µg/ml TFL or 75/150 µg/ml TFL + 2 mM leucine. The cultures were incubated at 28 ^{o}C with shaking for 36 h with OD readings at 600 nm taken every 30 min. The error bar represent SD±, n = 5 (biological replicates).

8 References

ÆVARSSON, A., SEGER, K., TURLEY, S., SOKATCH, J. R. & HOL, W. G. J. 1999. Crystal structure of 2-oxoisovalerate and dehydrogenase and the architecture of 2-oxo acid dehydrogenase multienzyme complexes. *Nature Structural Biology,* 6**,** 785-792.

ALEXANDER, P., BROWN, C., ARNETH, A., DIAS, C., FINNIGAN, J., MORAN, D. & ROUNSEVELL, M. D. A. 2017. Could consumption of insects, cultured meat or imitation meat reduce global agricultural land use? *Global Food Security-Agriculture Policy Economics and Environment,* 15**,** 22-32.

ALEXANDRATOS, N. & BRUINSMA, J. 2012. World agriculture towards 2030/2050: the 2012 revision. Rome: FAO.

ALISAAC, E. & MAHLEIN, A. K. 2023. *Fusarium* head blight on wheat: Biology, modern detection and diagnosis and integrated disease management. *Toxins (Basel),* 15.

ALTAMURA, E., BORGATTI, M., FINOTTI, A., GASPARELLO, J., GAMBARI, R., SPINELLI, M., CASTALDO, R. & ALTAMURA, N. 2016. Chemical-induced read-through at premature termination codons determined by a rapid dual-fluorescence system based on *S. cerevisiae*. *PLoS One,* 11**,** e0154260.

ALTOMARE, C., LOGRIECO, A., BOTTALICO, A., MULÉ, G., MORETTI, A. & EVIDENTE, A. 1995. Production of type A trichothecenes and enniatin B by *Fusarium sambucinum* Fuckel sensu lato. *Mycopathologia,* 129**,** 177-81.

ANDERSON, C., LONGTON, J., C., M., W., S. G. & SOLOMONS, G. L. 1975. The growth of microfungi on carbohydrates.

ANDERSON, C. & SOLOMONS, G. L. 1984. *Primary metabolism and biomass production from Fusarium*, Cambridge University Press.

ANGELI, V., MIGUEL SILVA, P., CRISPIM MASSUELA, D., KHAN, M. W., HAMAR, A., KHAJEHEI, F., GRAEFF-HÖNNINGER, S. & PIATTI, C. 2020. Quinoa (*Chenopodium quinoa Willd*.): an overview of the potentials of the "Golden Grain" and socio-economic and environmental aspects of its cultivation and marketization. *Foods,* 9.

ANGOLD, R., BEECH, G. A. & TAGGART, J. 1989. *Food Biotechnology*, Cambridge University Press.

ARMESTO, J., ROCCHETTI, G., SENIZZA, B., PATEIRO, M., BARBA, F. J., DOMINGUEZ, R., LUCINI, L. & LORENZO, J. M. 2020. Nutritional characterization of butternut squash (*Cucurbita moschata D.*): Effect of variety (Ariel vs. Pluto) and farming type (conventional vs. organic). *Food Research International* 132**,** 109052.

ARUN, K. B., MADHAVAN, A., SINDHU, R., BINOD, P., PANDEY, A., R, R. & SIROHI, R. 2020. Remodeling agro-industrial and food wastes into value-added bioactives and biopolymers. *Industrial Crops and Products,* 154**,** 112621.

ASHTON, G. D. & DYER, P. S. 2016. Sexual development in fungi and its uses in gene expression systems. *In:* SCHMOLL, M. & DATTENBÖCK, C. (eds.) *Gene Expression Systems in Fungi: Advancements and Applications.* Cham: Springer International Publishing.

AZIZI, S., AZIZI, M. H., MOOGOUEI, R. & RAJAEI, P. 2020. The effect of Quinoa flour and enzymes on the quality of gluten-free bread. *Food Sci Nutr,* 8**,** 2373-2382.

BAE, M., AHMED, K. & YIM, J. E. 2022. Beneficial effects of taurine on metabolic parameters in animals and humans. *Journal of Obesity & Metabolic Syndrome,* 31**,** 134-146.

BAI, Z., HARVEY, L. M. & MCNEIL, B. 2003. Oxidative Stress in Submerged Cultures of Fungi. *Critical Reviews in Biotechnology,* 23**,** 267-302.

BANOVIC, M., ARVOLA, A., PENNANEN, K., DUTA, D. E., BRÜCKNER-GÜHMANN, M., LÄHTEENMÄKI, L. & GRUNERT, K. G. 2018. Foods with increased protein content: A qualitative study on European consumer preferences and perceptions. *Appetite,* 125**,** 233-243.

BAR-ON, Y. M., PHILLIPS, R. & MILO, R. 2018. The biomass distribution on Earth. *Proceedings of the National Academy of Sciences,* 115**,** 6506-6511.

BARSOUM, M., KUSCH, S., FRANTZESKAKIS, L., SCHAFFRATH, U. & PANSTRUGA, R. 2020. Ultraviolet mutagenesis coupled with next-generation sequencing as a method for functional interrogation of powdery mildew genomes. *Molecular Plant-Microbe Interactions,* 33**,** 1008-1021.

BARTOLOMEO, M. P. & MAISANO, F. 2006. Validation of a reversed-phase HPLC method for quantitative amino acid analysis. *Journal of Biomolecular Techniques,* 17**,** 131-7.

BATISTA, B. G., CHAVES, M. A., REGINATTO, P., SARAIVA, O. J. & FUENTEFRIA, A. M. 2020. Human fusariosis: An emerging infection that is difficult to treat. *Revista da Sociedade Brasileira de Medicina Tropical,* 53**,** e20200013.

BAUM, J. I., KIM, I. Y. & WOLFE, R. R. 2016. Protein consumption and the elderly: What is the optimal level of intake? *Nutrients,* 8.

BELLIVEAU, N. M., CHURE, G., HUESCHEN, C. L., GARCIA, H. G., KONDEV, J., FISHER, D. S., THERIOT, J. A. & PHILLIPS, R. 2021. Fundamental limits on the rate of bacterial growth and their influence on proteomic composition. *Cell Systems,* 12**,** 924-944.e2.

BELTZER, J. P., MORRIS, S. R. & KOHLHAW, G. B. 1988. Yeast LEU4 encodes mitochondrial and nonmitochondrial forms of alpha-isopropylmalate synthase. *Journal of Biological Chemistry,* 263**,** 368-74.

BEREMAND, M. N., VAN MIDDLESWORTH, F., TAYLOR, S., PLATTNER, R. D. & WEISLEDER, D. 1988. Leucine auxotrophy specifically alters the pattern of trichothecene production in a T-2 toxin-producing strain of *Fusarium sporotrichioides*. *Applied and Environmental Microbiology,* 54**,** 2759-66.

BERG, M. D., HOFFMAN, K. S., GENEREAUX, J., MIAN, S., TRUSSLER, R. S., HANIFORD, D. B., O'DONOGHUE, P. & BRANDL, C. J. 2017. Evolving mistranslating trnas through a phenotypically ambivalent intermediate in *Saccharomyces cerevisiae*. *Genetics,* 206**,** 1865-1879.

BLOMSTRAND, E., ELIASSON, J., KARLSSON, H. K. & KÖHNKE, R. 2006. Branched-chain amino acids activate key enzymes in protein synthesis after physical exercise. *The Journal of Nutrition,* 136**,** 269s-73s.

BRAT, D., WEBER, C., LORENZEN, W., BODE, H. B. & BOLES, E. 2012. Cytosolic re-localization and optimization of valine synthesis and catabolism enables inseased isobutanol production with the yeast *Saccharomyces cerevisiae*. *Biotechnology for Biofuels and Bioproducts,* 5**,** 65.

BROBERG, M. C., UDDLING, J., MILLS, G. & PLEIJEL, H. 2017. Fertilizer efficiency in wheat is reduced by ozone pollution. *The Science of the Total Environnment,* 607-608**,** 876-880.

BRYAN, D., ABBOTT, D. A. & CLASSEN, H. L. 2018. Development of an in vitro protein digestibility assay mimicking the chicken digestive tract. *Animal Nutrition,* 4**,** 401-409.

BURLEY, V. J., PAUL, A. W. & BLUNDELL, J. E. 1993. Influence of a high-fibre food (myco-protein) on appetite: effects on satiation (within meals) and satiety (following meals). *European Journal of Clinical Nutrition,* 47**,** 409-18.

CARBERRY, S. & DOYLE, S. 2007. Proteomic studies in biomedically and industrially relevant fungi. *Cytotechnology,* 53**,** 95-100.

CARILLO, P., CACACE, D., DE PASCALE, S., RAPACCIUOLO, M. & FUGGI, A. 2012. Organic vs. traditional potato powder. *Food Chemistry,* 133**,** 1264-1273.

CASSELTON, L. & ZOLAN, M. 2002. The art and design of genetic screens: Filamentous fungi. *Nature Reviews Genetics,* 3**,** 683-697.

CAVALIERI, D., CASALONE, E., BENDONI, B., FIA, G., POLSINELLI, M. & BARBERIO, C. 1999. Trifluoroleucine resistance and regulation of alpha-isopropyl malate synthase in *Saccharomyces cerevisiae*. *Molecular & General Genetics,* 261**,** 152-60.

CHEE, J. Y., LAKSHMANAN, M., JEEPERY, I. F., MOHAMAD HAIRUDIN, N. H. & SUDESH, K. 2019. The potential application of cupriavidus necator as polyhydroxyalkanoates producer and single cell protein: A review on scientific, cultural and religious perspectives. *Applied Food Biotechnology,* 6**,** 19-34.

CHEN, H., ERCANBRACK, C., WANG, T., GAN, Q. & FAN, C. 2020. A synthetic reporter for probing mistranslation in living cells. *Frontiers in Bioengineering and Biotechnology,* 8**,** 623.
CHING, X. L., ZAINAL, N. A. A. B., LUANG-IN, V. & MA, N. L. 2022. Lab-based meat the future food. *Environmental Advances,* 10**,** 100315.
CIA 1977. The Soviet hydrocarbon based single cell protein program.
COCHEMÉ, H. M. & MURPHY, M. P. 2008. Complex I is the major site of mitochondrial superoxide production by paraquat. *Journal of Biological Chemistry,* 283**,** 1786-1798.
COELHO, M. O. C., MONTEYNE, A. J., DIRKS, M. L., FINNIGAN, T. J. A., STEPHENS, F. B. & WALL, B. T. 2021. Daily mycoprotein consumption for 1 week does not affect insulin sensitivity or glycaemic control but modulates the plasma lipidome in healthy adults: a randomised controlled trial. *British Journal of Nutrition,* 125**,** 147-160.
COLLINS, L. 2021. *The amount of energy required by direct air carbon capture proves it is an exercise in futility* [Online]. Available: https://www.rechargenews.com/energy-transition/the-amount-of-energy-required-by-direct-air-carbon-capture-proves-it-is-an-exercise-in-futility/2-1-1067588 [Accessed 25.12 2023].
COZMA, E., RAO, M., DUSICK, M., GENEREAUX, J., RODRIGUEZ-MIAS, R. A., VILLÉN, J., BRANDL, C. J. & BERG, M. D. 2023. Anticodon sequence determines the impact of mistranslating tRNAAla variants. *RNA Biology,* 20**,** 791-804.
CROUS, P. W., LOMBARD, L., SANDOVAL-DENIS, M., SEIFERT, K. A., SCHROERS, H. J., CHAVERRI, P., GENÉ, J., GUARRO, J., HIROOKA, Y., BENSCH, K., KEMA, G. H. J., LAMPRECHT, S. C., CAI, L., ROSSMAN, A. Y., STADLER, M., SUMMERBELL, R. C., TAYLOR, J. W., PLOCH, S., VISAGIE, C. M., YILMAZ, N., FRISVAD, J. C., ABDEL-AZEEM, A. M., ABDOLLAHZADEH, J., ABDOLRASOULI, A., AKULOV, A., ALBERTS, J. F., ARAÚJO, J. P. M., ARIYAWANSA, H. A., BAKHSHI, M., BENDIKSBY, M., BEN HADJ AMOR, A., BEZERRA, J. D. P., BOEKHOUT, T., CÂMARA, M. P. S., CARBIA, M., CARDINALI, G., CASTAÑEDA-RUIZ, R. F., CELIS, A., CHATURVEDI, V., COLLEMARE, J., CROLL, D., DAMM, U., DECOCK, C. A., DE VRIES, R. P., EZEKIEL, C. N., FAN, X. L., FERNÁNDEZ, N. B., GAYA, E., GONZÁLEZ, C. D., GRAMAJE, D., GROENEWALD, J. Z., GRUBE, M., GUEVARA-SUAREZ, M., GUPTA, V. K., GUARNACCIA, V., HADDAJI, A., HAGEN, F., HAELEWATERS, D., HANSEN, K., HASHIMOTO, A., HERNÁNDEZ-RESTREPO, M., HOUBRAKEN, J., HUBKA, V., HYDE, K. D., ITURRIAGA, T., JEEWON, R., JOHNSTON, P. R., JURJEVIĆ, Ž., KARALTI, İ., KORSTEN, L., KURAMAE, E. E., KUŠAN, I., LABUDA, R., LAWRENCE, D. P., LEE, H. B., LECHAT, C., LI, H. Y., LITOVKA, Y. A., MAHARACHCHIKUMBURA, S. S. N., MARIN-FELIX, Y., MATIO KEMKUIGNOU, B., MATOČEC, N., MCTAGGART, A. R., MLČOCH, P., MUGNAI, L., NAKASHIMA, C., NILSSON, R. H., NOUMEUR, S. R., PAVLOV, I. N., PERALTA, M. P., PHILLIPS, A. J. L., PITT, J. I., POLIZZI, G., QUAEDVLIEG, W., RAJESHKUMAR, K. C., RESTREPO, S., RHAIEM, A., ROBERT, J., ROBERT, V., RODRIGUES, A. M., et al. 2021. Fusarium: more than a node or a foot-shaped basal cell. *Studies in Mycology,* 98**,** 100116.
CUMMINGS, J. H. & EDWARDS, D. G. 2010. The protein quality of mycoprotein. *Proceedings of the Nutrition Society,* 69**,** E331.
CVETESIC, N., SEMANJSKI, M., SOUFI, B., KRUG, K., GRUIC-SOVULJ, I. & MACEK, B. 2016. Proteome-wide measurement of non-canonical bacterial mistranslation by quantitative mass spectrometry of protein modifications. *Scientific Reports,* 6**,** 28631.
DE MARCHI, L., WANGORSCH, A. & ZOCCATELLI, G. 2021. Allergens from edible insects: Cross-reactivity and effects of processing. *Current Allergy and Asthma Reports,* 21**,** 35.
DE MELLO, A. F. M., VANDENBERGHE, L. P. D. S., MACHADO, C. M. B., VALLADARES-DIESTRA, K. K., DE CARVALHO, J. C. & SOCCOL, C. R. 2023. Polyhydroxybutyrate production by Cupriavidus necator in a corn biorefinery concept. *Bioresource Technology,* 370**,** 128537.

DE VRIES-TEN HAVE, J., OWOLABI, A., STEIJNS, J., KUDLA, U. & MELSE-BOONSTRA, A. 2020. Protein intake adequacy among Nigerian infants, children, adolescents and women and protein quality of commonly consumed foods. *Nutrition Research Reviews,* 33**,** 1-19.

DEL CASTILLO, D. S., PARRA, D., NOCEDA, C. & PÉREZ-MARTÍNEZ, S. 2016. Co-occurrence of pathogenic and non-pathogenic *Fusarium decemcellulare* and *Lasiodiplodia theobromae* isolates in cushion galls disease of cacao (*Theobroma cacao L.*). *Journal of Plant Protection Research,* 56**,** 129-138.

DELBRUCK, M. 1910. Woschschr. *Brau,* 27**,** 375.

DEVLIN, E. 2023. *Quorn owner hit by cost hikes and falling demand in meat-free* [Online]. Available: https://www.thegrocer.co.uk/results/quorn-owner-hit-by-cost-hikes-and-falling-demand-in-meat-free/684215.article#:~:text=Marlow%20grew%20its%20retail%20market,than%2021%2C000%20additional%20distribution%20points. [Accessed 15.12.2023].

DIAS, G. J., HATHTHOTUWA, T. N., ROWLANDS, D. S., GRAM, M. & BEKHIT, A. E.-D. A. 2022. Wool keratin – A novel dietary protein source: Nutritional value and toxicological assessment. *Food Chemistry,* 383**,** 132436.

DITA, M., BARQUERO, M., HECK, D., MIZUBUTI, E. S. G. & STAVER, C. P. 2018. *Fusarium* wilt of banana: Current knowledge on epidemiology and research needs toward sustainable disease management. *Frontiers in Plant Science,* 9.

DIZIGAN, M., KELLY, R., VOYLES, D., LUETHY, M., MALVAR, T. & MALLOY, K. 2007. *High lysine maize compositions and event LY038 maize plants*. US patent application.

DRUMMEN, M., TISCHMANN, L., GATTA-CHERIFI, B., ADAM, T. & WESTERTERP-PLANTENGA, M. 2018. Dietary protein and energy balance in relation to obesity and co-morbidities. *Frontiers in Endocrinology,* 9.

DRUMMOND, M. J. & RASMUSSEN, B. B. 2008. Leucine-enriched nutrients and the regulation of mammalian target of rapamycin signalling and human skeletal muscle protein synthesis. *Current Opinion in Clinical Nutrition & Metababolic Care,* 11**,** 222-6.

DYER, P. S., INDERBITZIN, P. & DEBUCHY, R. 2016. 14 mating-type structure, function, regulation and evolution in the Pezizomycotina. *In:* WENDLAND, J. (ed.) *Growth, Differentiation and Sexuality.* Cham: Springer International Publishing.

DYER, P. S. & KÜCK, U. 2017. Sex and the imperfect fungi. *Microbiology Spectrum,* 5**,** 10.1128/microbiolspec.funk-0043-2017.

EBI, K. L., VANOS, J., BALDWIN, J. W., BELL, J. E., HONDULA, D. M., ERRETT, N. A., HAYES, K., REID, C. E., SAHA, S., SPECTOR, J. & BERRY, P. 2021. Extreme weather and climate change: Population health and health system implications. *Annual Review of Public Health,* 42**,** 293-315.

EL-SAYED, A. S. A., YASSIN, M. A. & ALI, G. S. 2015. Transcriptional and proteomic profiling of *Aspergillus flavipes* in response to sulfur starvation. *PLOS ONE,* 10**,** e0144304.

ELLIS, N. & GALLANT, J. 1982. An estimate of the global error frequency in translation. *Molecular and General Genetics MGG,* 188**,** 169-172.

ENGLER, K. H., COKER, R. & EVANS, I. H. 1999. A novel colorimetric yeast bioassay for detecting trichothecene mycotoxins. *Journal of Microbiological Methods,* 35**,** 207-18.

ESKOLA, M., KOS, G., ELLIOTT, C. T., HAJŠLOVÁ, J., MAYAR, S. & KRSKA, R. 2020. Worldwide contamination of food-crops with mycotoxins: Validity of the widely cited 'FAO estimate' of 25. *Critical Reviews in Food Science and Nutrition,* 60**,** 2773-2789.

ESPOSITO, M. M., TURKU, S., LEHRFIELD, L. & SHOMAN, A. 2023. The impact of human activities on zoonotic infection transmissions. *Animals,* 13.

FAN-MINOGUE, H. & BEDWELL, D. M. 2008. Eukaryotic ribosomal RNA determinants of aminoglycoside resistance and their role in translational fidelity. *RNA,* 14**,** 148-57.

FAO 2000. The state of food and agriculture 2000. Rome.

FAO 2009. Global argiculture towards 2050. Rome.

FAO 2013. Dietary protein quality evaluation in human nutrition. Rome, Italy: Food and Agriculture Organisation of the United Nations.
FAO 2021. The state of the world's land and water resources for food and agriculture – Systems at breaking point. Synthesis report. Rome.
FARSI, D. N., GALLEGOS, J. L., FINNIGAN, T. J. A., CHEUNG, W., MUNOZ, J. M. & COMMANE, D. M. 2023a. The effects of substituting red and processed meat for mycoprotein on biomarkers of cardiovascular risk in healthy volunteers: an analysis of secondary endpoints from Mycomeat. *European Journal of Nutrition,* 62**,** 3349-3359.
FARSI, D. N., GALLEGOS, J. L., KOUTSIDIS, G., NELSON, A., FINNIGAN, T. J. A., CHEUNG, W., MUÑOZ-MUÑOZ, J. L. & COMMANE, D. M. 2023b. Substituting meat for mycoprotein reduces genotoxicity and increases the abundance of beneficial microbes in the gut: Mycomeat, a randomised crossover control trial. *European Journal of Nutrition*.
FIJALKOWSKA, I. J., SCHAAPER, R. M. & JONCZYK, P. 2012. DNA replication fidelity in *Escherichia coli*: A multi-DNA polymerase affair. *FEMS Microbiology Reviews,* 36**,** 1105-21.
FINNIGAN, T. 2012. Mycoprotein: origins, production and properties. *In:* PHILLIPS GO & WILLIAMS PA (eds.) *Handbook of food proteins.* Cambridge: Woodhead Publishing.
FINNIGAN, T., NEEDHAM, L. & ABBOTT, C. 2017a. Chapter 19 - Mycoprotein: A Healthy New Protein With a Low Environmental Impact. *In:* NADATHUR, S. R., WANASUNDARA, J. P. D. & SCANLIN, L. (eds.) *Sustainable Protein Sources.* San Diego: Academic Press.
FINNIGAN, T., NEEDHAM, L. & ABBOTT, C. 2017b. Mycoprotein: A Healthy New Protein With a Low Environmental Impact. *Sustainable Protein Sources,* 3**,** 305-325.
FINNIGAN, T. J. A. Mycoprotein: origins, production and properties. 2011.
FINNIGAN, T. J. A., WALL, B. T., WILDE, P. J., STEPHENS, F. B., TAYLOR, S. L. & FREEDMAN, M. R. 2019. Mycoprotein: The future of nutritious nonmeat protein, a symposium review. *Current Developments in Nutrition,* 3**,** nzz021.
GALILI, G. & AMIR, R. 2013. Fortifying plants with the essential amino acids lysine and methionine to improve nutritional quality. *Plant Biotechnology Journal,* 11**,** 211-222.
GAO, S., ZENG, R., XU, L., SONG, Z., GAO, P. & DAI, F. 2020. Genome sequence and spore germination-associated transcriptome analysis of *Corynespora cassiicola* from cucumber. *BMC Microbiology,* 20**,** 199.
GEOGHEGAN, I. A., EMES, R. D., ARCHER, D. B. & AVERY, S. V. 2020. Method for RNA extraction and transcriptomic analysis of single fungal spores. *MethodsX,* 7**,** 50-55.
GFI. 2020. *$1.5 billion invested in alternative proteins in 2020, including a record $435 million in the next pillar—fermentation* [Online]. Available: https://gfi.org/press/1-5-billion-invested-in-alternative-proteins-in-2020-including-a-record-435-million-in-the-next-pillar-fermentation/ [Accessed 25.12 2023].
GFI. 2023. *Alternative proteins in the European Union* [Online]. Available: https://gfieurope.org/alternative-proteins-in-the-european-union/ [Accessed 25.12 2023].
GILANI, G. S., XIAO, C. W. & COCKELL, K. A. 2012. Impact of Antinutritional Factors in Food Proteins on the Digestibility of Protein and the Bioavailability of Amino Acids and on Protein Quality. *British Journal of Nutrition,* 108**,** S315-S332.
GORISSEN, S. H. M., CROMBAG, J. J. R., SENDEN, J. M. G., WATERVAL, W. A. H., BIERAU, J., VERDIJK, L. B. & VAN LOON, L. J. C. 2018. Protein content and amino acid composition of commercially available plant-based protein isolates. *Amino Acids,* 50**,** 1685-1695.
GORNALL, J., BETTS, R., BURKE, E., CLARK, R., CAMP, J., WILLETT, K. & WILTSHIRE, A. 2010. Implications of climate change for agricultural productivity in the early

twenty-first century. *Philosophical Transactions of the Royal Society of London. Series B, Biological Sciences,* 365**,** 2973-89.
GRAF, M., HAAS, T., MÜLLER, F., BUCHMANN, A., HARM-BEKBENBETOVA, J., FREUND, A., NIEß, A., PERSICKE, M., KALINOWSKI, J., BLOMBACH, B. & TAKORS, R. 2019. Continuous adaptive evolution of a fast-growing *Corynebacterium glutamicum* strain independent of protocatechuate. *Frontiers in Microbiology,* 10.
GRAHAM, A. E. & LEDESMA-AMARO, R. 2023. The microbial food revolution. *Nature Communications,* 14**,** 2231.
GRANT PEARCE, F., HUDSON, A. O., LOOMES, K. & DOBSON, R. C. J. 2017. Dihydrodipicolinate synthase: Structure, dynamics, function, and evolution. *Subcellular Biochemistry,* 83**,** 271-289.
GRAPES, M., WHITING, P. & DINAN, L. 1989. Fatty acid and lipid analysis of the house cricket, *Acheta domesticus*. *Insect Biochemistry,* 19**,** 767-774.
GROMADSKI, K. B. & RODNINA, M. V. 2004. Streptomycin interferes with conformational coupling between codon recognition and GTPase activation on the ribosome. *Nature Structural & Molecular Biology,* 11**,** 316-322.
GROSSI, G., GOGLIO, P., VITALI, A. & WILLIAMS, A. G. 2018. Livestock and climate change: impact of livestock on climate and mitigation strategies. *Animal Frontiers,* 9**,** 69-76.
HALFORD, N. G. 2019. Legislation governing genetically modified and genome-edited crops in Europe: the need for change. *Journal of the Science of Food and Agriculture,* 99**,** 8-12.
HAMM, D. 1981. Amino acid composition of breast and thigh meat from broilers produced in 4 locations of the United States. *Journal of Food Science,* 46**,** 1122-1124.
HARRIS, E. E. 1949. *Food-yeast Production from Wood-processing Byproducts*, U.S. Forest Service, Forest Products Laboratory.
HARTMANN, C., SHI, J., GIUSTO, A. & SIEGRIST, M. 2015. The psychology of eating insects: A cross-cultural comparison between Germany and China. *Food Quality and Preference,* 44**,** 148-156.
HASHEMPOUR-BALTORK, F., HOSSEINI, S. M., ASSAREHZADEGAN, M. A., KHOSRAVI-DARANI, K. & HOSSEINI, H. 2020. Safety assays and nutritional values of mycoprotein produced by *Fusarium venenatum* IR372C from date waste as substrate. *Journal of the Science of Food and Agriculture,* 100**,** 4433-4441.
HAUG, A., HOSTMARK, A. T. & HARSTAD, O. M. 2007. Bovine milk in human nutrition - a review. *Lipids in Health and Disease,* 6.
HAYEK, M. N. 2022. The infectious disease trap of animal agriculture. *Science Advances,* 8**,** eadd6681.
HÉBERT, A., FORQUIN-GOMEZ, M. P., ROUX, A., AUBERT, J., JUNOT, C., HEILIER, J. F., LANDAUD, S., BONNARME, P. & BECKERICH, J. M. 2013. New insights into sulfur metabolism in yeasts as revealed by studies of *Yarrowia lipolytica*. *Applied and Environmental Microbiology,* 79**,** 1200-11.
HERMANS, W. J. H., SENDEN, J. M., CHURCHWARD-VENNE, T. A., PAULUSSEN, K. J. M., FUCHS, C. J., SMEETS, J. S. J., VAN LOON, J. J. A., VERDIJK, L. B. & VAN LOON, L. J. C. 2021. Insects are a viable protein source for human consumption: from insect protein digestion to postprandial muscle protein synthesis in vivo in humans: a double-blind randomized trial. *American Journal of Clinical Nutrition,* 114**,** 934-944.
HERNANDEZ-VALDES, J. A., AAN DE STEGGE, M., HERMANS, J., TEUNIS, J., VAN TATENHOVE-PEL, R. J., TEUSINK, B., BACHMANN, H. & KUIPERS, O. P. 2020. Enhancement of amino acid production and secretion by Lactococcus lactis using a droplet-based biosensing and selection system. *Metabolic Engineering Communications,* 11**,** e00133.
HOLLAND, S., LODWIG, E., SIDERI, T., READER, T., CLARKE, I., GKARGKAS, K., HOYLE, D. C., DELNERI, D., OLIVER, S. G. & AVERY, S. V. 2007. Application of the comprehensive set of heterozygous yeast deletion mutants to elucidate the molecular basis of cellular chromium toxicity. *Genome Biology,* 8**,** R268.

HOLLAND, S. L., GHOSH, E. & AVERY, S. V. 2010. Chromate-induced sulfur starvation and mRNA mistranslation in yeast are linked in a common mechanism of Cr toxicity. *Toxicology in Vitro,* 24**,** 1764-1767.
HOLLO, G., CSAPO, J., SZUCS, E., TOZSER, J., REPA, I. & HOLLO, I. 2001. Influence of breed, slaughter weight and gender on chemical composition of beef. Part 2. Fatty acid composition of fat in rib samples. *Asian-Australasian Journal of Animal Sciences,* 14**,** 1719-1723.
HOUSTON, D. K., NICKLAS, B. J., DING, J., HARRIS, T. B., TYLAVSKY, F. A., NEWMAN, A. B., LEE, J. S., SAHYOUN, N. R., VISSER, M. & KRITCHEVSKY, S. B. 2008. Dietary protein intake is associated with lean mass change in older, community-dwelling adults: The health, aging, and body composition (Health ABC) study. *American Journal of Clinical Nutrition,* 87**,** 150-5.
HUANG, M. & HULL, C. M. 2017. Sporulation: how to survive on planet Earth (and beyond). *Current Genetics,* 63**,** 831-838.
HUMPENÖDER, F., BODIRSKY, B. L., WEINDL, I., LOTZE-CAMPEN, H., LINDER, T. & POPP, A. 2022. Projected environmental benefits of replacing beef with microbial protein. *Nature,* 605**,** 90-96.
HUNTER, J. 2014. Investigation of symptoms reported after eating mycoprotein. Interim report of 2 year study. *Marlow Foods Document*.
IMASHIMIZU, M., OSHIMA, T., LUBKOWSKA, L. & KASHLEV, M. 2013. Direct assessment of transcription fidelity by high-resolution RNA sequencing. *Nucleic Acids Research,* 41**,** 9090-104.
IPCC 2019. Climate change and land: an IPCC special report on climate change, desertification, land degradation, sustainable land management, food security, and greenhouse gas fluxes in terrestrial ecosystems. *In:* P.R. SHUKLA, J. S., E. CALVO BUENDIA, V. MASSON-DELMOTTE, H.-O. PÖRTNER, D. C. ROBERTS, P. ZHAI, R. SLADE, S. CONNORS, R. VAN DIEMEN, M. FERRAT, E. HAUGHEY, S. LUZ, S. NEOGI, M. PATHAK, J. PETZOLD, J. PORTUGAL PEREIRA, P. VYAS, E. HUNTLEY, K. KISSICK, M. BELKACEMI, J. MALLEY, (EDS.) (ed.). In press: IPCC.
JÄGERMEYR, J., MÜLLER, C., RUANE, A. C., ELLIOTT, J., BALKOVIC, J., CASTILLO, O., FAYE, B., FOSTER, I., FOLBERTH, C., FRANKE, J. A., FUCHS, K., GUARIN, J. R., HEINKE, J., HOOGENBOOM, G., IIZUMI, T., JAIN, A. K., KELLY, D., KHABAROV, N., LANGE, S., LIN, T.-S., LIU, W., MIALYK, O., MINOLI, S., MOYER, E. J., OKADA, M., PHILLIPS, M., PORTER, C., RABIN, S. S., SCHEER, C., SCHNEIDER, J. M., SCHYNS, J. F., SKALSKY, R., SMERALD, A., STELLA, T., STEPHENS, H., WEBBER, H., ZABEL, F. & ROSENZWEIG, C. 2021. Climate impacts on global agriculture emerge earlier in new generation of climate and crop models. *Nature Food,* 2**,** 873-885.
JANSSEN, M., WIJFFELS, R. H. & BARBOSA, M. J. 2022. Microalgae based production of single-cell protein. *Current Opinion in Biotechnology,* 75**,** 102705.
JANZEN, D. H. 1977. Why Fruits Rot, Seeds Mold, and Meat Spoils. *The American Naturalist,* 111**,** 691-713.
JASTRZEBOWSKA, K. & GABRIEL, I. 2015. Inhibitors of amino acids biosynthesis as antifungal agents. *Amino Acids,* 47**,** 227-49.
JAYAWARDENA, D. M., HECKATHORN, S. A. & BOLDT, J. K. 2021. A meta-analysis of the combined effects of elevated carbon dioxide and chronic warming on plant %N, protein content and N-uptake rate. *AoB Plants,* 13**,** plab031.
JENKINS, T. C. & MCGUIRE, M. A. 2006. Major advances in nutrition: Impact on milk composition. *Journal of Dairy Science,* 89**,** 1302-1310.
JI, F., HE, D., OLANIRAN, A. O., MOKOENA, M. P., XU, J. & SHI, J. 2019. Occurrence, toxicity, production and detection of *Fusarium* mycotoxin: a review. *Food Production, Processing and Nutrition,* 1**,** 6.
JONES, S. W., KARPOL, A., FRIEDMAN, S., MARU, B. T. & TRACY, B. P. 2020. Recent advances in single cell protein use as a feed ingredient in aquaculture. *Current Opinion in Biotechnology,* 61**,** 189-197.

JONES, T. E., ALEXANDER, R. W. & PAN, T. 2011. Misacylation of specific nonmethionyl tRNAs by a bacterial methionyl-tRNA synthetase. *Proceedings of the National Academy of Sciences,* 108**,** 6933-6938.
KAPUR, M. & ACKERMAN, S. L. 2018. mRNA translation gone awry: Translation fidelity and neurological disease. *Trends in Genetics,* 34**,** 218-231.
KEELING, K. M., XUE, X., GUNN, G. & BEDWELL, D. M. 2014. Therapeutics based on stop codon readthrough. *Annual Review of Genomics and Human Genetics,* 15**,** 371-94.
KFC. 2019. *KFC UK adds imposter to the roster* [Online]. Available: https://global.kfc.com/press-releases/kfc-uk-adds-imposter-to-the-roster/ [Accessed 15.12.2023 2023].
KING, R., BROWN, N. A., URBAN, M. & HAMMOND-KOSACK, K. E. 2018. Inter-genome comparison of the Quorn fungus *Fusarium venenatum* and the closely related plant infecting pathogen *Fusarium graminearum*. *BMC Genomics,* 19**,** 269.
KINGSBURY, J. M. & MCCUSKER, J. H. 2010. Cytocidal amino acid starvation of *Saccharomyces cerevisiae* and *Candida albicans* acetolactate synthase (ilv2Δ) mutants is influenced by the carbon source and rapamycin. *Microbiology,* 156**,** 929-939.
KLENK, F., GLEICH, K., MEISTER, F., HÄFNER, B. & LANZA, G. 2020. Approach for developing implementation strategies for circular economy in global production networks. *Procedia CIRP,* 90**,** 127-132.
KOHANSKI, M. A., DWYER, D. J., WIERZBOWSKI, J., COTTAREL, G. & COLLINS, J. J. 2008. Mistranslation of membrane proteins and two-component system activation trigger antibiotic-mediated cell death. *Cell,* 135**,** 679-90.
KOHLHAW, G. B. 2003. Leucine biosynthesis in fungi: Entering metabolism through the back door. *Microbiology and Molecular Biology Reviews,* 67**,** 1-+.
KOIVURINTA, J., KURKELA, R. & KOIVISTOINEN, P. 1979. Uses of Pekilo, a microfungus biomass from *Paecilomyces varioti* in sausage and meat balls. *International Journal of Food Science & Technology,* 14**,** 561-570.
KOLKMAN, A., DARAN-LAPUJADE, P., FULLAONDO, A., OLSTHOORN, M. M., PRONK, J. T., SLIJPER, M. & HECK, A. J. 2006. Proteome analysis of yeast response to various nutrient limitations. *Molecular Systems Biology,* 2**,** 2006.0026.
KRAMER, E. B. & FARABAUGH, P. J. 2007. The frequency of translational misreading errors in *E. coli* is largely determined by tRNA competition. *RNA,* 13**,** 87-96.
LARABA, I., MCCORMICK, S. P., VAUGHAN, M. M., GEISER, D. M. & O'DONNELL, K. 2021. Phylogenetic diversity, trichothecene potential, and pathogenicity within *Fusarium sambucinum* species complex. *PLOS ONE,* 16**,** e0245037.
LAROSSA, R. A., VAN DYK, T. K. & SMULSKI, D. R. 1987. Toxic accumulation of alpha-ketobutyrate caused by inhibition of the branched-chain amino acid biosynthetic enzyme acetolactate synthase in *Salmonella typhimurium*. *Journal of Bacteriology,* 169**,** 1372-8.
LARSSON, L., GRIMBY, G. & KARLSSON, J. 1979. Muscle strength and speed of movement in relation to age and muscle morphology. *Journal of applied physiology: respiratory, environmental and exercise physiology,* 46**,** 451-6.
LAURENCE, M. H., WALSH, J. L., SHUTTLEWORTH, L. A., ROBINSON, D. M., JOHANSEN, R. M., PETROVIC, T., VU, T. T. H., BURGESS, L. W., SUMMERELL, B. A. & LIEW, E. C. Y. 2016. Six novel species of *Fusarium* from natural ecosystems in Australia. *Fungal Diversity,* 77**,** 349-366.
LEGER, D., MATASSA, S., NOOR, E., SHEPON, A., MILO, R. & BAR-EVEN, A. 2021. Photovoltaic-driven microbial protein production can use land and sunlight more efficiently than conventional crops. *PNAS,* 118.
LEVINE, R. L., MOSONI, L., BERLETT, B. S. & STADTMAN, E. R. 1996. Methionine residues as endogenous antioxidants in proteins. *Proc Natl Acad Sci U S A,* 93**,** 15036-40.
LI, Y., HUANG, X. M., ZHAO, D. M., LIU, Y. Z., HE, K. W., LIU, Y. X., CHEN, C. H., LONG, L. P., XU, Y., XIE, X. X., HAN, K. K., LIU, X. Y., YANG, J., ZHANG, Y. F., FAN, F., WEBBY, R. & WAN, X. F. 2016. Detection of avian H7N9 influenza a viruses in the

Yangtze Delta region of China during early H7N9 outbreaks. *Avian Disease* 60**,** 118-25.
LI, Z., HOSHINO, Y., TRAN, L. & GAUCHER, E. A. 2022. Phylogenetic articulation of uric acid evolution in mammals and how it informs a therapeutic uricase. *Molecular Biology and Evolution,* 39.
LIN, X., ALSPAUGH, J. A., LIU, H. & HARRIS, S. 2014. Fungal morphogenesis. *Cold Spring Harbor Perspectives in Medicine,* 5**,** a019679.
LIVINGSTON, N. M., KWON, J., VALERA, O., SABA, J. A., SINHA, N. K., REDDY, P., NELSON, B., WOLFE, C., HA, T., GREEN, R., LIU, J. & WU, B. 2023. Bursting translation on single mRNAs in live cells. *Molecular Cell,* 83**,** 2276-2289.e11.
LONG, C. P. & ANTONIEWICZ, M. R. 2018. How adaptive evolution reshapes metabolism to improve fitness: recent advances and future outlook. *Current Opinion in Chemical Engineering,* 22**,** 209-215.
LONNIE, M., HOOKER, E., BRUNSTROM, J. M., CORFE, B. M., GREEN, M. A., WATSON, A. W., WILLIAMS, E. A., STEVENSON, E. J., PENSON, S. & JOHNSTONE, A. M. 2018. Protein for life: Review of optimal protein intake, sustainable dietary sources and the effect on appetite in ageing adults. *Nutrients,* 10.
LOURENÇO, R. & CAMILO, M. E. 2002. Taurine: a conditionally essential amino acid in humans? An overview in health and disease. *Nutricion Hospitalaria,* 17**,** 262-70.
LUCAS, D. M., TAYLOR, M. L., HARTNELL, G. F., NEMETH, M. A., GLENN, K. C. & DAVIS, S. W. 2007. Broiler performance and carcass characteristics when fed diets containing lysine maize (LY038 or LY038 x MON 810), control, or conventional reference maize. *Poultry Science,* 86**,** 2152-61.
MACUSI, E. D., CAYACAY, M. A., BORAZON, E. Q., SALES, A. C., HABIB, A., FADLI, N. & SANTOS, M. D. 2023. Protein fishmeal replacement in aquaculture: A systematic review and implications on growth and adoption viability. *Sustainability,* 15.
MÆHRE, H. K., JENSEN, I. J. & EILERTSEN, K. E. 2016. Enzymatic pre-treatment increases the protein bioaccessibility and extractability in dulse (*Palmaria palmata*). *Marine Drugs,* 14.
MAGGIO-HALL, L. A., LYNE, P., WOLFF, J. A. & KELLER, N. P. 2008. A single acyl-CoA dehydrogenase is required for catabolism of isoleucine, valine and short-chain fatty acids in *Aspergillus nidulans*. *Fungal Genetics and Biology,* 45**,** 180-9.
MARANGONI, F., CORSELLO, G., CRICELLI, C., FERRARA, N., GHISELLI, A., LUCCHIN, L. & POLI, A. 2015. Role of poultry meat in a balanced diet aimed at maintaining health and wellbeing: an Italian consensus document. *Food & Nutrition Research,* 59**,** 27606.
MARLOW INGREDIENTS 2023. Marlow Foods, parent company of Quorn®, sets up ingredients division to make its mycoprotein available to others.
MARSTRAND, P. 1981. Production of microbial protein: a study of the development and introduction of a new technology *Research Policy* 10**,** 148–171.
MARTINEZ-FORCE, E. & BENITEZ, T. 1995. Effects of varying media, temperature, and growth rates on the intracellular concentrations of yeast amino acids. *Biotechnology Progress,* 11**,** 386-92.
MARTINEZ-PORCHAS, M. & MARTINEZ-CORDOVA, L. R. 2012. World aquaculture: environmental impacts and troubleshooting alternatives. *The Scientific World Journal,* 2012**,** 389623.
MCCORMICK, S. P., STANLEY, A. M., STOVER, N. A. & ALEXANDER, N. J. 2011. Trichothecenes: from simple to complex mycotoxins. *Toxins* 3**,** 802-14.
MCDANIEL, L. E. & BAILEY, E. G. 1969. Effect of shaking speed and type of closure on shake flask cultures. *Applied Microbiology,* 17**,** 286-90.
MD NOH, M. F., GUNASEGAVAN, R. D., MUSTAFA KHALID, N., BALASUBRAMANIAM, V., MUSTAR, S. & ABD RASHED, A. 2020. Recent techniques in nutrient analysis for food composition database. *Molecules,* 25.
MECHA, E., ALVES, M. L., BENTO DA SILVA, A., PEREIRA, A. B., RUBIALES, D., VAZ PATTO, M. C. & BRONZE, M. R. 2023. High inter- and intra- diversity of amino acid content and protein digestibility disclosed in five cool season legume species with a growing market demand. *Foods,* 12**,** 1383.

MEHMOOD, A., LIU, G., WANG, X., MENG, G., WANG, C. & LIU, Y. 2019. Fungal quorum-sensing molecules and inhibitors with potential antifungal activity: A review. *Molecules,* 24.

MILLER, J. D. & MACKENZIE, S. 2000. Secondary metabolites of *Fusarium venenatum* strains with deletions in the tri5 gene encoding trichodiene synthetase. *Mycologia,* 92**,** 764-771.

MILLER, S. A. & DWYER, J. T. 2001. Evaluating the safety and nutritional value of mycoprotein. *Food Technology,* 55**,** 42-47.

MIRANDA, I., SILVA-DIAS, A., ROCHA, R., TEIXEIRA-SANTOS, R., COELHO, C., GONCALVES, T., SANTOS, M. A., PINA-VAZ, C., SOLIS, N. V., FILLER, S. G. & RODRIGUES, A. G. 2013. Candida albicans CUG mistranslation is a mechanism to create cell surface variation. *mBio,* 4.

MOHANTY, B., MAHANTY, A., GANGULY, S., SANKAR, T. V., CHAKRABORTY, K., RANGASAMY, A., PAUL, B., SARMA, D., MATHEW, S., ASHA, K. K., BEHERA, B., AFTABUDDIN, M., DEBNATH, D., VIJAYAGOPAL, P., SRIDHAR, N., AKHTAR, M. S., SAHI, N., MITRA, T., BANERJEE, S., PARIA, P., DAS, D., DAS, P., VIJAYAN, K. K., LAXMANAN, P. T. & SHARMA, A. P. 2014. Amino Acid compositions of 27 food fishes and their importance in clinical nutrition. *Journal of Amino Acids,* 2014**,** 269797.

MOHANTY, C. S., SINGH, V. & CHAPMAN, M. A. 2020. Winged bean: An underutilized tropical legume on the path of improvement, to help mitigate food and nutrition security. *Scientia Horticulturae,* 260**,** 108789.

MOHLER, K. & IBBA, M. 2017. Translational fidelity and mistranslation in the cellular response to stress. *Nature Microbiology,* 2.

MONTEYNE, A. J., COELHO, M. O. C., PORTER, C., ABDELRAHMAN, D. R., JAMESON, T. S. O., FINNIGAN, T. J. A., STEPHENS, F. B., DIRKS, M. L. & WALL, B. T. 2020. Branched-chain amino acid fortification does not restore muscle protein synthesis rates following ingestion of lower- compared with higher-dose mycoprotein. *The Journal of Nutrition,* 150**,** 2931-2941.

MONTEYNE, A. J., DUNLOP, M. V., MACHIN, D. J., COELHO, M. O. C., PAVIS, G. F., PORTER, C., MURTON, A. J., ABDELRAHMAN, D. R., DIRKS, M. L., STEPHENS, F. B. & WALL, B. T. 2021. A mycoprotein-based high-protein vegan diet supports equivalent daily myofibrillar protein synthesis rates compared with an isonitrogenous omnivorous diet in older adults: a randomised controlled trial. *British Journal of Nutrition,* 126**,** 674-684.

MOORE, D., ROBSON, G. D. & TRINCI, A. P. J. 2011. *21st century guidebook to fungi,* Cambridge, Cambridge University Press Cambridge.

MORDRET, E., DAHAN, O., ASRAF, O., RAK, R., YEHONADAV, A., BARNABAS, G. D., COX, J., GEIGER, T., LINDNER, A. B. & PILPEL, Y. 2019. Systematic detection of amino acid substitutions in proteomes reveals mechanistic basis of ribosome errors and selection for translation fidelity. *Molecular Cell,* 75**,** 427-+.

NEFF, R. A., EDWARDS, D., PALMER, A., RAMSING, R., RIGHTER, A. & WOLFSON, J. 2018. Reducing meat consumption in the USA: a nationally representative survey of attitudes and behaviours. *Public Health Nutrition,* 21**,** 1835-1844.

NELSON, P. E., DESJARDINS, A. E. & PLATTNER, R. D. 1993. Fumonisins, mycotoxins produced by fusarium species: biology, chemistry, and significance. *Annual Review of Phytopathology,* 31**,** 233-52.

NETZER, N., GOODENBOUR, J. M., DAVID, A., DITTMAR, K. A., JONES, R. B., SCHNEIDER, J. R., BOONE, D., EVES, E. M., ROSNER, M. R., GIBBS, J. S., EMBRY, A., DOLAN, B., DAS, S., HICKMAN, H. D., BERGLUND, P., BENNINK, J. R., YEWDELL, J. W. & PAN, T. 2009. Innate immune and chemically triggered oxidative stress modifies translational fidelity. *Nature,* 462**,** 522-526.

NORVIENYEKU, J., ZHONG, Z., LIN, L., DANG, X., CHEN, M., LIN, X., ZHANG, H., ANJAGO, W. M., LIN, L., ABDUL, W. & WANG, Z. 2017. Methylmalonate-semialdehyde dehydrogenase mediated metabolite homeostasis essentially regulate conidiation, polarized germination and pathogenesis in *Magnaporthe oryzae*. *Environmental Microbiology,* 19**,** 4256-4277.

NUCCI, M. & ANAISSIE, E. 2007. Fusarium infections in immunocompromised patients. *Clinical Microbiology Reviews* 20**,** 695-704.
NYYSSÖLÄ, A., OJALA, L. S., WUOKKO, M., PEDDINTI, G., TAMMINEN, A., TSITKO, I., NORDLUND, E. & LIENEMANN, M. 2021. Production of endotoxin-free microbial biomass for food applications by gas fermentation of gram-positive H_2-oxidizing bacteria. *Acs Food Science & Technology,* 1**,** 470-479.
NYYSSÖLÄ, A., SUHONEN, A., RITALA, A. & OKSMAN-CALDENTEY, K.-M. 2022. The role of single cell protein in cellular agriculture. *Current Opinion in Biotechnology,* 75**,** 102686.
O'DONNELL, K., CIGELNIK, E. & CASPER, H. H. 1998. Molecular phylogenetic, morphological, and mycotoxin data support reidentification of the Quorn mycoprotein fungus as *Fusarium venenatum*. *Fungal Genetetics and Biology,* 23**,** 57-67.
OBA, T., NOMIYAMA, S., HIRAKAWA, H., TASHIRO, K. & KUHARA, S. 2005. Asp578 in LEU4p is one of the key residues for leucine feedback inhibition release in sake yeast. *Bioscience Biotechnology and Biochemistry,* 69**,** 1270-1273.
OBA, T., YAMAMOTO, Y., NOMIYAMA, S., SUENAGA, H., MUTA, S., TASHIRO, K. & KUHARA, S. 2006. Properties of a trifluoroleucine-resistant mutant of Saccharomyces cerevisiae. *Bioscience Biotechnology and Biochemistry,* 70**,** 1776-1779.
OLIVER, J. D., KAYE, S. J., TUCKWELL, D., JOHNS, A. E., MACDONALD, D. A., LIVERMORE, J., WARN, P. A., BIRCH, M. & BROMLEY, M. J. 2012. The *Aspergillus fumigatus* dihydroxyacid dehydratase Ilv3A/IlvC is required for full virulence. *PLoS One,* 7**,** e43559.
OU, X., CAO, J., CHENG, A., PEPPELENBOSCH, M. P. & PAN, Q. 2019. Errors in translational decoding: tRNA wobbling or misincorporation? *PLoS Genetics,* 15.
PAOLETTI, M., RYDHOLM, C., SCHWIER, E. U., ANDERSON, M. J., SZAKACS, G., LUTZONI, F., DEBEAUPUIS, J. P., LATGE, J. P., DENNING, D. W. & DYER, P. S. 2005. Evidence for sexuality in the opportunistic fungal pathogen *Aspergillus fumigatus*. *Current Biology,* 15**,** 1242-8.
PEGG, K. G., COATES, L. M., O'NEILL, W. T. & TURNER, D. W. 2019. The epidemiology of *Fusarium* wilt of banana. *Frontiers in Plant Science,* 10**,** 1395.
PEREIRA, A. G., FRAGA-CORRAL, M., GARCIA-OLIVEIRA, P., OTERO, P., SORIA-LOPEZ, A., CASSANI, L., CAO, H., XIAO, J., PRIETO, M. A. & SIMAL-GANDARA, J. 2022. Single-cell proteins obtained by circular economy intended as a feed ingredient in aquaculture. *Foods,* 11.
POORE, J. & NEMECEK, T. 2018. Reducing food's environmental impacts through producers and consumers. *Science,* 360**,** 987-992.
PRASANNA, B. M., VASAL, S. K., KASSAHUN, B. & SINGH, N. N. 2001. Quality protein maize. *Current Science,* 81**,** 1308-1319.
PUBLIC HEALTH ENGLAND 2020. NDNS: results from years 9 to 11 (2016 to 2017 and 2018 to 2019). London.
QUORN. 2020. *Quorn driving success for the 'vegan high street'* [Online]. Available: https://www.quorn.co.uk/company/press/quorn-driving-success-for-the-vegan-high-street [Accessed 15.12.2023].
RANSY, C., VAZ, C., LOMBÈS, A. & BOUILLAUD, F. 2020. Use of H_2O_2 to cause oxidative stress, the catalase issue. *International Journal of Molecular Sciences,* 21.
REALMONTE, G., DROUET, L., GAMBHIR, A., GLYNN, J., HAWKES, A., KÖBERLE, A. C. & TAVONI, M. 2019. An inter-model assessment of the role of direct air capture in deep mitigation pathways. *Nature Communications,* 10**,** 3277.
RECANATI, F., ALLIEVI, F., SCACCABAROZZI, G., ESPINOSA, T., DOTELLI, G. & SAINI, M. 2015. Global meat consumption trends and local deforestation in Madre de Dios: assessing land use changes and other environmental impacts. *Defining the Future of Sustainability and Resilience in Design, Engineering and Construction,* 118**,** 630-638.
REDMOND, H. P., STAPLETON, P. P., NEARY, P. & BOUCHIER-HAYES, D. 1998. Immunonutrition: the role of taurine. *Nutrition,* 14**,** 599-604.

REITZER, L. 2014. Amino acid synthesis. *Reference Module in Biomedical Sciences.* Elsevier.
REVERBERI, M., RICELLI, A., ZJALIC, S., FABBRI, A. A. & FANELLI, C. 2010. Natural functions of mycotoxins and control of their biosynthesis in fungi. *Applied Microbiology and Biotechnology,* 87**,** 899-911.
RIBAS DE POUPLANA, L., SANTOS, M. A. S., ZHU, J.-H., FARABAUGH, P. J. & JAVID, B. 2014. Protein mistranslation: friend or foe? *Trends in Biochemical Sciences,* 39**,** 355-362.
RIEL, M., EIDEN, F., BLANK, L.M., FREYER, N., HARTMANN, I. 2020. Optimal bioreactor inoculum preparation in shake flasks with automated seed inoculation, conditioning and online monitoring. *Application Note No. 431*.
RIPPS, H. & SHEN, W. 2012. Review: taurine: a "very essential" amino acid. *Molecular Vision,* 18**,** 2673-86.
RIQUELME, M., AGUIRRE, J., BARTNICKI-GARCÍA, S., BRAUS, G. H., FELDBRÜGGE, M., FLEIG, U., HANSBERG, W., HERRERA-ESTRELLA, A., KÄMPER, J., KÜCK, U., MOURIÑO-PÉREZ, R. R., TAKESHITA, N. & FISCHER, R. 2018. Fungal morphogenesis, from the polarized growth of hyphae to complex reproduction and infection structures. *Microbiology and Molecular Biology Reviews,* 82.
RISNER, D., MCDONALD, K. A., JONES, C. & SPANG, E. S. 2023. A techno-economic model of mycoprotein production: achieving price parity with beef protein. *Frontiers in Sustainable Food Systems,* 7.
RITALA, A., HAKKINEN, S. T., TOIVARI, M. & WIEBE, M. G. 2017. Single cell protein-state-of-the-art, industrial landscape and patents 2001-2016. *Frontiers in Microbiology,* 8.
RODRIGUEZ-MIAS, R. A., HESS, K. N., RUIZ, B. Y., SMITH, I. R., BARENTE, A. S., ZIMMERMAN, S. M., LU, Y. Y., NOBLE, W. S., FIELDS, S. & VILLÉN, J. 2022. Proteome-wide identification of amino acid substitutions deleterious for protein function. *bioRxiv***,** 2022.04.06.487405.
RONDANELLI, M., NICHETTI, M., PERONI, G., FALIVA, M. A., NASO, M., GASPARRI, C., PERNA, S., OBERTO, L., DI PAOLO, E., RIVA, A., PETRANGOLINI, G., GUERRESCHI, G. & TARTARA, A. 2021. Where to find leucine in food and how to feed elderly with sarcopenia in order to counteract loss of muscle mass: Practical advice. *Frontiers in Nutrition,* 7.
ROSZKOWSKA, A., PAWLICKA, M., MROCZEK, A., BAŁABUSZEK, K. & NIERADKO-IWANICKA, B. 2019. Non-Celiac Gluten Sensitivity: A Review. *Medicina (Kaunas),* 55.
SÁENZ, V., ALVAREZ-MORENO, C., PAPE, P. L., RESTREPO, S., GUARRO, J. & RAMÍREZ, A. M. C. 2020. A one health perspective to recognize *Fusarium* as important in clinical practice. *Journal of Fungi* 6.
SAINT-MACARY, M. E., BARBISAN, C., GAGEY, M. J., FRELIN, O., BEFFA, R., LEBRUN, M. H. & DROUX, M. 2015. Methionine biosynthesis is essential for infection in the rice blast fungus *Magnaporthe oryzae*. *PLOS ONE,* 10**,** e0111108.
SAJEENA, A., NAIR, D. S. & SREEPAVAN, K. 2020. Non-pathogenic *Fusarium oxysporum* as a biocontrol agent. *Indian Phytopathology,* 73**,** 177-183.
SAMHITA, L., P, K. R., STEPHENSON, G., THUTUPALLI, S. & AGASHE, D. 2021. The impact of mistranslation on phenotypic variability and fitness. *Evolution,* 75**,** 1201-1217.
SAMHITA, L., RAVAL, P. K. & AGASHE, D. 2020. Global mistranslation increases cell survival under stress in *Escherichia coli*. *PLoS Genetics,* 16.
SCHMUTZER, M. & WAGNER, A. 2023. Not quite lost in translation: Mistranslation alters adaptive landscape topography and the dynamics of evolution. *Molecular Biology and Evolution,* 40.
SCHUNTERMANN, D. B., FISCHER, J. T., BILE, J., GAIER, S. A., SHELLEY, B. A., AWAWDEH, A., JAHN, M., HOFFMAN, K. S., WESTHOF, E., SOLL, D., CLARKE, C. R. & VARGAS-RODRIGUEZ, O. 2023. Mistranslation of the genetic code by a new family of bacterial transfer RNAs. *Journal of Biological Chemistry,* 299**,** 104852.

SIDDIQUI, F., SALAM, R. A., LASSI, Z. S. & DAS, J. K. 2020. The intertwined relationship between malnutrition and poverty. *Frontiers in Public Health,* 8**,** 453.
SIDDIQUI, S. A., ALVI, T., SAMEEN, A., KHAN, S., BLINOV, A. V., NAGDALIAN, A. A., MEHDIZADEH, M., ADLI, D. N. & ONWEZEN, M. 2022. Consumer acceptance of alternative proteins: A systematic review of current alternative protein sources and interventions adapted to increase their acceptability. *Sustainability,* 14**,** 15370.
SIMPSON, D., WITHERS, J., WIEBE, M., ROBSON, G. & TRINCI, A. 1998. Mutants with general growth rate advantages are the predominant morphological mutants to be isolated from the Quorn® production plant. *Mycological Research,* 102**,** 221-227.
SINGH, B. K., DELGADO-BAQUERIZO, M., EGIDI, E., GUIRADO, E., LEACH, J. E., LIU, H. & TRIVEDI, P. 2023a. Climate change impacts on plant pathogens, food security and paths forward. *Nature Reviews Microbiology,* 21**,** 640-656.
SINGH, P., GOLLAPALLI, K., MANGIOLA, S., SCHRANNER, D., YUSUF, M. A., CHAMOLI, M., SHI, S. L., LOPES BASTOS, B., NAIR, T., RIERMEIER, A., VAYNDORF, E. M., WU, J. Z., NILAKHE, A., NGUYEN, C. Q., MUIR, M., KIFLEZGHI, M. G., FOULGER, A., JUNKER, A., DEVINE, J., SHARAN, K., CHINTA, S. J., RAJPUT, S., RANE, A., BAUMERT, P., SCHÖNFELDER, M., IAVARONE, F., DI LORENZO, G., KUMARI, S., GUPTA, A., SARKAR, R., KHYRIEM, C., CHAWLA, A. S., SHARMA, A., SARPER, N., CHATTOPADHYAY, N., BISWAL, B. K., SETTEMBRE, C., NAGARAJAN, P., TARGOFF, K. L., PICARD, M., GUPTA, S., VELAGAPUDI, V., PAPENFUSS, A. T., KAYA, A., FERREIRA, M. G., KENNEDY, B. K., ANDERSEN, J. K., LITHGOW, G. J., ALI, A. M., MUKHOPADHYAY, A., PALOTIE, A., KASTENMÜLLER, G., KAEBERLEIN, M., WACKERHAGE, H., PAL, B. & YADAV, V. K. 2023b. Taurine deficiency as a driver of aging. *Science,* 380**,** eabn9257.
SKIDMORE, M. E., MOFFETTE, F., RAUSCH, L., CHRISTIE, M., MUNGER, J. & GIBBS, H. K. 2021. Cattle ranchers and deforestation in the Brazilian Amazon: Production, location, and policies. *Global Environmental Change,* 68**,** 102280.
SOKATCH, J. R., SANDERS, L. E. & MARSHALL, V. P. 1968. Oxidation of methylmalonate semialdehyde to propionyl coenzyme A in *Pseudomonas aeruginosa* grown on valine. *Journal of Biological Chemistry,* 243**,** 2500-6.
SOLAR FOODS. 2023. *Solar Foods' Solein® makes its debut in Singapore's resilient food culture* [Online]. Available: https://solarfoods.com/solar-foods-solein-makes-its-debut-in-singapores-resilient-food-culture/#:~:text=Singapore%20is%20now%20the%20first,potential%20of%20this%20novel%20food. [Accessed 25/12 2023].
SPALVINS, K., ZIHARE, L. & BLUMBERGA, D. 2018. Single cell protein production from waste biomass: comparison of various industrial by-products. *International Scientific Conference Environmental and Climate Technologies, Conect 2018,* 147**,** 409-418.
SPECHT, L. 2020. An analysis of culture medium cost and production volumes for cultivated meat. Good Food Institute.
SPITZE, A. R., WONG, D. L., ROGERS, Q. R. & FASCETTI, A. J. 2003. Taurine concentrations in animal feed ingredients; cooking influences taurine content. *The Journal of Animal Physiology and Animal Nutrition,* 87**,** 251-62.
STEPHENS, N., DI SILVIO, L., DUNSFORD, I., ELLIS, M., GLENCROSS, A. & SEXTON, A. 2018. Bringing cultured meat to market: Technical, socio-political, and regulatory challenges in cellular agriculture. *Trends in Food Science & Technology,* 78**,** 155-166.
STOHS, S. J. & BAGCHI, D. 1995. Oxidative mechanisms in the toxicity of metal ions. *Free Radical Biology and Medicine,* 18**,** 321-36.
SUBRAMANIAM, R., NARAYANAN, S., WALKOWIAK, S., WANG, L., JOSHI, M., ROCHELEAU, H., OUELLET, T. & HARRIS, L. J. 2015. Leucine metabolism regulates TRI6 expression and affects deoxynivalenol production and virulence in Fusarium graminearum. *Molecular Microbiology,* 98**,** 760-9.

SUMMERELL, B. A. 2019. Resolving *Fusarium*: Current status of the genus. *The Annual Review of Phytopathology,* 57**,** 323-339.
SUN, M. & ZHANG, J. 2022. Preferred synonymous codons are translated more accurately: Proteomic evidence, among-species variation, and mechanistic basis. *Science Advances,* 8**,** eabl9812.
SWIFT, R. J., CRAIG, S. H., WIEBE, M. G., ROBSON, G. D. & TRINCI, A. P. 2000. Evolution of *Aspergillus niger* and *A. nidulans* in glucose-limited chemostat cultures, as indicated by oscillations in the frequency of cycloheximide resistant and morphological mutants. *Mycological Research,* 104**,** 333-337.
SZEPE, K. J., DYER, P. S., JOHNSON, R. I., SALTER, A. M. & AVERY, S. V. 2021. Influence of environmental and genetic factors on food protein quality: current knowledge and future directions. *Current Opinion in Food Science,* 40**,** 94-101.
TAKAGI, H., HASHIDA, K., WATANABE, D., NASUNO, R., OHASHI, M., IHA, T., NEZUO, M. & TSUKAHARA, M. 2015. Isolation and characterization of awamori yeast mutants with L-leucine accumulation that overproduce isoamyl alcohol. *The Journal of Bioscience and Bioengineering,* 119**,** 140-7.
TANZI, A. S., EAGLETON, G. E., HO, W. K., WONG, Q. N., MAYES, S. & MASSAWE, F. 2019. Winged bean (Psophocarpus tetragonolobus (L.) DC.) for food and nutritional security: synthesis of past research and future direction. *Planta,* 250**,** 911-931.
TAUB, D. R., MILLER, B. & ALLEN, H. 2008. Effects of elevated CO2 on the protein concentration of food crops: a meta-analysis. *Global Change Biology,* 14**,** 565-575.
TEVATIA, R., ALLEN, J., RUDRAPPA, D., WHITE, D., CLEMENTE, T. E., CERUTTI, H., DEMIREL, Y. & BLUM, P. 2015. The taurine biosynthetic pathway of microalgae. *Algal Research-Biomass Biofuels and Bioproducts,* 9**,** 21-26.
THAM, E. H. & LEUNG, D. Y. M. 2018. How different parts of the world provide new insights into food allergy. *Allergy, Asthma & Immunology Resesearch,* 10**,** 290-299.
TILLICH, U. M., LEHMANN, S., SCHULZE, K., DÜHRING, U. & FROHME, M. 2012. The optimal mutagen dosage to induce point-mutations in Synechocystis sp. PCC6803 and its application to promote temperature tolerance. *PLoS One,* 7**,** e49467.
TRAIL, F. 2009. For blighted waves of grain: *Fusarium graminearum* in the postgenomics era. *Plant Physiology,* 149**,** 103-110.
TRAYNOR, A. M., SHERIDAN, K. J., JONES, G. W., CALERA, J. A. & DOYLE, S. 2019. Involvement of sulfur in the biosynthesis of essential metabolites in pathogenic fungi of animals, particularly *Aspergillus* spp.: Molecular and therapeutic implications. *Frontiers in Microbiology,* 10**,** 2859.
TRINCI, A. P. 1994. The 1994 Marjory Stephenson Prize Lecture. Evolution of the Quorn myco-protein fungus, *Fusarium graminearum* A3/5. *Microbiology,* 140 (Pt 9)**,** 2181-8.
TRINCI, A. P. J. 1992. Myco-protein: A twenty-year overnight success story. *Fungal Biology,* 96**,** 1-13.
TURNBULL, W. H., LEEDS, A. R. & EDWARDS, D. G. 1992. Mycoprotein reduces blood lipids in free-living subjects. *The American Journal of Clinical Nutrition,* 55**,** 415-9.
UGALDE, U. O. & CASTRILLO, J. I. 2002. Single cell proteins from fungi and yeasts. *In:* KHACHATOURIANS, G. G. & ARORA, D. K. (eds.) *Applied Mycology and Biotechnology.* Elsevier.
UKRI. 2023. *Understanding hyphal branching in Fusarium venenatum to design improved strains* [Online]. Available: https://gtr.ukri.org/projects?ref=BB%2FW008734%2F1 [Accessed 08.09.2023 2023].
ULM, E. H., BOHME, R. & KOHLHAW, G. 1972. Alpha-isopropylmalate synthase from yeast: purification, kinetic studies, and effect of ligands on stability. *Journal of Bacteriology,* 110**,** 1118-26.
UN 2017. World Population Prospects: The 2017 Revision, Key Findings and Advance Tables. Working paper No. ESA/P/WP/248 ed. New York: United Nations.

UN 2022. World Population Prospects 2022: Summary of Results. New York.
UN. 2023. *Water – at the center of the climate crisis* [Online]. Available: https://www.un.org/en/climatechange/science/climate-issues/water#:~:text=Climate%20change%20is%20exacerbating%20both,climate%20change%20are%20inextricably%20linked. [Accessed 07.12.2023 2023].
VAN HUIS, A. 2013. Potential of insects as food and feed in assuring food security. *Annual Review of Entomology,* 58**,** 563-83.
VAN HUIS, A. & OONINCX, D. G. A. B. 2017. The environmental sustainability of insects as food and feed. A review. *Agronomy for Sustainable Development,* 37**,** 43.
VIDAL, M. A., KILROY, G. E., JOHNSON, J. R., LOPEZ, M. J., MOORE, R. M. & GIMBLE, J. M. 2006. Cell growth characteristics and differentiation frequency of adherent equine bone marrow-derived mesenchymal stromal cells: adipogenic and osteogenic capacity. *Vet Surg,* 35**,** 601-10.
VISSER, M., HUNG, Y. & VERBEKE, W. 2021. Protein knowledge of older adults and identification of subgroups with poor knowledge. *Nutrients,* 13**,** 1006.
VOLLSET, S. E., GOREN, E., YUAN, C. W., CAO, J., SMITH, A. E., HSIAO, T., BISIGNANO, C., AZHAR, G. S., CASTRO, E., CHALEK, J., DOLGERT, A. J., FRANK, T., FUKUTAKI, K., HAY, S. I., LOZANO, R., MOKDAD, A. H., NANDAKUMAR, V., PIERCE, M., PLETCHER, M., ROBALIK, T., STEUBEN, K. M., WUNROW, H. Y., ZLAVOG, B. S. & MURRAY, C. J. L. 2020. Fertility, mortality, migration, and population scenarios for 195 countries and territories from 2017 to 2100: a forecasting analysis for the Global Burden of Disease Study. *Lancet,* 396**,** 1285-1306.
VÖLTZ, W. 1916. Über die Verwertung der Hefe als Nährmittel für Mensch und Tier. *Naturwissenschaften,* 4**,** 705-710.
VON DER HAAR, T., LEADSHAM, J. E., SAUVADET, A., TARRANT, D., ADAM, I. S., SAROMI, K., LAUN, P., RINNERTHALER, M., BREITENBACH-KOLLER, H., BREITENBACH, M., TUITE, M. F. & GOURLAY, C. W. 2017. The control of translational accuracy is a determinant of healthy ageing in yeast. *Open Biology,* 7.
VOUTILAINEN, E., PIHLAJANIEMI, V. & PARVIAINEN, T. 2021. Economic comparison of food protein production with single-cell organisms from lignocellulose side-streams. *Bioresource Technology Reports,* 14**,** 100683.
WANG, X. & PAN, T. 2016. Stress response and adaptation mediated by amino acid misincorporation during protein synthesis. *Advances in Nutrition,* 7**,** 773s-9s.
WANG, Y., GUAN, Y., LIN, W., YAN, H., NENG, J. & SUN, P. 2021. Quantitative proteomic profiling of fungal growth, development, and ochratoxin a production in *Aspergillus ochraceus* on high- and low-NaCl cultures. *Toxins* 13.
WARD, J. F., EVANS, J. W., LIMOLI, C. L. & CALABRO-JONES, P. M. 1987. Radiation and hydrogen peroxide induced free radical damage to DNA. *The British Journal of Cancer,* 8**,** 105-12.
WEST, S., MONTEYNE, A. J., WHELEHAN, G., ABDELRAHMAN, D. R., MURTON, A. J., FINNIGAN, T. J. A., BLACKWELL, J. R., STEPHENS, F. B. & WALL, B. T. 2023. Mycoprotein ingestion within or without its wholefood matrix results in equivalent stimulation of myofibrillar protein synthesis rates in resting and exercised muscle of young men. *British Journal of Nutrition,* 130**,** 20-32.
WHITTAKER, J. A. 2022. *Is Your Sweetness My Weakness?: The Impact of Carbon Source on Mycotoxigenesis in Fusarium venenatum.* PhD Thesis, University of Nottingham.
WHITTAKER, J. A., JOHNSON, R. I., FINNIGAN, T. J. A., AVERY, S. V. & DYER, P. S. 2020. The biotechnology of Quorn mycoprotein: past, present and future challanges. *In:* NEVALAINEN, H. (ed.) *Grand Challenges in Fungal Biotechnology.* Cham: Springer.
WHO 2007. Amino acid requirements of adults. *Protein and Amino Acid Requirements in Human Nutrition: Report of a Joint Who/Fao/Unu Expert Consultation,* 935**,** 135-159.

WIEBE, M. G., ROBSON, G. D., OLIVER, S. G. & TRINCI, A. P. 1994a. Evolution of *Fusarium graminearum* A3/5 grown in a glucose-limited chemostat culture at a slow dilution rate. *Microbiology* 140 (Pt 11)**,** 3023-9.
WIEBE, M. G., ROBSON, G. D., OLIVER, S. G. & TRINCI, A. P. 1994b. Use of a series of chemostat cultures to isolate 'improved' variants of the Quorn mycoprotein fungus, *Fusarium graminearum* A3/5. *Microbiology,* 140 (Pt 11)**,** 3015-21.
WILHELM, J. M., JESSOP, J. J. & PETTITT, S. E. 1978. Aminoglycoside antibiotics and eukaryotic protein synthesis: stimulation of errors in the translation of natural messengers in extracts of cultured human cells. *Biochemistry,* 17**,** 1149-53.
WILTROUT, E., GOODENBOUR, J. M., FRECHIN, M. & PAN, T. 2012. Misacylation of tRNA with methionine in *Saccharomyces cerevisiae*. *Nucleic Acids Research,* 40**,** 10494-10506.
WITHERS, J. M., WIEBE, M. G., ROBSON, G. D. & TRINCI, A. P. J. 1994. Development of morphological heterogeneity in glucose-limited chemostat cultures of *Aspergillus oryzae*. *Mycological Research,* 98**,** 95-100.
WOHLGEMUTH, I., GAROFALO, R., SAMATOVA, E., GUNENC, A. N., LENZ, C., URLAUB, H. & RODNINA, M. V. 2021. Translation error clusters induced by aminoglycoside antibiotics. *Nature Communications,* 12**,** 1830.
WONG, H. E., HUANG, C. J. & ZHANG, Z. 2018. Amino acid misincorporation propensities revealed through systematic amino acid starvation. *Biochemistry,* 57**,** 6767-6779.
WTO 1994. General agreement on tarrifs and trade.
XIE, J., DE SOUZA ALVES, V., VON DER HAAR, T., O'KEEFE, L., LENCHINE, R. V., JENSEN, K. B., LIU, R., COLDWELL, M. J., WANG, X. & PROUD, C. G. 2019. Regulation of the elongation phase of protein synthesis enhances translation accuracy and modulates lifespan. *Current Biology,* 29**,** 737-749 e5.
XING, R. Y. & WHITMAN, W. B. 1991. Characterization of enzymes of the branched-chain amino acid biosynthetic pathway in *Methanococcus* spp. *Journal of Bacteriology,* 173**,** 2086-92.
YODER, W. T. & CHRISTIANSON, L. M. 1998. Species-specific primers resolve members of *Fusarium* section *Fusarium*. Taxonomic status of the edible "Quorn" fungus reevaluated. *Fungal Genet Biol,* 23**,** 68-80.
YOO, H. C., YU, Y. C., SUNG, Y. & HAN, J. M. 2020. Glutamine reliance in cell metabolism. *Experimental & Molecular Medicine,* 52**,** 1496-1516.
ZHA, X., TSAPEKOS, P., ZHU, X., KHOSHNEVISAN, B., LU, X. & ANGELIDAKI, I. 2021. Bioconversion of wastewater to single cell protein by methanotrophic bacteria. *Bioresource Technology,* 320**,** 124351.
ZHANG, J., DEBETS, A. J., VERWEIJ, P. E., MELCHERS, W. J., ZWAAN, B. J. & SCHOUSTRA, S. E. 2015. Asexual sporulation facilitates adaptation: The emergence of azole resistance in *Aspergillus fumigatus*. *Evolution,* 69**,** 2573-86.
ZOHEIR, A. E., SPÄTH, G. P., NIEMEYER, C. M. & RABE, K. S. 2021. Microfluidic evolution-on-a-chip reveals new mutations that cause antibiotic resistance. *Small,* 17**,** e2007166.
ZOTTE, A. D., RICCI, R., CULLERE, M., SERVA, L., TENTI, S. & MARCHESINI, G. 2020. Research Note: Effect of chicken genotype and white striping-wooden breast condition on breast meat proximate composition and amino acid profile. *Poultry Science,* 99**,** 1797-1803.